TECHNISCHE UNIVERSITÄT MÜNCHEN

Lehrstuhl für Experimentelle Genetik

Long-term effects of low and moderate doses of ionising radiation on learning and memory formation in the neonatal mouse brain

Stefan J. Kempf

Vollständiger Abdruck der von der Fakultät Wissenschaftszentrum Weihenstephan für Ernährung, Landnutzung und Umwelt der Technischen Universität München zur Erlangung des akademischen Grades eines

Doktors der Naturwissenschaften

genehmigten Dissertation.

Vorsitzender:	Univ.-Prof. Dr. S. Scherer
Prüfer der Dissertation:	1. apl.Prof. Dr. J. Adamski
	2. Univ.-Prof. Dr. M. W. Pfaffl
	3. Univ.-Prof. Dr. M. J. Atkinson

Die Dissertation wurde am 04.11.2014 bei der Technischen Universität München eingereicht und durch die Fakultät Wissenschaftszentrum Weihenstephan für Ernährung, Landnutzung und Umwelt am 25.11.2014 angenommen.

Memories are for life time

to Anna

Eidesstattliche Erklärung

Ich erkläre hiermit an Eides statt, dass die vorliegende Arbeit von mir selbst und ohne fremde Hilfe verfasst und noch nicht anderweitig für Prüfungszwecke vorgelegt wurde. Es wurden keine anderen als die angegebenen Quellen oder Hilfsmittel benutzt. Wörtliche und sinngemäße Zitate sind als solche gekennzeichnet.

München, den …….

.....
Stefan Kempf

Table of Contents

1 Abstract

The number of computed tomography (CT) scans, especially those involving the head region, is sharply rising in the western world. Children may be of increased risk for possible adverse effects due to the greater susceptibility of the growing brain. Indeed, epidemiological data strongly suggest that intellectual development is adversely affected when the infant brain is exposed to radiation doses that are equivalent to those delivered by CT of the head. However, the biological mechanisms behind the potential damage from low-dose and also moderate-dose radiation are unknown. Neonatal NMRI mice (postnatal day 10) were irradiated with total body doses ranging from 0.02 to 1.0 Gy. The molecular investigation of irradiated mouse brain included global and targeted proteomics, pathway-focused transcriptomics and targeted miRNAomics analysis at 7 months post-irradiation. Immunohistochemistry was used to confirm alterations in adult neurogenesis. Immunofluorescence was performed to evaluate changes in synaptic proteins. Significant signalling pathway changes were found at doses of 0.5 and 1.0 Gy. An alteration of synaptic plasticity was indicated by impaired Rac1-Cofilin and CREB pathways in irradiated brains. Increased TNFα levels suggesting neuroinflammation as well as a decline in adult neurogenesis in the hippocampus were additional hallmarks. Further, a potential deregulation of molecules involved in circadian rhythm was noted. In a second study, neonatal C57BL/6 mice (postnatal day 10) were irradiated with total body doses of 0.1, 0.5 Gy or 2.0 Gy. The analysis 6 months post-irradiation showed impaired Rac1-Cofilin signalling and CREB pathways similar to irradiated NMRI mice. In addition, mitochondrial dysfunction in isolated hippocampal and cortical synaptosomes was found.

These data imply that mainly moderate but also low doses of irradiation target signalling pathways of synaptic plasticity that may explain the abnormal cognition even after a prolonged time of radiation insult. Overall, this work (i) emphasises the important role of synapses in radiation science which is still an unenlightened target in this field although it is the origin of neurotransmission and storage of information (synaptic plasticity) and (ii) connects several molecular targets of radiation to neurodegenerative diseases such as Alzheimer´s. The results are essential in minimising radiation-associated health risks.

2 Zusammenfassung

Die Zahl der Computertomographie (CT) basierter Bildgebung, vor allem im Bereich des Kopfes, ist in der westlichen Welt stark gestiegen. Besonders Kinder weisen ein erhöhtes Risiko für mögliche Nebenwirkungen auf, was begründet ist in der höheren Empfindlichkeit des sich entwickelnden Gehirns. Tatsächlich zeigen epidemiologische Daten, dass die geistige Entwicklung beeinträchtigt ist, wenn das Gehirn des Kindes mit Strahlendosen bestrahlt wird, die bereits denen von CT Scans entsprechen. Die biologischen und mechanistischen Effekte von niedrigen aber auch mittleren Strahlendosen, die das Gehirn schädigen können, sind unbekannt.

Neugeborene NMRI-Mäuse (Tag 10 postnatal) wurden mit Gesamtkörperdosen im Bereich von 0,02 bis 1,0 Gy bestrahlt. Die molekulare Untersuchung der bestrahlten Mäusehirne umfasste eine Analyse des Proteoms, Transkriptoms und miRNAoms sieben Monate nach der Bestrahlung. Zudem wurden immunhistochemische Veränderungen in der adulten Neurogenese untersucht. Mittels Immunfluoreszenzfärbung wurden Änderungen in der Expressionsstärke synaptischer Proteine bewertet. Es zeigten sich signifikante Veränderungen in Signalwegen bei Dosen von 0,5 und 1,0 Gy. Eine Veränderung der synaptischen Plastizität wurde durch eine Störung des Rac1-Cofilin und CREB Signalweges im bestrahlten Gehirn nachgewiesen. Eine erhöhte TNFα Expression, welche auf eine neuronale Entzündungsreaktion im Gehirn hindeutet, sowie ein Rückgang der adulten Neurogenese im Hippocampus waren weitere Kennzeichen. Ferner wurde eine mögliche Deregulierung von Molekülen des zirkadianen Biorhythmus festgestellt.

Im zweiten Teil dieser Arbeit wurden neugeborene C57BL/6 Mäuse (Tag 10 postnatal) mit einer Gesamtkörperdosis von 0,1, 0,5 oder 2,0 Gy bestrahlt. Die Analyse sechs Monate nach der Bestrahlung zeigte Defekte des Rac1-Cofilin-Signalwegs und des CREB-vermittelten Signalwegs vergleichbar zu bestrahlten NMRI Mäusen. Darüber hinaus wurden mitochondriale Fehlfunktionen in isolierten hippocampalen und kortikalen Synaptosomen gefunden.

Diese Daten implizieren, dass vor allem mittlere, aber auch niedrige Strahlendosen einen Effekt auf Signalwege der synaptischen Plastizität haben, welche die anormale

Kognition selbst nach einem langen Zeitraum der Strahlenschädigung erklären könnte. Zudem betont diese Arbeit die wichtige Rolle der Synapse in der Strahlenwissenschaft, welche immer noch ein unbeleuchtetes Forschungsgebiet ist obwohl es den Ursprung der Neutransmission und Informationsspeicherung (synaptische Plastizität) darstellt. Des Weiteren stellt diese Arbeit eine Verbindung zwischen Strahlung und neurodegenerative Erkrankungen, wie zum Beispiel Alzheimer, anhand mehrerer überlappender molekularer Targets her.
Die Ergebnisse sind wichtig bei der Minimierung von strahlungsassoziierten Gesundheitsrisiken.

3 Introduction

3.1 Increase in medical-associated radiation exposure

The exposure of ionising radiation relevant for mankind comes from natural and man-made sources. Temporal trends show that the usage of medical radiation is rapidly increasing and is leading to a worldwide increase in the population exposure: around 20 % of the global annual per capita effective radiation dose was received from diagnostic medical and dental radiation in the period 1997 to 2007; the increase exceeded more than 60 % that of the years 1991 to 1996 (Schonfeld et al., 2011). Importantly, the annual dose for individuals who had not received ionising radiation for medical purposes was not, or only slightly, changed since 1987 (Gerber et al., 2009). As an optimal diagnosis is often dependent on high-resolution imaging methods, usually based on ionising radiation, medical radiation is the main artificial source of ionising radiation exposure (Bernier et al., 2012). Within this class, X-ray computed tomography (CT) scanning is a commonly and widely used radiodiagnostic method. Generally, the absorbed tissue doses range from 10-100 mGy for a single CT examination (Wiest et al., 2002). Repeated CT examinations can lead to higher cumulative radiation exposures. Although the application of CT scans is only around 11 % of all imaging procedures, it contributes approximately to 70 % of the total radiation exposure from all medical imaging methods (Smith-Bindman et al., 2008). Most CT scans are applied on the age group of 36-50 years (27 %), and 9 % of these patients are imaged on the head region (Mettler et al., 2000). Children receive approximately 11 % of all CT scans and 5 % of these are head CT scans (Mettler et al., 2000) corresponding to six children out of 1000 receiving head exposure. Approximately 15 % of children with minor traumatic brain injury are still imaged with ionising radiation in paediatric German hospitals (Oster et al., 2012). The number of CT scans for children may be higher than 1.5 million per year in the Western hemisphere (UNSCEAR, 2000). Importantly, the presumptive threshold of the brain dose still causing delayed damage may be as low as 0.1 Gy (Loganovsky, 2009).

3.2 Children and ionising radiation

Compared to adults, children are in general a highly radiation-sensitive group, especially regarding radiation-dependent side-effects on the brain. This may be reasoned in their higher life expectancy allowing radiation-induced effects with a prolonged latency to develop and in their immature and developing brain.

During early phases of childhood the volume of the grey matter – a major component of the central nervous system (CNS) with neuronal cell bodies including their axons and dendrites and glial cells - increases rapidly and peaks at around four years of age (Holland et al., 1986). This specific phase of rapid brain maturation is called the brain growth spurt (Dobbing and Sands, 1979) and involves phases of axonal and dendritic growth including establishment and breakup of neuronal circuits (synaptogenesis) (Huttenlocher and Dabholkar, 1997, Dekaban, 1978). Further, motor and sensory skills are increasingly acquired at that age (Kelly et al., 1988). In rodents, the comparable time window for the brain growth spurt is restricted to the second and fourth postnatal week and lasts in human until the third to fourth postnatal year (Dobbing and Sands, 1973). It has been shown that toxic agents administered to neonatal mice within this susceptibility window can lead to disruption of adult brain function (Eriksson et al., 2000). This can increase the more pronounced detrimental effects on cognition-based spontaneous behaviour if combined with low-dose ionising radiation on postnatal day ten (Eriksson et al., 2010). Exposure of ionising radiation at this specific developmental stage may lead to long-term associated neurocognitive deficits due to disruption of distinct molecular and cellular processes (Zhu et al., 2009).

3.3 Epidemiological evidence of radiation and cognitive deficits

One of the most valuable cohort studies showing that low-dose ionising radiation exposure affects cognitive skills in exposed children later in life was published by Hall et al. (Hall et al., 2004). The children studied were treated for cutaneous haemangioma before the age of 18 months with an average absorbed brain dose of

around 52 mGy (median 20 mGy, range 0 - 2,800 mGy including multiple radiation treatments). Hall et al. showed impaired intellectual skills at the age of 18-19 years (Hall et al., 2004). A study of children treated with X-ray radiation against scalp ringworm (Tinea capitis) indicated that children receiving head doses ranging from 0.7 to 1.7 Gy (Schulz and Albert, 1968) developed more psychiatric symptoms, and were more often treated for psychiatric disorders than unexposed ones (Omran et al., 1978), and had a slightly higher frequency of mental retardation (Ron et al., 1982).

In adults, a cohort study of nuclear workers at the Mayak Production Association (Mayak PA) demonstrated a significantly increased incidence of cerebrovascular disease (CVD) among workers who received cumulative doses of external gamma-rays higher than 0.2 Gy, compared with those who received less than 0.2 Gy (Azizova et al., 2011). Disturbances of the cerebrovascular system have been considered as a relevant pathogenic factor in Alzheimer´s disease (Tong et al., 2012, Kurata et al., 2011, Viticchi et al., 2012), a progressive neurodegenerative disease attributed with learning and memory loss. A French-UK cohort study with childhood brain cancer survivors treated with radiotherapy showed an increased risk in long-term cerebrovascular mortality (relative risk of 22 per Gy with a 95 % confidence interval of 1-44) (Haddy et al., 2011). However, this study did not take into consideration any confounding factors such as hypertension, smoking or obesity. Generally, these studies indicate that ionising radiation could indirectly cause neurological symptoms via effects on the microvasculature of the brain. Further, these epidemiological studies suggest that there is a correlation between exposure to low (≤ 0.1 Gy) or moderate (≤ 2.0 Gy) doses of ionising radiation and altered neurocognitive outcome. These observations are consistent with the outcomes of patients exposed to much higher doses fractionated during cranial irradiation (cumulative doses ≥ 40 Gy, single doses 2 – 4 Gy) to treat brain tumours; patients suffer shortly after treatment from distinct long-lasting decline in cognition and visual memory (Hoffman and Yock, 2009, Spiegler et al., 2004) strongly affecting the patient´s life quality. Moreover, there are indications that the linear no-threshold (LNT) model assuming that the risk of ionising radiation is directly proportional to the whole range of doses may not be valid for non-cancer endpoints, especially at low and moderate radiation doses (≤ 2.0 Gy) (Little, 2010). In particular, this seems to be

the case for cerebrovascular disease (Shimizu et al., 2010, Azizova et al., 2010, Azizova et al., 2011).

3.4 The brain and the memory

Numerous studies showed that the hippocampus is necessary for certain types of memories such as for memories of daily experiences (episodic memory) and personal history (autographical memory) (Squire et al., 2004, Milner, 2005, Moscovitch et al., 2006). The hippocampus consists of three sub-regions namely dentate gyrus (DG), cornu ammonis area 3 (CA3) and cornu ammonis area 1 (CA1). It is considered that the hippocampus is involved in distinct projection processes from the entorhinal cortex to DG, DG to CA3, CA3 to CA1 and CA1 to the cortex (Amaral and Witter, 1989). Each of these brain regions has specific cell types and regulatory tasks contributing to memory processes (Nakazawa et al., 2004, Nakazawa et al., 2002, Gold and Kesner, 2005, Kesner, 2007, De Jaeger et al., 2014, Bero et al., 2014). The DG is of particular interest as it is capable to generate new neurons throughout life – a process called adult neurogenesis (Ming and Song, 2011) - and is important for regulation of cognition and mood (Bero et al., 2014, Zhao et al., 2008). Moreover, it has been proposed that adult neurogenesis is involved for efficient cortical storage of new memories (Kitamura et al., 2009).

The process of adult neurogenesis originates from stem cells in the subgranular zone (SGZ) of the DG giving rise to a large population of proliferative progenitor cells and mature neurons but only a part of them functionally integrate within existing neuronal circuits (van Praag et al., 2002). Irradiation leads to changes in these steps of adult neurogenesis that is associated with micro-environmental changes such as microglia-dependent neuroinflammation (Rola et al., 2004a, Allen et al., 2013, Raber et al., 2004, Mizumatsu et al., 2003). However, as both the number of integrated neurons is relatively small and adult neurogenesis is a time-dependent process over several weeks (Basak and Taylor, 2009), the immediate alterations in adult neurogenesis by ionising radiation may not completely explain the radiation-induced learning and memory deficits seen rapidly after start of radiotherapy treatment. In addition, radiation exposure may cause changes directly in mature neuronal

networks as demonstrated recently in the murine hippocampus (Parihar et al., 2014, Parihar and Limoli, 2013). This could include alterations in the level of structural and synaptic plasticity of the dendritic spine - a membranous protrusion on a neuron´s dendrite receiving input from another neuronal dendritic spine to form a synapse with a pre- and post-synapse - congruent with the current most influential memory storage model that learning-related activity structurally shapes synapses and that leads to preserved memory (McGaugh, 2000). Alterations in the dendritic spine tree have been observed in cognitive brain disorders such as Alzheimer´s (Tsamis et al., 2010), Rett syndrome (Armstrong et al., 1998) and Down´s syndrome (Becker et al., 1986), not only in the hippocampus but also in the cortex.

The ability of synapses to undergo structural modifications in response to increases or decreases in their activity to strengthen or weaken the information flow is called synaptic plasticity (Hughes, 1958). This is an important mechanism to store new information but also to recall them after a prolonged time (Takeuchi et al., 2014). In this context, the actin cytoskeleton plays an important role in mature dendritic spines to modulate these processes by enabling a scaffold to sustain synaptic morphology and to integrate neurotransmitter receptors necessary for neurotransmission that is based on its rapid dynamic potential (Star et al., 2002, Sheng and Hoogenraad, 2007, Hotulainen and Hoogenraad, 2010); spines would be unable to immediately change their morphology and volume in response to stimuli if the cytoskeleton is not dynamic.

Neuronal communication is primarily mediated via the pre-synaptic release of neurotransmitters such as glutamate binding to neuronal receptors on the postsynapse. The glutamatergic neurotransmitter receptors N-methyl-D-aspartate receptors (NMDARs), α-amino-2-hydroxy-5-methyl-4-isoxazole propionic acid receptors (AMPARs) and metabotropic G-protein coupled glutamate receptors (mGluRs) represent important neuronal receptors (Bourne and Harris, 2008) along with their intracellular downstream signalling pathways affecting long-term potentiation (LTP) and –depression (LTD) (Bellot et al., 2014a, Cortes-Mendoza et al., 2013). LTP is a long-lasting elevation in synaptic transmission resulting from synchronic or strong stimulation and leads to synaptic strength increase (Bliss and Gardner-Medwin, 1973, Kaibara and Leung, 1993). In contrast to LTP, LTD is a long-lasting decrease in synaptic transmission relying on weak and low-frequency

stimulation (Lee et al., 1998). While LTP is in part due to activation of protein kinases such as calmodulin-kinases (Camk´s), protein kinases A (PKA`s) and –C (PKC`s) phosphorylating target proteins, LTD arises from activation of calcium-dependent phosphatases such as types 1 (PP1) and 2 (PP2), accounting for the majority of serine/threonine phosphatase activity in the brain (Cohen, 1997), dephosphorylating proteins (Bellot et al., 2014a, Colbran, 2004).

3.5 Loss of memory

Memory impairment in patients suffering from Alzheimer´s is related to the loss of synapses in the cortex and hippocampus (Terry et al., 1991, DeKosky and Scheff, 1990, DeKosky et al., 1996). Importantly, as the loss of synapses and aberrant synaptic sprouting in patients incipient for Alzheimer´s is greater than the neuronal loss and neurofibrillary tangle formation (Masliah, 1995), synapses are a good marker to access cognitive deficits (Overk and Masliah, 2014). The process of damaging to synapses could be associated with defects on NMDA and AMPA glutamate receptor signalling (Mota et al., 2014, Hsieh et al., 2006) but also on metabotropic G-protein coupled glutamate receptors (Renner et al., 2010) as early molecular events in an altered synaptic plasticity. This may manifest into a loss of synaptic terminals, dendritic spines and neurons (Overk and Masliah, 2014).

3.6 Mechanisms of ionising radiation on memory formation

A proposed model outlining the state of knowledge of ionising radiation and neurodegeneration is shown in Figure 1.

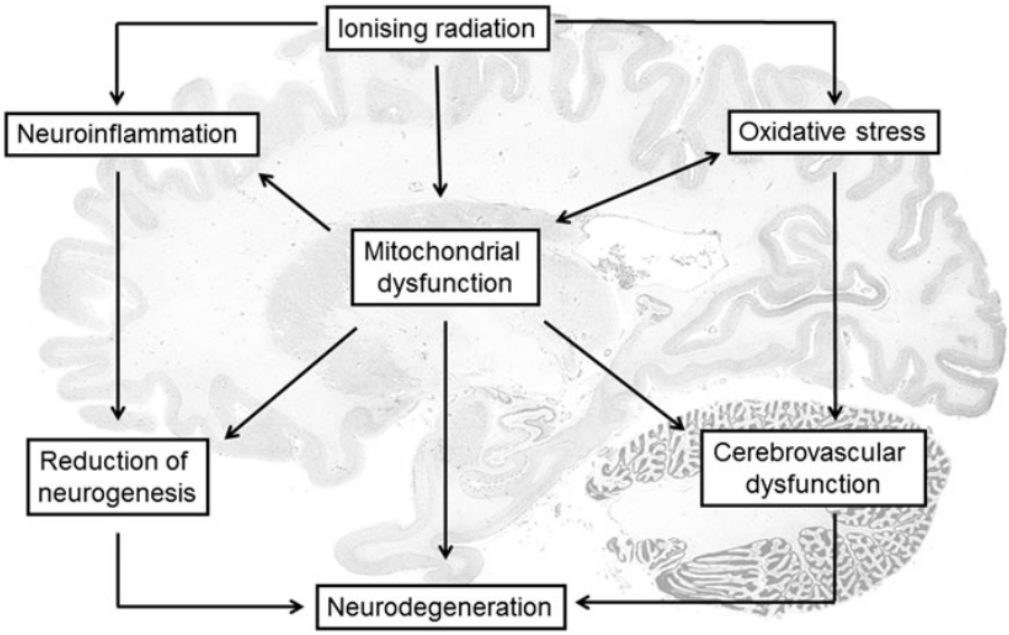

Figure 1: Targets of ionising radiation in neurodegeneration.
Neurodegeneration after radiation exposure is a multicellular process and may be associated to various targets such as reduction of adult neurogenesis, cerebrovascular dysfunctions, neuroinflammation and oxidative stress and their intrinsic cellular signalling pathways. Yet, there is a growing body of evidence that mitochondria play an important central role in these processes. The image is adapted after own publication (Kempf et al., 2013) and is based on both *in vitro* and *in vivo* data of radiation experiments as tabular listed in this mentioned publication.

4 Aim of the thesis

The ***hypothesis*** of this work is that exposure to low- / moderate-doses of ionising radiation in neonatal mice leads to long-term alterations in synaptogenesis / dendrite shape causing persistent neurocognitive decline due to an altered synaptic plasticity.

In detail, the ***aims*** of the studies presented here were:

i) To estimate the initial triggering dose needed to manifest detrimental long-term effects of radiation on synaptic plasticity in the brain
ii) To elucidate the molecular mechanism by analysing altered signalling pathways that explain the synaptic defects
iii) To challenge the hypothesis by using two mouse models by characterising the involvement of synaptic signalling pathways
iv) To find potential overlapping molecular connections between radiation-induced learning and memory dysfunction and neurodegenerative diseases such as Alzheimer´s

5 Materials

5.1 Chemicals and Reagents

Acetic acid	Merck KG
Acrylamid / Bisacrylamide (30 % / 0.8 %)	National Diagnostics
APS	Merck KG
Acetone	Merck KG
Acetonitrile	Merck KG
Ammonium bicarbonate	Sigma Aldrich Chemie GmbH
ADP	Sigma Aldrich Chemie GmbH
Antimycin A	Sigma Aldrich Chemie GmbH
Bradford-Reagent	Sigma-Aldrich Chemie GmbH
Bromophenol blue	Roche Molecular Diagnostics
Beta-Mercaptoethanol	Merck KG
BSA, fatty acid free	ROTH GmbH
Coomassie® Brilliant Blue R250	Serva Electrophoresis
Concentrated Formalin, neutral buffered (7x)	BioOptica
Diaminobenzidine	DCS Diagnostics
DMSO	Sigma Aldrich Chemie GmbH
EDTA	SIGMA-Aldrich Chemie GmbH
Ethanol (absolute)	Merck KG
Fluoresent Mounting Medium	Dako
Ficoll®PM400	Sigma Aldrich Chemie GmbH
Formic Acid	Sigma Aldrich Chemie GmbH
FCCP	Sigma Aldrich Chemie GmbH
Geltrex^{TM} LDEV-free reduced Growth Factor Basement Membrane Mix	Life Technologies
GnHCl (6 M)	Serva Electrophoresis
Glycerine	Sigma-Aldrich Chemie GmbH
Goat serum (Immunofluorescence)	Life Technologies
HCl	Sigma Aldrich Chemie GmbH
Hoechst 33258	SIGMA-Aldrich Chemie GmbH
Isopropanol	Merck KG
Methanol	Merck KG
Milk powder, skimmed	ROTH GmbH
Non-immune antibody diluent solution	DCS Diagnostics
NaOH	Sigma Aldrich Chemie GmbH
Nitrocellulose membrane (Whatman BA83 Protran)	GE Healthcare

Oligomycin	Sigma Aldrich Chemie GmbH
peqGold Protein Marker V	Peqlab
Paraffin	Sigma Aldrich Chemie GmbH
pH stripes (range of 7.5 – 9.5)	Machery Nagel
Ponceau-S-Red	SIGMA-Aldrich Chemie GmbH
Protogel TM	National Diagnostics
Phenol / Chloroform (AM9720) (5:1 solution, pH 4.5, MB grade)	Sigma-Aldrich Chemie GmbH
Rotenone	Sigma Aldrich Chemie GmbH
R6k Screen Tape (5067-5367)	Agilent Technologies
Roti^{R} Block, 10x	ROTH GmbH
SDS	Serva Electrophoresis
Sucrose	Merck KG
Sudan Black B	Sigma Aldrich Chemie GmbH
TES	Sigma Aldrich Chemie GmbH
TEMED	GE Healthcare
Tris	Merck KG
Trypsin (T6567 – proteomics grade)	Sigma Aldrich Chemie GmbH
TFA	Sigma Aldrich Chemie GmbH
Water, distilled	Sigma Aldrich Chemie GmbH
Water, nuclease-free	Life technologies
W-Cap Citrate Buffer pH 6.0	Biooptica
Xylene	Sigma Aldrich Chemie GmbH

5.2 Instruments and lab wares

Brushes, sizes 2 to 12 (L242.1)	Roth GmbH
BIO-RAD criterion^{TM} Blotter	BioRad
Centrifuges	
- SpeedVac centrifuge RVC 2-18	CHRIST
- Ultracentrifuge Optima L70	Beckman
- Lab centrifuge 1-15 PK and 5424R	Sigma Aldrich and Eppendorf
Centrifuge tubes (15 ml and 50 ml)	BD Biosciences
Cell culture incubator (37°C)	Heraeus
Disposable plastic gel cassettes (1.5 mm)	Invitrogen
FluorChem® HD2 (chemiluminescent Imaging of immunoblots)	Alpha Innotech
Filter paper for immunoblotting	Biorad
Fluorescence microscope BZ-9000	Keyence
Glas douncer - loose and thight pestles	Wheaton

HM 355 S Rotationsmikrotom	Microm
LTQ-Orbitrap XL	Thermo Fisher
Nanodrop Spectrophotometer ND1000	PeqLap
Nano-HPLC Ultimate 3000	Dionex Softron GmbH
Nunc® CryoTubes® (1.8ml)	Sigma Aldrich Chemie GmbH
Petri dishes, cell culture grade	Greiner Labortechnik GmbH
pH-Meter, Lab850	Schott Instruments
Plate spectrophotometer infinite M200	Tecan
Shaker MS3 basic	IKA
Sonic bath S30H	Elma
StepONePlusTM Real-Time PCR System	Applied Biosystems
SuperFrost®Plus glass slides	Kobe Laborbedarf
Stereomicroscope – Model Stemi 1000	Zeiss
Seahorse XF96	Seahorse Bioscience
TapeStation, Lab901	Genomax technologies
Thermomixer compact	Eppendorf
Voltage source, PowerPac Basic	Biorad
Vacuum infiltration processor - V.I.P.5	Sacura

5.3 Animals

C57BL/6NCrl, female (strain code: 027)	Charles River, Germany
Crl:NMRI(Han), male (strain code: not available)	Charles River, Germany

Animals were bred at least 6 generations on the genetic background. C57BL/6NCrl and Crl:NMRI(Han) mice will be named in the following sections only with C57BL/6 and NMRI mice, respectively.

5.4 Buffers and solutions

All dilutions / solutions were made with distilled water if not otherwise mentioned. All reagents were in analytical quality.

Blocking buffer for immunoblotting
1x Roti^{R}-Block solution using 10x Roti^{R}-Block solution diluted in water

Blocking buffer for immunofluorescence

Goat serum	5 % in PBS (v/v)

Electrophoresis buffer

1x Rotiphorese^{R} solution from 10x Rotiphorese^{R} solution diluted in water

Laemlli buffer (4x)

Tris-HCl, pH 6.8	240 mM
SDS	10 %
Glycerine	40 %
Bromphenolblue	0.08 %
Beta-Mercaptoethanol	20 %

PBS buffer

NaCl	9 g
Water	up to 1000 ml

SDS-PAGE - Seperating gel (12 %)

Acrylamide / Bisacrylamide 30 %	3 ml
Tris-HCl (1.5 M), pH 8.8	2.5 ml
Water	4.35 ml
SDS (10 %)	100 µl
APS (10 %) (w/v)	50 µl
TEMED	5 µl

Stacking gel (4 %)

Acrylamide / Bisacrylamide 30%	0.5 ml
Tris-HCl (0.5 M), pH 6.8	1.26 ml
Water	3.18 ml
SDS (10 %)	50 µl
APS (10 %) (w/v)	25 µl
TEMED	5 µl

TBST (10 x)

Tris	4.24 g
Tris-HCl	26.0 g
NaCl	80.0 g
pH	7.5
Tween 20	10 ml
Water	up to 1 l

Ponceau solution (0.2 %) for immunoblotting

Ponceau-S	1 g
Acetic acid solution (5% in water)	25 ml
Water	500 ml

Towbin-Buffer

Tris	3.03 g
Glycine	14.4 g
Water	800 ml
Methanol	up to 1l

Fixing solution for colloidal Coomassie blue dye (10x)

Methanol	500 ml
Acetic acid	120 ml
Water	380 ml

Coomassie Blue dye staining solution

0.4 % Brilliant Blue R
1x Fixing solution for colloidal Coomasie blue dye

Isolation buffer for synaptosomes and mitochondria (IBS)

Sucrose (0.32 M)	109.5 g
Tris-HCl (10 mM)	1.58 g
EDTA-K (1 mM)	0.44 g
pH	7.4
water	filled up to 1 l

Ficoll solution (20 %)

Ficoll (20 %) (w/v)	20 g
Isolation buffer (IBS)	up to 100 ml

Formalin fixation solution

Concentrated Formalin, neutral buffered (7x)	100 ml
Water	600 ml

Fresh prepared
Stored at room temperature and light protected

PEI (polyethylenimine) solution

PEI	1:30000 (v/v) in water (three dilution steps)

Geltrex solution

Geltrex	1:100 (v/v) in Isolation buffer (IBS)

Assay buffer (SAS) for XF96 Seahorse

KCl	3.5 mM
NaCl	120 mM
$CaCl_2$	1.3 mM
KH_2PO_4	0.4 mM
Na_2SO_4	1.2 mM
D-Glucose	15 mM
Pyruvate	10 mM
BSA, fatty acid-free	0.4 % (w/v)
TES	10 mM
pH 7.4	

5.5 Kits

DAB chromogen system (GV82511)	Dako North American
ECL™ Advance Western-Blotting Detection Kit (RPN2232)	Amersham Biosciences
HistoMouse MAX Kit (87-9551)	Invitrogen Corporation
ICPL triplex kit (39231.01), ICPL quadruplex Kit (39232.01)	Serva Electrophoresis
mirVana™ miRNA isolation kit (AM1560)	Life Technologies
MoMap Kit (760-137)	Ventana
RT^2 Profiler PCR Arrays - PI3K-AKT Signalling Pathway (PAMM-058Z) - Synaptic Plasticity (PAMM-126Z) - Circadian Rhythms (PAMM-153Z)	Qiagen
RestoreTM Plus Western-Blot Stripping Buffer (46430)	Thermo Scientific
TaqMan MicroRNA Reverse Transcription Kit (4366596)	Life Technologies
TaqMan Univ. PCR Master Mix, No AmpErase UNG (4324020)	Life Technologies
Vector NovaRED Substrate Kit (SK-4800)	Vector Laboratories
QuantiTect Reverse Transcription Kit (205311)	Qiagen

5.6 Antibodies

Table 1 and Table 2 show the antibodies used for immunoblotting and immunohistochemistry / immunofluorescence with the appropriate secondary antibodies.

Table 1: Antibodies used for immunoblotting

Antigen	Source of primary antibody	Species of primary antibody	Dilution of primary antibody	Source of secondary antibody	Dilution of secondary antibody
β-Actin	Santa cruz (sc-1616)	goat - polyclonal	1 to 5000	donkey anti-goat IgG-HRP / Santa cruz (sc-2020)	1 to 40000
Arc	Abcam (ab118929)	rabbit - polyclonal	1 to 1000	goat anti-rabbit IgG-HRP / Santa cruz (sc-2004)	1 to 66667
Cdc42	Abcam (ab106374)	chicken - polyclonal	1 to 1000	goat anti-chicken IgG-HRP / Santa cruz (sc-2428)	1 to 40000
COX IV subunit IV	Mitosciences (MS407)	mouse - monoclonal	1 to 1000	goat anti-mouse IgG-HRP / Santa cruz (sc-2005)	1 to 40000
Cofilin	Cell signalling (3312)	rabbit - polyclonal	1 to 1000	goat anti-rabbit IgG-HRP / Santa cruz (sc-2004)	1 to 66667
CREB	Cell signalling (4820)	rabbit - monoclonal	1 to 1000	goat anti-rabbit IgG-HRP / Santa cruz (sc-2004)	1 to 66667
c-Fos	Santa cruz (sc-52)	rabbit - polyclonal	1 to 200	goat anti-rabbit IgG-HRP / Santa cruz (sc-2004)	1 to 66667
Fascin	Abcam (ab78487)	mouse - monoclonal	1 to 500	goat anti-mouseIgG-HRP / Santa cruz (sc-2005)	1 to 40000
GAPDH	Santa cruz (Sc-47724)	mouse - monoclonal	1 to 200	goat anti-mouse IgG-HRP / Santa cruz (sc-2005)	1 to 40000
LIMK1	Cell signalling (3842)	rabbit - polyclonal	1 to 1000	goat anti-rabbit IgG-HRP / santa cruz (sc-2004)	1 to 66667
LSD1	Cell signalling (2139)	rabbit - polyclonal	1 to 1000	goat anti-rabbit IgG-HRP / Santa cruz (sc-2004)	1 to 66667
Malondialdehyde (MDA)	Alpha diagnostic (MDA11-S)	rabbit - polyclonal	1 to 1000	goat anti-rabbit IgG-HRP / Santa cruz (sc-2004)	1 to 66667
phospho-CREB	Cell signalling (9191)	rabbit - polyclonal	1 to 200	goat anti-rabbit IgG-HRP / Santa cruz (sc-2004)	1 to 66667
phospho-IGF1Rβ/INSRβ	Cell signalling (3021)	rabbit - polyclonal	1 to 1000	goat anti-rabbit IgG-HRP / Santa cruz (sc-2004)	1 to 66667
phospho-RhoGDIα	Santa cruz (sc-33047)	rabbit - polyclonal	1 to 200	goat anti-rabbit IgG-HRP / Santa cruz (sc-2004)	1 to 66667
phospho-Cofilin	Cell signalling (3311)	rabbit - polyclonal	1 to 200	goat anti-rabbit IgG-HRP / Santa cruz (sc-2004)	1 to 66667
phospho-LIMK1/2	Santa cruz (sc-28409-R)	rabbit - polyclonal	1 to 200	goat anti-rabbit IgG-HRP / Santa cruz (sc-2004)	1 to 66667
phospho-PAK1/2	Cell signalling (2601)	rabbit - polyclonal	1 to 1000	goat anti-rabbit IgG-HRP / Santa cruz (sc-2004)	1 to 66667
PLP	Santa cruz (sc-98781)	rabbit - polyclonal	1 to 200	goat anti-rabbit IgG-HRP / Santa cruz (sc-2004)	1 to 66667
Rac1	Abcam (ab33186)	mouse - monoclonal	1 to 1000	goat anti-mouse IgG-HRP / Santa cruz (sc-2005)	1 to 40000
RhoGDIα	Epitomics (2751-1)	rabbit - monoclonal	1 to 1000	goat anti-rabbit IgG-HRP / Santa cruz (sc-2004)	1 to 66667
SNAP-25	Covance (SMI-81R)	mouse - monoclonal	1 to 5000	goat anti-mouse IgG-HRP / Santa cruz (sc-2005)	1 to 40000
TNFα	Cell signalling (3707)	rabbit - polyclonal	1 to 1000	goat anti-rabbit IgG-HRP / Santa cruz (sc-2004)	1 to 66667

Table 2: Antibodies used for immunohistochemistry and immunofluorescence

Antigen	Source of primary antibody	Species of primary antibody	Dilution of primary antibody	Source of secondary antibody	Dilution of secondary antibody
Ki67	Abcam (ab15580)	rabbit - polyclonal	1 to 1000	Goat Anti-Rabbit IgG, biotinylated (BA-1000 - Vector Laboratories) + avidin conjugated horseradish immunoperoxidase (43-4423 Life technologies) + DAB chromogen system	1 to 750
MAP-2	Abcam (ab32454)	rabbit - polyclonal	1 to 500	Cy™3-conjugated AffiniPure Fab Fragment Goat Anti-Rabbit IgG (H+L) / JacksonImmunoResearch (111-167-003)	1 to 100
NeuN	Millipore (MAB377)	mouse - monoclonal	1 to 10	soluble immune complex of biotinylated secondary and mouse primary antibody [MoMap Kit (760-137, Ventana)] + avidin conjugated horseradish immunoperoxidase (43-4423 Life technologies) + DAB chromogen system	1 to 1000
PSD-95	Abcam (ab18258)	rabbit - polyclonal	1 to 1000	Alexa fluor®488-conjugated AffiniPure Goat Anti-Rabbit IgG (H+L) / JacksonImmunoResearch (111-545-144)	1 to 100

5.7 Primers

The following primers (Life Technologies) for miRNA / mRNA quantification were used:

mmu-miR-132 (ID000457)
mmu-miR-134 (ID001186)
mmu-miR-212 (ID002551)
snoRNA135 (ID001239)
Tnfα (Mm00443260_g1)
Gapdh (Mm99999915_g1)
Mecp2 (Mm01193537_g1)
Limk1 (Mm01196310_m1)

5.8 Software and Databases

Adobe Photoshop CS	Adobe Inc.
TotalLab TL100	www.totallab.com
Ingenuity Pathway analysis software	http://www.ingenuity.com
PANTHER classification system	http://www.pantherdb.org
UniProt	http://www.uniprot.org
Proteome discoverer (version 1.3)	Thermo Fisher
MASCOT search engine (version 2.3.02)	Matrix Science
Ensembl mouse database (version: 2.4, 56416 sequences)	Ensembl

6 Methods

6.1 Irradiation of animals

a) NMRI mice

Experiments were carried out in accordance with the European Communitites Council Directive of 24 November 1986 (86/609/EEC), after approval from the local ethical committees (Uppsala University and the Agricultural Reseach Council) and by the Swedish Committee for Ethical Experiments on Laboratory Animals.

Male NMRI mice were total body irradiated on postnatal day 10 (PND 10) with a single exposure of gamma irradiation (^{60}Co, 0.025 Gy/min) at doses of 0 (sham), 0.02, 0.1, 0.5 and 1.0 Gy (Rudbeck Laboratory, Uppsala University). Dose verification was done with an ionisation chamber (Markus chamber type 23343, PTW-Freiburg) and was homogeneous within ± 3 % over the 10 cm dish area where mice were positioned during irradiation procedure. Neonates from each litter were irradiated at the same time. Three litters were used within each irradiation group to minimise litter effects. Irradiation of mice and dose verification was performed in Uppsala by S. Buratovic, P. Eriksson and B. Stenerlöw.

Mice were kept at Uppsala University until the age of 5 months and were sent then to Helmholtz Centre Munich, Germany where they received a routine treatment for intestinal parasites with Ivomac (Merial, 0.03 mg/mouse, over 1 week) (Baumans et al., 1988). At the age of 7 months, animals were sacrificed. Animals were kept at all times under standard housing conditions.

b) C57BL/6 mice

Experiments were carried out according to protocol number 139-12-30 approved by animal experiments committee dec-consult (EMCnr. 3018). Female C57BL/6 mice were total body irradiated on postnatal day 10 (PND10) with a single exposure to gamma irradiation (^{137}Cs, 0.082 Gy/min) at doses of 0 (sham), 0.1, 0.5 and 2.0 Gy

(Erasmus University Medical Center EDC [Erasmus Dierexperimenteel Centrum]). The radiation field was homogenous within ± 3 % as verified with a TLD-100 dosimeter. Three litters were used within each irradiation group to minimise litter effects. Irradiation of mice and dose verification was performed in Rotterdam by S. Sepe and P. Mastroberardino.
Animals were shipped to Helmholtz Centre Munich, Germany 1-2 weeks post-irradiation and were kept under standard housing conditions. 4-5 weeks post-irradiation and 6 months post-irradiation, mice were sacrificed.

6.2 Sacrifice of animals

Animals were sacrificed by $C0_2$ asphyxiation for immunohistochemistry and immunofluorescence or cervical dislocation for all other studies.

6.3 Tissue sampling for isolation of total protein and RNA content

The isolated brains were placed into ice-cold PBS, rinsed carefully and dissected using a stereomicroscope whilst being maintained on ice. Hippocampi and cortices without meninges were separately sampled from each hemisphere, gently rinsed in fresh ice-cold PBS and snap-frozen in liquid nitrogen for molecular studies and stored at -20°C until analysis. For the isolation of intact synaptosomes from hippocampi and cortices, samples were maintained chilled but not frozen until the final isolation procedure (~ 5 hours *ex vivo* until frozen).

a) Isolation and determination of total protein content

Frozen hippocampi / cortices were homogenised in 6 M guanidine hydrochloride (GnHCl) on ice using a manual plastic mortar. Homogenates were briefly vortexed (1 minute), sonicated and pelleted by centrifugation (20000xg, 1 hour, 4°C). The supernatants were collected and stored at -20°C before further use.

Total protein content was determined in the supernatants using Bradford assay (Bradford, 1976). The principle of this spectrophotometric method is based on an absorbance shift of the Coomassie Brilliant Blue G-250 dye from its red (470 nm) into its blue (595 nm) form under acidic conditions binding to proteins. The absorbance of the samples at 595 nm wavelength was measured against a bovine serum albumin (BSA) standard curve (concentrations of 0 (blank), 0.25, 0.5, 0.75, 1.0, 1.25, 1.5 and 2 mg / ml) dissolved in 1.2 M GnHCl. Volumes (5 µl) and GnHCl concentrations were kept equal in all standard curve and biological samples. Standard curve samples were measured in duplicate; biological samples in triplicate. After adding 200 µl Bradford reagent to standards and biological samples, the assay plate was incubated for 5 minutes at room temperature before spectrophotometric measurement at 595 nm. Finally, the protein concentration in the biological samples (mean of triplicate) was read via the standard curve constructed from the means of the standard curve samples.

b) Total RNA isolation and RNA purity / concentration determination

Total RNA from frozen hippocampi and cortices was extracted and purified by the mirVana^{TM} Isolation kit using the manufacturer´s instructions. The samples were homogenised by a manual plastic mortar in the kit manufacturer´s lysis buffer. After addition of 1 / 10 (v/v) manufacturer´s homogenate additive, the lysates were incubated for 30 minutes on ice. Subsequently, an equal volume of acid-phenol / chloroform mixture (5:1, pH 4.5) was added to the lysates at the same volume ratio, vortexed for 1 minute and centrifuged (10000xg, 10 minutes, room temperature). The aqueous upper phase containing total RNA was transferred to a new tube without disturbing the lower organic phase. After mixing this transferred solution with an equal volume of 100 % ethanol to precipitate the total RNA content, the solution was transferred to the kit manufacturer´s filter cartridges and centrifuged (10000xg, 20 seconds, room temperature). After discarding the flow-through, the filters were washed with 700 µl manufacturer´s wash solution 1 and centrifuged again (10000xg, 20 seconds, room temperature). The flow-through was again discarded and the filters were washed twice with 500 µl manufacturer´s wash solution 2/3 followed by

centrifugation (10000xg, 20 seconds, room temperature) and the discard of flow-throughs. Finally, the filter cartridges were transferred to a fresh tube and the bound RNA was eluted with 50 µl nuclease-free water (preheated to 95°C) using centrifugation (10000xg, 20 seconds, room temperature).

For both microRNA and mRNA expression studies the optical density (OD) ratio of 260/280 (260 nm: spectrophotometric absorbance of RNA; 280 nm: spectrophotometric absorbance of proteins) from total RNA lysates from the brain tissues was measured using a Nanodrop spectrophotometer. An OD ratio reflecting high RNA purity ranges between 2.0 and 2.1 whereas lower ratios indicate contamination with proteins. The obtained RNA integrity number (RIN) ranged between 8.6 to 9.0 measured with R6k Screen Tapes (Agilent Technologies) by the TapeStation device after manufacturer's instructions. Eluates were stored at -20°C until further analysis.

6.4 1D-SDS-PAGE gels – preparation and electrophoresis

Protein lysates were resolved on 1D-SDS-PAGE (1 dimensional sodium dodecyl sulfate-polyacrylamide gel electrophoresis) gels for mass spectrometry-based proteome analysis and immunoblotting of single proteins. This procedure enables the separation of proteins according to their molecular weight by denaturing and complex formation with SDS (Laemmli, 1970). SDS leads to a high negatively charged protein status regardless of original protein charge enabling the separation of proteins according to their molecular weight. Disposable plastic cassettes were used to cast the polyacrylamide gels. The separating gel solution (12 %) was prepared first as described under section 5.4. After casting, the separating gel was overlaid with isopropanol to exclude air and was incubated for 2 hours to allow polymerisation. Subsequently, the isopropanol was discarded and the gel surface was washed twice with water followed by gently blotting with filter paper. The stacking gel (4 %) was prepared as described under section 5.4 and poured on top of the separating gel. A 10 slot-plastic comb was carefully placed into the stacking gel without generating air bubbles. After 2 hours incubation for final polymerisation,

the gel cassettes were wrapped in wet tissue to prevent dehydration and stored at 4°C until used the next day. The combs were carefully removed and the wells rinsed with electrophoresis buffer. The gels were placed in an electrophoresis chamber and electrophoresis buffer added. Protein samples were incubated at 95°C for 15 minutes with Laemmli buffer as mentioned in section 5.4 at defined protein concentrations, samples were briefly centrifuged (1000xg, 30 seconds, room temperature) and transferred into the wells of the prepared gels. Each gel was run with a lane containing the protein ladder molecular weight marker (2 µl in Laemmli buffer) with the same volume as samples. A voltage of 90 V was used until the tracking dye reached the separating gel. Thereafter, the voltage was increased to 120 V until the tracking dye reached the bottom of the gel. Subsequently, the plastic cassettes were removed and the gels were processed for either mass spectrometry-based proteome analysis (see section 6.5) or for the immunoblotting of selected proteins (see section 6.7).

6.5 Mass spectrometry-based proteome analysis

a) Isotope coded protein label (ICPL) of proteins, 1D PAGE separation / Coomassie Blue staining

Protein extracts from hippocampi and cortices were labelled with ICPL reagent after manufacturer´s instructions (ICPL Triplex / Quadruplex Kit). The method is based on the recent experiences gained using an ICPL Duplex approach at the Institute of Radiation Biology, Helmholtz Centre Munich, Munich (Azimzadeh et al., 2013, Barjaktarovic et al., 2011). The proteomic ICPL workflow is illustrated in Figure 2. Briefly, individually protein lysates (50 µg in 20 µl of 6 M GnHCl from each cortex or hippocampus) were adjusted to a pH of 8.5 by the addition of HCl (2 M HCl, 0.5 µl, measured by pH stripes), followed by reduction with 0.5 µl manufacturer´s reduction solution of disulphide bonds (30 min at 60°C) and subsequent carbamidomethylation of sulfhydryl groups with 0.5 µl of manufacturer´s iodoacetamide solution.

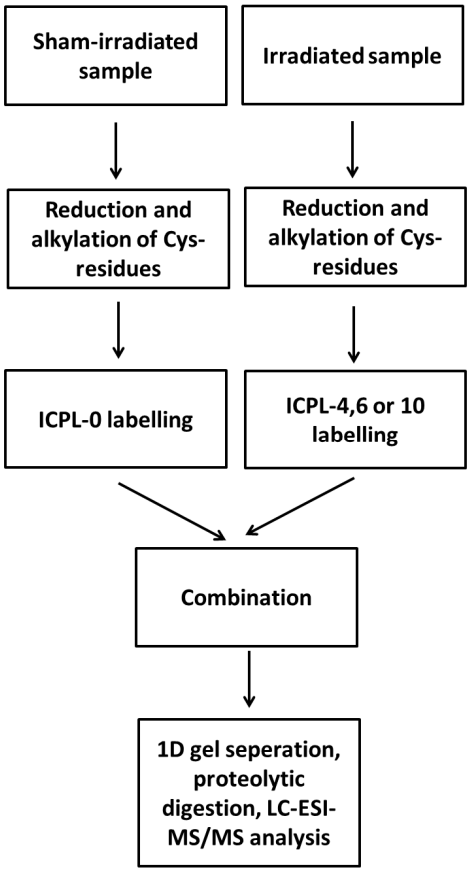

Figure 2: Schematic illustration of the ICPL proteomic approach work flow.
The protein samples from sham-irradiated and irradiated brain regions were reduced and alkylated before labelling with ICPL-0 (for sham-irradiated samples) or ICPL-4/6/10 (for irradiated samples) depending on the study design. Detailed information can be found in the text. Samples were mixed and further separated by 1D gel electrophoresis and tryptic digested. The peptides were analysed by LC-ESI-MS/MS.

The labelling with the respective ICPL-reagents (ICPL-0, ICPL-4, ICPL-6 or ICPL-10 leading to a mass shift of 0, 4, 6 or 10 kDa, respectively) was performed by incubating the reduced and carbamidomethylated protein mixture for 3 hours at 25°C as following: for studies with NMRI mice, sham-irradiated samples were labelled with ICPL-0, 0.02 Gy / 0.1 Gy exposed samples with ICPL-4 and 0.5 Gy / 1.0 Gy exposed samples with ICPL-6, respectively. For C57BL/6 mice studies, sham-irradiated samples were labelled with ICPL-0, 0.1 Gy / 0.5 Gy / 2.0 Gy exposed samples with ICPL-4 / ICPL-6 / ICPL-10, respectively. Subsequently, the labelled samples from each study were combined in the following order: sham - 0.02 Gy - 0.5 Gy and sham - 0.1 Gy - 1.0 Gy (NMRI mice study); sham – 0.1 Gy – 0.5 Gy – 2.0 Gy (C57BL/6 mice study). Afterwards, the pH of the combined solutions was raised to 12 by adding NaOH (2 M NaOH, 2 µl, measured by pH stripes). Samples were incubated

for 20 minutes to hydrolyse esters potentially generated during the labelling procedure. This step was followed by acidification by adding HCl (2 M HCl, 2 µl) to restore the original pH of 8.5 verified by pH stripes. Finally, the ICPL labelled proteins of the biological replicates were overnight precipitated with 80 % acetone in water at -20 °C.

The biological replicates included animals drawn from at least three different litters. ICPL-labelled precipitates were separated by 12 % SDS-polyacrylamide gel electrophoresis as described in section 6.4 followed by Coomassie Blue staining. The Coomassie dye molecules bind to proteins and form a dye-protein complex allowing the visualisation of major protein bands. Gels were fixed for 30 minutes in Fixing Solution (see section 5.4) followed by incubation in Coomassie Blue Dye Staining Solution (see section 5.4) overnight at 4°C. On the next day, the Coomassie-stained gels were destained with water until protein bands were clearly distinguishable against the gel background.

b) In-gel digestion

For in-gel digestion to prepare samples for mass spectrometry-based analysis, the individual gel lanes were excised and cut into six equal slices, destained and trypsinised overnight as described recently (Merl et al., 2012). In-gel digestion was done by S. Helm of the Protein Science Department, Helmholtz Centre Munich, Munich, Germany. Briefly, each gel slice was destained with 200 µl 60 % acetonitrile for 10 minutes, followed by a washing step with 200 µl water for 10 minutes. During this step, the gel pieces are dehydrated and hydrated again that removes the Coomassie staining dye; the gel pieces shrink and become white. This procedure of dehydration and hydration was repeated until the gel pieces were completely destained. Subsequently, the proteins were enzymatically digested within the gel slices by adding 20 µl trypsin (0.01 µg/µl diluted in 50 mM ammoniumbicarbonat solution) and incubated overnight at 37°C. On the next day, 2 µl of 0.5 % trifluoroacetic acid (TFA) was added to inactivate trypsin. The supernatant was collected and pooled with the eluates of repeated elution steps (2x) using 60 %

acetonitrile / 0.1 % TFA. The pooled peptide eluates were dried completely in a SpeedVac centrifuge and re-dissolved in 60 µl of 2 % acetonitrile / 0.5 % TFA in water by incubation for 30 minutes at room temperature under agitation. The peptide solutions were stored at -20°C until measurement via LC-MS/MS.

c) LC-MS/MS analysis

The LC-MS/MS runs were performed by S. Helm and C. von Toerne, Department of Protein Sciences, Helmholtz Centre Munich, Munich, Germany.

Before loading the peptide samples on the LC-MS/MS device, the samples were centrifuged for 5 minutes at 4°C. LC-MS/MS analysis was performed on a linear quadrupole ion trap (LTQ-Orbitrap XL - Thermo Fisher) equipped with a nano electrospray ionisation spray (ESI) source (von Toerne et al., 2013). Briefly, pre-fractionated samples were automatically injected and loaded onto the trap column (Acclaim PepMap100, C18, 5 µm, 100 Å pore size, 300 µm ID x 5 mm µ-Precolumn - No 160454 [Thermo Scientific]) of the liquid chromatography system. After 5 minutes, peptides were eluted and separated on the analytical column (Acclaim PepMap100, C18, 3 µm, 100 Å pore size, 75 µm ID x 15 cm, nanoViper - No 164568 [Thermo Scientific]) by reversed phase chromatography operated on a nano-HPLC (Ultimate 3000, Dionex) with a nonlinear 170 min gradient with the following gradients of acetonitrile in 0.1 % formic acid (FA) at a flow rate of 300 nl/min: 135 minutes of a 7% to 32% gradient and 10 minutes of a 32 % to 93 % acetonitrile gradient. Between each gradient, the acetonitrile in 0.1 % formic acid (FA) concentration was set back to starting conditions for 20 minutes. The mass spectrometer was operated in the data-dependent mode switching automatically between Orbitrap-MS and LTQ-MS/MS acquisition. Thus, from the MS pre-scan, the 10 most abundant peptide ions were selected for fragmentation in the linear ion trap if they exceeded an intensity of at least 200 counts and were at least doubly charged. During fragment analysis via collision-induced fragmentation, a high-resolution (60,000 full-width half maximum) MS spectrum was acquired in the

Orbitrap with a mass range of 300 to 1500 Da. Target peptides were dynamically excluded for 30 seconds if already selected for MS/MS.

d) Identification and quantification of proteins

MS/MS spectra were searched against the ENSEMBL mouse database via the MASCOT database with a mass error and fragment tolerance of 10 ppm and 0.6 Da, respectively, including not more than one missed cleavage. Fixed modifications were set to carbamidomethylation of cysteine and variable modifications to ICPL-0, ICPL-4 and ICPL-6, ICPL-10 for lysine (N-termini and side chain). Proteins were identified and quantified based on the ICPL pairs using the Proteome Discoverer software (Version 1.3 – Thermo Fisher). To ensure that only high-confident peptides were used for protein quantification, the MASCOT percolator algorithm was newly established. The percolator is an algorithm that improves the discrimination between correct and incorrect spectrum identifications and gives a q value sizing the statistical confidence assigned to each peptide-spectra-match (Brosch et al., 2009); the q value was set to 0.01 representing strict peptide ranking. Thus, only the best ranked peptides were used for quantification. Further, these peptides were filtered against a decoy database resulting in a false discovery rate (FDR) of each LC-MS-run; the significance threshold of FDR was set to 0.01 as well to ensure that only highly confident peptides were used for protein quantification. Proteins from each LC-MS-run were normalised against the median of all quantifiable proteins (minimum protein count: 20). Proteins were considered to be significantly deregulated if they fulfilled the following criteria: (i) identification by at least two unique peptides in n-1 biological replicates where n represents the number of biological replicates, (ii) quantification with an ICPL-4/ICPL-0, ICPL-6/ICPL-0, ICPL-10/ICPL-0 variability of ≤ 30 % in all biological replicates and (iii) a fold-change of ≥ 1.3 or ≤ -1.3. The threshold of ±1.3 was based on the average experimental technical variance of 13.8 % from the multiple analysis of hippocampal and cortical technical replicates during this work (Table 3).

Table 3: Evaluation of the experimental technical variance
Three technical replicates from cortex and hippocampus at 0 Gy, 0.02 Gy and 1.0 Gy (NMRI mouse study) were individually processed (ICPL labelling, 1D gel electrophoresis, tryptic digestion) and analysed via mass spectrometry under identical conditions. The technical variance was calculated from the median ICPL-variabilities of all quantifiable proteins from the three technical replicates. The samples were run under cyclic conditions meaning that each technical replicate from the samples was measured first followed by the others to access the technical variance from a long measuring time.

	Technical variance [%]	Average technical variance [%]
Cortex 0.02 Gy	12.7	13.8
Cortex 1.0 Gy	8.9	
Hippocampus 0.02 Gy	18.9	
Hippocampus 1.0 Gy	14.7	

Thus, a threshold of ±1.3 enabled a confident quantification of protein changes. Proteins showing borderline values for ICPL-value variability (30 %) and/or fold-change (±1.3) were manually scrutinised and were regarded as significantly deregulated if they fulfilled the following criteria: (i) MS/MS spectra showed a long, nearly complete y- and/or b-series without gaps in the ICPL-pairs, (ii) MS/MS signal intensities of the proteins were at least three times higher than the noise and (iii) at least one mass of an ICPL-modified lysine was included in the detected partial fragment series. Further, proteins regarded as significantly deregulated after fulfilling the first set of criteria were also manually investigated to prevent outliers and thus false-positive hits.

6.6 Bioinformatics analysis of protein classes and affected signalling pathways

Deregulated proteins were categorised into protein classes using PANTHER (Protein Analysis Through Evolutionary Relationships) classification system software (http://www.pantherdb.org) and the general annotation from UniProt (http://uniprot.org). The analyses of affected signalling pathways from all deregulated proteins were performed with the INGENUITY Pathway Analysis (IPA) (http://www.ingenuity.com) software tool that comprises curated information from databases of experimental and predictive origin, enabling discovery of highly represented functions and pathways from large quantitative data sets. To get

information about affected signalling pathways, deregulated proteins with their protein accession number and fold-changes were imported into the IPA core analysis and IPA comparison analysis. The IPA comparison analysis takes into account the signalling pathway rank according to the calculated p-value and reports it hierarchically. The software generates significance values (p-values) between each biological or molecular event and the imported proteins based on the Fischer´s exact test ($p \leq 0.05$).

6.7 Immunoblotting

Hippocampal and cortical protein extracts (15 µg) were separated on 12 % sodium dodecyl sulphate-polyacrylamide gel electrophoresis (SDS-PAGE) gels as described in section 6.4 and transferred to nitrocellulose membranes via a BIO-RAD criterion^{TM} Blotter at 100 V for 2 hours. The stacking gel was carefully peeled off from the separating gel and the separating gel, filter paper, nitrocellulose membrane and blotter foam pads were equilibrated in Towbin buffer for 15 min. Subsequently, the separating gel was laid on top of a nitrocellulose membrane and both were placed in the blotting apparatus between two stacks of filter paper with blotter foam pads on both sides. The proteins electrophoretically transferred onto the nitrocellulose membranes were stained with Ponceau-S for 5 minutes to evaluate protein transfer quality followed by washing with water to remove all dye. Membranes were blocked with Roti^{R}-Block solution for 1 hour to prevent non-specific binding of antibodies and incubated overnight at 4°C with primary antibodies diluted in Roti^{R}-Block solution as indicated in Table 1. On the next day, blots were washed for 3 x 15 minutes with 1x TBST for 15 minutes each and incubated with appropriate horseradish peroxidase-conjugated secondary antibody in 8 % milk made from skimmed milk powder diluted in 1x TBST for 1 h at room temperature. After a washing step (3 times with 1x TBST for 15 minutes each), blots were developed using the ECL system with a mixture of Luminogen A and Luminogen B (ratio 1:1) solutions and chemiluminescence was detected by an Alpha Innotech FluorChem HD2 device.

Nitrocellulose membranes were reused for primary antibodies that were derived from different species or if proteins of interest had different molecular weights. Thus,

membranes were stripped with Restore^{TM} PLUS Western Blot Stripping Buffer for 20 minutes at room temperature followed by a washing step (3 times with 1x TBST for 15 minutes each) and blocking in Roti^{R}-Block solution for 1 hour. Subsequently, membranes were incubated overnight at 4°C with primary antibody dilution suspended in Roti^{R}-Block solution. Further steps were identical to that described above.

GAPDH was not significantly deregulated either at the mRNA or protein level in any sample and was therefore used as the loading control. Proteins from each irradiated group were run on separate immunoblots with corresponding control samples under identical conditions on the same day. Immunoblots were only considered for quantification (TotalLab TL100 software – www.totallab.com) if the ratios between control samples and endogenous GAPDH did not differ than maximal 10 % after software-suggested background correction. Three biological replicates were used for statistical analysis (unpaired Student´s t-test) with a significance threshold of at least 0.05.

6.8 Quantification of malondialdehyde-tagged protein content

Detection of global lipid peroxidation was done by quantification of malondialdehyde-tagged proteins and immunoblotting. 50 µg of total protein were used following section 6.7. The immunoblot was performed with sham-irradiated samples and irradiated samples (hippocampus) or sham-irradiated samples and 1.0 Gy-irradiated samples (cortex) from all the different dose groups (n=4). Immunoblots were considered for quantification if (i) the pattern and Ponceau-S-stained intensity of lanes were equal on the blot and (ii) if the total lane intensity of malondialdehyde-tagged proteins was similar in the biological replicates. Statistical analysis was performed with unpaired Student´s t-test.

6.9 Gene expression analysis of pathway-focused genes

Hippocampal and cortical RNA isolates (100 ng) were used to quantify the expression of 84 mRNA´s related to synaptic plasticity, PI3K/Akt signalling pathway

and circadian rhythm using the RT^2 Profiler PCR array (Qiagen) detecting one single mRNA per well of a 96-well-plate. The assays were performed according to the manufacturer´s instructions and included genomic DNA elimination, first-strand cDNA synthesis, pre-amplification of cDNA target templates and real time PCR via RT^2 SYBR Green Mastermix on a StepOnePlus device as indicated in Table 4.

Table 4: Workflow of gene expression analysis via RT^2 Profiler PCR arrays

Quantification of mRNA via RT^2 profiler assay	
Genomic DNA elimation (5 minutes, 42°C)	
Component	**Volume / reaction**
Genomic Elemination Buffer	2 µl
RNA	100 ng in 8 µl nuclease-free water
Reverse-ranscription (RT) reaction (15 minutes, 42°C; 5 minutes, 95°C)	
Component	**Volume / reaction**
5x Buffer BC3	4 µl
Control P2	1 µl
RE3 Reverse Transcriptase Mix	2 µl
nuclease-free water	3 µl
RNA, genomic DNA eliminated	10 µl
Preamplification (10 minutes, 95°C; 12 cylces [15 seconds, 95°C; 2minutes; 60°C])	
Component	**Volume / reaction**
RT^2 PreAmp PCR Mastermix	12.5 µl
RT^2 PreAmp Pathway Primer Mix	7.5 µl
c-DNA	5 µl
Side reduction (15 minutes, 37°C; 5 minutes; 95°C)	
Component	**Volume / reaction**
Side Reaction Reducer	2 µl
c-DNA, preamplified	25 µl
Preparation of solution 1	
Component	**Volume**
RT^2 SYBR Green Mastermix	1275 µl
c-DNA, preamplified and side-reduced	27 µl
nuclease-free water	1458 µl
Quantitative RT-PCR reaction (10 minutes, 95°C; 40 cycles including cycling stage and melt curve stage [15 seconds, 95°C; 1 minute, 60°C; 15 seconds; 95°C; 1 minute, 60°C; 15 seconds; 95°C])	
Component	**Volume / well**
Solution 1	25 µl

Corresponding controls on each assay plate showed no detectable genomic DNA contamination. The relative expression of each mRNA was normalised against the median of all 84 target mRNA´s on the same assay plate using the equation $2^{-\Delta\Delta Ct}$, where $\Delta\Delta Ct = \Delta Ct_{irradiated} - \Delta Ct_{sham}$ and $\Delta Ct = Ct_{target\text{-}mRNA} - Ct_{median\text{-}of\text{-}84\text{-}target\text{-}genes}$. The Ct-value is the number of cycles which are required for crossing the fluorescence signal against a significant cycle threshold (Ct) within the exponential phase of the quantitative polymerase chain reaction (qPCR) reaction. The Ct-value is inversely proportional to the amount of the target mRNA in the original sample. Only Ct-values ≤ 32 were used for quantification. Three biological replicates from three different litters were used within each group. Gene expression changes were considered significant if they reached a p-value of ≤ 0.05 and if they had a fold-change of ≥ 1.2 or ≤ -1.2. This threshold of ±1.2 fold-change was based on the average experimental technical variance (8.4 %) and biological variance (6.9 %) of a set of 14 overlapping target mRNAs (Table 5).

Table 5: Evaluation of technical and biological variance of RT² profiler arrays used for mRNA expression analysis
14 mRNAs overlapped between the "PI3K/Akt pathway" and "synaptic plasticity" RT² profiler arrays (*Akt1, c-Fos, Igf1, Jun, Mapk1, Nfkb1, Prkca, Rheb, Srf, Gusb, Hprt, Hsp90ab1, Gapdh* and *Actb*). The corresponding technical replicates from in total 3 biological replicates employed for the two different sets of arrays were used to calculate the median technical variance, mean technical variance and finally the average technical variance (8.4 %). For this purpose, the same c-DNA from 3 biological replicates was used. The biological variance was calculated from the standard deviation of the fold-changes obtained from the three biological replicates in the two different sets of arrays giving the total variance of 15.3 %. Thus, the biological variance can be calculated with 6.9 %.

Calculation of technical variance	Median replicate 1	Median replicate 2	Median replicate 3	Mean technical variance	Average technical variance [%]
cortex 0.5 Gy	0.17	0.05	0.14	0.12	8.4
hippocampus 0.5 Gy	0.12	0.09	0.04	0.09	
hippocampus 1.0Gy	0.09	0.07	0.06	0.08	
cortex 1.0 Gy	0.03	0.03	0.09	0.05	
Calculation of biological variance	**Median**				**Average biological variance [%]**
cortex 0.5 Gy	0.08				6.9
hippocampus 0.5 Gy	0.06				
hippocampus 1.0Gy	0.07				
cortex 1.0 Gy	0.07				

Thus, a threshold of ±1.2 enables confident identification of changes in the gene expression analysis as it overcomes the sum of both technical and biological variance (±1.20 * [8.4 + 6.9] / 100 = ±0.19; 1.20 - 0.19 = 1.01; -1.20 + 0.19 = -1.01). Data from overlapping gene targets arising from the use of different RT^2 profiler arrays were only regarded being significantly deregulated if (i) they were consistently up- or down-regulated and significantly changed and (ii) they had overlapping confidence intervals.

6.10 Analysis of individual mRNA expression

Total hippocampal and cortical RNA isolates (10 ng) were used to quantify the expression of individual mRNA´s using the QuantiTect Reverse Transcription Kit following manufacturer´s protocol. Briefly, steps included a genomic DNA, reverse transcription and real-time PCR (StepOnePlus device) via TaqMan Universal PCR Master Mix and Taqman-primers (mentioned in section 5.7) according to Table 6. Potential contamination with genomic DNA was verified using same conditions without reverse transcriptase but nuclease-free water; genomic DNA was not detectable in any samples.

Table 6: Workflow of mRNA quantification

Quantification of mRNA	
Genomic DNA elimation (10 minutes, 42°C)	
Component	**Volume / reaction**
genomic DNA Wipeout Buffer, 7x	2 µl
RNA	10 ng in 12 µl nuclease-free water
Reverse-ranscription (RT) reaction (30 minutes, 42°C; 3 minutes, 95°C)	
Component	**Volume / reaction**
RT-master mix "Quantiscript Reverse Transcriptase"	1 µl
Quantiscript RT Buffer, 5x	4 µl
RT Primer Mix	1 µl
RNA, genomic DNA eliminated	14 µl
Quantitative RT-PCR reaction (40 cycles [2 minutes, 16°C; 1 minute, 42°C; 1 minute, 50°C), 1 cylce [5 minutes, 85°C])	
Component	**Volume / reaction**
Master mix	5 µl
nuclease-free water	2.5 µl
primer of interest	0.5 µl
c-DNA	2 µl

Expression of mRNA were calculated based on the $2^{-\Delta\Delta Ct}$ method, where $\Delta\Delta Ct = \Delta Ct_{irradiated} - \Delta Ct_{sham}$ and $\Delta Ct = Ct_{target\text{-}mRNA} - Ct_{\textit{Gapdh}}$. Normalisation of mRNA data was performed against endogenous *Gapdh*. Changes were considered significance if they reached a p-value of ≤ 0.05 (unpaired Student´s t-test, n=3).

6.11 Analysis of miRNA expression

Total hippocampal and cortical RNA isolates (10 ng) were used to quantify miRNA´s using TaqMan MicroRNA Reverse Transcription Kit following manufacturer´s protocol. Briefly, steps included reverse transcription and real-time PCR

(StepOnePlus device) via TaqMan Universal PCR Master Mix and Taqman-primers (mentioned in section 5.7) according to Table 7.

Table 7: Workflow of miRNA quantification

Quantification of miRNA	
Reverse-ranscription (RT) reaction (30 minutes, 16°C; 30 minutes, 42°C, 5 minutes 85°C)	
Component	**Volume / reaction**
dNTPs	0.15 µl
10x buffer	1.5 µl
Reverse transcriptase	0.5 µl
RNAse inhibitor	0.19 µl
nuclease-free water	9.16 µl
RNA (5ng/µl dilution)	2 µl
primer of interest	1.5 µl
Quantitative RT-PCR reaction	
Component	**Volume / reaction**
Master mix	5 µl
nuclease-free water	2.5 µl
primer of interest	0.5 µl
c-DNA	2 µl

Expression of miRNA were calculated based on the $2^{-\Delta\Delta Ct}$ method, where $\Delta\Delta Ct = \Delta Ct_{irradiated} - \Delta Ct_{sham}$ and $\Delta Ct = Ct_{target\text{-}miRNA} - Ct_{snoRNA135}$. Normalisation of miRNA data was performed against endogenous snoRNA135 as used recently by Shaltiel et al. for quantification of hippocampal miRNA´s (Shaltiel et al., 2013). Changes were considered significant if they reached a p-value of ≤ 0.05 (unpaired Student´s t-test, n=3).

6.12 Immunohistochemistry

The procedure of formalin fixation and paraffin embedding, sections cutting, drying and rehydration / dewaxing and immunohistochemistry was performed with technical support by J. Mueller and D. Janik, Institute of Pathology, Helmholtz Centre Munich, Munich, Germany.

a) Formalin fixation and paraffin embedding

The isolated brains were removed and immediately transferred to formalin fixation solution (at least 7x tissue volume of 3.7 % neutral buffered formalin) and kept for 2 - 3 days light protected at room temperature. Formalin crosslinks proteins and inactivates tissue, stops proteolysis and stabilises the tissue for the following dehydration and paraffination process. After formalin fixation, brains were washed with water for 1 hour and samples were transferred to dehydration (Vacuum infiltration processor - V.I.P.5 – Sacura) as indicated in Table 8. Subsequently, dehydrated formalin-fixed samples were embedded in paraffin using plastic containers and stored at room temperature until section cutting.

Table 8: Dehydration conditions of formalin-fixed tissue.
After each incubation with the reagent, the solution was aspirated and incubated with the next one

reagent	time [h]
ethanol 70%	1
ethanol 70%	1
ethanol 80%	1
ethanol 96%	2
ethanol 96%	2
ethanol 100%	1
ethanol 100%	2
ethanol 100%	2
xylene	1
xylene	2
paraffin (60°C)	1
paraffin (60°C)	1
paraffin (60°C)	1
paraffin (60°C)	1

b) Sections cutting, drying and rehydration / dewaxing

1 µm-thick sections were cut from paraffin-embedded samples using a microtome. The sections were laid into a warm water bath for complete unfolding of the cut sections followed by capture of the sections onto glass slides. After a short drying of the glass slides in air, the slides were put into a rack and stored at 60°C in an incubator overnight to melt the paraffin from the sections and to prevent

displacement of the brain sections from the glass slides during subsequent rehydration / dewaxing procedure as shown in Table 9.

Table 9: Rehydration conditions of formalin-fixed paraffin embedded tissue sections on glass slides.
After each incubation with the reagent, the solution was dripped off and incubated with the next one

reagent	time [min]
xylene	15
xylene	15
ethanol 96%	5
ethanol 96%	5
ethanol 70%	5
ethanol 70%	5
water	2
water	2

c) Immunohistochemistry analysis of adult neurogenesis markers

After rehydration / dewaxing, the samples were heated in W-Cap Citrate Buffer pH 6.0 for heat-induced epitope retrieval (microwave: 450 W for 30 minutes, steamed-pressure) followed by quenching of endogenous peroxidase by incubation with 3 % H_2O_2 in methanol (30 minutes at room temperature). Brain sections were incubated overnight with a soluble immune complex of mouse primary antibody against NeuN + biotinylated anti-mouse secondary antibody or with rabbit primary antibody against Ki67 followed by incubation with biotinylated anti-rabbit secondary antibody as shown in Table 2. The slides were incubated with avidin-conjugated horseradish immunoperoxidase and were visualised with diaminobenzidine (DAB) according to the manufacturer´s instructions. Semi-quantitative analysis of labelling was performed on single sections. The number of positive cells for Ki67 in the subgranular zone (SGZ) was determined and expressed per μm^2 of dentate gyrus (DG). To assess the neuronal density in the granule cell layer of the DG, immunohistochemical staining for NeuN was performed. Counting was carried out in a rectangular field of 4000 μm^2 in the suprapyramidal (SB) and infrapyramidal blade (IB) and in the crest area (CR) of the DG. Cells touching the upper and left limits of

the field where counted, whereas cells touching the lower and right limits where not taken into account. The number of positive cells in any of the areas was recorded separately and the mean from the three regions of each biological replicate was used for statistical analysis.

All images were analysed using identical software settings. Statistical analysis (Student´s t-test, unpaired) was performed with three biological replicates for stainings with Ki67 and at least three biological replicates for NeuN stainings. Differences were considered to be significant when p-values were ≤0.05.

6.13 Immunofluorescence

The method of sequential immunofluorescence as described here is a newly established method in the laboratory.

Steps as mentioned in 6.12 a) and b) were identical for immunofluorescence. If not otherwise mentioned, all incubation steps were performed in a humid chamber in the dark. After rehydration / dewaxing, the tissue sections were heated in W-Cap Citrate Buffer pH 6.0 (microwave: 450 W for 30 minutes, steamed-pressure) and washed with PBS (3x). Auto-fluorescence was blocked with Sudan Black B solution (0.1 % in 70% ethanol [w/v]) (20 minutes, RT) followed by PBS washing (3x). After a goat serum block with 100 µl (5 % in PBS, 30 minutes, RT – 0005-000-121, JacksonimmunoResearch), slides were incubated with 100 µl MAP-2 primary antibody solution overnight (4°C) followed by 100 µl Cy3-Fab-fragment IgG secondary antibody for 1 hour (4°C). After washing with PBS (3x), the same slides were incubated with a 100 µl PSD-95 primary antibody overnight (4°C) followed by 100 µl Alexa-Fluor IgG secondary antibody for 1 hour (4°C, in dark of a humid chamber) (Figure 3).

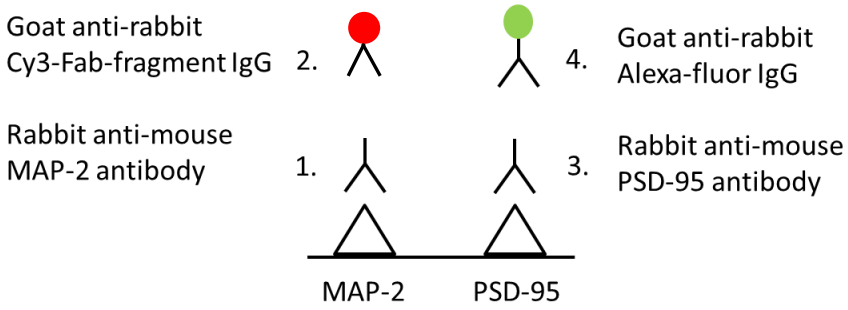

Figure 3: Workflow of sequential immunofluorescence of MAP-2 and PSD95 proteins.
The workflow consisted of incubation with rabbit anti-mouse MAP-2 antibody (1.) followed by a washing step and incubation with secondary Cy3-labelled antibody (2.). After a washing step, rabbit anti-mouse PSD-95 antibody was incubated (3.) followed by a washing step and secondary Alexa-fluor-labelled antibody incubation (4.)

Slides were nuclear stained with Hoechst 33258 (1:1000 in PBS [v/v]) and were afterwards mounted with antifade fluorescence mounting medium. Sample processing and analysis was done under identical conditions on the same day using a fluorescence microscope. Each fluorescent label was excited and recorded separately with only single channels and were afterwards merged with the software. All images were analysed using identical software settings. The MAP-2 / PSD-95 intensity in the hippocampus and dentate gyrus was normalised against the Hoechst intensity within this region. Three biological replicates were used for all cases. Statistical significance was calculated with unpaired Student´s t-test and a p-value of ≤0.05.

As both primary antibodies were raised in the same species leading to the use of same species-dependent secondary antibodies for detection, it was necessary to evaluate the different possible combinations of negative controls of the antibodies as used during this workflow (Figure 3). Figure 4 represents the associated results using the same biological sample from serial cuts.

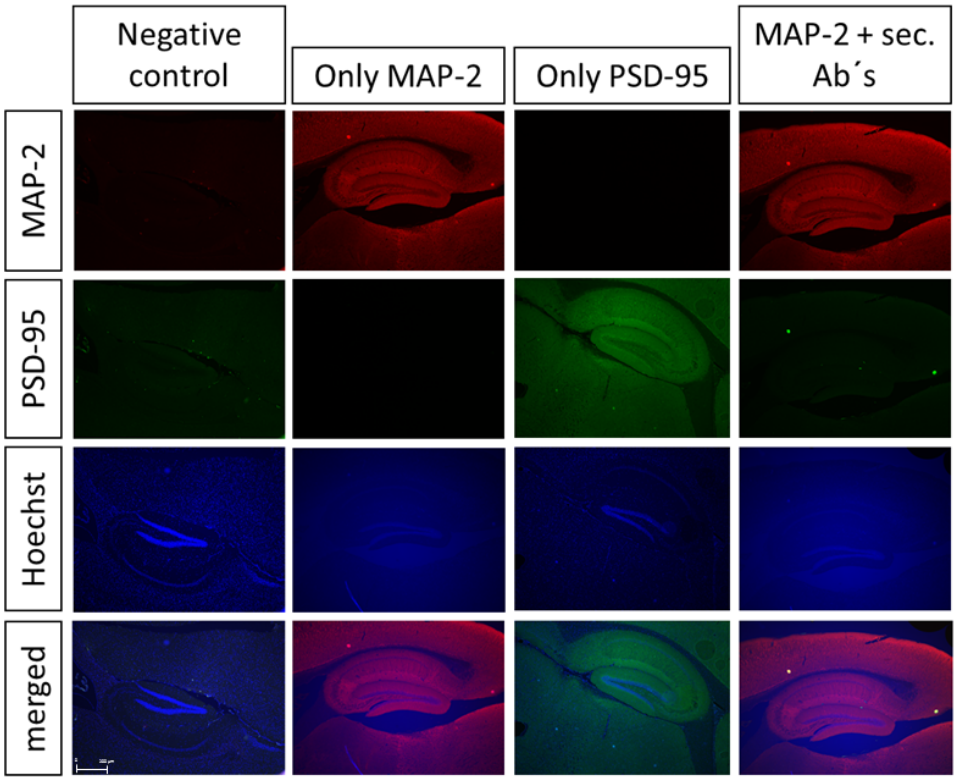

Figure 4: Images of sequential immunofluorescence from hippocampus to evaluate the different aspects of negative controls of used antibodies.

"Negative control" – only secondary antibodies and Hoechst; "only MAP-2" – primary antibody against MAP-2, Cy3-Fab-fragment IgG secondary antibody, Hoechst; "only PSD-95" – primary antibody against PSD-95, Alexa-fluor IgG secondary antibody, Hoechst; "MAP-2 + sec. Ab´s" – primary antibody against MAP-2, Cy3-Fab-fragment IgG secondary antibody, Alexa-fluor IgG secondary antibody, Hoechst. Images indicate specific binding of secondary antibodies ("negative control"), binding sites of primary MAP-2 antibody are saturated via Cy3-Fab-fragment IgG ("MAP-2 + sec. Ab´s") and sequential immunofluorescence is also working on single protein detection ("Only MAP-2" and "Only PSD-95"). Each fluorescent label was excited and recorded separately with only single channels and were afterwards merged with the software

First, only the secondary antibodies ("negative control") were added on the glass slides (step 2, incubation and washing, step 4, incubation and washing, Hoechst – [Figure 3]). The images show that the primary antibodies were necessary for efficient binding of the secondary antibodies (Figure 4 – negative control). Next, it was tested if the binding sites from the primary MAP-2 antibody were saturated from the Cy3-Fab-fragment preventing false-positive results from additional Alexa-fluor IgG binding to this complex. The images ("MAP-2 + sec. antibodies") indicated that the binding sites from the primary antibody against MAP-2 were saturated (Figure 4) (step 1, incubation and washing, step 2, incubation and washing, step 4, incubation and

washing, Hoechst – [Figure 3]); the observable PSD-95 signal (green dots) was based on artefacts due to tissue folding as manually investigated under phase contrast microscopy. Taken together, the sequential immunofluorescence procedure detected only one epitope at each glass slide. The images (“Only MAP-2” [step 1, incubation and washing, step 2, incubation and washing, Hoechst] and “Only PSD-95” [step 3, incubation and washing, step 4, incubation and washing, Hoechst] (Figure 4) showed that (i) immunofluorescence-based detection of MAP-2 and PSD-95 worked also separately and (ii) signal intensity of MAP-2 from “Only MAP-2”-approach and “MAP-2 + sec. Ab´s” were comparable (Figure 4).

Thus, the workflow of sequential immunofluorescence as depicted in Figure 3 was specific for the sequential quantification of the MAP-2 and PSD-95 proteins and provides a confident evaluation of the synaptic proteins MAP-2 and PSD-95 in the hippocampus.

6.14 Isolation and enrichment of synaptosomes and non-synaptosomal mitochondria

The method to isolate / enrich synaptosomes and non-synaptosomal mitochondria was established in the laboratory using the protocol of Kiebish et al. (Kiebish et al., 2008) with slight modifications. Briefly, isolated brain tissues were transferred to a precooled glass douncer tissue grinder. Tissues were homogenised in isolation buffer (IBS) using 8 strokes with a “loose” and 8 strokes with a “tight” pestle. All steps were done on ice. The homogenates were centrifuged (4°C, 1000xg, 5 minutes) and the supernatant containing synaptosomes / non-synaptosomal mitochondria was collected. The residual pellet was resuspended and washed twice with IBS by centrifugation (4°C, 1000xg, 5 minutes). Each time the supernatants were collected. Subsequently, the pooled supernatants were centrifuged again (4°C, 1000xg, 5 minutes) and the supernatants were transferred to fresh tubes. The supernatants were centrifuged (4°C, 14000xg, 15 minutes) to pellet non-synaptosomal mitochondria / synaptosomes. The supernatants were discarded and the pellets were resuspended in 3 ml ice-cold IBS and layered on a 12 % / 7.5 %

discontinuous Ficoll gradient (4 °C). The gradient was ultracentrifuged (4°C, 73000xg, 36 minutes). The interfaces with myelin and synaptosomes and the pellet of non-synaptosomal mitochondria are depicted in Figure 5.

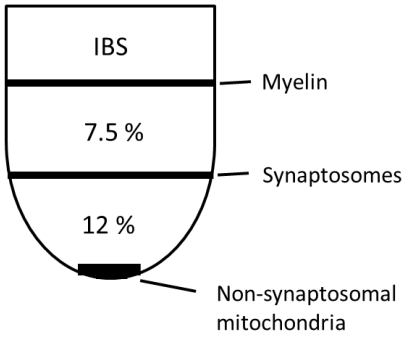

Figure 5: The gradient consists of a 12% / 7.5% / IBS containing brain homogenates to isolate synaptosomes and non-synaptosomal mitochondria.

The myelin fraction was gently taken off to avoid contamination of the other fractions and discarded whereas the synaptosomes layer was transferred to fresh tubes and resuspended in IBS (1:3, v/v, final volume 2 ml). Next, the non-synaptosomal mitochondria were collected as a pellet and gently resuspended using a fine brush in IBS to a final volume of 2 ml. The synaptosomes / non-synaptosomal mitochondria fractions were pelleted by centrifugation (4°C, 16000xg, 15 minutes) and the pellets washed with IBS containing 0.5 mg/ml bovine serum albumin [(BSA), fatty-acid free]. Subsequently, the samples were centrifuged again (4°C, 16000xg, 15 minutes) and washed with IBS. Finally, synaptosomes / non-synaptosomal mitochondria were pelleted by centrifugation (4°C, 16000xg, 15 minutes), supernatants discarded and pellets frozen (-20°C) until further analysis (proteomics of synaptosomes) or stored on ice (measurement of mitochondrial respiration in synaptosomes) immediately after isolation.

The following section describes two approaches used for the evaluation of the synaptosomes intactness (mitochondrial respiration) and enrichment / purity quality (immunoblotting) including the associated results.

6.15 Evaluation of synaptosomes intactness and enrichment quality

a) Mitochondrial respiration from non-irradiated synaptosomes

Evaluation of the intactness of mitochondria within the synaptosome fraction (see section 6.14) was first investigated using mitochondrial respiration measurement (Seahorse XF96 analyzer, Seahorse Bioscience) from non-irradiated test animals. As mitochondria are highly sensitive to changes to osmolarity or mechanical / shear forces leading to disruption of both the mitochondrial potential and the mitochondria themselves, mitochondrial respiration capacity is a good marker to measure mitochondrial intactness within synaptosomes.

Mitochondrial respiration was performed under technical assistance by M. Kutschke and M. Jastroch (Institute for Diabetes and Obesity, Division of Mitochondrial Biology, Helmholtz Centre Munich, Munich, Germany).

Synaptosome preparation for mitochondrial respiration measurement was newly established based on a protocol of Choi et al. (Choi et al., 2011) with slight modifications. Briefly, one calibration and one sample plate were coated before use with PEI polymer solution (100 µl/well) at room temperature overnight to avoid effects from the plastic plate surface on the synaptosomes. On the next day, both PEI-coated plates were washed with isolation buffer and were incubated with Geltrex suspension (100 µl) for 1 hour at 37°C enabling synaptosome attachment to the bottom of the plate where mitochondrial measurement took place. Isolated synaptosomes corresponding to 10 µg of total protein (measured via Bradford assay as described above) were diluted with SAS to 200 µl and transferred to the sample plate by centrifugation (200xg, 20 minutes at 4°C). 200 µl of manufacturer´s Calibrant was added to each well of the calibration plate. Before measuring the sample plate with synaptosomes, the calibration plate was measured and the ports were loaded and time-dependently injected following Table 10. After calibration, the sample plate was incubated at 37°C for 10 minutes and transferred to the XF96 Analyzer for measurement under identical conditions as the calibration plate (Table 10).

Table 10: Scheme of port loading with compounds for mitochondrial respiration measurement of synaptosomes and the XF protocol.
The compounds were prepared as 10x stocks in DMSO.

Compound	Port	Concentration in port (10x)	final concentration	Inected volume
ADP	A	40 mM	4 mM	20
Oligomycin	B	40 µg / ml	4 µg/ml	22
FCCP	C	40 µM	4 µM	25
Rotenone	D	20 µM	2 µM	30
Antimycin A		20 µM	2 µM	

Command	Time [min]
Calibrate	
Measure	3.0
Mix	1.0
Measure	3.0
Mix	1.0
Inject Port A	
Mix	1.0
Measure	3.0
Mix	1.0
Measure	3.0
Mix	1.0
Inject Port B	
Mix	1.0
Measure	3.0
Mix	1.0
Inject Port C	
Mix	1.0
Measure	3.0
Mix	1.0
Inject Port D	
Mix	1.0
Measure	3.0

Results showed that the mitochondria within synaptosomes responded qualitatively to the added chemicals by altering their oxygen consumption rate in a manner that is typical for intact respiring mitochondria (Figure 6). It is noteworthy that the maximal respiration was not higher than the expected basal respiration. Although the addition of FCCP led to an increase in the oxygen consumption rate, the FCCP concentration has to be increased in further experiments until the maximal oxygen consumption rate can be determined to get quantitative information.

Overall, the method can be used to isolate intact and respiratory-active mitochondria from synaptosomes.

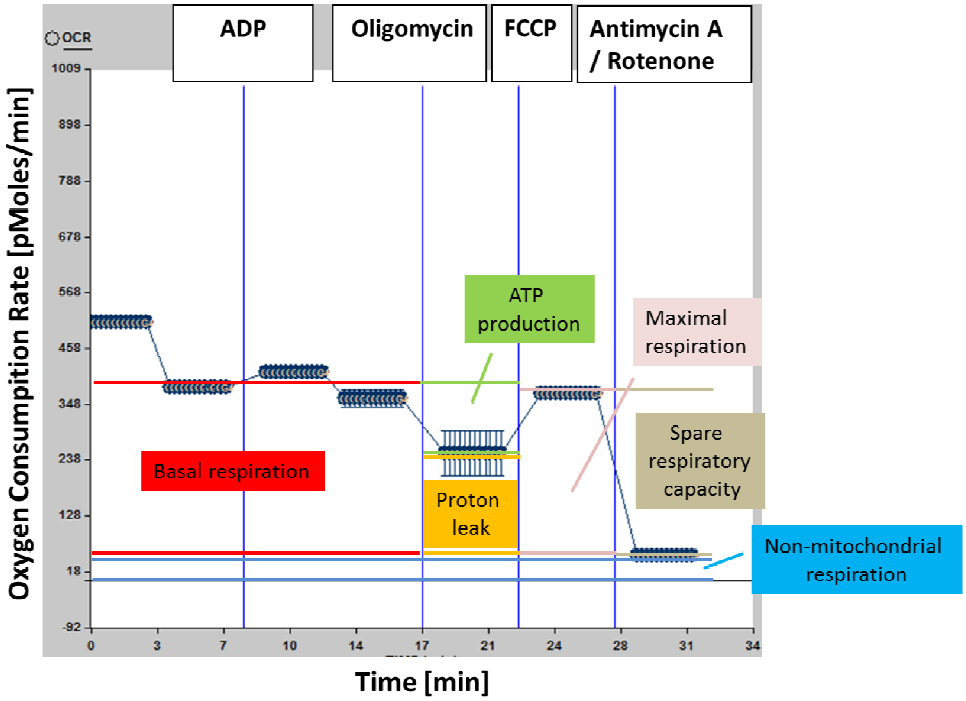

Figure 6: Mitochondrial respiration using 10 µg of synaptosomal mitochondria from non-irradiated mice hippocampi.
The added chemical substances are shown. The graph shows the mean with standard deviation from two technical replicates. OCR: Oxygen Consumption Rate; FCCP: Carbonyl cyanide-4-(trifluoromethoxy)phenylhydrazone); ADP: Adenosine diphosphate. Mitochondria have a basal respiration capacity (red). Addition of oligomycin which inhibits ATP synthase leads to reduction in the electron flow through the electron transport chain. However, the electron flow is not completely inhibited as protons diffuse into the mitochondrial matrix via e.g. uncoupling proteins (UCPs), thus, ATP production (green) and proton leakage (orange) can be calculated. Addition of the ionophore FCCP [Carbonyl cyanide-4-(trifluoromethoxy)phenylhydrazone] inhibits oxidative phosphorylation and leads to maximal mitochondrial respiration rate (pink). Addition of Antimycin A / Rotenone inhibits Complex III leading to inhibition of oxygen consumption via Complex IV and the synthesis of ATP in Complex V which gives information about the spare respiratory capacity (olive). Non-mitochondrial respiration (blue) is characterised as the area between no oxygen consumption and spare respiratory capacity.

b) Verification of the synaptosomes enrichment by immunoblotting

To evaluate the quality of synaptosome enrichment, subcellular fractions during the isolation workflow were analysed by immunoblotting with protein markers of inner

mitochondria membrane (Complex IV, subunit IV), nucleus (LSD1 - lysine-specific demethylase 1), myelin sheath (PLP - proteolipid protein), synaptosomal membrane (SNAP25 - Synaptosomal-associated protein 25) and cytoskeleton (β-actin) (see Table 1) using non-irradiated animals.

Results are depicted in Figure 7 indicating that, based on the synaptosomal marker SNAP25, synaptosomes were enriched more than 2.5 fold (fraction f) compared to total homogenate (a) and were separated from the non-synaptosomal mitochondria (fraction e).

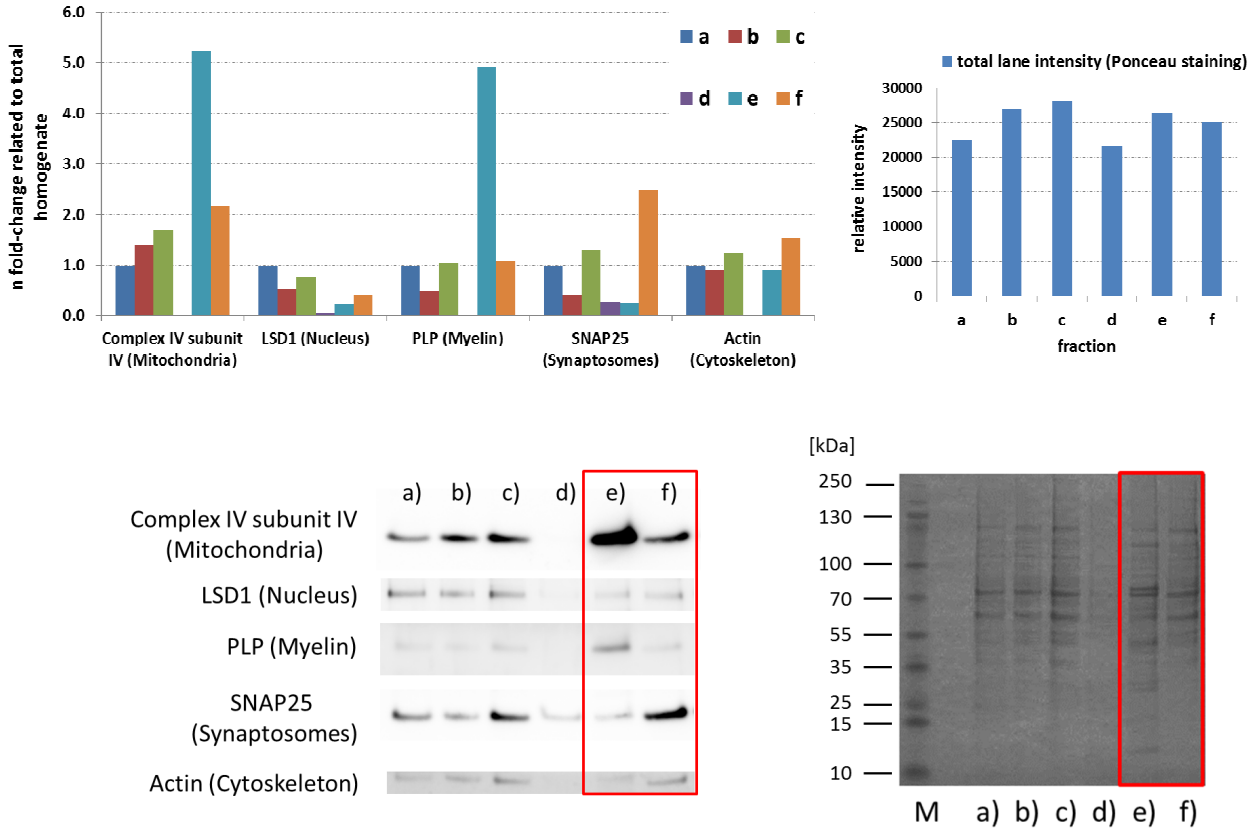

Figure 7: Distribution of protein markers in subcellular fractions from mouse hippocampus using immunoblotting for characterisation of synaptosome enrichment.

Subcellular fractions included total homogenate (a), supernatant with non-synaptosomal mitochondria and synaptosomes after low spin centrifugation (b), crude non-synaptosomal mitochondria and synaptosomes pellet after high spin centrifugation (c), myelin fraction from Ficoll gradient (d), non-synaptosomal mitochondria from Ficoll gradient (e) and synaptosomes from Ficoll gradient (f); the workflow with its subcellular fractions is depicted in Figure 41 (Supplementary information). Western blots were performed to determine the distribution of specific protein markers for the inner mitochondria membrane (Complex IV, subunit IV), nucleus (LSD1 – lysine-specific demethylase 1), myelin (PLP - proteolipid protein), synaptosomal membrane (SNAP25 - Synaptosomal-associated protein 25) and cytoskeleton (β-actin). All lanes correspond to 10 µg protein lysate, originating from a pool of three hippocampi from control mice. M: protein marker. Ponceau staining was used to normalise the level of protein of interest against the total Ponceau-stained lane of each loaded fraction. As data correspond to one technical experiment, no error bar is depicted.

Furthermore, based on the mitochondrial marker Complex IV subunit IV, it was possible to enrich non-synaptosomal mitochondria more than 5.0 fold (fraction e) and synaptosomal mitochondria more than 2.0 fold (fraction f) compared to total homogenate (fraction a). Nuclear debris, based on the presence of the protein marker LSD1, was removed during the workflow. Cytoskeletal proteins, based on the level of marker protein actin, were slightly enriched in the synaptosomal fraction (fraction f). As filamentous actin represents the major cytoskeletal component in dendritic spines to ensure morphological integrity (Bellot et al., 2014b), the increase in β-actin within the synaptosomal fraction is in good agreement. Importantly, myelin contamination that was measured by the marker PLP was increased in the mitochondrial fraction (fraction e) but was not detectable in the myelin fraction itself (fraction d) compared to total homogenate (fraction a). However, there was no enrichment in myelin in the synaptosomal fraction (fraction f) compared to total homogenate (fraction a). The reason for that is unclear, but may be associated to its highly hydrophobic properties attaching to plastic surfaces; during dissolution of the non-synaptosomal mitochondria fraction, it may be eluted from the plastic surface into the mitochondrial sample. Importantly, the protein marker intensities were normalised against the total lane intensity from Ponceau-S staining; the total lane intensities were similar in all the lanes (Figure 7) although visual inspection of the Ponceau-stained bands of each lane may suggest a lower protein content in the myelin fraction (lane d) (Figure 7).

In total, it was possible to isolate and enrich synaptosomes with their mitochondrial content. The method can be applied to successfully isolate and purify synaptosomes from brain regions. Similar approaches to isolate synaptic terminals were also applied to study synaptosomes from Alzheimer´s cortex (Sokolow et al., 2012).

7 Study design

In this work, two different mouse strains were used, namely male NMRI (outbred) and female C57BL/6 (inbred) to obtain long-term radiation data from different strains. The study designs are shown in Figure 8 with the methods applied at distinct post-irradiation time points. 0.1 Gy and 0.5 Gy was used in both studies; 0.02 Gy did not show any long-term alteration in signalling pathways in the NMRI mouse study, thus, it was not used in the C57BL/6 mouse study. 2.0 Gy instead of 1.0 Gy was used to get more information in the moderate-dose range used in radiotherapy such as treatment of brain malignancies. Cobalt and caesium sources were used due to the different availability in the two labs but both were γ-rays. The slight discrepancies within the follow-up time points were based on quarantine capacity limitations at the Helmholtz Centre Munich, Munich, Germany. Moreover, female C57BL/6 mice were used to overcome in part the quarantine capacity limitations as they can be housed at higher number in the cages compared to male mice (territory demands). Further, partly different assays were used due to its tedious nature (synaptosomes enrichment, immunohistochemistry) but they were overall focussed to the context of synapses.

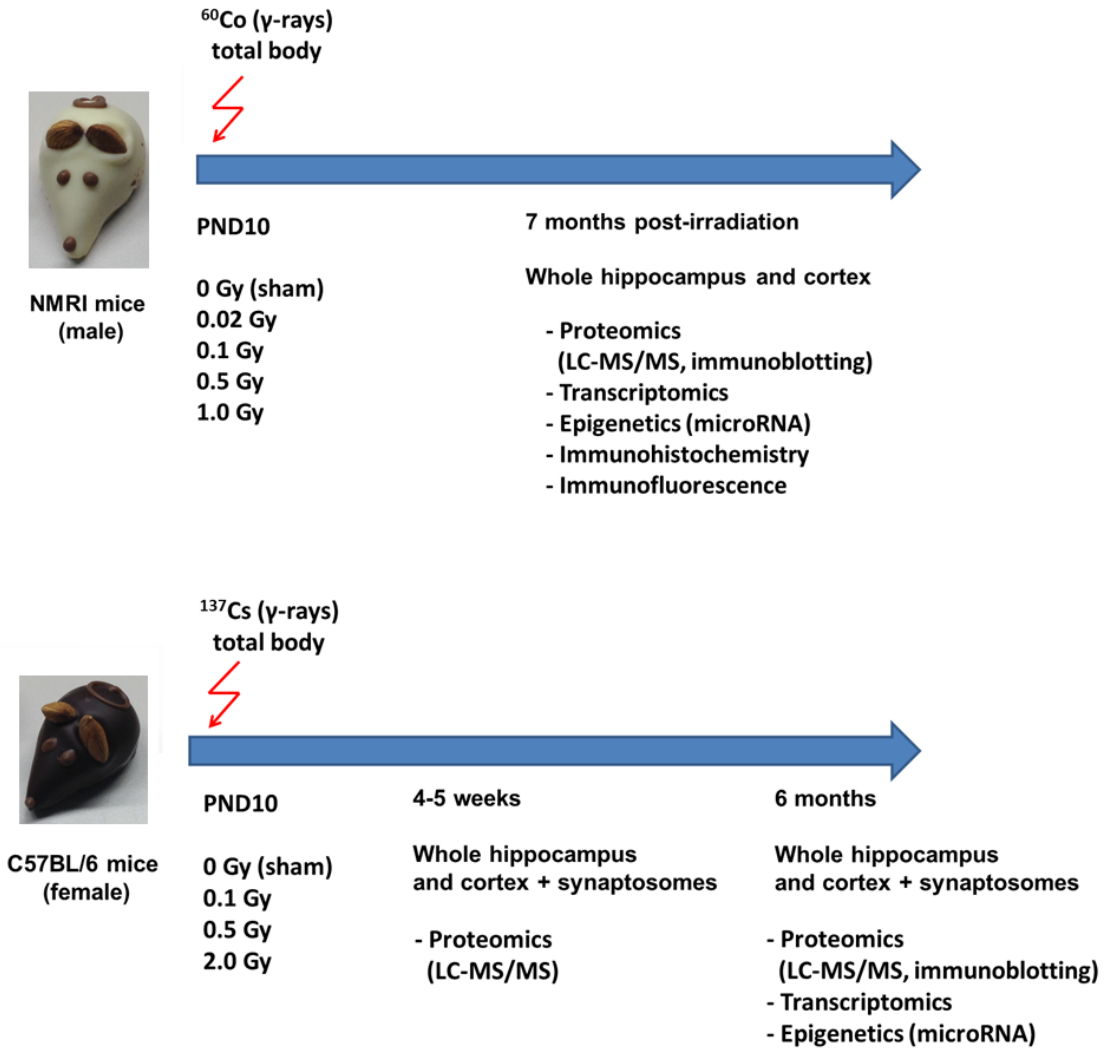

Figure 8: Study designs of NMRI and C57BL/6 mice study.

For NMRI mice study, male mice were irradiated (^{60}Co – γ-rays – total body) with doses of 0 Gy (sham), 0.02 Gy, 0.1 Gy, 0.5 Gy and 1.0 Gy on PND10 at the Uppsala university – Department of Environmental Toxicology (S. Buratovic, P. Eriksson, B. Stenerlöw). Mice were shipped to Munich (Institute of Radiation Biology, Helmholtz Zentrum München) for molecular studies in the hippocampus and cortex 7 month post-irradiation. For C57BL/6 mice study, female mice were irradiated (^{137}Cs – γ-rays – total body) with doses of 0 Gy (sham), 0.1 Gy, 0.5 Gy and 2.0 Gy on PND10 at the Erasmus Medical Centre – Department of Genetics in Rotterdam (S. Sepe, P. G. Mastroberardino). Following irradiation, animals were shipped to Munich (Institute of Radiation Biology, Helmholtz Zentrum München) for the indicated molecular studies and targets using whole hippocampus and cortex and isolated synaptosomes from whole hippocampus and cortex. PND: postnatal day; LC-MS/MS: liquid chromatography tandem-mass spectrometry

8 Results

Results from the NMRI mouse study

8.1 Radiation-induced changes in actin cytoskeleton-associated signalling pathways are persistent in hippocampus and cortex

A cognition-based behaviour test of irradiated NMRI mice 2 and 4 months post-irradiation showed that only mice exposed to 0.5 Gy and 1.0 Gy had cognitive deficits but not at lower doses (spontaneous behaviour observation over 60 minutes period of testing time in a novel environment) (personal communication with S. Buratovic and P. Eriksson, University of Uppsala).

To obtain information about the alteration in cognitive performance due to radiation exposure, a global quantitative proteome analysis by liquid-chromatography-mass-spectrometry (LC-MS) was performed in these mice 7 month post-irradiation after shipment of material to Helmholtz Centre Munich, Munich, Germany to quantify deregulation in the protein composition. The cortex and hippocampus - important brain regions for cognitive functions - were isolated 7 months post-irradiation and used for LC-MS-based proteome analysis. The in-gel digestion and LC-MS/MS runs on the mass spectrometer were done by S. Helm and C. von Toerne (Department of Protein Science, Helmholtz Centre Munich, Munich, Germany). The protein quantification illustrated a dose-dependency in the absolute number of significantly deregulated proteins from the lower dose (0.02 Gy and 0.1 Gy) towards a plateau at moderate doses (0.5 Gy and 1.0 Gy) (cortex/hippocampus: 0.02 Gy – 6/7, 0.1 Gy – 6/12, 0.5 Gy - 27/34, 1.0 Gy – 22/36) as shown in Figure 9 A and B in Venn diagrams. The complete list of deregulated proteins is presented in Table 25 and Table 26 (Supplementary information).

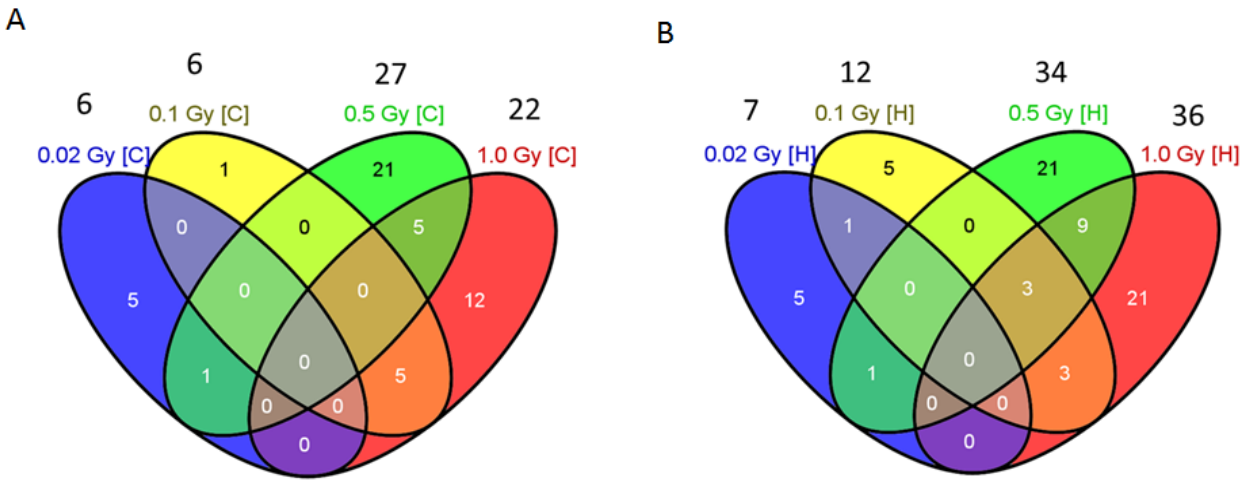

Figure 9: Venn diagrams of deregulated proteins from cortex [C] (A) and hippocampus [H] (B) from global proteomics approach.
Animals were exposed to 0.02 Gy, 0.1 Gy, 0.5 Gy and 1.0 Gy. H: n=4; C: n=5. The number above each dose shows the total number of deregulated proteins at this dose

Importantly, the behavioural data from Uppsala indicated defects only at doses of 0.5 and 1.0 Gy (personal communication with S. Buratovic and P. Eriksson, University of Uppsala), the deregulated proteins at these doses were partly overlapping and distinct from the deregulated proteins induced by the two lower doses (Figure 9). Table 11 shows the unique overlapping proteins between 0.5 Gy and 1.0 Gy in the cortex and hippocampus, respectively. Importantly, the direction of the change of proteins (up- and down-regulation) was consistent between these doses (Table 11).

Table 11: Unique overlapping deregulated proteins between cortex and hippocampus at doses of 0.5 Gy and 1.0 Gy with their fold-changes and variabilities.

The variability corresponds to the total variance in % from the fold-change of the protein of interest from all the biological replicates used; n=5 (Cortex), n=4 (Hippocampus)

Distinct unique overlapping proteins between 0.5 Gy and 1.0 Gy - Cortex						
#	**Symbol**	**Entrez Gene Name**	**n-fold change (0.5 Gy)**	**Variability [%] (0.5 Gy)**	**n-fold change (1.0 Gy)**	**Variability [%] (1.0 Gy)**
1	Cox6a1	cytochrome c oxidase, subunit VI a, polypeptide 1	2.43	22.3	2.34	27.6
2	Uqcrc1	ubiquinol-cytochrome c reductase core protein 1	2.03	21.5	1.92	27.1
3	Gnb2	guanine nucleotide binding protein (G protein), beta 2	1.49	11.8	1.42	27.6
4	Gnb1	guanine nucleotide binding protein (G protein), beta 1	1.43	13.5	1.33	15.8
5	Hnrnpl	heterogeneous nuclear ribonucleoprotein L	1.40	18.5	1.68	13.6
Distinct unique overlapping proteins between 0.5 Gy and 1.0 Gy - Hippocampus						
#	**Symbol**	**Entrez Gene Name**	**n-fold change (0.5 Gy)**	**Variability [%] (0.5 Gy)**	**n-fold change (1.0 Gy)**	**Variability [%] (1.0 Gy)**
1	Rap1gds1	RAP1, GTP-GDP dissociation stimulator 1	1.61	18.0	1.59	14.5
2	Ank2	ankyrin 2, brain	1.49	21.8	1.79	24.0
3	Gnb2	guanine nucleotide binding protein (G protein), beta 2	1.37	3.5	1.35	6.4
4	Gnb1	guanine nucleotide binding protein (G protein), beta 1	1.42	6.6	1.37	4.6
5	Cnrip1	cannabinoid receptor interacting protein 1	1.42	13.7	1.34	11.2
6	Tubb3	tubulin, beta 3 class III	1.33	7.8	1.41	7.0
7	Tuba4a	tubulin, alpha 4A	1.32	7.9	1.36	9.3
8	Sgip1	SH3-domain GRB2-like (endophilin) interacting protein 1	-1.31	17.9	-1.30	27.5
9	Necab2	N-terminal EF-hand calcium binding protein 2	-1.51	25.5	-1.52	28.3

Only two proteins deregulated at 0.5 Gy and 1.0 Gy were found changed in brain regions, namely the guanine nucleotide binding proteins beta 1 and beta 2 (Gnb1 and Gnb2) involved in G-protein coupled receptor signalling (Table 11). Annotation

of the altered proteins into functionally defined protein classes demonstrated that a number of changed proteins at 0.5 Gy and 1.0 Gy belonged to the protein class of cytoskeleton / cytoskeleton-associated proteins (cortex - 0.5 Gy: 22 %, 1.0 Gy: 9 %; hippocampus – 0.1 Gy: 20 %, 1.0 Gy: 16 %) (Figure 10 and Figure 11). However, only one hit was found within this class at 0.02 Gy in the cortex but not in hippocampus at 0.02 Gy and 0.1 Gy (Figure 10 and Figure 11). Table 25 and Table 26 (Supplementary information) show the proteins grouped into their respective protein classes according to PANTHER classification software and information from UniProt database. As cytoskeletal proteins are important in the morphology of cells and synapses, these data indicated that there may be defects in these structures particularly at 0.5 Gy and 1.0 Gy 7 month post-irradiation.

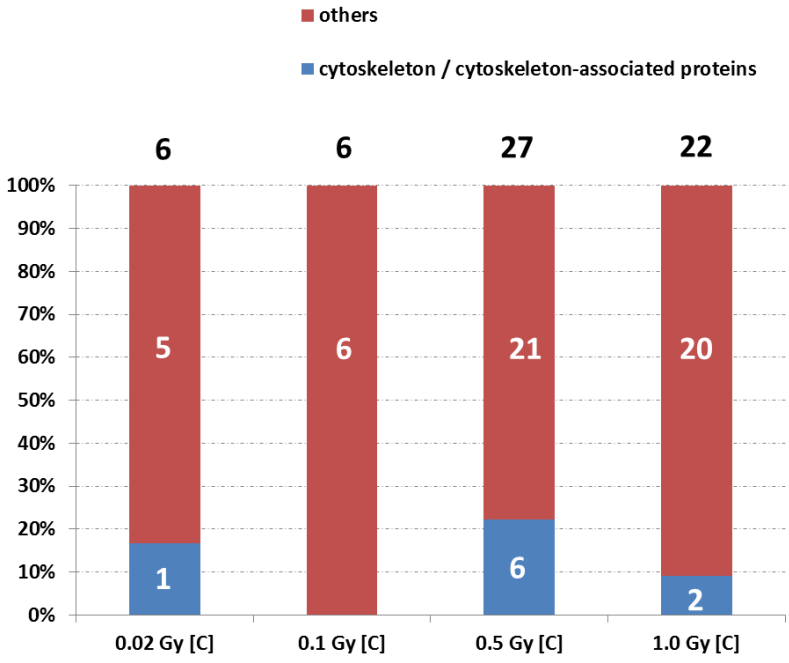

Figure 10: Comparable representation of the number of deregulated proteins from cortical global proteomics approach (NMRI mouse study) grouped into the protein class cytoskeleton / cytoskeleton-associated proteins and others.

The classes are based on information from the PANTHER software (PANTHER protein class) and UniProt-database. The numbers within the columns represent the number of proteins involved in this protein class. The number above the columns represents the total number of deregulated proteins at this dose and brain region; C: Cortex

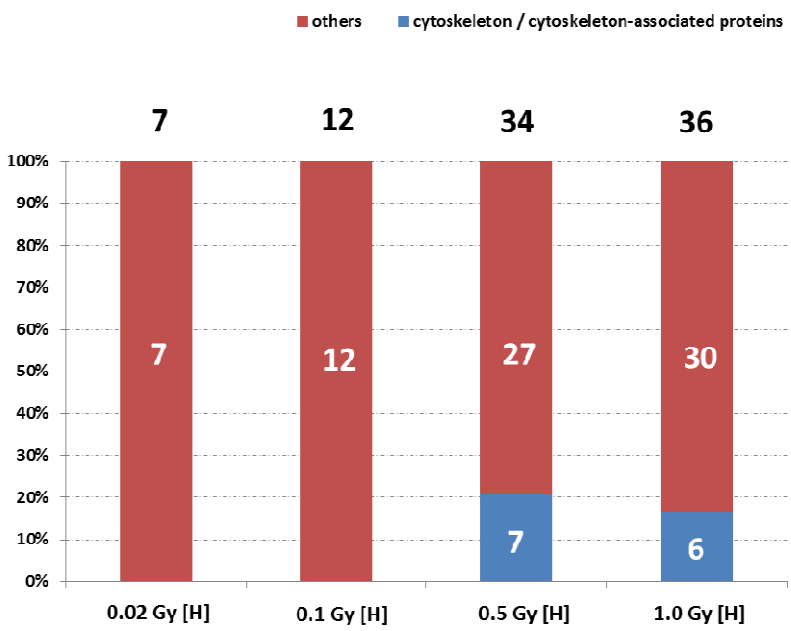

Figure 11: Comparable representation of the number of deregulated proteins from hippocampal global proteomics approach (NMRI mouse study) grouped into the protein class cytoskeleton / cytoskeleton-associated proteins and others.

The classes are based on information from the PANTHER software (PANTHER protein class) and UniProt-database. The numbers within the columns represent the number of proteins involved in this protein class. The number above the columns represents the total number of deregulated proteins at this dose and brain region; H: Hippocampus

Next, the Ingenuity Pathway analysis (IPA) software tool was used to identify the long-term radiation-affected signalling pathways possibly affecting synapses by the changes in observed protein levels. Thus, a comparison analysis from all the deregulated proteins found at the different doses in the two brain regions was applied. Figure 12 shows the associated signalling pathways involved which are ephrin B / ephrin receptor signalling, signalling by Rho family GTPases, RhoGDI signalling and axonal guidance signalling. Evaluation of these signalling pathways showed that there were shared proteins including the small Rho family GTPases Rac1 and Cdc42, the kinases PAK and LIMK1, and the actin-modulating cofilin (Figure 40) (Supplementary information); all these proteins are regulating axonal maturation, spine- and synapse-formation, maturation and neuronal morphology via

regulation of actin polymerisation (Rac1-Cofilin pathway) (Asrar and Jia, 2013, Saneyoshi and Hayashi, 2012, Saneyoshi et al., 2010).

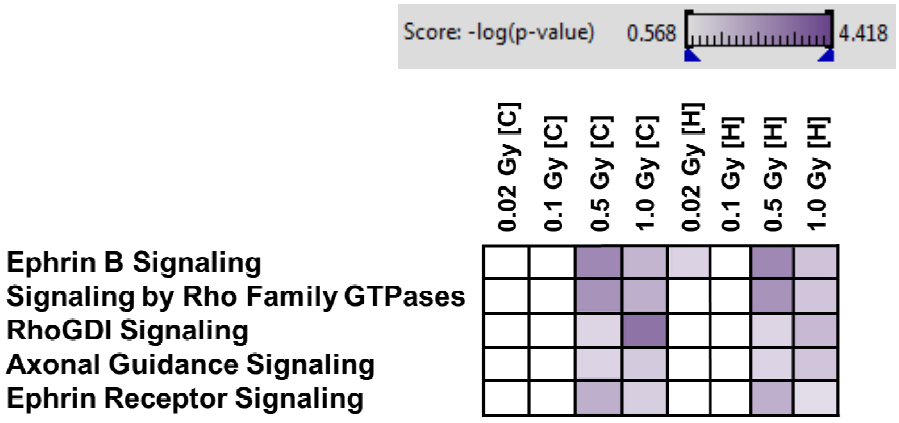

Figure 12: Associated signalling pathways of all dose-dependent significantly deregulated proteins found by LC-MS/MS analysis using the Ingenuity Pathway Analysis (IPA) software.
Higher colour intensity represents higher significance (p-value) whereas all coloured boxes have a p-value of ≤ 0.05. Hippocampal and cortical data result from four and five biological replicates, respectively. H: Hippocampus, C: Cortex

8.2 Ionising radiation exposure impairs the Rac1-Cofilin pathway

Both the cognitive studies (data of cognition-related spontaneous behaviour from Uppsala University) and the protein profiling data (LC-MS/MS proteome analysis) indicated detrimental effects on synapses only at doses of 0.5 Gy and 1.0 Gy. The Rac1-Cofilin pathway was characterised in more detail by immunoblotting, miRNA and mRNA quantification at these two doses. Figure 13 shows the Rac1-Cofilin pathway (Saneyoshi et al., 2010, DerMardirossian et al., 2004) and its regulatory network.

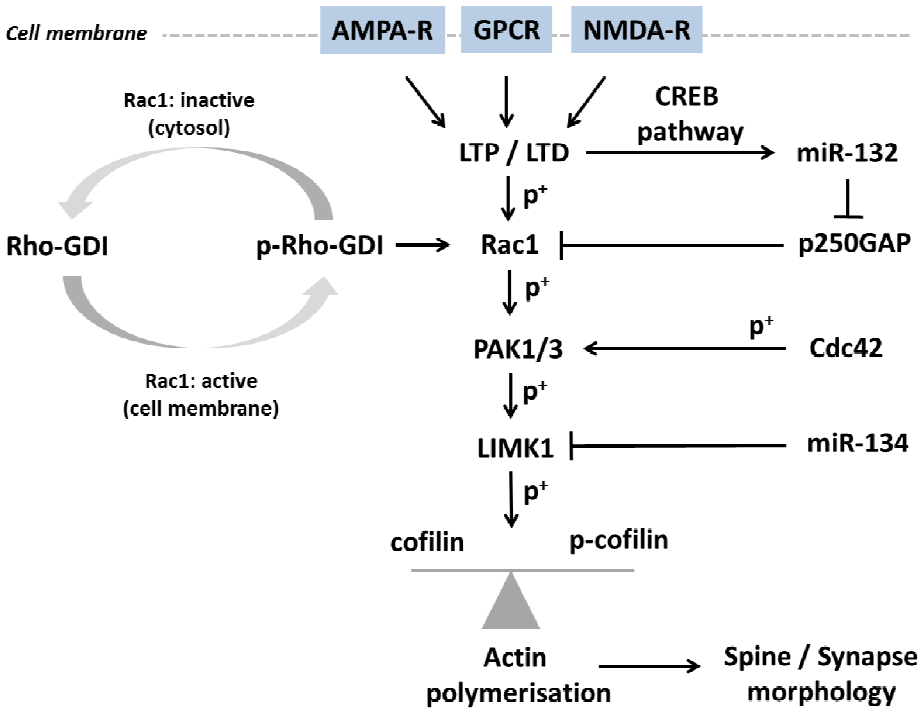

Figure 13: The Rac1-Cofilin signalling pathway.
Signalling from AMPA, NMDA and GPC receptors lead to activation (phosphorylation) of Rac1 via LTP / LTD (long-term potentiation / long-term depression) associated signalling pathways. This leads to downstream activation (phosphorylation) of PAK1/3, LIMK1 and final inactivation of cofilin via phosphorylation. Further, Cdc42 can also phosphorylate PAK1/3. Associated microRNAs are the CREB-mediated miR-132 regulating Rac1 activity via modulation of a GTP hydrolysis protein (p250GAP) and miR-134 suppressing LIMK1 levels. Rac1 activity is regulated via phosphorylation of RhoGDI releasing Rac1 from RhoGDI inhibitory complex. The Rac1-Cofilin signalling pathway regulates in the end actin polymerisation and, thus, spine / synapse morphology. The image is adapted after own publication (Kempf et al. – in preparation).

Irradiation with 0.5 Gy and 1.0 Gy significantly decreased Rac1 and LIMK1 protein expression levels in the cortex and hippocampus (Figure 14 and Figure 15). As Rac1 is an upstream negative regulator of cofilin, the levels of both cofilin and phospho-cofilin were quantified. Phospho-cofilin is the inactive form of the protein that is unable to disassemble actin filaments. A significantly marked increase in cofilin levels in cortex and hippocampus at 0.5 Gy and 1.0 Gy was noted whereas levels of phosphorylated cofilin were only slightly increased in the cortex at 1.0 Gy and slightly decreased in the hippocampus at 0.5 and 1.0 Gy (Figure 14 and Figure 15). This suggests imbalances in cofilin / phospho-cofilin ratios in hippocampus and cortex at 0.5 Gy and 1.0 Gy. Further, quantification of Cdc42 demonstrated an increase only at 0.5 Gy in the hippocampus (Figure 14) correlating with the proteomics data

showing at 0.5 Gy a fold-change of 1.66 (Table 26 [Supplementary information]) whereas Cdc42 protein levels were unchanged in the cortex at any dose (Figure 15). Thus, these data may indicate a predominant role of the Rho GTPases Rac1, but with Cdc42 complementary in the hippocampus, in the radiation-induced long-term alteration of cytoskeletal remodelling of the synapse.

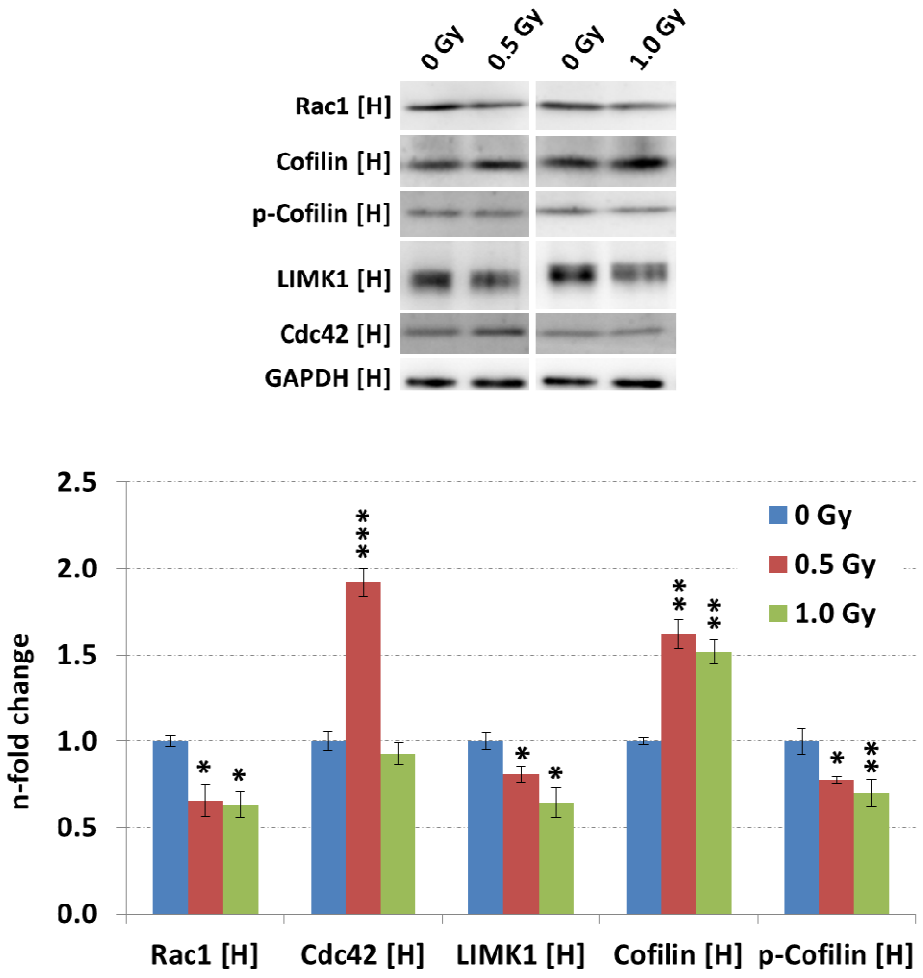

Figure 14: Data from immunoblots associated to the Rac1-Cofilin pathway in hippocampus from sham-irradiated, 0.5 Gy and 1.0 Gy exposed mice.

The columns represent the fold-changes with standard errors of the mean (SEM) from three biological replicates. The visualisation of protein bands shows the representative change from three biological replicates. *p<0.05; **p<0.01; ***p<0.001 (unpaired Student´s t-test). Normalisation was performed against endogenous GAPDH; H: Hippocampus

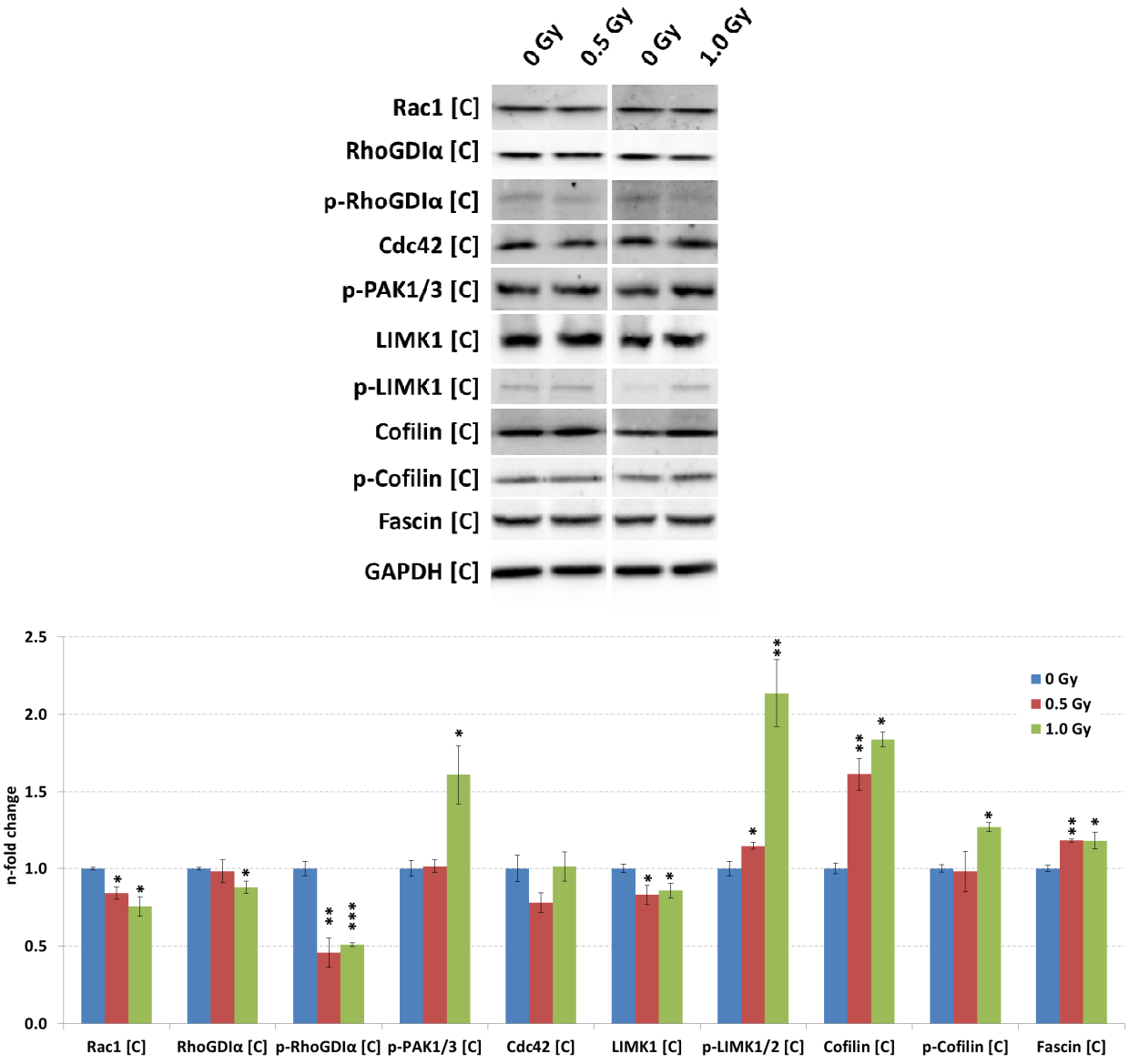

Figure 15: Data from immunoblots associated to the Rac1-Cofilin pathway in cortex from sham-irradiated, 0.5 Gy and 1.0 Gy exposed mice.

The columns represent the fold-changes with standard errors of the mean (SEM) from three biological replicates. The visualisation of protein bands shows the representative change from three biological replicates. *p<0.05; **p<0.01; ***p<0.001 (unpaired Student´s t-test). Normalisation was performed against endogenous GAPDH; C: Cortex

Further characterisation of the Rac1-Cofilin pathway in the cortex by immunoblotting demonstrated alterations in both expression and phosphorylation levels of RhoGDIα, PAK1/3 and LIMK1. The level of RhoGDIα in the cortex was slightly decreased at 1.0 Gy and unchanged at 0.5 Gy whereas the phosphorylated form was strongly decreased at both doses (Figure 15) suggesting less active Rac1 in the cortex at both doses as un-phosphorylated RhoGDIα keeps Rac1 in the cytosol and thus

inactive (Figure 13). Cortical levels of phosphorylated PAK1/3 were increased only at 1.0 Gy consistent with the strongly increased phospho-LIMK1/2 levels at 1.0 Gy (Figure 15) reflected in the increased levels of phosphorylated cofilin at this dose (Figure 15).

Immunoblotting analysis demonstrated a significant increase in cortical fascin levels at both doses (Figure 15) and this was in accordance with proteomics data of fascin1 (Fscn1) levels at 0.5 Gy (0.5 Gy: fold-change of 1.53 - Table 25 [Supplementary information]) whereas at 1.0 Gy, fascin1 was not confidently quantifiable (1 unique peptide); fascin plays an important role in the organisation of actin filament bundles whereas cofilin may play a cooperative role in disassembly of filopodial actin filaments as demonstrated *in vitro* (Breitsprecher et al., 2011).

LIMK1 was down-regulated without corresponding change in gene expression (Figure 16) in both cortex and hippocampus at 0.5 Gy and 1.0 Gy. The microRNA miR-134 is a well-known negative regulator of LIMK1 (Schratt et al., 2006) and therefore, levels of miR-134 were determined in irradiated hippocampus and cortex. Notably, the decrease of LIMK1 was paralleled by a significant increase in miR-134 levels both in cortex and hippocampus (Figure 17) implying a role of the increased mir-134 in LIMK1 down-regulation. Importantly, evaluation of the levels of miR-132 and its tandem miRNA miR-212 showed a significant increase in hippocampus and cortex at both doses (Figure 17). These miRNAs share a close sequence similarity and they both are implicated in a number of neurocognitive disorders characterised by aberrant synaptogenesis such as Alzheimer´s (Lukiw, 2007, Lau et al., 2013, Wong et al., 2013).

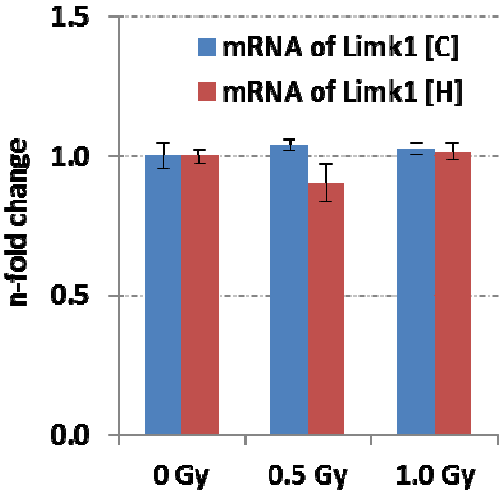

Figure 16: Data from *Limk1* quantification associated to the Rac1-Cofilin pathway in hippocampus and cortex from sham-irradiated, 0.5 Gy and 1.0 Gy exposed mice.
The columns represent the fold-changes with standard errors of the mean (SEM) from three biological replicates. *p<0.05; **p<0.01; ***p<0.001 (unpaired Student´s t-test). Normalisation was performed against endogenous *GAPDH*; H: Hippocampus, C: Cortex

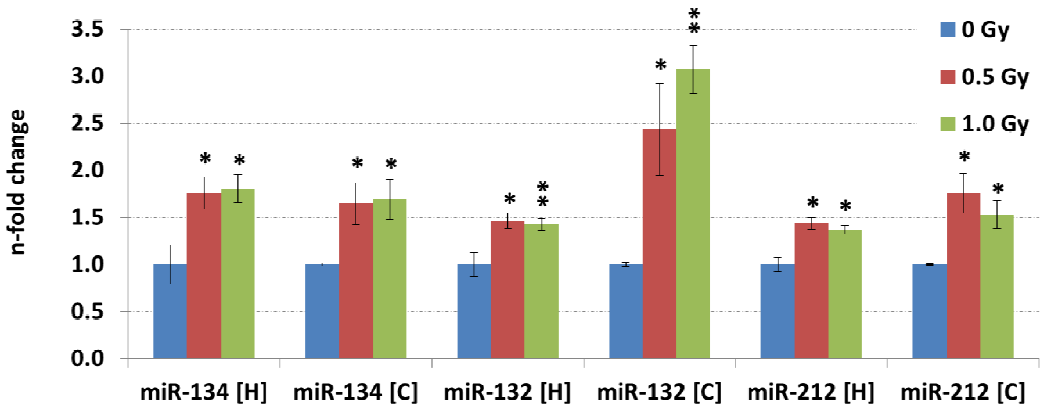

Figure 17: Data from miRNA quantification associated to the Rac1-Cofilin pathway and synaptogenesis in hippocampus and cortex from sham-irradiated, 0.5 Gy and 1.0 Gy exposed mice.
The columns represent the fold-changes with standard errors of the mean (SEM) from three biological replicates. *p<0.05; **p<0.01; ***p<0.001 (unpaired Student´s t-test). Normalisation was performed against endogenous snoRNA135; H: Hippocampus, C: Cortex

Taken together the changes in protein, RNA and miRNA levels all indicate the dysregulation of the Rac1-Cofilin pathway in the cortex and hippocampus after irradiation of 0.5 Gy and 1.0 Gy even 7 months post-irradiation. Furthermore, these

data are suggestive of an aberrant modulation of the actin filament polymerisation process due to imbalances in the ratios of cofilin and phospho-cofilin that may play a role in the neuropathological alteration of neuronal spine and synapse morphology manifested by irradiation.

7.4 Ionising radiation induces changes in synaptic proteins in the hippocampus and dentate gyrus

To investigate the potential radiation-induced changes in synaptic density and associated processes that are indicated by the observed alterations in the Rac1-Cofilin pathway, the level of the postsynaptic density protein 95 (PSD-95) and the microtubule-associated protein 2 (MAP-2) were analysed using sequential immunofluorescence. PSD-95 plays a key role in regulating synaptic plasticity via NMDA receptors; MAP-2 is a neuron-specific cytoskeletal protein enriched in dendrites and is implicated in determining and stabilising dendritic shape during neuron development (Harada et al., 2002, Woods et al., 2011). Negative controls are depicted in section 6.13 highlighting specificity and confident quantification of the sequential immunofluorescence workflow. The quantification of MAP-2 and PSD-95 levels showed significant increases at 1.0 Gy both in hippocampus and dentate gyrus (Figure 18).

These data indicate that ionising radiation can elevate the level of neuronal synaptic proteins over a prolonged period.

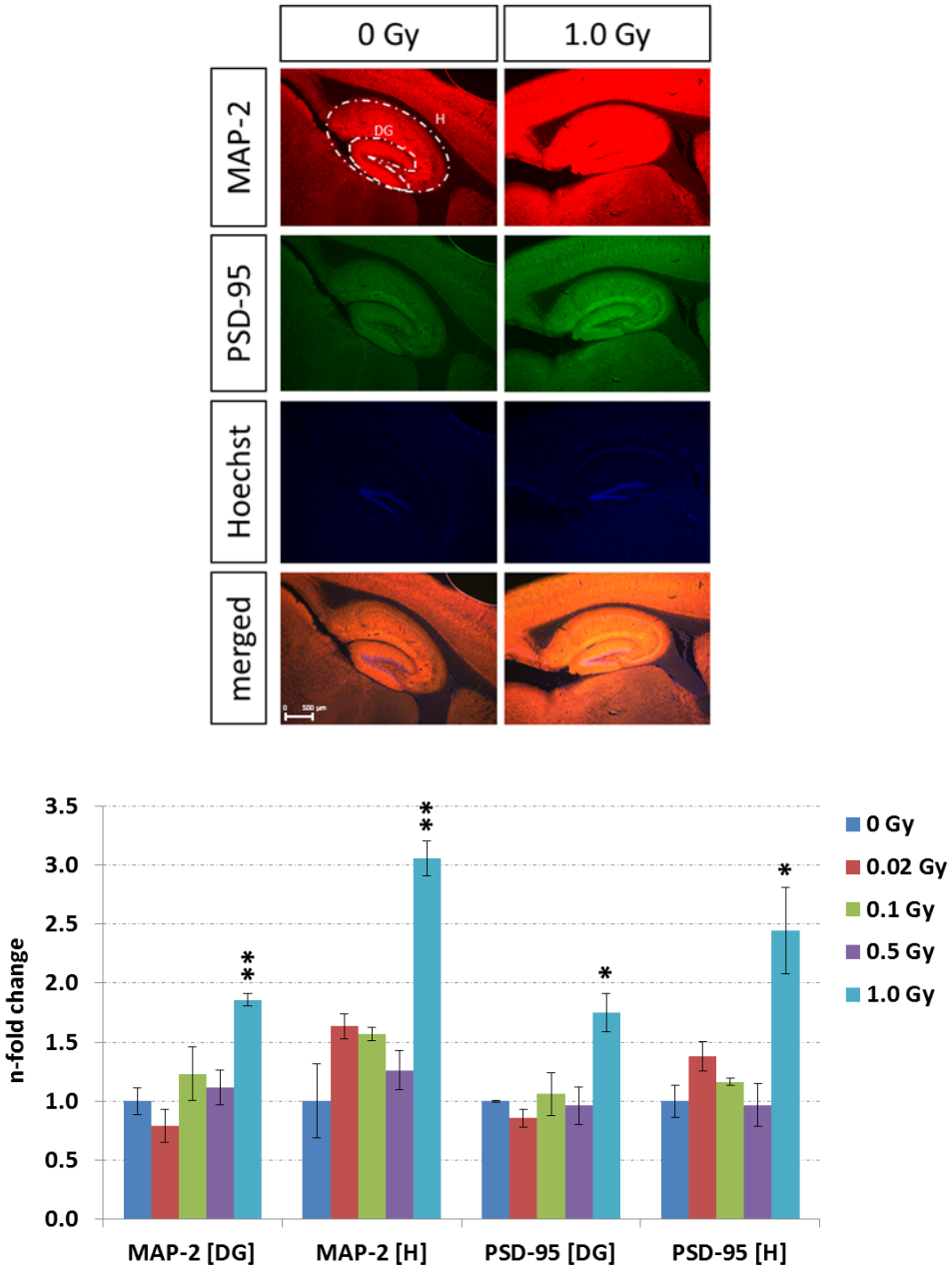

Figure 18: Data from sequential immunofluorescence from hippocampus (H) and dentate gyrus (DG) at different doses.

The columns represent the fold-changes with standard errors of the mean (SEM) from three biological replicates. The visualisation shows the representative intensity from three biological replicates of 0 Gy and 1.0 Gy regarding MAP-2 (red - Microtubule-associated protein 2), PSD-95 (green - Disks large homolog 4 (DLG4)), Hoechst (blue) and merged intensity within the hippocampal region. The MAP-2 / PSD-95 intensity was normalised against nuclear Hoechst intensity in the region of interest as indicated by white dashes. *p<0.05; **p<0.01; ***p<0.001 (unpaired Student´s t-test). Each fluorescent label was excited and recorded separately with only single channels and were afterwards merged with the software.

7.5 Radiation-induced changes in long-term potentiation / long-term depression-dependent signalling cascades are associated with imbalances in CREB-dependent neuronal signalling

Structural changes to synapses lead to an altered neuronal activity pattern regulated by transcription of immediate-early / -late response genes. Particularly, immediate-early genes (IEG´s) are transcribed in the first minutes after a neuronal stimulation event e.g. via neurotransmitters or growth factors (Kovacs, 2008).

To investigate such changes in irradiated brains, total RNA from hippocampus and cortex were isolated and used to quantify mRNAs related to the above processes to gain insight into radiation-affected synapses and the basal neuronal activity. The expressions of several of the early response genes were mainly down-regulated in the hippocampus (Table 12) and cortex (Table 13).

Table 12: Significantly changed expressed genes associated to the gene affiliation "Immediate-early response genes and late response genes" from hippocampus at doses of 0.5 Gy and 1.0 Gy using RT² Profiler PCR Arrays.
The table shows the genes which are significantly up-regulated or down-regulated with the fold-changes±SEM in brackets and its p-value; *p<0.05; **p<0.01; ***p<0.001 (unpaired Student´s t-test, n=3) after normalisation to the median of 84 target genes from each assays plate. The grouping of genes into the gene affiliation is after manufacturer; genes which are in one than one group arising according to the manufacturer were manually verified via literature

	Hippocampus - 0.5 Gy		Hippocampus - 1.0 Gy	
Gene affiliation	Gene description	Gene symbol with fold-change±SEM and p-value	Gene description	Gene symbol with fold-change±SEM and p-value
Immediate-early response genes and late response genes	Nuclear factor of kappa light polypeptide gene enhancer in B-cells inhibitor, beta	*Nfkbib* (3.64±1.31)*	Plasminogen activator, tissue	*Plat* (-1.24±0.02)**
	CCAAT/enhancer binding protein (C/EBP), beta	*Cebpb* (1.31±0.04)***	CCAAT/enhancer binding protein (C/EBP), beta	*Cebpb* (-1.34±0.10)*
	Kruppel-like factor 10	*Klf10* (-1.26±0.09)*	Early growth response 3	*Egr3* (-1.35±0.06)***
	Homer homolog 1 (Drosophila)	*Homer1* (-1.26±0.12)*	Homer homolog 1 (Drosophila)	*Homer1* (-1.39±0.05)***
	Regulator of G-protein signaling 2	*Rgs2* (-1.27±0.05)**	Early growth response 4	*Egr4* (-1.46±0.15)*
	Ras homolog enriched in brain	*Rheb* (-1.38±0.08)*	Activity regulated cytoskeletal-associated protein	*Arc* (-1.50±0.02)*
	Synaptopodin	*Synpo* (-1.40±0.05)***	Protocadherin 8	*Pcdh8* (-1.57±0.16)*
	Nuclear factor of kappa light polypeptide gene enhancer in B-cells 1, p105	*Nfkb1* (-1.42±0.06)*	Jun-B transcription factor	*Junb* (-1.65±0.17)**
	Early growth response 3	*Egr3* (-1.59±0.12)***	Early growth response 2	*Egr2* (-2.80±0.06)*
	Protocadherin 8	*Pcdh8* (-2.13±0.20)***	c-Fos transcription factor	*c-Fos* (-3.33±0.21)**

Table 13: Significantly changed expressed genes associated to the gene affiliation "Immediate-early response genes and late response genes" from cortex at doses of 0.5 Gy and 1.0 Gy using RT² Profiler PCR Arrays.
The table shows the genes which are significantly up-regulated or down-regulated with the fold-changes±SEM in brackets and its p-value; *p<0.05; **p<0.01; ***p<0.001 (unpaired Student´s t-test, n=3) after normalisation to the median of 84 target genes from each assays plate. The grouping of genes into the gene affiliation is after manufacturer; genes which are in one than one group arising according to the manufacturer were manually verified via literature

	Cortex - 0.5 Gy		Cortex - 1.0 Gy	
Gene affiliation	Gene description	Gene symbol with fold-change±SEM and p-value	Gene description	Gene symbol with fold-change±SEM and p-value
Immediate-early response genes and late response genes	Synaptopodin	*Sympo* (-1.22±0.08)*	Serine / threonine-protein kinase pim-1	*Pim1* (1.68±0.31)*
	Beta nerve growth factor	*Ngf* (-1.26±0.09)*	Matrix metallopeptidase 9	*Mmp9* (1.25±0.08)*
	Nuclear factor of kappa light polypeptide gene enhancer in B-cells 1, p105	*Nfkb1* (-1.27±0.04)*	p65 transcription factor	*Rela* (1.21±0.04)*
	Neurotrophin-3	*Ntf3* (-1.30±0.07)*	Homer protein homolog 1	*Homer1* (-1.44±0.02)*
	Brain derived neurotrophic factor	Bdnf (-1.36±0.11)*	Inhibin beta-A	Inhba (-1.45±0.39)**
	Early growth response 3	*Egr3* (-1.47±0.19)*	Early growth response 1	*Egr1* (-1.48±0.15)*
	Serine / threonine-protein kinase pim-1	*Pim1* (-1.47±0.08)*	Early growth response 4	*Egr4* (-1.63±0.28)*
	Inhibin beta A	Inhba (-2.20±0.38)*	Brain derived neurotrophic factor	Bdnf (-1.69±0.03)**
			Early growth response 3	*Egr3* (-2.16±0.22)**
			Early growth response 2	*Egr2* (-2.95±0.94)*
			c-Fos transcription factor	*c-Fos* (-3.53±0.33)**
			Jun-B transcription factor	*Junb* (-4.41±0.82)**
			Activity regulated cytoskeletal-associated protein	*Arc* (-5.25±0.66)***

Two genes, namely *Arc* and *c-Fos* were significantly decreased in both cortex and hippocampus at 1.0 Gy but not 0.5 Gy (Table 12 and Table 13); lower doses were not tested. This result was verified via quantification of protein expression (immunoblotting) that also showed a decrease at the protein level both in the hippocampus and cortex at 1.0 Gy (Figure 19). Importantly, it is generally accepted that the IEG c-Fos is an important generic marker to access neuronal activity (Kovacs, 2008) and the activity-regulated cytoskeletal-associated protein (Arc) is an "effector" IEG that is induced by neuronal excitation and plays a fundamental role in activity-dependent synaptic modifications at dendrites (Kovacs, 2008, Lyford et al., 1995).

Taken together, these results may indicate a reduced basal neuronal activity in the cortex and hippocampus 7 month post-irradiation due to the overall reduction in immediate-early response genes needed to react on neurotransmission efficiently.

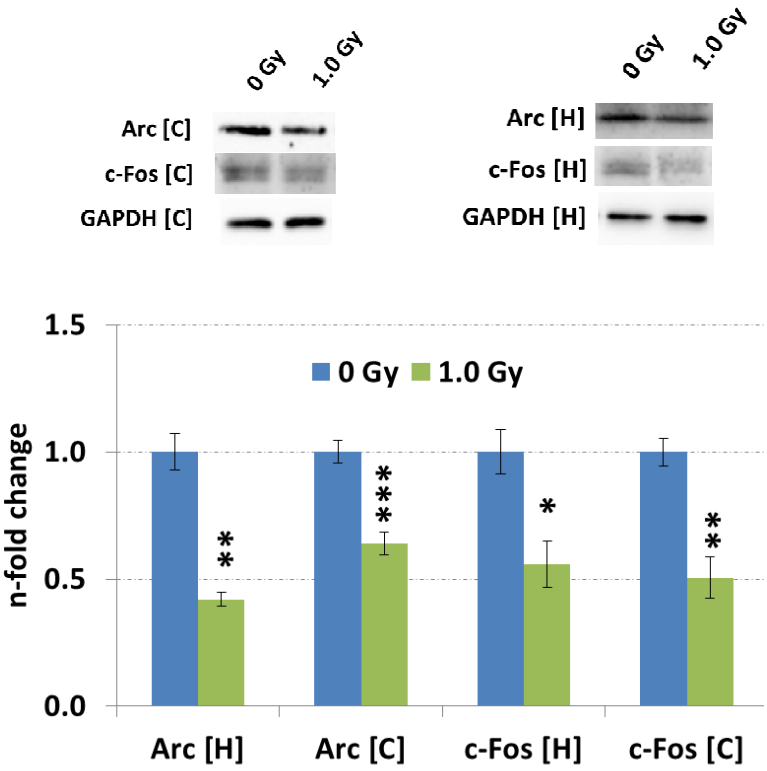

Figure 19: Immunblots of Arc and c-Fos in hippocampus and cortex of sham-irradiated and 1.0 Gy irradiated mice 7 months post-irradiation.
The columns represent the fold-changes with standard errors of the mean (SEM) from three biological replicates. The visualisation of protein bands shows the representative change from three biological replicates. *p<0.05; **p<0.01; ***p<0.001 (unpaired Student´s t-test). Normalisation was performed against endogenous GAPDH; H: Hippocampus, C: Cortex

Further, both synaptic alterations and reduced neuronal activity as indicated by reductions in the expression level of immediate-early / -late response genes may lead in turn to changes in the neuronal receptor profile.

Gene expression quantification of a panel of 27 neuronal receptors (Table 35) showed alterations mainly in the expression of G-protein coupled receptors for glutamate (*Grm´s*) but also α-amino-3-hydroxy-5-methyl-4-isoxazolepropionic acid

receptor (AMPA)-selective glutamate receptors (*Gria´s*) and N-methyl-D-aspartate (NMDA) receptors (*Grin´s*) in hippocampus (Table 14) and cortex (Table 15) at 0.5 Gy and 1.0 Gy doses; lower doses were not tested as mass spectrometry-based signalling pathway analysis did not indicate any changes at these doses. Noteworthy, the gene expression of several G-protein coupled receptors was down-regulated at 0.5 Gy in hippocampus (reduced levels of *Grm3, Grm5, Grm8)* (Table 14).

Table 14: Significantly changed expressed genes associated to the gene affiliation "neuronal receptors" from hippocampus at doses of 0.5 Gy and 1.0 Gy using RT² Profiler PCR Arrays.

The table shows the genes which are significantly up-regulated or down-regulated with the fold-changes±SEM in brackets and its p-value; *p<0.05; **p<0.01; ***p<0.001 (unpaired Student´s t-test, n=3) after normalisation to the median of 84 target genes from each assays plate. The grouping of genes into the gene affiliation is according to the manufacturer; genes which are in more than one group were manually verified via literature

	Hippocampus - 0.5 Gy		Hippocampus - 1.0 Gy	
Gene affiliiation	Gene description	Gene symbol with fold-change±SEM and p-value	Gene description	Gene symbol with fold-change±SEM and p-value
Neuronal receptors	Glutamate receptor, ionotropic, NMDA2C (epsilon 3)	*Grin2c* (1.32±0.02)*	Glutamate receptor, ionotropic, NMDA2C (epsilon 3)	*Grin2c* (1.35±0.05)*
	Gamma-aminobutyric acid (GABA) A receptor, subunit alpha 5	*Gabra5* (-1.25)**±0.03	Glutamate receptor, metabotropic 4	*Grm4* (1.34±0.01)*
	Glutamate receptor, metabotropic 3	*Grm3* (-1.31±0.03)**	Nerve growth factor receptor (TNFR superfamily, member 16)	*Ngfr* (-1.80±0.33)*
	Glutamate receptor, metabotropic 5	*Grm5* (-1.31±0.03)*		
	Glutamate receptor, ionotropic, NMDA2B (epsilon 2)	*Grin2b* (1.31±0.07)*		
	Glutamate receptor, ionotropic, AMPA1 (alpha 1)	*Gria1* (-1.36+0.03)**		
	Cannabinoid receptor 1 (brain)	*Cnr1* (-1.37±0.08)**		
	Glutamate receptor, metabotropic 8	*Grm8* (-1.73±0.15)**		
	Glutamate receptor, ionotropic, AMPA2 (alpha 2)	*Gria2* (1.84±0.18)**		
	Nerve growth factor receptor (TNFR superfamily, member 16)	*Ngfr* (-2.29±0.26)**		

Table 15: Significantly changed expression of genes associated to the gene affiliation "neuronal receptors" from cortex at doses of 0.5 Gy and 1.0 Gy using RT² Profiler PCR Arrays.
The table shows the genes which are significantly up-regulated or down-regulated with the fold-changes±SEM in brackets and its p-value; *p<0.05; **p<0.01; ***p<0.001 (unpaired Student´s t-test, n=3) after normalisation to the median of 84 target genes from each assays plate. The grouping of genes into the gene affiliation is after manufacturer; genes which are in one than one group arising according to the manufacturer were manually verified via literature

	Cortex - 0.5 Gy		Cortex - 1.0 Gy	
Gene affiliiation	Gene description	Gene symbol with fold-change±SEM and p-value	Gene description	Gene symbol with fold-change±SEM and p-value
Neuronal receptors	Glutamate receptor, metabotropic 8	*Grm8* (-1.35±0.10)*	Glutamate receptor, metabotropic 5	*Grm5* (1.33±0.04)**
			Glutamate receptor, metabotropic 7	*Grm7* (1.32±0.04)*
			Glutamate receptor, metabotropic 3	*Gria3* (1.21±0.06)*
			5-hydroxytryptamine (serotonin) receptor 7	*Htr7* (-1.25±0.10)*
			Prokineticin receptor 2	*Prokr2* (-1.99±0.16)**

Immediate-early / -late response genes are transcribed from activated transcription factors originating from the upstream signalling cascades regulated by neuronal receptors and its expression / activation status. Widely accepted nuclear transcription factors involved in learning and memory formation are the cAMP responsive element binding protein (CREB) and cAMP response element modulator (CREM) (Cortes-Mendoza et al., 2013, Greer and Greenberg, 2008). The crucial event in the activation of CREB is the phosphorylation of Ser133 in the kinase-inducible domain including consensus phosphorylation sites for Protein Kinase-A (PKA), Protein-Kinase-C (PKC), calmodulin kinases (Camk´s) and casein kinases (Csnk´s). All of them can either increase or decrease CREB activity (Johannessen and Moens, 2007, Johannessen et al., 2004).

Gene expression analysis showed alterations in the modulators and upstream-regulators of CREB such as protein kinases (Prk´s), adenylate cyclases (*Adcy´s*), serine/threonine-protein kinases (*Akt´s)*, calmodulin kinases (*Camk*), and casein kinases (*Csnk´s*) in both hippocampus (Table 16) and cortex (Table 17). Additionally, significant changes in the expression of *Creb1* in the hippocampus (0.5 Gy: -1.30 1 Gy: -1.35) and *Crem* in the cortex (0.5 Gy: -1.24) and hippocampus (0.5 Gy: -1.38; 1 Gy: -1.26) were noted.

As there are several forms of CREB protein, total CREB and phosphorylated CREB (Ser133) levels were further quantified by immunoblotting. A markedly decreased expression of total CREB protein accompanied with a slight increase in the phosphorylated form of CREB was found in both hippocampus and cortex at 1.0 Gy (Figure 20).

Table 16: Significantly changed expressed genes associated to the gene affiliation "Long-term potentiation / Long-term depression (LTP/LTD)" from hippocampus at doses of 0.5 Gy and 1.0 Gy using RT² Profiler PCR Arrays.
The table shows the genes which are significantly up-regulated or down-regulated with the fold-changes±SEM in brackets and its p-value; *p<0.05; **p<0.01; ***p<0.001 (unpaired Student´s t-test, n=3) after normalisation to the median of 84 target genes from each assays plate. The grouping of genes into the gene affiliation is according to the manufacturer; genes which are in more than in one group were manually verified via literature

	Hippocampus - 0.5 Gy		Hippocampus - 1.0 Gy	
Gene affiliation	Gene description	Gene symbol with fold-change±SEM and p-value	Gene description	Gene symbol with fold-change±SEM and p-value
Long-term potentiation / Long-term depression (LTP/ LTD)	Adenylate cyclase 1	*Adcy1* (1.36±0.09)*	Kinesin family member 17	*Kif17* (1.92±0.12)**
	Src homology 2 domain-containing transforming protein C1	*Shc1* (-1.27±0.02)*	Calcium/calmodulin-dependent protein kinase II alpha	*Camk2a* (1.42±0.03)*
	CAMP responsive element binding protein 1	*Creb1* (-1.30±0.14)*	Protein kinase, cAMP dependent regulatory, type I beta	*Prkar1b* (1.35±0.12)*
	Casein kinase 2, alpha 1 polypeptide	*Csnk2a1* (-1.34±0.11)*	Protein kinase C, beta	*Prkcb* (1.31±0.08)*
	CAMP responsive element modulator	*Crem* (1.38±0.06)**	Son of sevenless homolog 1	*Sos1* (1.21±0.02)***
	Protein phosphatase 2 (formerly 2A), catalytic subunit, alpha isoform	*Ppp2ca* (-1.44±0.13)**	Protein phosphatase 1, catalytic subunit, alpha isoform	*Ppp1ca* (-1.21±0.06)*
	RAB3A, member RAS oncogene family	*Rab3a* (1.45±0.17)*	Calcium/calmodulin-dependent protein kinase II, beta	*Camk2b* (1.23±0.04)*
	Glutamate receptor interacting protein 1	*Grip1* (-1.50±0.09)**	CAMP responsive element modulator	*Crem* (-1.26±0.06)*
	Adenylate cyclase 8	*Adcy8* (-1.59±0.06)**	Calcium/calmodulin-dependent protein kinase II gamma	*Camk2g* (-1.31±0.05)**
	Protein phosphatase 1, catalytic subunit, alpha isoform	*Ppp1ca* (-1.67±0.21)**	CAMP responsive element binding protein 1	*Creb1* (-1.35±0.09)**
	Calcium/calmodulin-dependent protein kinase II gamma	*Camk2g* (-1.68±0.16)**	Phosphatase and tensin homolog	*Pten* (-1.38±0.03)*
	Phosphatase and tensin homolog	*Pten* (-1.91±0.21)**	Conserved helix-loop-helix ubiquitous kinase	*Chuk* (-1.38±0.03)*
	Conserved helix-loop-helix ubiquitous kinase	*Chuk* (-5.88±5.58)*	GTPase Hras	*Hras1* (-2.03±0.47)*

Table 17: Significantly changed expressed genes associated to the gene affiliation "Long-term potentitiation / Long-term depression (LTP/LTD)" from cortex at doses of 0.5 Gy and 1.0 Gy using RT² Profiler PCR Arrays.
The table shows the genes which are significantly up-regulated or down-regulated with the fold-changes ± SEM in brackets and its p-value; *p<0.05; **p<0.01; ***p<0.001 (unpaired Student´s t-test, n=3) after normalisation to the median of 84 target genes from each assays plate. The grouping of genes into the gene affiliation is according to the manufacturer; genes which are in more than in one group were manually verified via literature

	Cortex - 0.5 Gy		Cortex - 1.0 Gy	
Gene affiliation	Gene description	Gene symbol with fold-change±SEM and p-value	Gene description	Gene symbol with fold-change±SEM and p-value
Long-term potentiation / Long-term depression (LTP / LTD)	Phosphatidylinositol 3-kinase, regulatory subunit, polypeptide 2 (p85 beta)	*Pik3r2* (1.60±0.23)*	Kinesin family member 17	*Kif17* (1.89±0.15)***
	Rac-beta serine / theronine protein kinase	*Akt2* (1.34±0.06)***	Ras-related protein Rab-3A	*Rab3a* (1.38±0.04)**
	Calcium/calmodulin-dependent protein kinase II alpha	*Camk2a* (1.25±0.08)*	Protein phosphatase 3, catalytic subunit, alpha isoform	*Ppp3ca* (1.36±0.08)*
	Protein kinase C, beta	*Prkcb* (1.23±0.08)*	Calcium/calmodulin-dependent protein kinase II gamma	*Camk2g* (1.32±0.07)*
	Protein phosphatase 2 (formerly 2A), catalytic subunit, alpha isoform	*Ppp2ca* (-1.23±0.06)*	Protein interacting with C kinase 1	*Pick1* (1.20±0.04)*
	CAMP responsive element modulator	*Crem* (-1.24±0.05)*	Protein kinase C, alpha	*Prkca* (-1.23±0.05)**
	Protein phosphatase 1, catalytic subunit, alpha isoform	*Ppp1ca* (-1.32±0.10)*	Mitogen-activated protein kinase 3	*Mapk3* (-1.23±0.04)**
	Adenylate cyclase 8	*Adcy8* (-1.33±0.04)**	Casein kinase 2, alpha prime polypeptide	*Csnk2a2* (-1.23±0.06)*
	Ras-related protein Rab-3A	*Rab3a* (-1.35±0.11)*	Casein kinase 1, alpha 1	*Csnk1a1* (-1.24±0.03)**
	Rac-gamma serine / theronine protein kinase	*Akt3* (-1.44±0.09)*	Methionine adenosyltransferase II, alpha	*Mat2a* (-1.26±0.05)*
	Phosphatase and tensin homolog	*Pten* (-1.45±0.10)*	Casein kinase 2, alpha 1 polypeptide	*Csnk2a1* (-1.29±0.05)*
	Casein kinase 2, alpha 1 polypeptide	*Csnk2a1* (-1.42±0.05)***	Nitric oxide synthase 1, neuronal	*Nos1* (-1.33±0.04)***
			Casein kinase 1, epsilon	*Csnk1e* (-1.35±0.08)*
			GTPase Hras	*Hras1* (-2.87±0.48)**

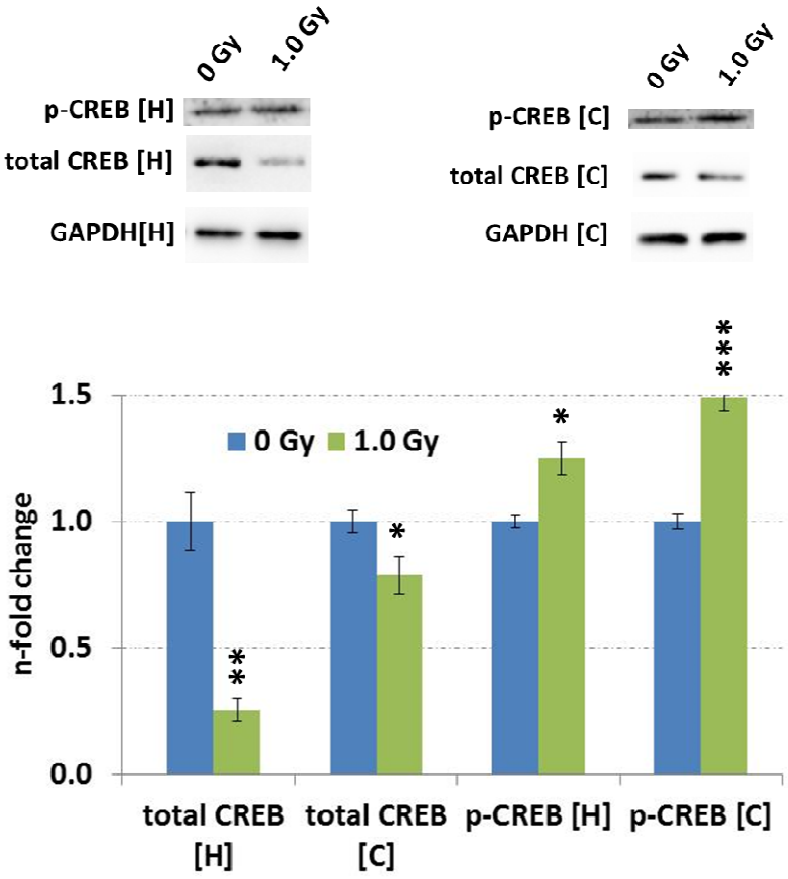

Figure 20: Immunoblotting of CREB and phosphorylated CREB in hippocampus and cortex of sham-irradiated and 1.0 Gy irradiated mice 7 months post-irradiation.
The columns represent the fold-changes with standard errors of the mean (SEM) from three biological replicates. The visualisation of protein bands shows the representative change from three biological replicates. *p<0.05; **p<0.01; ***p<0.001 (unpaired Student´s t-test). Normalisation was performed against endogenous GAPDH; H: Hippocampus, C: Cortex

Learning processes may be affected by changes in the circadian clock through modulation of LTP / LTD signalling pathways (Nakatsuka and Natsume, 2014, Chaudhury et al., 2005). Thus, gene expression analysis to quantify alterations in circadian rhythm was performed in 1.0 Gy exposed mice as alterations in CREB and p-CREB levels were detected at this dose in cortex and hippocampus.

Quantification of circadian clock genes showed significant alterations in 2 out of 14 genes (Table 35) in the cortex (downregulation of *Arntl*; upregulation of *Bhihe41*) and 4 out of 14 (Table 35) in the hippocampus (upregulation of *Arntl2, Bhihe41, Per1,*

Cry2) at 1.0 Gy (Table 18). Further, quantification of a panel of 35 circadian-rhythm regulated transcription factors / -regulated genes (Table 35) showed that 12 were significantly changed in the cortex (upregulation: *Tef*; downregulation: *Wee1, Tgfb1, Sp1, Stat5a, Nr2f6, Npas2, Ccrn4l, Cartpt, Prf1, Nfil3, Epo*) and 2 in the hippocampus (upregulation: *Srebf1*; downregulation: *Epo*) at 1.0 Gy (Table 18).

Table 18: Significantly changed expressed genes associated to the gene affiliation "circadian rhythm" from cortex and hippocampus at doses of 1.0 Gy using RT² Profiler PCR Arrays.
The table shows the genes which are significantly up-regulated or down-regulated with the fold-changes±SEM in brackets and its p-value; *p<0.05; **p<0.01; ***p<0.001 (unpaired Student´s t-test, n=3) after normalisation to the median of 84 target genes from each assays plate. The grouping of genes into the gene affiliation is according to the manufacturer; genes which are in more than in one group were manually verified via literature

	Cortex - 1.0 Gy			Hippocampus - 1.0 Gy	
Gene affiliation	Gene description	Gene symbol with fold-change±SEM and p-value	Gene affiliation	Gene description	Gene symbol with fold-change±SEM and p-value
Circadian rhythm	Thyrotroph embryonic factor	Tef (1.30±0.02)*	Circadian rhythm	Aryl hydrocarbon receptor nuclear translocator-like 2	*Arntl2* (2.32±0.24)*
	Basic helix-loop-helix family, member e41	Bhlhe41 (1.28±0.03)*		Basic helix-loop-helix family, member e41	*Bhlhe41* (1.63±0.19)*
	WEE 1 homolog 1 (S. pombe)	Wee1 (-1.21±0.03)*		Sterol regulatory element binding transcription factor 1	*Srebf1* (1.30±0.02)***
	Transforming growth factor, beta 1	Tgfb1 (-1.22±0.02)*		Period homolog 1 (Drosophila)	*Per1* (1.24±0.09)*
	Trans-acting transcription factor 1	Sp1 (-1.26±0.04)**		Cryptochrome 2 (photolyase-like)	*Cry2* (1.24±0.05)*
	Signal transducer and activator of transcription 5A	Stat5a (-1.43±0.10)*		Erythropoietin	*Epo* (-5.09±1.80)*
	Nuclear receptor subfamily 2, group F, member 6	Nr2f6 (-1.49±0.06)***			
	Neuronal PAS domain protein 2	Npas2 (-1.51±0.10)**			
	Aryl hydrocarbon receptor nuclear translocator-like	Arntl (-1.52±0.10)*			
	CCR4 carbon catabolite repression 4-like (S. cerevisiae)	Ccrn4l (-1.55±0.02)***			
	CART prepropeptide	Cartpt (-2.04±0.33)*			
	Nuclear factor, interleukin 3, regulated	Nfil3 (-2.20±0.16)*			
	Perforin 1 (pore forming protein)	Prf1 (-4.22±1.07)*			
	Erythropoietin	Epo (-5.12±1.25)*			

Due to the several changes of circadian clock genes showing significant expression changes in the irradiated hippocampus, the CREB-miR-132-regulated chromatin

remodelling gene *Mecp2* (Methyl-CpG-binding protein 2) (Klein et al., 2007) was quantified on gene expression level as an increase in miR-132 levels was noted at 0.5 Gy and 1.0 Gy in the hippocampus (Figure 17). The *Mecp2* gene is a broad transcriptional regulator by chromatin remodelling with implications in Rett syndrome, a neurodevelopmental disorder; mutations in *Mecp2* are a common genetic cause of mental retardation (Heckman et al., 2014). Irradiation with 0.5 Gy and 1.0 Gy induced a significant decrease in the mRNA expression level of *Mecp2* in the hippocampus (Figure 21); lower doses were not tested.

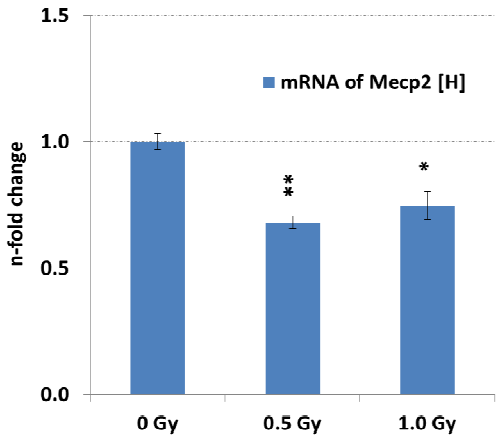

Figure 21: Gene expression levels of *Mecp2* in hippocampus at doses of 0, 0.5 Gy and 1.0 Gy.
Normalisation was performed against endogenous *Gapdh;* columns represent the fold-changes with standard errors of the mean (SEM) from 3 biological replicates; *p<0.05; **p<0.01; ***p<0.001 (unpaired Student´s t-test); H: Hippocampus, C: Cortex

7.6 Irradiation impairs adult neurogenesis in the hippocampus

A considerable amount of data has been obtained in the field of adult neurogenesis and ionising radiation at relatively high doses (Rola et al., 2004a, Allen et al., 2013, Raber et al., 2004, Mizumatsu et al., 2003) but neither at low doses nor after longer follow-up time point.

Adult neurogenesis in the hippocampal region of subgranular zone (SGZ) of the dentate gyrus (DG) was elucidated in more detail using immunohistochemistry. This work was done under technical assistance with J. Mueller and D. Janik (Institute of Pathology, Helmholtz Centre Munich, Munich, Germany). Proneural markers

expressed during specific stages of adult neurogenesis from defined subpopulations were used to characterise changes 7 month post-irradiation. These markers were antigen Ki67 to quantify the number of proliferating progenitors and neuronal nuclear antigen NeuN to quantify mature granule neurons (Namba et al., 2005).

A marked reduction of proliferating precursor cells in the DG labelled with Ki67 at doses of 0.1 Gy, 0.5 Gy and 1.0 Gy was noted (Figure 22 A and B). Moreover, quantification of $NeuN^+$-cells demonstrated reductions of this population in the crest area, suprapyramidal- and infrapyramidal-blade area of DG based on 4000 μm^2 of counted areas (Figure 22 C and D). The combined data from these three subregions showed significant dose-dependent reductions in the number of NeuN-labelled cells at 0.1 Gy, 0.5 Gy and 1.0 Gy in the whole DG (Figure 22 C and D).

Importantly, mRNA expression analysis of *Bad* – a cell death promoting gene - indicated the absence of radiation-persistent apoptosis in both hippocampus and cortex at 0.5 Gy and 1.0 Gy (Figure 23) suggesting that the observed alterations in adult neurogenesis marker were not due to radiation-induced persistent apoptotic cell death.

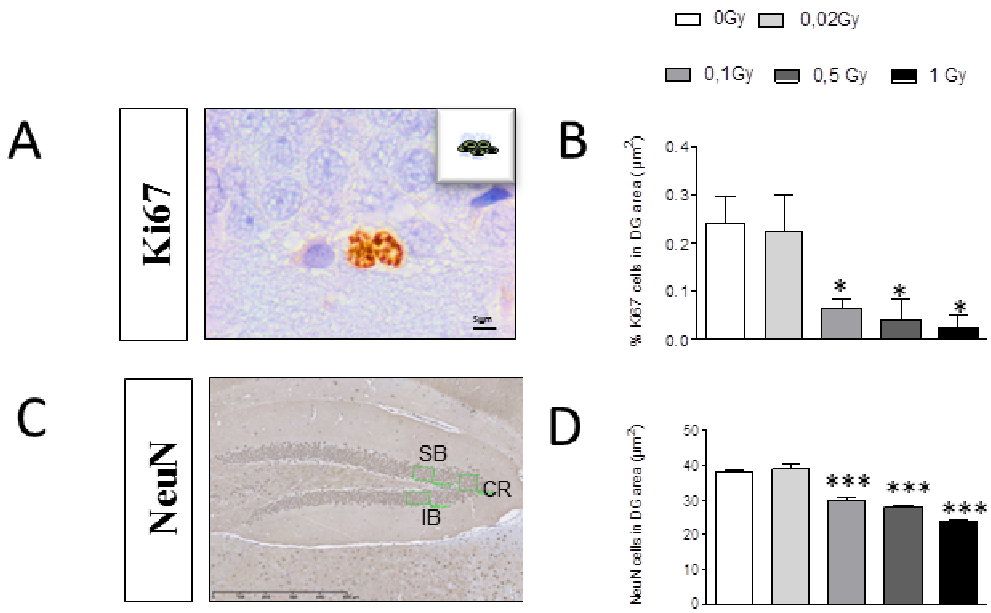

Figure 22: Representative image of proliferating progenitor cells labelled with Ki67 (A) and mature neurons labelled with NeuN (C) and relative quantifications (B, D).

$NeuN^+$ cells were counted in 4000 μm^2 areas (in green). *p<0.05; **p<0.01; ***p<0.001 (unpaired Student´s t-test). Data are reported as mean ± S.E.M (n=3 for Ki67, n≥3 for NeuN); DG, dentate gyrus; CR, crest area of dentate gyrus; SB, suprapyramidal blade of dentate gyrus; IB, infrapyramidal blade of dentate gyrus

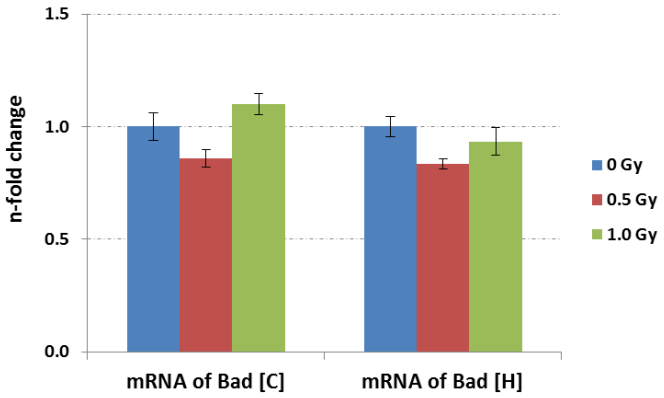

Figure 23: Evaluation of persistent radiation-induced apoptosis
Bad mRNA expression using RT^2 Profiler PCR Arrays 7 month post-irradiation in hippocampus and cortex at 0.5 Gy and 1.0 Gy; n=3, error bars representing SEM, *p<0.05; **p<0.01; ***p<0.001 (unpaired Student´s t-test). Data were normalised to the median of 84 target genes; C: Cortex; H: hippocampus

7.7 Radiation exposure induces neuroinflammation

Next, neuroinflammation was quantified within the hippocampus. It is known that neuroinflammation plays a role in neurocognitive disorders such as Alzheimer´s and in cognitive decline (Daulatzai, 2014).

As neuroinflammation is characterised by an increase of cytokines during inflammatory responses, the cytokine TNFα was quantified both at gene and protein expression level. An increased *TNFα* expression was noted in the hippocampus at 1.0 Gy whereas levels were unchanged at 0.5 Gy (Figure 24). This is consistent with TNFα protein levels at 1.0 Gy (Figure 24).

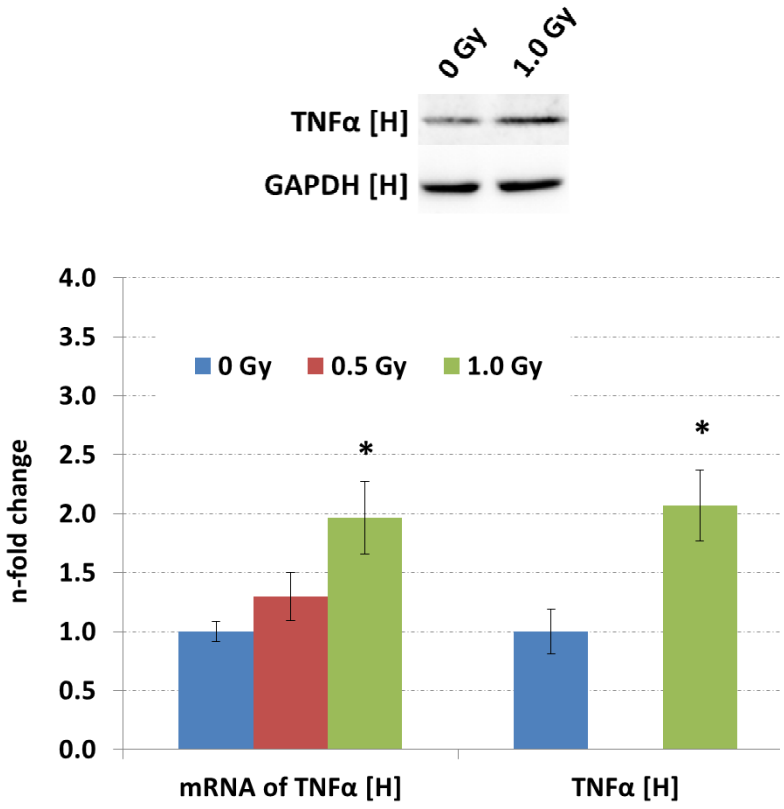

Figure 24: Gene expression analysis / immunoblots of TNFα within the hippocampus [H].
All data are reported as fold-change ± S.E.M (n=3); *p<0.05; **p<0.01; ***p<0.001 (unpaired Student´s t-test). Data normalisation was done against *Gapdh* (mRNA expression) and Gapdh (immunoblotting).

7.8 Radiation exposure may lead to changes in neuroprotective capacity

As neuroinflammation may increase oxidative stress (di Penta et al., 2013), the level of total malondialdehyde-modified protein content was quantified as a marker for the oxidative stress of lipid peroxidation. Reactive radicals produced under oxidative stress cause oxidation of polyunsaturated fatty acids such as arachidonic acids in lipid membranes (lipid peroxidation) and can elevate in that way modified proteins such as malondialdheyde-modified proteins (Pizzimenti et al., 2013). As lipid polyunsaturated fatty acids are highly enriched in synaptic membranes (Marza et al., 2008), the quantification of malondialdehyde-modified proteins serves as a good marker for the oxidative stress of lipid peroxidation. The method of immunoblotting

was used to get from several quantifiable bands a more detailed evaluation of the malondialdehyde-modified protein content. The analysis demonstrated a significant decrease at 1.0 Gy in the hippocampus (Figure 25) but not in the cortex (Figure 26).

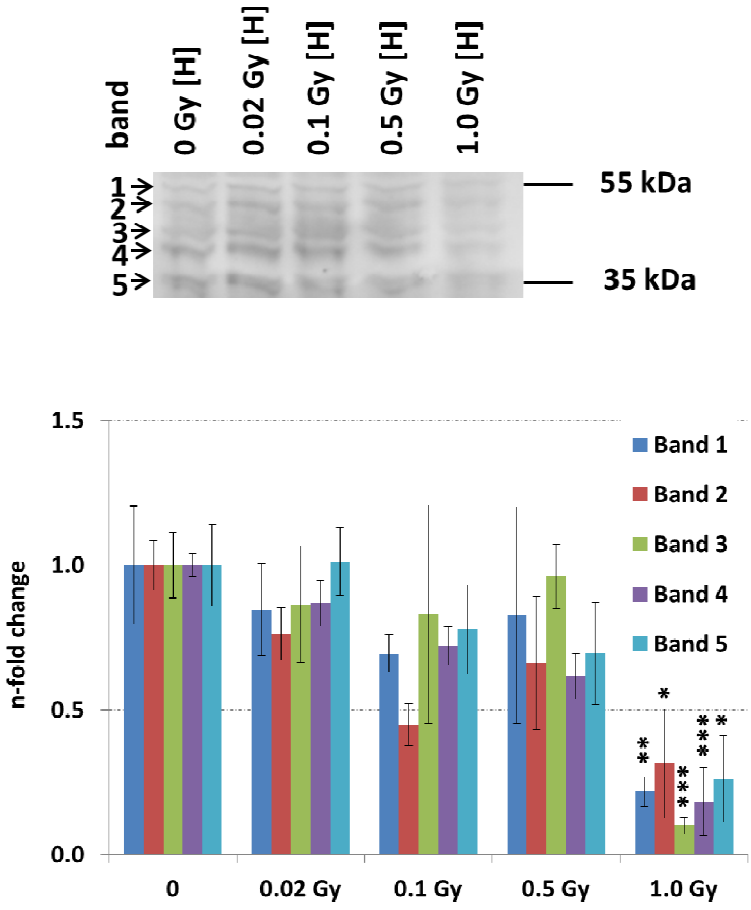

Figure 25: Immunoblot of total malondialdehyde (MDA)-tagged proteins within the hippocampus [H] at all doses.
The visualisation of protein bands shows the representative change from the biological replicates; MDA content quantification was performed with 5 bands in the range of 35 kDa to 55 kDa after total lane normalisation in hippocampus. All data are reported as fold-change ± S.E.M (n=4 for immunoblotting against MDA content); *p<0.05; **p<0.01; ***p<0.001 (unpaired Student´s t-test)

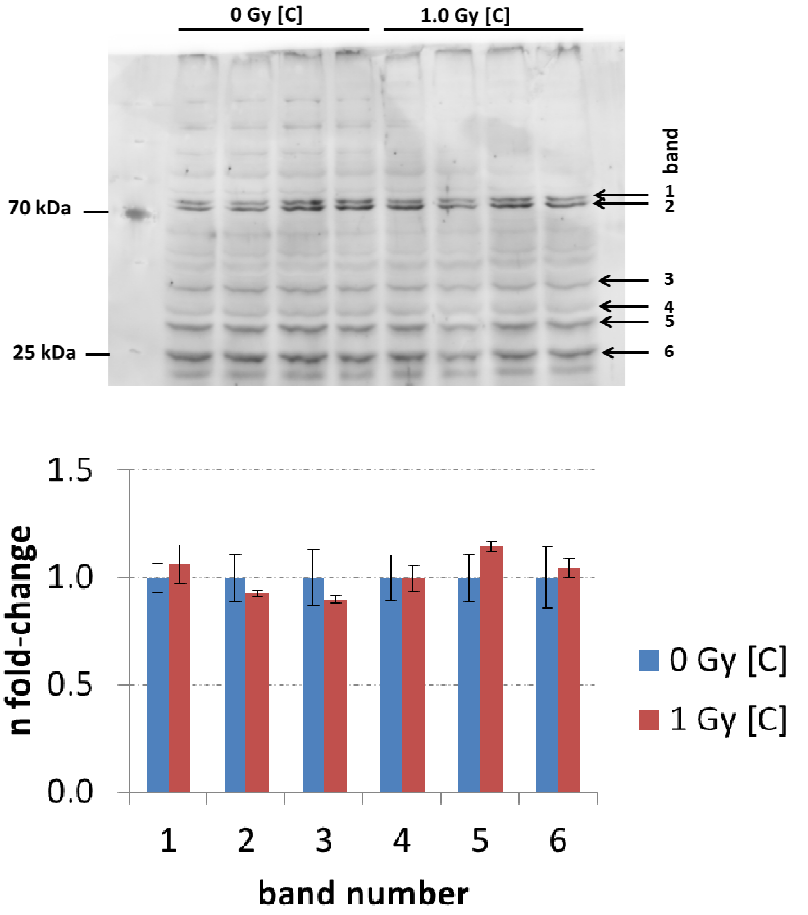

Figure 26: Immunoblot of total malondialdehyde (MDA)-tagged proteins within the cortex [C] at 1.0 Gy.
The visualisation of protein bands shows the representative change from the biological replicates; MDA content quantification was performed with 6 bands in the range of 25 kDa and 70 kDa after total lane normalisation. All data are reported as fold-change ± S.E.M (n=4 for immunoblotting against MDA content); *p<0.05; **p<0.01; ***p<0.001 (unpaired Student´s t-test)

The decrease of oxidative stress characterised by evaluation of malondialdehyde-modified proteins is against the observation of increased neuroinflammation. It is known that the IGF-1 pathway may reduce the level of oxidative stress (Grinberg et al., 2012). Immunoblotting demonstrated an increase in the phosphorylation status of insulin-like growth factor receptor β / insulin receptor β (IGF1Rβ / INSRβ) in the hippocampus at 1.0 Gy (Figure 27) indicative for activation of the IGFR1 / INSR signalling pathway.

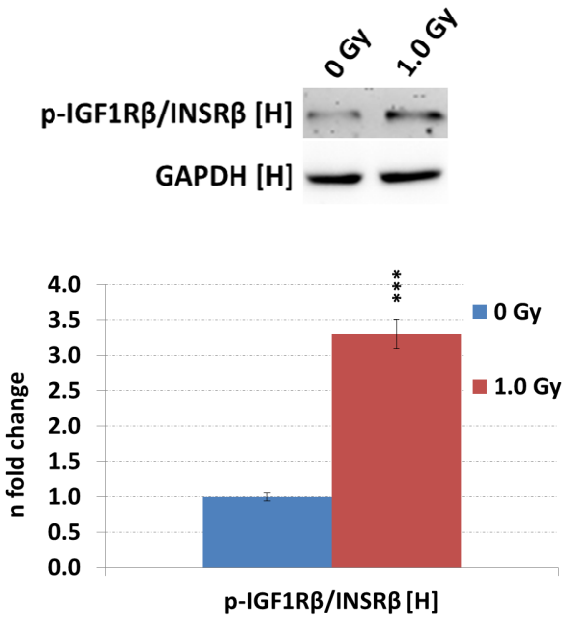

Figure 27: Immunoblots of phospho-IGF1Rβ / INSRβ within the hippocampus [H]. The visualisation of protein bands shows the representative change from the biological replicates. Data are reported as mean / fold-change ± S.E.M (n=3) *p<0.05; **p<0.01; ***p<0.001 (unpaired Student´s t-test)

Results from the C57BL/6 mouse study

Next, we wanted to investigate whether the radiation-induced alteration in the brain were comparable in a different mouse model. For this purpose, we analysed C57BL/6 female mice. Similar to the NMRI mouse study, C57BL/6 mice were irradiated with 0 Gy (sham irradiated control), 0.1 Gy, 0.5 Gy and 2.0 Gy (total body) on PND10; 2.0 Gy was used to mimic the radiation dose used in the fractionated radiotherapy and thus get more clinically relevant information from side-effects. Follow-up time points were 4 weeks or 5 weeks and 24 weeks post-irradiation to trace the radiation-induced manifestation in synaptic signalling pathways in the hippocampus and cortex. The animals were irradiated at the Erasmus Medical Centre – Department of Genetics, Rotterdam (S. Sepe, P. G. Mastroberardino) and were shipped to Helmholtz Centre Munich, Munich, Germany for molecular analysis.

7.9 Radiation-induced changes in actin cytoskeleton-associated signalling pathways are persistent in the hippocampus and cortex

Global quantitative proteome analysis via liquid-chromatography-mass-spectrometry (LC-MS) was performed to quantify alterations in hippocampal and cortical proteins at 4 weeks and 24 weeks post-irradiation. Enzymatic protein digestion and performance of LC-MS/MS runs were done by S. Helm and C. von Toerne (Department of Protein Science, Helmholtz Centre Munich, Munich, Germany). The deregulated proteins are depicted in Table 27, Table 28, Table 29 and Table 30 (Supplementary information). The protein quantification showed significantly changed proteins at 4 weeks post-irradiation (cortex/hippocampus: 0.1 Gy – 9/4 proteins, 0.5 Gy – 31/24 proteins, 2.0 Gy - 14/10 proteins) and 24 weeks post-irradiation (cortex/hippocampus: 0.1 Gy – 6/6 proteins, 0.5 Gy – 22/29 proteins, 2.0 Gy – 29/11 proteins) (Figure 28 and Figure 29). Interestingly, the overall highest number of deregulated proteins was found at 0.5 Gy and that is quantitatively similar to NMRI study (7 month post-irradiation: 34 deregulated proteins in hippocampus, 27

deregulated proteins in cortex). Annotation of the deregulated proteins into protein classes demonstrated that a large number of proteins were changed at later time points at 0.5 Gy and 2.0 Gy in cortex (4 weeks – 0.5 Gy: 29 %; 2.0 Gy: 7 % and 24 weeks - 0.5 Gy: 27 %; 2.0 Gy: 10 %) and hippocampus (4 weeks – 0.5 Gy: 20 %; 2.0 Gy: 4 % and 24 weeks - 0.5 Gy: 17 %; 2.0 Gy: 33 %) that belonged to the protein class of cytoskeleton / cytoskeleton-associated proteins (Figure 28 and Figure 29; Table 27, Table 28, Table 29 and Table 30 [Supplementary information]). However, doses of 0.1 Gy showed only some hits in this protein class mainly at 0.1 Gy in the cortex 4 weeks post-irradiation.

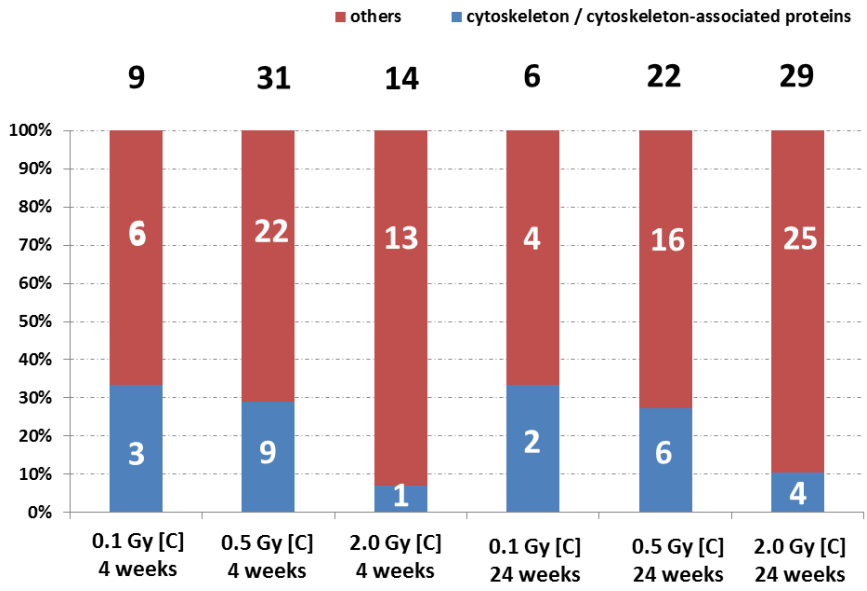

Figure 28: Comparable representation of the number of deregulated proteins from global proteomics approach (C57BL/6 mouse study) at 4 weeks and 24 weeks post-irradiation in cortex grouped into the protein class cytoskeleton / cytoskeleton-associated proteins and others.

The classes are based on information from the PANTHER software (PANTHER protein class) and UniProt-database. The numbers within the columns represent the number of proteins involved in this protein class. The number above the columns represents the total number of deregulated proteins at this dose and brain region; C: Cortex; n=6 in dose group

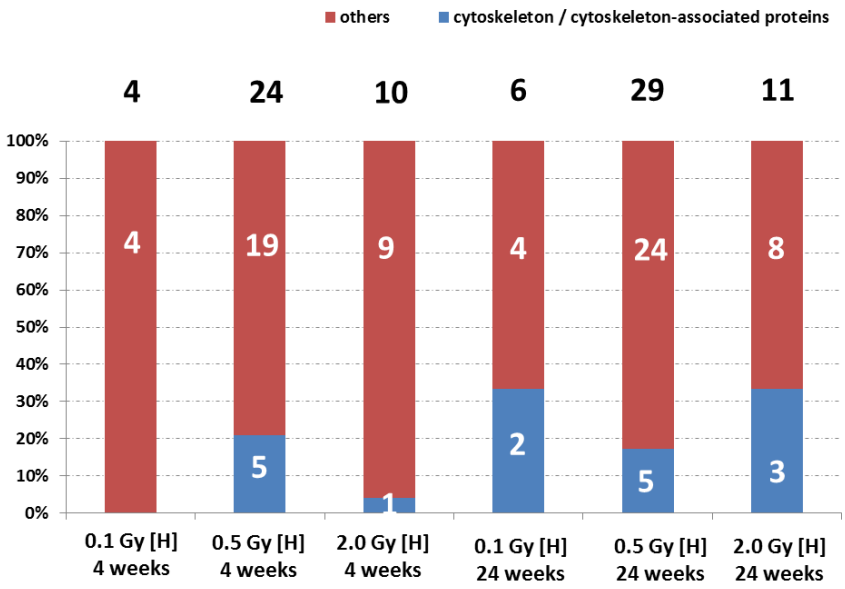

Figure 29: Comparable representation of the number of deregulated proteins from global proteomics approach (C57BL/6 mouse study) at 4 weeks and 24 weeks post-irradiation in hippocampus grouped into the protein class cytoskeleton / cytoskeleton-associated proteins and others.
The classes are based on information from the PANTHER software (PANTHER protein class) and UniProt-database. The numbers within the columns represent the number of proteins involved in this protein class. The number above the columns represents the total number of deregulated proteins at this dose and brain region; H: Hippocampus; n=6 in dose group

Next, Ingenuity pathway analysis of all the deregulated proteins showed that the signalling pathways ephrin B / ephrin receptor signalling, signalling by Rho family GTPases, RhoGDI signalling and axonal guidance signalling were persistently altered after radiation exposure at 0.5 Gy and 2.0 Gy 4 weeks and 24 weeks post-irradiation (Figure 30). Importantly, signalling pathways were not significantly altered 24 weeks post-irradiation in cortex and hippocampus at 0.1 Gy dose. This observation is comparable to NMRI mouse study showing defects at 0.5 Gy and 1.0 Gy in both brain regions.

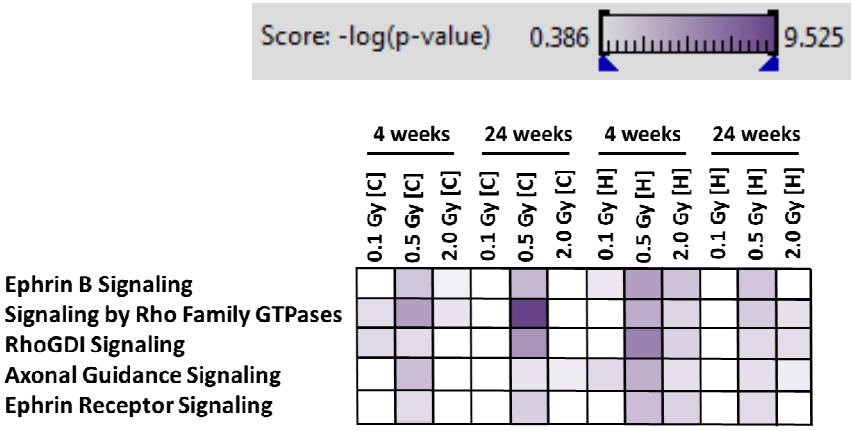

Figure 30: Associated signalling pathways to all deregulated proteins found in hippocampus and cortex 4 weeks and 24 weeks post-irradiation using the Ingenuity Pathway Analysis (IPA) software.
Higher colour intensity represents higher significance (p-value) whereas all coloured boxes have a p-value of ≤ 0.05. Hippocampal and cortical data result from six biological replicates, respectively. H: Hippocampus, C: Cortex; n=6

7.10 Radiation-induced alterations in the Rac1-Cofilin pathway are persistent in hippocampus and cortex

Next, using immunoblotting and miRNA quantification, the Rac1-Cofilin signalling pathway was studied in more detail 24 weeks post-irradiation as this was the optimal follow-up time point to evaluate potential persistent radiation-induced changes. Figure 31 shows that Rac1 levels were significantly reduced in both hippocampus and cortex (0.5 Gy and 2.0 Gy) correlating with mass spectrometry data (24 weeks: hippocampus – 0.5 Gy: -1.31; 2.0 Gy: -1.39 and cortex – 0.5 Gy: -1.33; 2.0 Gy: -1.35 (Table 29 and Table 30 [Supplementary information]). Furthermore, proteomics data showed that the reduced Rac1 protein levels post-irradiation were also found at 4 weeks (4 weeks: hippocampus – 0.5 Gy: -1.36; 2.0 Gy: -1.31 and cortex – 0.5 Gy: -1.47; 2.0 Gy: -1.30 (Table 27 and Table 28 [Supplementary information]). In addition, the downstream modulator cofilin was significantly increased in hippocampus (0.5 Gy and 2.0 Gy) and cortex (0.1 Gy, 0.5 Gy and 2.0 Gy) at the protein level (Figure 31). The phosphorylated form of cofilin was reduced only at 2.0 Gy in the cortex but not in the hippocampus at any dose (Figure 31). Persistent reductions in Rac1 levels

were similarly noted in the NMRI mouse study accompanied with imbalances in the cofilin / phospho-cofilin ratios favouring cofilin.

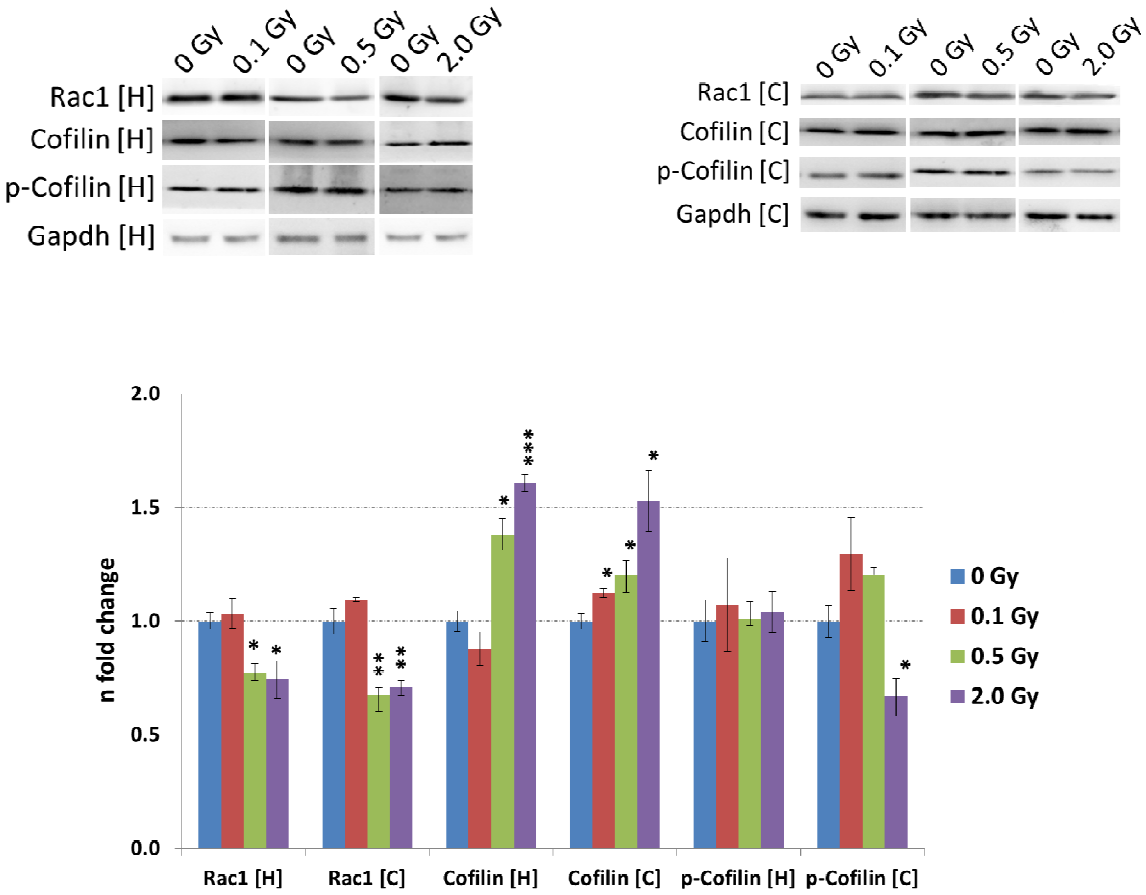

Figure 31: Data from immunoblots associated to the Rac1-Cofilin pathway in hippocampus and cortex from sham-irradiated, 0.1 Gy, 0.5 Gy and 2.0 Gy exposed mice 6 month post-irradiation.
The columns represent the fold-changes with standard errors of the mean (SEM) from three biological replicates. The visualisation of protein bands shows the representative change from three biological replicates. *p<0.05; **p<0.01; ***p<0.001 (unpaired Student´s t-test). Normalisation was performed against endogenous GAPDH; H: Hippocampus, C: Cortex

Expression levels of miR-132 were significantly increased in both cortex and hippocampus at all doses 24 weeks post-irradiation whereas miR-134 was significantly increased in cortex (0.1 Gy, 0.5 Gy and 2.0 Gy). In hippocampus, miR-134 levels were decreased at 0.1 Gy, unchanged at 0.5 Gy and increased at 2.0 Gy (Figure 32). The overall increase in these two miRNAs is comparable with those obtained from the NMRI mouse study.

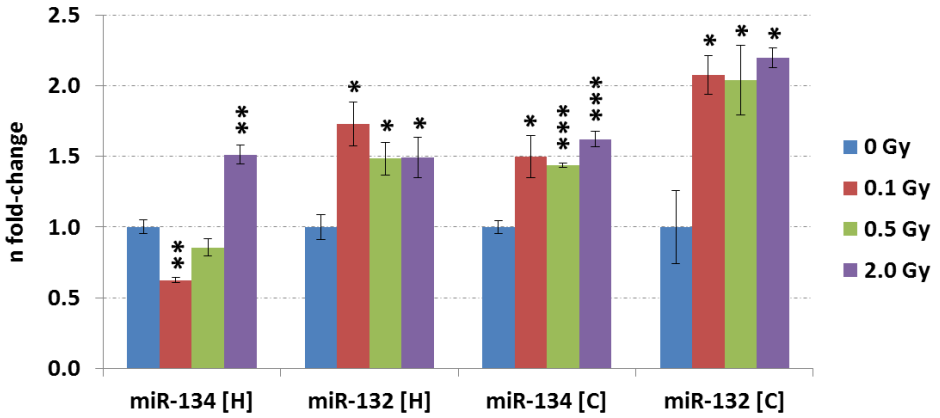

Figure 32: Data from miRNA quantification associated to the Rac1-Cofilin pathway in hippocampus and cortex from sham-irradiated, 0.1 Gy, 0.5 Gy and 2.0 Gy exposed mice 6 month post-irradiation.
The columns represent the fold-changes with standard errors of the mean (SEM) from three biological replicates. *p<0.05; **p<0.01; ***p<0.001 (unpaired Student´s t-test). Normalisation was performed against endogenous snoRNA135; H: Hippocampus, C: Cortex

7.11 Radiation-induced changes in neuronal receptor expression and processes in LTP / LTD signalling pathways

Similar to NMRI mouse study, alterations in the mRNA expression of neuronal receptors and LTP / LTD signalling pathways were observed but only at 2.0 Gy 24 weeks post-irradiation in both brain regions; 4 weeks post-irradiation time point was not analysed. Gene expression analysis demonstrated an increase in ephrin receptor B2 mRNA expression (*Ephb2*) only in the cortex at the highest dose (2.0 Gy) but not in the hippocampus (Table 19). Further, alterations in mainly G-protein coupled receptors for glutamate (*Grm´s*) but also in α-amino-3-hydroxy-5-methyl-4-isoxazolepropionic acid receptor (AMPA)-selective glutamate receptors (*Gria´s*) and N-methyl-D-aspartate (NMDA) receptors (*Grin´s*) in hippocampus and cortex only at 2.0 Gy were found but not at lower doses (0.1 Gy and 0.5 Gy) (Table 19). A number of G-protein coupled receptors for glutamate were up-regulated in the cortex at 2.0 Gy (*Grm1, Grm3, Grm4 and Grm7*) whereas in the hippocampus, there was only one significantly reduced mRNA at 2.0 Gy (*Grm5*) (Table 19).

Table 19: Significantly changed expressed genes associated to the gene affiliation "neuronal receptors" from cortex and hippocampus at 2.0 Gy using RT² Profiler PCR Array "Synaptic plasticity".
The table shows the genes which are significantly up-regulated or down-regulated with the fold-changes±SEM in brackets and its p-value; *p<0.05; **p<0.01; ***p<0.001 (unpaired Student´s t-test, n=3) after normalisation to the median of 84 target genes from each assays plate

	Cortex - 2.0 Gy			Hippocampus - 2.0 Gy	
Gene affiliation	Gene description	Gene symbol with fold-change±SEM and p-value	Gene affiliation	Gene description	Gene symbol with fold-change±SEM and p-value
Neuronal receptors	Eph receptor B2	*Ephb2* (1.42±0.13)*	Neuronal receptors	Gamma-aminobutyric acid (GABA) A receptor, subunit alpha 5	*Gabra5* (-5.74±1.72)**
	Glutamate receptor, ionotropic, AMPA4 (alpha 4)	*Gria4* (1.49±0.08)**		Glutamate receptor, ionotropic, AMPA1 (alpha 1)	*Gria1* (-5.43±1.80)*
	Glutamate receptor, ionotropic, NMDA2A (epsilon 1)	*Grin2a* (1.47±0.13)*		Glutamate receptor, ionotropic, AMPA2 (alpha 2)	*Gria2* (-3.29±1.10)*
	Glutamate receptor, ionotropic, NMDA2C (epsilon 3)	*Grin2c* (1.37±0.11)*		Glutamate receptor, metabotropic 5	*Grm5* (-2.43±0.69)*
	Glutamate receptor, metabotropic 1	*Grm1* (1.39±0.16)*			
	Glutamate receptor, metabotropic 3	*Grm3* (1.37±0.09)*			
	Glutamate receptor, metabotropic 4	*Grm4* (1.46±0.14)*			
	Glutamate receptor, metabotropic 7	*Grm7* (1.20±0.02)**			

To verify if the changes in the neuronal receptor profile may affect intracellular protein kinases and phosphates playing an important role in LTP / LTD processes, a subset of these proteins were quantified on the gene expression level. This showed that protein kinases and phosphates were only deregulated at 2.0 Gy but not at lower doses (0.1 Gy and 0.5 Gy) in cortex and hippocampus 24 weeks post-irradiation (Table 20) correlating with the observations on the altered neuronal receptor profile quantification only at this dose.

Table 20: Significantly changed expressed genes associated to the gene affiliation "Protein kinases and phosphatases involved in LTP/LTD" from cortex and hippocampus at 2.0 Gy using RT² Profiler PCR Array "Synaptic plasticity".

The table shows the genes which are significantly up-regulated or down-regulated with the fold-changes±SEM in brackets and its p-value; *p<0.05; **p<0.01; ***p<0.001 (unpaired Student´s t-test, n=3) after normalisation to the median of 84 target genes from each assays plate

	Cortex - 2.0 Gy			Hippocampus - 2.0 Gy	
Gene affiliation	Gene description	Gene symbol with fold-change±SEM and p-value	Gene affiliation	Gene description	Gene symbol with fold-change±SEM and p-value
Protein kinases and phosphates involved in LTP and LTD	Protein phosphatase 1, regulatory (inhibitor) subunit 14A	*Ppp1r14a* (1.40±0.11)*	Protein kinases and phosphates involved in LTP and LTD	Protein phosphatase 1, catalytic subunit, gamma isoform	*Ppp1cc* (-3.08±0.80)*
	Protein kinase C, alpha	*Prkca* (1.28±0.03)*		Protein phosphatase 3, catalytic subunit, alpha isoform	*Ppp3ca* (-2.67±0.80)*
	Protein kinase C, gamma	*Prkcc* (1.30±0.05)*		Protein kinase C, alpha	*Prkca* (-2.71±0.73)*
	Protein kinase, cGMP-dependent, type I	*Prkg1* (1.33±0.02)**		Protein kinase C, gamma	*Prkcc* (2.95±0.88)*
				Protein kinase, cGMP-dependent, type I	*Prkg1* (-2.37±0.64)*

Taken together, the mRNA expression analysis of neuronal receptors and LTP / LTD associated molecules showed only at 2.0 Gy in both brain regions alterations in the C57Bl/6 mouse study. However, changes of mRNAs associated to these processes were also seen at lower doses (0.5 Gy) during analysis in NMRI mouse study at 7 months post-irradiation in hippocampus and cortex.

7.12 Radiation exposure lead to persistent alterations in synaptic proteins affecting synaptic signalling pathways and synaptic mitochondria

To get more insight into the deregulation of signalling pathways associated with synapses, synaptosomes were isolated from hippocampus and cortex samples at 5 weeks and 24 weeks post-irradiation followed by global mass spectrometry and signalling pathway analysis using the Ingenuity software.

a) Signalling pathways related to synaptic morphology and plasticity are affected by ionising radiation in isolated synaptosomes of hippocampus and cortex

Isolated and enriched synaptosomes from hippocampus and cortex were used to identify protein expression changes 5 weeks and 24 weeks post-irradiation at doses of 0.1 Gy, 0.5 Gy and 2.0 Gy by mass spectrometry-based protein quantification (ICPL approach). The isolation of intact and enriched synaptosomes was evaluated with mitochondrial respiration by Seahorse XF analyser and immunoblotting. The analysis showed that synaptosomes are intact and enriched after a workflow involving differential centrifugation and a Ficoll gradient density (see section 6.15).

Mass-spectrometry based protein analysis was done with technical assistance (enzymatic digestion of proteins, LC-MS/MS run performance) by S. Helm and C. von Toerne (Department of Protein Science, Helmholtz Centre Munich, Munich). All deregulated proteins identified from these experiments are listed in Table 31, Table 32, Table 33 and Table 34 (Supplementary information).

The protein quantification showed a dose-dependency in the number of significantly deregulated proteins 5 weeks post-irradiation (cortex/hippocampus: 0.1 Gy – 47/59 proteins, 0.5 Gy – 43/64 proteins, 2.0 Gy - 106/106 proteins) and 24 weeks post-irradiation (cortex/hippocampus: 0.1 Gy – 73/40 proteins, 0.5 Gy – 91/84 proteins, 2.0 Gy – 152/168 proteins) (Figure 33 and Figure 34) .

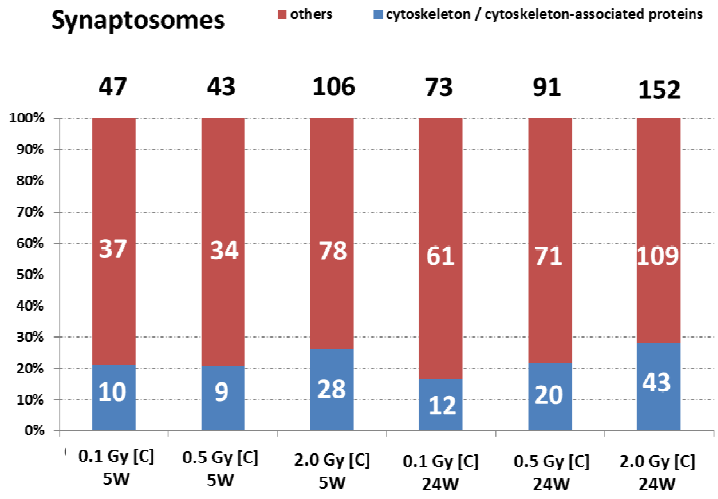

Figure 33: Comparative representation of the number of deregulated proteins from global proteomics approach (synaptosomes of C57BL/6 mouse study) at 5 weeks and 24 weeks post-irradiation in cortex grouped into the protein class "cytoskeleton / cytoskeleton-associated proteins" and "others".

The classes are based on information from the PANTHER software (PANTHER protein class) and UniProt-database. The numbers within the columns represent the counts of proteins involved in this protein class. The number above the columns represents the total count of deregulated proteins at this dose and brain region; C: Cortex; n=3 where each biological replicate corresponded to a pooled sample from two animals

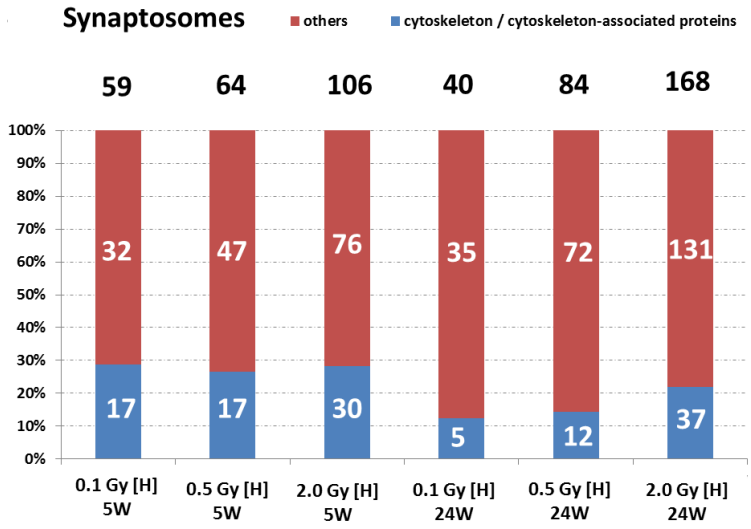

Figure 34: Comparative representation of the number of deregulated proteins from global proteomics approach (synaptosomes of C57BL/6 mouse study) at 5 weeks and 24 weeks post-irradiation in hippocampus grouped into the protein class "cytoskeleton / cytoskeleton-associated proteins" and "others".

The classes are based on information from the PANTHER software (PANTHER protein class) and UniProt-database. The numbers within the columns represent the counts of proteins involved in this protein class. The number above the columns represents the total count of deregulated proteins at this dose and brain region; H: Hippocampus; n=3 where each biological replicate corresponded to a pooled sample from two animals

Interestingly, the highest number of deregulated proteins was found at 2.0 Gy independent of the time point and brain region. Notably, annotation of all the deregulated proteins into protein classes demonstrated an overall dose-dependent and time-dependent increase in proteins involved in the protein class cytoskeleton / cytoskeleton-associated proteins particularly in the cortex (Figure 33 and Figure 34). An increased number of proteins at 0.1 Gy were also noted to be involved in cytoskeletal processes (Figure 33 and Figure 34). Notably, no single protein involved in this class was found at 0.1 Gy in the NMRI mouse study whereas both whole tissue and synaptosomes approach in C57BL/6 mouse study demonstrated alterations.

Ingenuity pathway analysis from all deregulated proteins from isolated hippocampal and cortical synaptosomes showed, that the signalling pathways ephrin B / ephrin receptor signalling, signalling by Rho family GTPases, RhoGDI signalling and axonal guidance signalling were affected after radiation (Figure 35).

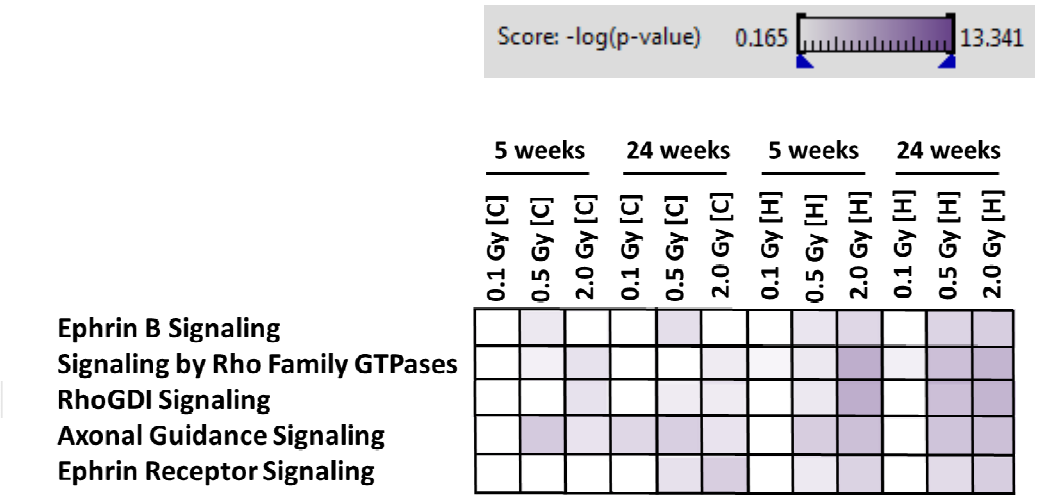

Figure 35: Associated signalling pathways of all significantly deregulated proteins from hippocampal and cortical synaptosomes 5 weeks and 24 weeks post-irradiation using the Ingenuity Pathway Analysis (IPA) software.
Higher colour intensity represents higher significance (p-value) whereas all coloured boxes have a p-value of ≤ 0.05. Hippocampal and cortical data result from three biological replicates where each biological replicate represent a pool from two mice. The radiation doses are shown. H: Hippocampus, C: Cortex

The results are highly comparable with the obtained data from whole tissue approaches of both NMRI and C57BL/6 mouse studies suggesting that these

signalling pathways may not be altered at 0.1 Gy at the latest time point. Importantly, compared with the analysis of synaptosomes (Figure 33 and Figure 34), the number of proteins affiliated at 0.1 Gy in cytoskeletal processes may not cluster in significant alterations of synaptic signalling pathways (Figure 35). Further, an altered protein profile for neuronal receptors was notable (Table 21). Particularly in the cortex, ion channels for calcium, sodium or potassium were differentially expressed at all doses whilst changes in the expression of a number of glutamate receptors (NMDA receptors and metabotropic glutamate receptors) were observed also at all doses (Table 21).

Table 21: Significantly deregulated proteins involved as neuronal receptors during mass spectrometry-based proteomics of cortical and hippocampal synaptosomes at doses of 0.1 Gy, 0.5 Gy and 2.0 Gy 24 weeks post-irradiation.

The table shows the protein name and fold-change and variability. Data resulted from three biological replicates where each biological replicate represents a pool of two samples

Neuronal receptors - 0.1 Gy - cortical synaptosomes - 24 weeks					Neuronal receptors - 0.1 Gy - hippocampal synaptosomes - 24 weeks				
#	Symbol	Entrez Gene Name	n-fold change	Variability [%]	#	Symbol	Entrez Gene Name	n-fold change	Variability [%]
1	Grm2	glutamate receptor, metabotropic 2	2.79	20.0					
2	Kcnq2	potassium voltage-gated channel, subfamily Q, member 2	1.54	9.7					
3	Scn2a1	sodium channel, voltage-gated, type II, alpha 1	1.40	5.1			-		
4	Gabbr1	gamma-aminobutyric acid (GABA) B receptor, 1	1.38	15.9					
5	Grin1	glutamate receptor, ionotropic, NMDA1 (zeta 1)	1.38	19.7					
6	Cacng8	calcium channel, voltage-dependent, gamma subunit 8	1.33	5.1					
Neuronal receptors - 0.5 Gy - cortical synaptosomes - 24 weeks					**Neuronal receptors - 0.5 Gy - hippocampal synaptosomes - 24 weeks**				
#	Symbol	Entrez Gene Name	n-fold change	Variability [%]	#	Symbol	Entrez Gene Name	n-fold change	Variability [%]
1	Grm2	glutamate receptor, metabotropic 2	2.02	2.8	1	Gria1	glutamate receptor, ionotropic, AMPA1 (alpha 1)	-1.34	8.7
2	Kcnab2	potassium voltage-gated channel, shaker-related subfamily, beta member 2	-1.38	1.8			-		
Neuronal receptors - 2.0 Gy - cortical synaptosomes - 24 weeks					**Neuronal receptors - 2.0 Gy - hippocampal synaptosomes - 24 weeks**				
#	Symbol	Entrez Gene Name	n-fold change	Variability [%]	#	Symbol	Entrez Gene Name	n-fold change	Variability [%]
1	Cacna2d1	calcium channel, voltage-dependent, alpha2/delta subunit 1	1.51	11.6	1	Grin1	glutamate receptor, ionotropic, NMDA1 (zeta 1)	-1.41	29.2
2	Kcnq2	potassium voltage-gated channel, subfamily Q, member 2	1.34	7.5	2	Cacng8	calcium channel, voltage-dependent, gamma subunit 8	-1.42	4.5
3	Kcnab2	potassium voltage-gated channel, shaker-related subfamily, beta member 2	-1.44	4.1					
4	Grin1	glutamate receptor, ionotropic, NMDA1 (zeta 1)	-1.81	22.0					

Additionally, mass spectrometry-based proteomics of synaptosomes demonstrated that protein kinases and –phosphatases associated to LTP / LTD signalling were deregulated in the cortex and hippocampus 24 weeks after radiation exposure at doses of 0.1 Gy and 0.5 Gy, but mainly at 2.0 Gy (Table 22).

Table 22: Significantly deregulated proteins involved as protein kinases or protein phosphatases in LTP / LTD processes identified by mass spectrometry-based proteomics of cortical and hippocampal synaptosomes at doses of 0.1 Gy, 0.5 Gy and 2.0 Gy 24 weeks post-irradiation.

The table shows the protein name and fold-change and variability. Data resulted from three biological replicates whereeach biological replicate represent a pooled sample from two mice

Protein kinases and phosphatases involved in LTP and LTD - 0.1 Gy - cortical synaptosomes - 24 weeks					Protein kinases and phosphatases involved in LTP and LTD - 0.1 Gy - hippocampal synaptosomes - 24 weeks				
#	Symbol	Entrez Gene Name	n-fold change	Variability [%]	#	Symbol	Entrez Gene Name	n-fold change	Variability [%]
1	Prkar2b	protein kinase, cAMP dependent regulatory, type II beta	1.33	20.9	1	Prkacb	protein kinase, cAMP dependent, catalytic, beta	-1.96	18.8
					2	Ppfia3	protein tyrosine phosphatase, receptor type, f polypeptide (PTPRF), interacting protein (liprin), alpha 3	1.34	11.6
Protein kinases and phosphatases involved in LTP and LTD - 0.5 Gy - cortical synaptosomes - 24 weeks					Protein kinases and phosphatases involved in LTP and LTD - 0.5 Gy - hippocampal synaptosomes - 24 weeks				
#	Symbol	Entrez Gene Name	n-fold change	Variability [%]	#	Symbol	Entrez Gene Name	n-fold change	Variability [%]
1	Prkacb	protein kinase, cAMP dependent, catalytic, beta	-1.38	25.7	1	Prkacb	protein kinase, cAMP dependent, catalytic, beta	-1.31	15.1
Protein kinases and phosphatases involved in LTP and LTD - 2.0 Gy - cortical synaptosomes - 24 weeks					Protein kinases and phosphatases involved in LTP and LTD - 2.0 Gy - hippocampal synaptosomes - 24 weeks				
#	Symbol	Entrez Gene Name	n-fold change	Variability [%]	#	Symbol	Entrez Gene Name	n-fold change	Variability [%]
1	Cask	calcium/calmodulin-dependent serine protein kinase (MAGUK family)	2.09	17.9	1	Ppp1r9b	protein phosphatase 1, regulatory subunit 9B	1.46	27.9
2	Prkar2b	protein kinase, cAMP dependent regulatory, type II beta	2.06	9.1	2	Ppp2r2a	protein phosphatase 2 (formerly 2A), regulatory subunit B (PR 52), alpha isoform	1.33	13.6
3	Camk2b	calcium/calmodulin-dependent protein kinase II, beta	1.66	26	3	Prkacb	protein kinase, cAMP dependent, catalytic, beta	-2.28	2.2
4	Ppfia3	protein tyrosine phosphatase, receptor type, f polypeptide (PTPRF), interacting protein (liprin), alpha 3	1.55	18.4					
5	Ppp2r2a	protein phosphatase 2 (formerly 2A), regulatory subunit B (PR 52), alpha isoform	-1.32	25.7					
6	Prkcb	protein kinase C, beta	-1.34	13.8					
7	Prkacb	protein kinase, cAMP dependent, catalytic, beta	-1.61	16.2					
8	Ppp1r7	protein phosphatase 1, regulatory (inhibitor) subunit 7	-1.83	24.6					

Overall, IPA analysis indicated that the global protein alterations found in cortical and hippocampal synaptosomes were associated with synaptic LTP / LTD processes and CREB signalling in neurons presumably at all doses and time points in both brain regions (Figure 36).

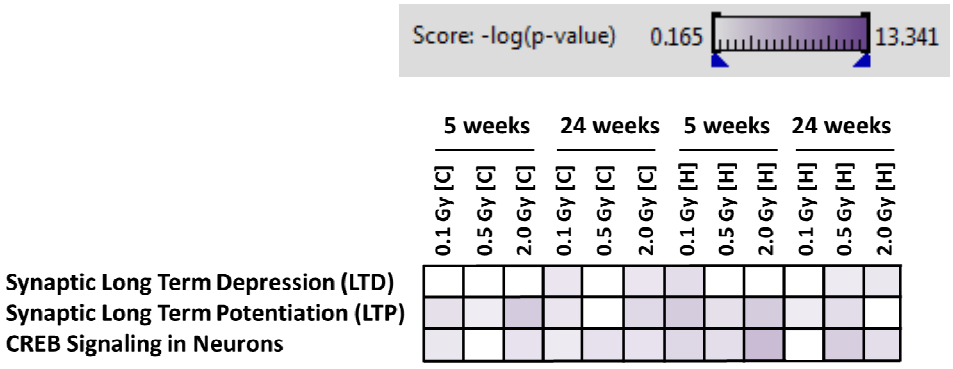

Figure 36: Associated signalling pathways of Synaptic Long Term Depression (LTD), Synaptic Long Term Potentiation (LTP) and CREB Signalling in Neurons of all significantly deregulated proteins from hippocampal and cortical synaptosomes 5 weeks and 24 weeks post-irradiation using the Ingenuity Pathway Analysis (IPA) software. Higher colour intensity represents higher significance (p-value) where all coloured boxes have a p-value of ≤ 0.05. Hippocampal and cortical synaptosomes data resulted from three biological replicates whereas each biological replicate represent a pooled sample from two mice; H: Hippocampus, C: Cortex

As CREB is a transcription factor regulated downstream by LTP / LTD signalling, total CREB and phosphorylated CREB was quantified by immunoblotting from total hippocampal and cortical protein lysates at 6 month post-irradiation time point; the time point 4 week post-irradiation was not analysed. The analysis showed that total CREB levels were only elevated in the hippocampus at 0.5 Gy and 2.0 Gy 24 weeks post-irradiation whilst it was not changed at 0.1 Gy or at all doses in the cortex (Figure 37). However, the phosphorylated CREB levels were significantly increased in the hippocampus at 0.5 Gy and 2.0 Gy whereas in the cortex, they were increased at all doses (Figure 37). This indicates that CREB signalling is altered in the hippocampus at 0.5 Gy and 2.0 Gy and cortex at 0.1 Gy, 0.5 Gy and 2.0 Gy at 24 week time point (Figure 37) consistent with IPA analysis suggesting defects of CREB signalling in neurons in cortex at all doses and hippocampus at 0.5 Gy and 2.0 Gy but not at 0.1 Gy dose 24 weeks post-irradiation (Figure 36). Mentionable, an

increase in phosphorylated CREB is indicative for an activation of LTP signalling pathways where protein kinases phosphorylate CREB (Paul et al., 2010, Cao et al., 2009). An increase in phosphorylated CREB was also noted in NMRI mouse study (1.0 Gy) in both brain regions whilst total CREB levels were reduced (1.0 Gy) in hippocampus and cortex.

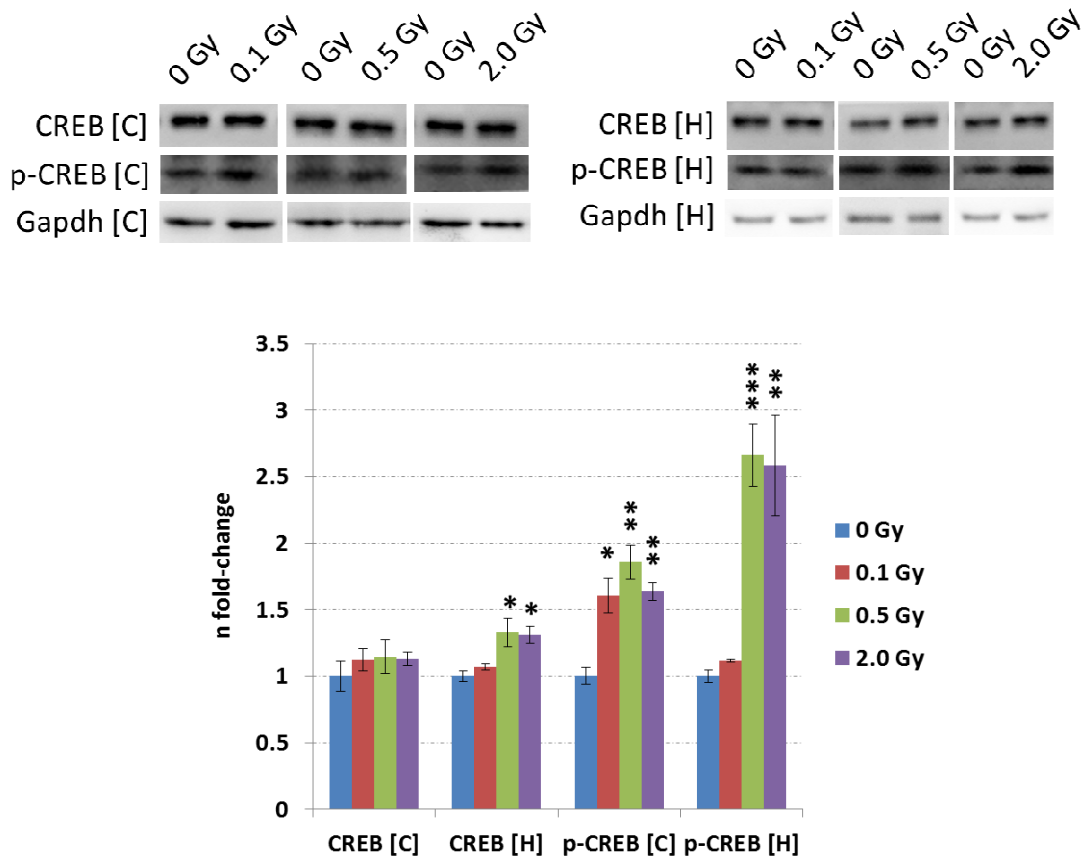

Figure 37: Immunoblotting of CREB and phospho-CREB levels from whole hippocampus and cortex (non synaptosomes approach) 24 weeks post-irradiation using the Ingenuity Pathway Analysis (IPA) software.
The columns represent the fold-changes with standard errors of the mean (SEM) from three biological replicates. The visualisation of protein bands shows the representative change from three biological replicates. *p<0.05; **p<0.01; ***p<0.001 (unpaired Student´s t-test). Normalisation was performed against endogenous GAPDH; H: Hippocampus, C: Cortex

b) Ionising radiation leads to long-term mitochondrial defects in hippocampal and cortical synapses

Further, the signalling pathways associated with oxidative phosphorylation and mitochondrial dysfunctions were found to be the most important pathways affected in the synaptosomes (Figure 38). Neurons transport mitochondria from the nucleus to dendrites / synapses via the cytoskeleton e.g. microtubuli and to axons, and anchor them at synapses to provide energy for signal transduction. In spines, energy is needed to support active synapse formation and structural spine remodelling processes (Sheng, 2014). As shown in Figure 38, the above mentioned signalling pathways were highly enriched in the synaptosomes particularly in the hippocampal synaptosomes compared to the whole hippocampus and cortex of irradiated C57BL/6 mice.

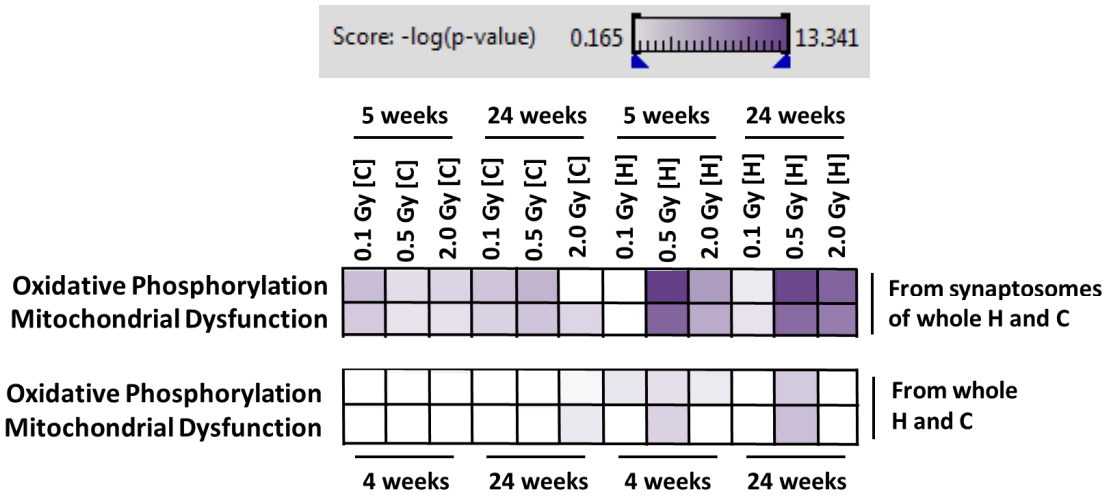

Figure 38: Associated signalling pathways of oxidative phosphorylation and mitochondrial dysfunction of all deregulated proteins from hippocampal and cortical synaptosomes 5 weeks and 24 weeks post-irradiation (upper panel) and from whole hippocampus and cortex 4 weeks and 24 weeks post-irradiation (lower panel) using the Ingenuity Pathway Analysis (IPA) software.

Higher colour intensity represents higher significance (p-value) where all coloured boxes have a p-value of ≤ 0.05. Hippocampal and cortical synaptosomes data result from three biological replicates where each biological replicate represents a pool from two samples; data from whole hippocampus and cortex correspond to six biological replicates; H: Hippocampus, C: Cortex

Importantly, bioinformatics analysis by IPA software indicated that the signalling pathways related to oxidative phosphorylation and mitochondrial dysfunction may be to a greater extent affected by irradiation in the hippocampal synaptosomes as compared to those in the whole hippocampus (Figure 38). Additionally, the signalling pathways were significantly altered in cortical synaptosomes at all doses but not in the whole cortex apart from 2.0 Gy dose showing significant changes 24 weeks post-irradiation (Figure 38).

8 Tabular list of results from both mouse studies

Table 23 and Table 24 show a tabular list of results from both NMRI and C57BL/6 mouse studies.

Table 23: Brief list of NMRI mouse study results 7 month post-irradiation and involvement/defects of targets

	NMRI mouse study (7 month post-irradiation)								
		0.02 Gy	0.1 Gy	0.5 Gy	1.0 Gy	0.02 Gy	0.1 Gy	0.5 Gy	1.0 Gy
		Cortex				Hippocampus			
whole tissue approach	Synaptic signalling pathways (LC-MS/MS)	No	No	Yes	Yes	No	No	Yes	Yes
	Rac1-cofilin pathway (immunoblotting, miRNA)	not analysed	not analysed	Yes	Yes	not analysed	not analysed	Yes	Yes
	Synaptic proteins (MAP-2 and PSD95) (immunofluorescence)	not analysed	not analysed	not analysed	not analysed	No	No	No	Yes
	Neuronal receptor profile (mRNA analysis)	not analysed	not analysed	Yes	Yes	not analysed	not analysed	Yes	Yes
	LTP / LTD dependent signalling (mRNA analysis)	not analysed	not analysed	Yes	Yes	not analysed	not analysed	Yes	Yes
	Total CREB / phosphorylated CREB levels (immunoblotting)	not analysed	not analysed	Yes	Yes	not analysed	not analysed	Yes	Yes
	Circadian rhythm (mRNA analysis)	not analysed	not analysed	not analysed	Yes	not analysed	not analysed	not analysed	Yes
	Adult neurogenesis (immunohistochemstry)	-				No	Yes	Yes	Yes
	Neuroinflammation (mRNA analysis, immunoblotting)	not analysed	not analysed	not analysed	not analysed	not analysed	not analysed	No	Yes
	Lipid peroxidation (immunoblotting)	not analysed	not analysed	not analysed	No	No	No	No	Yes

Table 24: Brief list of C57BL/6 study results 6 month post-irradiation and involvement/defects of targets

	C57BL/6 mouse study (6 month post-irradiation)						
		0.1 Gy	0.5 Gy	2.0 Gy	0.1 Gy	0.5 Gy	2.0 Gy
		Cortex			Hippocampus		
whole tissue approach	Synaptic signalling pathways (LC-MS/MS)	No	Yes	Yes	No	Yes	Yes
	Rac1-cofilin pathway (immunoblotting, miRNA)	Yes	Yes	Yes	Yes	Yes	Yes
	Synaptic proteins (MAP-2 and PSD95) (immunofluorescence)	not analysed			not analysed		
	Neuronal receptor profile (mRNA analysis)	No	No	Yes	No	No	Yes
	LTP / LTD dependent signalling (mRNA analysis)	No	No	Yes	No	No	Yes
	Total CREB / phosphorylated CREB levels (immunoblotting)	Yes	Yes	Yes	No	Yes	Yes
	Circadian rhythm (mRNA analysis)	not analysed			not analysed		
	Adult neurogenesis (immunohistochemstry)	not analysed			not analysed		
	Neuroinflammation (mRNA analysis, immunoblotting)	not analysed			not analysed		
	Lipid peroxidation (immunoblotting)	not analysed			not analysed		
Synaptosomes approach	Synaptic signalling pathways (LC-MS/MS)	No	Yes	Yes	No	Yes	Yes
	Neuronal receptors / channels (LC-MS/MS)	Yes	Yes	Yes	No	Yes	Yes
	LTP / LTD dependent signalling (LC-MS/MS)	Yes	Yes	Yes	Yes	Yes	Yes
	Synaptic mitochondrial dysfunction (LC-MS/MS)	Yes	Yes	Yes	Yes	Yes	Yes

9 Discussion

High doses of ionising radiation delivered to the brain may cause rapid cognitive impairment and memory loss (Spiegler et al., 2004). Previous studies have focused exclusively on the effect of high, clinically relevant doses on the adult neurogenesis in the hippocampus (Rola et al., 2004a, Allen et al., 2013, Raber et al., 2004, Mizumatsu et al., 2003). In contrast, very little is known about the implications of low- and moderate-dose radiation exposure in the hippocampus or other brain regions that also are important for cognition such as the cortex (Kirwan et al., 2008). Recent epidemiological evidence suggests that intellectual development can be adversely affected when the infant brain is exposed to ionising radiation at doses equivalent to those from a single CT scan of the head (Hall et al., 2004). Thus, it is crucial to understand the dose-dependence and persistence of biological alterations in the brain caused by such low-dose exposures.

The goal of this work was to investigate the long-term effects of neonatal exposure to low and moderate doses of ionising radiation in the mouse brain. Alterations in both the hippocampus and cortex were studied as the communication between these brain regions is important in the LTP / LTD process; memories that are first stored in the hippocampus are later transferred to the cortex (Kirwan et al., 2008, Clopath, 2012). Based on the data presented here, the alterations in cognitive performance (personal communication of S. Buratovic and P. Eriksson – Uppsala University) were associated with changes in hippocampal and cortical synaptic plasticity, marked hippocampal defects in adult neurogenesis and increased status of neuroinflammation (NMRI mouse study). Similar alterations were seen in the C57BL/6 mouse study including changes in hippocampal and cortical synaptic plasticity and synaptic mitochondrial defects.

The discussion is not split in separate sections in regard to NMRI mouse study and C57BL/6 mouse study to better compare the potential similarity in the biological changes of synapses found in these two approaches. If not in detail mentioned, the discussion is based on the results from the NMRI mouse study.

Reduced cognition-related behaviour after radiation exposure

Spontaneous behaviour (locomotion, rearing and total activity) in a novel environment was observed in 2- and 4-month-old control and irradiated NMRI mice by S. Buratovic and P. Eriksson (Uppsala University, Sweden). Mice irradiated with total body doses of 0.5 Gy and 1.0 Gy, but not control animals or mice irradiated with lower doses, showed persistent dose-related reductions in all three test variables (personal communication with S. Buratovic and P. Eriksson). Habituation which is a part of cognitive function (Daenen et al., 2001, Groves and Thompson, 1970), can be defined as a decrease in locomotion, rearing and total activity variables in response to the diminishing novelty of the test chamber (personal communication with S. Buratovic and P. Eriksson). The lack of habituation in the irradiated mice (0.5 Gy and 1.0 Gy) at two subsequent time points (2 and 4 month) suggested that they have lost the capacity to store or interpret new information (personal communication with S. Buratovic and P. Eriksson).

Irradiation leads to long-term changes in synaptic signalling pathways associated to synapse morphology

At 0.5 Gy and 1.0 Gy, but not at lower doses, proteins functionally involved in neuronal plasticity, synapse formation and strengthening including ephrin b and ephrin receptor signalling components (Sloniowski and Ethell, 2012) were altered. Ephrin signalling is involved in the maintenance of axonal guidance, synaptic plasticity and LTP in the adulthood (Kullander and Klein, 2002). In addition, proteins involved in the pathways RhoGDI signalling and signalling by Rho family GTPases were altered only at these higher doses which also link to ephrin-induced processes (Nishida and Okabe, 2007).

The studies in both NMRI and C57BL/6 mice irradiated with doses of 0.5 Gy showed both the same alterations in these mentioned pathways 6-7 month post-irradiation. Overall, these pathways share many proteins that are constituents of the Rac1-Cofilin pathway such as Rac1, PAK1/3, Cdc42, LIMK1 and cofilin.

It has been shown that selective deletion of Rac1 in excitatory neurons *in vivo* affects spine structure, impairs synaptic plasticity and spatial learning (Haditsch et al., 2009). Further, activation of cerebral RhoGTPases can enhance learning and memory for several weeks (Diana et al., 2007) and pharmacological inactivation of Rac1 impairs long-term plasticity in the mouse hippocampus (Martinez and Tejada-Simon, 2011). Additionally, the RhoGTPases Rac1 and Cdc42 regulate the synaptic maturation and integration of adult born hippocampal neurons (Vadodaria and Jessberger, 2013, Luo, 2002).

Alterations in the components of the Rac1-Cofilin pathway were identified in both hippocampus and cortex at 0.5 Gy and 1.0 Gy (NMRI mouse study) and 0.5 Gy and 2.0 Gy (C57BL/6 mouse study) at 6-7 month post-irradiation.

In the hippocampus, the radiation exposure to 0.5 Gy and 1.0 Gy may promote actin depolymerisation (Lisman, 2003) and thus impairment in axonal outgrowth and elongation (Lisman, 2003) as the level of inactive phopho-cofilin compared to total cofilin was down-regulated leading to an imbalanced ratio. In the cortex, the levels of both phospho-PAK1/3 and phospho-LIMK1/2 were up-regulated (1.0 Gy). Consequently, one would have expected an increased and not decreased phosphorylation and thus inactivation of the target protein cofilin at 1.0 Gy. However, both the total and phospho-cofilin were increased indicating a radiation-induced imbalance in the ratio between the two forms also in the cortex in favour of cofilin at 1.0 Gy but also at 0.5 Gy. Overall, a reduced expression level of Rac1 was noted in the hippocampus and cortex at both doses consistent with increased cofilin levels further downstream in the Rac1-Cofilin pathway.

Similar results were obtained using C57BL/6 female mice. At 0.5 Gy and 2.0 Gy, Rac1 protein levels decreased in hippocampus and cortex 6 month post-irradiation accompanied with an increase in total cofilin but not in its phosphorylation status – only a slight but significant decrease was noted at 2.0 Gy in the cortex.

Interestingly, it has been shown that amyloid beta can dephosphorylate the actin-polymerizing cofilin protein (Davis et al., 2011). Similarly to amyloid beta, the microtubule-associated Tau protein can induce stabilization and bundling of filamentous F-actin in Drosophila and mouse models of tauopathies (Fulga et al., 2007). Both amyloid beta and hyper-phosphorylated Tau protein accumulate in Alzheimer´s diseases and are thought to play an important role in neurodegeneration

shedding light on defects in actin dynamics and dysfunctions in learning and memory processes. Thus, the alterations found in the Rac1-Cofilin pathway regulating actin dynamics in dendritic spines indicate similarities in the biological target of cytoskeleton within the aetiology of neurodegenerative diseases such as Alzheimer´s. However, deregulation of amyloid beta or hyper-phosphorylation of Tau protein was not detected / analysed in both mouse studies but would be of importance to study in further experiments to access more information about the potential interaction of Alzheimer´s in the radiation-induced neuropathology (Kempf et al., 2013).

When analysing microRNA expression in hippocampus and cortex of irradiated NMRI mice, significant alterations were noted in the levels of miR-132 and miR-134 that are connected to the Rac1-Cofilin pathway (Schratt et al., 2006, Impey et al., 2010). As LIMK1 is a direct target of miR-134 (Schratt et al., 2006), the increased levels of miR-134 were in good agreement with the decreased levels of LIMK1 at 0.5 Gy and 1.0 Gy in both brain regions. Importantly, there was no change in *Limk1* levels either in hippocampus or cortex indicating translational LIMK1 repression as previously reported in primary neurons (Schratt et al., 2006). Of note *Limk1*-null mice show abnormal spine morphology, reduced dendritic branch size, alteration in hippocampal synaptic plasticity and impaired spatial learning (Meng et al., 2002). Thus, the reduction in LIMK1 levels at both doses and brain regions seems to be in good agreement with the increased cofilin levels highlighting defects in dendritic branching.

Quantification of miR-132 levels demonstrated a significant increase in both hippocampus and cortex at 0.5 Gy and 1.0 Gy (NMRI mouse study) but especially in the cortex. Overexpression of miR-132 in the rat perirhinal cortex has been shown to impair short-term recognition memory and this functional deficit was associated with a reduction in both LTD and LTP (Scott et al., 2012). Recently, a performing cohort study of Alzheimer´s patients illustrated a strong decrease in miR-132 levels in the prefrontal cortex and hippocampus (Lau et al., 2013); the deregulation of miR-132 seemed to occur predominately in neurons displaying Tau hyper-phosphorylation (Lau et al., 2013). Overall, these studies suggest a role of miR-132 in cognitive diseases. Quantification of miR-132 in irradiated C57BL/6 mice also showed a

persistent increase of miR-132 at the moderate doses (0.5 Gy and 2.0 Gy) but also at low dose (0.1 Gy) in both brain regions 6 month post-irradiation. This increase was quantitatively similar to that seen in NMRI mice at 0.5 Gy in hippocampus and cortex.

Quantification of miR-134 levels in the C57BL/6 study showed an increased expression in the cortex at 0.1, 0.5 Gy and 2.0 Gy. At 0.5 Gy, the increase was similar to that seen in irradiated NMRI mice. In the hippocampus, there was no noticeable alteration in miR-134 at 0.5 Gy whereas at 2.0 Gy, there was an increase and at 0.1 Gy a decrease, respectively. Quantification of LIMK1 protein levels may be supportive in further experiments to understand the potential miR-134-based translational repression of LIMK1 in the long-term radiation response in the C57BL/6 mouse background as NMRI mouse studies suggest a potential LIMK1 protein repression by miR-134.

The dose of 0.1 Gy in the NMRI mice study was not tested for alterations in the Rac1-Cofilin pathway as both behavioural data (obtained by Uppsala University) and global proteomics did not indicate any changes at this dose. Nevertheless, alterations particularly via epigenetic control such as miRNA´s may occur even at these low doses as shown in the C57BL/6 study. Further investigations are needed to characterise this in detail.

It is widely-accepted that the dendritic spines and their morphology to form synapses play an important role in modulating and storing of information (Kasai et al., 2003). Filamentous actin represents the major cytoskeletal component in dendritic spines to ensure morphological integrity (Urbanska et al., 2012). Generally, it seems that morphological defects in spine shape, size and number are dependent on local actin dynamics and signalling (Cohen et al., 1985, Fifkova and Delay, 1982). The persistent changes in the Rac1-Cofilin pathway in both irradiated mouse strains are indicative for alterations in these processes. In fact, spines induce rapid actin-based remodelling processes to change their morphology within seconds after neuronal receptor stimulation (Fischer et al., 2000).

Irradiation affects synaptic signalling pathways in isolated synaptosomes of hippocampus and cortex

Based on the observed radiation-induced changes in proteins and miRNA´s involved in the Rac1-Cofilin signalling pathway that leads to presumptive synaptic morphology changes, synaptosomes from the C57BL/6 mouse study were isolated and analysed for signalling pathway alterations in the synaptic compartment by global mass-spectrometry. The intactness and enrichment quality of synaptosomes was validated in detail (section 6.15). The results showed that synaptosomes are intact and can be confidently enriched after differential centrifugation and a Ficoll gradient density (section 6.15).

In irradiated C57BL/6 mice, the major alterations in synapse-associated signalling pathways were the ephrin / ephrin B signalling, axonal guidance signalling, RhoGDI signalling and signalling by Rho family GTPases. These were found to be deregulated after 6 months post-irradiation in the synaptosomes of both hippocampus and cortex at doses of 0.5 Gy and above. Importantly, these results correlated with the changes in signalling pathway alterations using whole hippocampus and cortex of irradiated C57BL/6 mice, emphasising the efficient and specific isolation of synaptosomes.

Alterations in CREB signalling pathway affect synaptic plasticity and neuronal receptor profile

The microRNA´s miR-132 and its tandem microRNA miR-212 have been characterised as neuronal activity-dependent rapid response genes in primary hippocampal neurons that are regulated by the CREB pathway (Wayman et al., 2008). Notably, increased miR-212 expression levels were observed in both hippocampus and cortex at 0.5 Gy and 1.0 Gy 7 month post-irradiation (NMRI mouse study). The CREB protein is a key regulator of dendritic growth (Redmond et al., 2002) and also regulates dendrite morphogenesis in mature neurons (Wayman et al., 2006). Thus, the observed alterations in the Rac1-Cofilin pathway were

indicative that the CREB pathway may be involved as miR-132 targets p250GAP (Wayman et al., 2008, Dhar et al., 2014) that is a component of the Rac1-Cofilin pathway. Notably, CREB is implicated in memory formation in a variety of species and its decrease in the hippocampus has been suggested in the rapid forgetting of aged rats (Morris and Gold, 2012).

Quantification of CREB protein levels in 1.0 Gy irradiated NMRI mice showed a strong decrease in total cortical and hippocampal CREB protein especially in the hippocampus whereas phospho-CREB levels were significantly increased but to a smaller extent. However, C57BL/6 mice irradiated with 0.5 Gy and 2.0 Gy showed in the hippocampus an increase of total CREB but particularly an increase in phospho-CREB levels whilst cortical phosphorylated CREB was increased with no changes in total CREB levels. The differences seen in these two studies may be based in the different exposed doses but also in strain and gender. Further experiments are needed particularly at the same doses to elucidate the changes in more detail. Taken together, these data indicate a role of CREB signalling in the long-term radiation-induced alterations in hippocampus and cortex. The increases in phosphorylated (active) CREB is consistent with increased miR-132 / mir-212 levels in NMRI mouse study and miR-132 in C57BL/6 mouse study. However, the small increase in phosphorylation may not be sufficient to compensate for the decrease in total basal CREB protein (NMRI mouse study). To elucidate this hypothesis, the target genes of the CREB pathway were quantified at the gene expression level; *c-Fos, Arc, and Crem* as CREB-dependent synaptic plasticity-related genes (Kadar et al., 2013) were all down-regulated, especially at 1.0 Gy in hippocampus and cortex 7 month post-irradiation in irradiated NMRI mice. Also the Arc and c-Fos protein levels were significantly reduced in both brain regions after exposure to 1.0 Gy (NMRI mouse study). This seems contradictory with the increased expression levels of miR-132 / miR-212 in irradiated NMRI mice. Yet, it has been demonstrated that the up-regulation of miR-132 transcription can partly result from an unidentified CREB-independent mechanism in neurons after treatment by neurotrophins such as Bdnf (Remenyi et al., 2010). In accordance with these data, it has been shown that the Bdnf-induced increase of miR-132 in $CREB^{-/-}$ cortical neurons is possible but to a much lesser extent than in wild type cells (Vo et al., 2005).

Regarding the target genes of CREB, it was shown that the c-Fos transcription factor regulates effector genes including growth factors, -signalling and cytoskeletal molecules which are necessary for LTP maintenance and memory consolidation (Guzowski, 2002, Lanahan and Worley, 1998). Indeed, it was demonstrated that the c-Fos knock-out in the mouse CNS leads to impaired hippocampus-dependent spatial and associative learning impairment accompained with LTP reduction in hippocampal synapses (Fleischmann et al., 2003).

Further, Arc has attracted attention due to its persistent long-term decrease in the hippocampus after irradiation (Rosi et al., 2008); it was demonstrated that after cranial irradiation with 10 Gy *Arc* mRNA and Arc protein levels were decreased in hippocampal neurons after 2 months of initial exposure, correlating with the observations in NMRI mice but at much lower dose (1.0 Gy) and at longer post-irradiation time point (7 months) than their observations. Reduced levels of Arc protein can impair maintenance of LTP and spatial memory consolidation (Guzowski et al., 2000) but most notable is its IEG-specific rapid mRNA translocation to the dendrites and thus to active synaptic sites where *Arc* is subsequently locally translated to functionally active Arc protein (Guzowski et al., 1999). It has been shown that acute inhibition of Arc synthesis at 2 hours after a LTP induction can induce a loss of nascent F-actin at these synaptic sites associated with dephosphorylation of cofilin (Messaoudi et al., 2007). Thus, Arc seems to be involved in the dephosphorylation of cofilin and at least in part, this may additionally explain the marked increase of unphosphorylated total cofilin as demonstrated during analysis of the Rac1-Cofilin pathway by immunoblotting in the NMRI mouse background.

Moreover, recent studies indicate a regulatory crosstalk between *Arc* and neuronal receptors, mainly glutamate (AMPA) receptors regulating the modulation of synaptic strength. The quantification of neuronal receptors on gene expression level indicated significant alterations of NMDAR, AMPAR but predominantly metabotropic G-protein coupled glutamate receptors mainly in hippocampus but also to a lesser extent in cortex at 0.5 Gy and 1.0 Gy. In contrast to these data, there were only mRNA alterations in the neuronal receptor profile at 2.0 Gy 6 month post-irradiation in the C57BL/6 mouse but not at lower doses. However, G-protein coupled glutamate receptors were also altered in this study but mainly in the cortex.

In the synaptosomes approach, there were also mainly cortical changes noticeable in the neuronal receptor profile involving primarily ion channels for potassium, calcium and sodium but also NMDAR and metabotropic G-protein coupled glutamate receptors.

Electrophysiological studies of metabotropic glutamate receptors have shown that activation of these receptors may lead to cellular changes involving the inhibition of calcium and potassium currents, mediation of a slow excitatory postsynaptic potential and the inhibition of neurotransmitter release from the presynapse (Anwyl, 1999, Marinissen and Gutkind, 2001, Losonczy et al., 2003). Further, it has been demonstrated that during memory formation, group I metabotropic glutamate receptors (Grm1 and Grm5) may interact in LTP and LTD whereas group II metabotropic glutamate receptors (Grm2 and Grm3) may be critically involved in LTD by influencing NMDAR activity potentiation (Manahan-Vaughan, 1997). However, various other members of the metabotropic glutamate system may be important for memory formation whereas generally the persistent activation or blockade of receptors are disadvantageous for this process (Holscher et al., 1999). Although gene (NMRI and C57BL/6 mouse study) and protein data (C57BL/6 study – synaptosomes approach) on glutamate receptor levels indicated changes speculative for an altered neurotransmission, it is still important to investigate their activation status with electrophysiological investigations. Indeed, global proteomics demonstrated that G-protein nucleotide binding proteins (Gnb´s) were increased in NMRI and C57BL/6 mouse studies. Particularly at 0.5 Gy, the levels of Gnb1 and Gnb2 in both studies including whole tissue and synaptosomes were similarly increased. As Gnb's are the effector proteins of metabotropic glutamate receptors, an increase on protein level may suggest chronic glutamatergic G-protein-coupled receptor activation.

Neurons regulate the expression of neuronal receptors, particularly glutamatergic AMPA and NMDA receptors, at synapses via changes in LTP / LTD synaptic signalling (Watt et al., 2000). However, the observed changes on the receptor profile after radiation may be inefficient to balance the intracellular LTP / LTD signalling cascades. Various gene expression and protein alterations such as protein kinase and protein phosphatases associated to LTP / LTD signalling were still observable in the long term in both mouse studies. Further, global mass spectrometry and

signalling pathway analysis using the Ingenuity software tool showed that the signalling pathways of synaptic LTD and LTP were also deregulated in isolated synaptosomes from irradiated C57BL/6 mice at the protein level. To decipher the exact pathway alterations in LTD and LTP, successive evaluation of the various protein phosphatases and –kinases will be necessary, with analysis of their phosphorylation status.

The postsynaptic density protein PSD-95 also influences synaptic AMPA / NMDA receptor content and may play a critical role in LTP / LTD (Xu et al., 2008). Previous studies showed that the proteins MAP-2 and PSD-95 are highly enriched in dendritic compartments of neurons and are involved in spine formation, stability and maturation (Harada et al., 2002, Woods et al., 2011). Quantification of both MAP-2 and PSD-95 proteins by immunofluorescence showed a marked increase in both hippocampus and DG at 1.0 Gy in the NMRI mouse study. These findings are consistent with recently published data showing that PSD-95 expression levels were increased in neurons of the granule cell layer of the hippocampus one month after radiation exposure (1.0 Gy) (Parihar and Limoli, 2013). Further, it was shown that immature filopodia were highly sensitive to irradiation compared to more mature spines (Parihar and Limoli, 2013). As filopodia are cytoplasmic projections containing actin filaments cross-linked into bundles by Rho family GTPases (Tatavarty et al., 2012), these data are in good agreement with the radiation-induced changes in the Rho family GTPase Rac1 in the hippocampus of irradiated NMRI mice.

Further, an increase in MAP-2 within the dentate gyrus has been also noted after irradiation with heavy ions (3 Gy, ^{56}Fe) 3 months post-irradiation in male mice (Villasana et al., 2013) consistent with the MAP-2 increase in NMRI mice at a lower dose (1.0 Gy) 7 month post-irradiation.

Ionising radiation induces neuroinflammation and activation of neuroprotective signalling pathways in the hippocampus

There is crosstalk between the CNS and the immune system influencing brain plasticity, neuronal networks and cognitive performance (Di Filippo et al., 2013). Interestingly, neuroinflammation has long been a study subject in Alzheimer´s

(Mosher and Wyss-Coray, 2014). Neuroinflammation is characterised by activation of microglia releasing pro-inflammatory cytokines such as TNFα (Olmos and Llado, 2014). Quantification of TNFα showed an increase on mRNA and protein level in the hippocampus at 1.0 Gy (NMRI mouse study). Hippocampal increase in *Tnfα* expression was demonstrated after acute ionising radiation (0.5 Gy) monitored during the first day after exposure (York et al., 2012) agreeing qualitatively with the long-term data obtained in the hippocampus at 1.0 Gy in the NMRI mouse study.

Interestingly, anti-inflammatory agents such as indomethacin prevented radiation-induced cognitive impairment in rodents by reducing microglia activation in the hippocampus restoring adult neurogenesis (Monje et al., 2003). Insulin-like growth factor 1 (IGF1)-dependent signalling has also been shown to modulate adult hippocampal neurogenesis and cognitive behaviour (Llorens-Martin et al., 2010). Further, a link between inflammation / neuronal dysfunction and defective insulin (INS) signalling in Alzheimer´s disease has been shown (Ferreira et al., 2014). Taken together, both insulin and insulin-like growth factors participate in neuroprotection and may modulate the pathophysiology of neurological diseases (Benarroch, 2012).

Quantification of the phosphorylation status of the IGF1 / INS receptor in the hippocampus at 1.0 Gy demonstrated a significant increase (NMRI mouse study). Insulin-like growth factor- and insulin-receptors are upstream regulators of PI3K/Akt and Ras/Raf/MAPK pathways but also the Rac1 pathway (Chiu et al., 2008, Lee et al., 2011). A successive investigation on protein levels of several targets of this pathway accompanied with evaluation of the phosphorylation status would be necessary to elucidate this in more detail. Yet, as activation of the PI3K pathway lowers lipid peroxidation in primary cortical neuronal cultures (Abdul and Butterfield, 2007) and mouse hippocampal neurons (HT22 cells) (Uranga et al., 2013), the PI3K pathway may be targeted as significant reductions of lipid peroxidation were detectable by immunoblotting of total malondialdehyde-modified protein content in the hippocampus at 1.0 Gy 7 month post-irradiation (NMRI mouse study).

Mitochondrial dysfunction

Alterations in mitochondrial function have emerged as an important aspect in age-related neurodegenerative diseases such as Alzheimer´s where a functional decline has been characterised in mitochondria (Pedros et al., 2014). Moreover, genetic mutations have been observed in oxidative phosphorylation (Biffi et al., 2014). As mitochondria are also concentrated in synapses (Vos et al., 2010), changes in synaptic morphology and signalling pathways may affect mitochondria of synapses (Cavallucci et al., 2013, Eckert et al., 2013).

Recently, our group demonstrated that ionising radiation (0.2 Gy and 2.0 Gy) led to biological alterations in the murine heart mitochondria several weeks post-irradiation whereas at 2.0 Gy, Complex I and III activities were significantly reduced (Barjaktarovic et al., 2011). Additionally, a reduced respiratory capacity was notable (2.0 Gy) (Barjaktarovic et al., 2013). Similar data were obtained *in vitro* (A7r5 cell line derived from rat aorta, thoracic / smooth muscle) demonstrating that 5.0 Gy gamma-ray irradiation can lead to decreased activity of NADH dehydrogenase (Complex I) at 12 hours post-irradiation (Yoshida et al., 2012). The mechanism of radiation-induced dysfunctions on mitochondria is not clear in both heart and brain, but may directly interact with mitochondrial DNA inducing mutations and deletions or indirectly by reactive oxygen species generated during radiation exposure (Prithivirajsingh et al., 2004).

Mass spectrometry-based quantification of isolated synaptosomes from hippocampi and cortices of irradiated C57BL/6 mice showed alterations in signalling pathways of oxidative phosphorylation and mitochondrial dysfunction. These data suggested that the mitochondria in the synaptic hippocampal compartment were more affected than those in the cortex. Importantly, the global proteomics tissue approach only showed a randomised evidence for the involvement of these signalling pathways in the whole hippocampus and cortex. In total, these results suggest that mitochondria in synapses may be affected by ionising radiation even after a considerable exposure time (6 month post-irradiation).

The damage to synapses could be associated with defects on NMDA and AMPA glutamate receptor signalling (Mota et al., 2014, Hsieh et al., 2006) but also changes in metabotropic G-protein coupled glutamate receptors (Renner et al., 2010) as an

early molecular event. This may result in changes in the axonal transport of synaptic vesicles and mitochondria to the dendritic spines and synapses (DuBoff et al., 2013) and manifesting finally with the loss of synaptic terminals, dendritic spines and neurons (Overk and Masliah, 2014). Synaptic mitochondria are necessary to sustain the high energy and calcium buffering levels that are required for synaptic signalling to load neurotransmitters in synaptic vesicles (Saxton and Hollenbeck, 2012) and a change in the expression profile of neuronal receptors may indicate mitochondrial dysfunctions.

Glutamate receptor changes have been noted at the mRNA level (NMRI and C57BL/6 mouse study) and protein level (C57BL/6 mouse study – synaptosomes approach) 6-7 months post-irradiation. Further, the observed alterations in the hippocampal and cortical Rac1-Cofilin signalling pathway may also suggest a defective cytoskeleton-dependent axonal transport of mitochondria to the synaptic sites. This may explain at least in part the mitochondrial dysfunctions seen in synapses during signalling pathway analysis of proteomic data. However, it is questionable if a presumable lower quantity of synaptic mitochondria may be the case and if this may be compensated by an increased aberrant mitochondrial activity. An increase in mitochondrial DNA copy number (polyploidisation) has been observed in the brain of gamma-irradiated (3.0 Gy) mice that was associated with the activation or amplification of intact or slightly damaged mitochondrial DNA molecules as a compensatory mechanism to the ATP deficiency originated from damaged mitochondrial DNA copies (Malakhova et al., 2005). Further, primary neurons of AβPP mice (Alzheimer´s model) showed defects in axonal transport of mitochondria and mitochondrial biogenesis (fission and fusion controlling mitochondrial morphology and number) and synaptic degeneration compared to wild-type neurons (Calkins et al., 2011). Moreover, Monteiro-Cardoso et al. showed that triple-transgenic Alzheimer mice (APPswe, PS1M146V and TauP301L) had a decrease of brain ATP levels and a 50 % decrease in Complex I activity originated essentially from the disruption of mitochondria in synapses (Monteiro-Cardoso et al., 2014).

Yet, the possibility of a lower number of synaptic mitochondria has to be validated by further investigation using mitochondrial respiration of irradiated synaptosomes and quantification of synaptic mitochondria content via imaging methods. Nevertheless,

mitochondrial dysfunction within the synaptic compartment is an important event in the neuropathology of Alzheimer´s associated with cognitive detriments.

Adult neurogenesis in the hippocampus

In addition to synapse-specific modulations, changes in the composition of the cellular population in the DG are affecting learning and memory (Song et al., 2012). This is highlighted by the fact that the DG has the capacity to continuously generate new granular cells (Cameron and McKay, 2001) to store new information not only in new synaptic circuits but also in new granular cells. Furthermore, dysfunctions in this process have been suggested to be involved in neurodegenerative diseases such as Alzheimer´s (Shruster and Offen, 2014, Zheng et al., 2013) and after cranial irradiation (Mizumatsu et al., 2003, Rola et al., 2004b).

The progression of stem cells to mature neurons is called adult neurogenesis and is a multistep process originating from stem cells that give rise to transient amplifying progenitor cells and finally to mature neurons.

Immunohistochemistry analysis showed that the DG of irradiated NMRI mice was depleted of transient amplifying progenitor cells ($Ki67^+$ cells) and mature neurons ($NeuN^+$ cells). Effective synaptic integration of adult-born hippocampal neurons into existing neuronal circuits depends *in vivo* on Rho GTPases (Cdc42 and Rac1) and defects in these enzymes may lead to a lower long term survival (Vadodaria and Jessberger, 2013, Luo, 2002). This correlates with the observed changes in Rac1 levels during analysis of the hippocampal Rac1-Cofilin pathway as described in the previous sections. Further, it is known that acute irradiation leads to immediate reductions in adult neurogenesis due to depletion of the highly proliferating neural progenitor cells (Limoli et al., 2004) consistent with the long-term reduction in the number of progenitor cells positive for Ki67 (NMRI mouse study). Importantly, a persistent cell death was not detectable in the hippocampus as verified by unchanged levels of cell death-promoting *Bad* (NMRI mouse study) which may affect adult neurogenesis. Thus, the reduced number of adult-born mature neurons seems to originate rather from defects in synaptic integration than from apoptotic effects.

Although apoptosis was not evaluated shortly after irradiation, a possible long-term effect on adult neurogenesis originating from acute apoptosis cannot be excluded. However, it has been shown that neural progenitors in the subgranular zone of the DG underwent p53-dependent apoptosis within 24 hours after irradiation but the reduction in newborn neurons within the DG 9 weeks post-irradiation in $p53^{-/-}$ mice was not significant different from that observed in $p53^{+/+}$ mice (Li et al., 2010) suggesting a non-causal role of immediate apoptosis in the long-term disruption of adult neurogenesis.

Overall, the results indicated that irradiation, by inducing synapse-specific modification at the sub-cellular level, may alter the dynamic composition of the DG and hippocampal circuitry affecting in that way learning and memory capacitiy. It is noteworthy at this point, that microglia are also contributing to hippocampal neurogenesis (Gemma and Bachstetter, 2013, Ming and Song, 2011) and the miR-132 / -212 cluster was classified as a "neurimmiR" operating within and between neural and immune compartment (Wanet et al., 2012). Thus, the alterations seen in hippocampal adult neurogenesis may be a process involving a discrete regulation of signalling by intrinsic epigenetic mechanisms and extrinsically by nearby neurogenic niche cells (Ma et al., 2010). This correlates with the increased TNFα levels and miR-132 / -212 levels found in the hippocampus 7 month post-irradiation in 1.0 Gy irradiated NMRI mice.

Circadian rhythm

Finally, the question arises if there is a presumable overall regulatory dysfunction which may explain the diverse persistent changes, particularly in the hippocampus.

The interplay between the circadian clock system and memory is highlighted by an aberrant regulation of clock timing in neurological disorders (Gerstner et al., 2009, Zelinski et al., 2014). In detail, neurotransmitter secretion and proficiency in cognitive tasks depend on biological circadian rhythms (Menet and Rosbash, 2011, Gerstner et al., 2009). The genes encoding clock proteins are expressed throughout the brain and their expression is synchronised from and to the suprachiasmatic nucleus (SCN) – the global zeitgeber to set the clocks in the other brain regions and organs.

The microRNA miR-132 has been shown to orchestrate chromatin remodeling and to modulate the circadian period (Per) genes within the SCN (Alvarez-Saavedra et al., 2011) and mouse brain cortex (Lusardi et al., 2010). Quantification of the miR-132 regulated *Mecp2* (Methyl-CpG-binding protein 2) that is necessary for both chromatin remodeling and neuronal synaptic contacts (Glaze, 2004) demonstrated a decrease in the hippocampus at 0.5 Gy and 1.0 Gy 7 month post-irradiation (NMRI mouse study); the cortex was not analysed. Alvarez-Saavedra et al. have shown that the regulation of Per1 and Per2 promoters occurs via Mecp2 in a miR-132-dependent manner and our mRNA expression analysis showed an increase in hippocampal *Per1* expression at 1.0 Gy 7 month post-irradiation in the NMRI mouse study; 0.5 Gy samples were not analysed. However, these results seem to be inconsistent with increases of miR-132 expression and it may be reasonable that the Per1 protein levels are decreased which may could correlate with increases in miR-132 expression. This has to be verified in further experiments.

Further, a number of significant changes were observable in other circadian clock-driven genes in hippocampus but also in cortex (1.0 Gy) (NMRI mouse study). Interestingly, the gene *Arntl* (synonym: *Bmal1*) was decreased in the cortex at 1.0 Gy which is a transcriptional activator forming a core component of the circadian clock via Clock:Bmal1 complex recruitment to chromatin (Eckel-Mahan et al., 2013).

Taken together, from these results it can be hypothesised that particularly miR-132 is essential in circadian-driven chromatin remodeling although only a few changes in circadian clock / circadian regulated transcription factor expressions were noticeable. However, a speculative defect in the orchestration of chromatin remodeling both in hippocampus and cortex in the long-term response to ionising radiation exposure could be reasonable. Further studies are needed to verify these preliminary data and to get more information in circadian rhythm dysfunctions after irradiation. This could be achieved by chromatin immunoprecipitation to investigate the interaction between proteins of the circadian clock system and DNA or by electroencephalographical studies to access information about the neural oscillations (frequency and periodicity) at different times during the day at distinct post-irradiation time points. Importantly, the sampling time between the different dose groups did not varied much (maximal 1 hour) and was performed in the morning when mice are out of their high behavioural nocturnal activity. Thus, a potential bias regarding different

sampling times of control and dose groups affecting the molecular analysis of circadian rhythm can be excluded.

10 Conclusion

It is of speculation if total-body irradiation may lead to systemic effects that indirectly influence brain function. However, cranial irradiation of neonatal mice is a sophisticated process including appropriate shielding and fixation mechanically or via anaesthesia. This may induce in turn additionally to irradiation early life time stress in a period of highest sensitivity to external cues (priming phase) (Lupien et al., 2009).
In this study, we used male NMRI and female C57BL/6 mice, irradiated them on postnatal day 10 and analysed alterations on the molecular level maximal 6-7 month post-irradiation. Interestingly, both mouse studies showed similar qualitative and quantitative overlapping events including the Rac1-Cofilin pathway, the CREB signalling pathway, the analysis of mir-132, neuronal receptor profile of glutamate and LTP/LTD signalling pathways although they are of different strains and gender. One explanation could be that the initial “storm” of ionising radiation affecting the brain molecules in a more randomised fashion disappeared 6-7 month post-irradiation and may leave only stable alterations in biological targets and molecules and that is presumably regardless of mouse strain and gender. Importantly, gender-specific responses to acute ionising radiation may be unlikely at the time of exposure on PND10 as mice did not reach puberty where the levels of the sexual hormones (oestrogen and testosterone) are distinct different. Further, if the irradiated animals get adolescent, the changes in the gender-specific hormone status may not affect the already manifested detriments over the time from PND10 to adolescence. However, it is known that estrogen levels may play a pivotal neuroprotective role in Alzheimer´s (Lan et al., 2014) and administration of 17-α-estradiol counteracts on behavioural and biochemical changes induced in irradiated rats probably by an antioxidant mechanism (Caceres et al., 2011). Thus, C57BL/6 mice experiments in females should be repeated also in males accompanied with an evaluation of hormone levels immediately after radiation exposure and at time of long-term analysis (6 month post-irradiation).
Animals were exposed on postnatal day 10 to the different radiation doses due to comparable times within the brain growth spurt of human beings (third to fourth postnatal years) where radiation originating from medical imaging methods (CT

scans) are applied; the long-term follow-up of maximal 6-7 months post-irradiation corresponds to the mouse reaching adolescence and represent the time window where children are also adolescent. Taken together, it was possible to identify and characterise the alterations in hippocampal and cortical synapses as an important biological target in the long-term response of ionising radiation exposure.

In general, irradiation of neonates with doses as low as 0.5 Gy induced long lasting neurological defects. The analysis showed strong associations between cognitive dysfunction, synaptic plasticity- and cytoskeletal signalling pathways, adult neurogenesis, synaptic mitochondrial dysfunction and neuroinflammation in the hippocampus and cortex after low / moderate doses of ionising radiation. Several deregulated molecules and signalling pathways seen in this study are also involved in neurocognitive disorders such as Alzheimer´s. Importantly, the accumulated data showed that no single cell type alteration can fully explain the complexity of long-term consequences of irradiation; a dynamic interaction between multiple cell types including neurons, astrocytes and microglia and different brain regions involving subtle molecular alteration, such as epigenetic modulations via miRNAs, and changes in both transcription and translation in an orchestrated response is likely to be involved in the pathogenesis of radiation-induced cognitive injury as highlighted in Figure 39.

Exposure to ionising radiation comes from many sources and concerns not only children but also adults involving radiation workers, astronauts, and persons subjected to radiotherapy / radiological medical diagnostics, or exposed to radiological accidents. A better understanding of the mechanisms of cognitive and neurological dysfunction at low / moderate radiation doses is of critical importance in establishing health risks and protection related policies; this work may support further investigations to reach these aims.

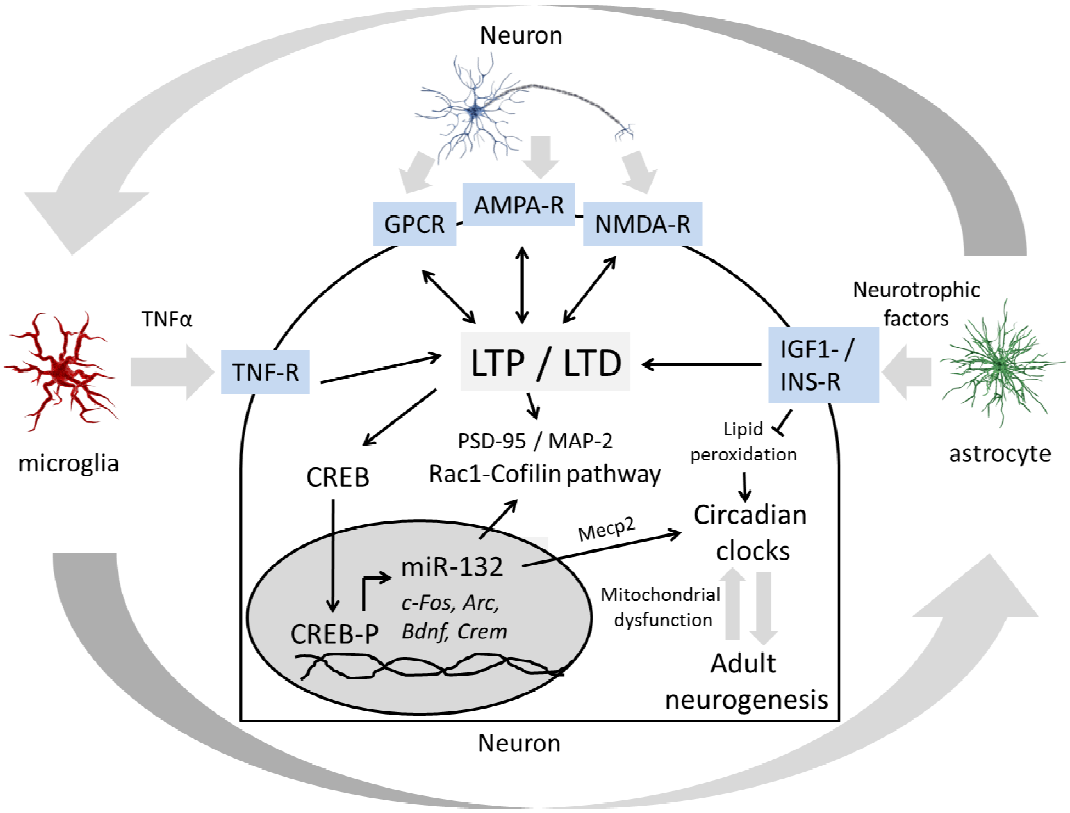

Figure 39: Schematic representation of long-term effects of ionising radiation on the brain combining all presented data.

Microglia and astrocytes regulate neuronal activity by influencing cytokines (TNFα) or neurotrophic factors. This results in changes in the receptor profile of G protein coupled receptors (GPCR´s), AMPA and NMDA receptors which are important for steady state signal transmission from neuron to neuron. In turn, this affects long-term potentiation / long-term depression (LTP / LTD) signalling pathways and leads to alterations in synaptic morphology (actin reorganisation via Rac1-Cofilin-pathway, changes in synaptic scaffold proteins such as PSD-95 / MAP-2) and synaptic plasticity (CREB pathway). Phosphorylated CREB (CREB-P) in the nucleus regulates the expression of miR-132 and immediate early genes such as *c-Fos*, *Arc* and *Crem* affecting both synaptic morphology and adult neurogenesis. Subsequently, circadian clocks affecting circadian rhythm may alter adult neurogenesis and vice versa but is not proven yet. However, synaptic mitochondrial dysfunction as seen in irradiated C57BL/6 mice may be involved in this process and in correct synapse formation. The figure is modified after own publication (Kempf et al. – in preparation). The involvement of microglia and astrocytes in this figure is based on the increases in the cytokine TNFα and increased phosphorylation status of the neurotrophic IGF1-/INSR within the hippocampus of 1.0 Gy-irradiated NMRI mice.

11 Supplementary information

Table 25: List of deregulated proteins 7 months post-irradiation from 20 mGy, 100 mGy, 500 mGy and 1000 mGy within the cortex (NMRI mouse study).

The table shows the up-regulated or down-regulated proteins with the fold-changes, their variability, their number of unique peptides used for protein identification and number of identifications in the biological replicates (ICPLx/ICPL0-Count). "PANTHER protein class" represents the protein class where the protein of interest can be annotated based on PANTHER software tool and UniProt database. Grey / brown highlighted "PANTHER protein classes" belong to the protein class of "small GTPase / associated G-protein" / "cytoskeleton / cytoskeleton-binding protein", respectively

20 mGy - Cortex

#	Symbol	Entrez Gene Name	Unique Peptides	n-fold change from ICPL-4/ICPL-0	ICPL-4/ICPL-0 Variability [%]	ICPL_4 / ICPL_0 Count	PANTHER protein class
1	Hsp90b1	heat shock protein 90, beta (Grp94), member 1	8	1.39	28.4	5;3;-;2;3	Hsp90 family chaperone
2	Npepps	aminopeptidase puromycin sensitive	11	1.34	25.5	5;4;4;4;4	metalloprotease
3	Tubb4a	tubulin, beta 4A class IVA	4	1.34	28.9	12;12;18;13;17	tubulin complex
4	Sfxn1	sideroflexin 1	7	1.31	19.0	1;5;3;4;1	cation transporter, transfer/carrier protein
5	Glod4	glyoxalase domain containing 4	4	-1.32	26.7	3;5;4;3;3	glyoxalase
6	Rab5b	RAB5B, member RAS oncogene family	2	-1.35	23.3	1;1;-;1;1	endosomal traffic, lipid metabolism, small GTPase

100 mGy - Cortex

#	Symbol	Entrez Gene Name	Unique Peptides	n-fold change from ICPL-4/ICPL-0	ICPL-4/ICPL-0 Variability [%]	ICPL_4 / ICPL_0 Count	PANTHER protein class
1	Auh	AU RNA binding protein/enoyl-coenzyme A hydratase	6	1.38	21.3	1;1;4;1;1	acetyltransferase, dehydrogenase, ligase
2	Hebp1	heme binding protein 1	3	1.35	14.5	2;2;1;-;2	heme metabolic process, heme binding
3	Bphl	biphenyl hydrolase-like (serine hydrolase, breast epithelial mucin-associated antigen)	8	1.31	21.9	4;-;3;2;1	serine protease
4	-	predicted pseudogene 9762	2	-1.32	12.4	1;1;2;2;2	-
5	Prrt2	proline-rich transmembrane protein 2	3	-1.42	12.7	2;1;3;3;4	response to biotic stimulus, cell junction
6	Pcp4	Purkinje cell protein 4	2	-1.46	24.4	1;-;1;1;1	calmodulin binding

500 mGy - Cortex

#	Symbol	Entrez Gene Name	Unique Peptides	n-fold change from ICPL-6/ICPL-0	ICPL-6/ICPL-0 Variability [%]	ICPL_6 / ICPL_0 Count	PANTHER protein class
1	Cox6a1	cytochrome c oxidase, subunit VI a, polypeptide 1	2	2.43	22.3	2;1;1;2;1	oxidase
2	Uqcrc1	ubiquinol-cytochrome c reductase core protein 1	11	2.03	21.5	5;5;7;9;7	metalloprotease, reductase, esterase
3	Prdx5	peroxiredoxin 5	2	2.03	14.2	5;6;3;5;2	proxidase
4	Cct7	chaperonin containing Tcp1, subunit 7 (eta)	3	1.95	28.7	2;4;1;1;1	protein folding, protein complex assembly
5	Psd3	pleckstrin and Sec7 domain containing 3	3	1.86	18.7	-;2;3;1;2	guanyl-nucleotide exchange factor
6	Ndufv2	NADH dehydrogenase (ubiquinone) flavoprotein 2	4	1.71	29.3	2;3;-;3;1	oxidative phosphorylation, respiratory electron transport
7	Cnrip1	cannabinoid receptor interacting protein 1	4	1.61	27.8	1;1;-;1;1	cannabinoid receptor signalling
8	Sept8	septin 8	5	1.58	28.9	6;4;4;5;3	small GTPase, cytoskeletal protein
9	Tubb3	tubulin, beta 3 class III	6	1.57	23.9	27;23;25;16;25	tubulin complex
10	Fscn1	fascin homolog 1, actin bundling protein	9	1.53	28.7	5;4;5;4;5	non-motor actin binding protein
11	Bin1	bridging integrator 1	4	1.52	11.0	5;2;3;2;2	membrane trafficking regulatory protein

12	Sept5	septin 5	6	1.51	18.6	11;6;2;7;3	small GTPase, cytoskeletal protein
13	Gnb2	guanine nucleotide binding protein (G protein), beta 2	6	1.49	11.8	6;8;7;1;6	hydrolyse, heterotrimeric G-protein
14	Napg	N-ethylmaleimide sensitive fusion protein attachment protein	2	1.45	28.8	3;3;2;4;1	membrane traffic protein
15	Gnb1	guanine nucleotide binding protein (G protein), beta 1	8	1.43	13.5	10;15;12;3;7	hydrolyse, heterotrimeric G-protein
16	Hnrnpl	heterogeneous nuclear ribonucleoprotein L	3	1.40	18.5	1;4;1;1;-	mRNA splicing factor, ribonucleoprotein
17	Atp1b2	ATPase, Na+/K+ transporting, beta 2 polypeptide	6	1.39	18.4	2;8;5;2;2	cation transporter
18	Ckb	creatine kinase, brain	13	1.37	13.2	52;52;50;55;59	ATP synthase, anion channel , hydrolase
19	Ak4	adenylate kinase 4	8	1.34	23.1	3;2;1;3;3	nucleotide kinase
20	Aldh6a1	aldehyde dehydrogenase family 6, subfamily A1	5	1.33	10.3	3;3;2;1;-	dehydrogenase
21	Alb	albumin	9	1.32	23.9	9;12;13;8;9	transfer / carrier protein
22	Npepps	aminopeptidase puromycin sensitive	11	1.31	23.7	4;4;4;4;5	small GTPase, cytoskeletal protein
23	Sept11	septin 11	2	1.30	24.5	4;5;5;3;3	small GTPase, cytoskeletal protein
24	Ufc1	ubiquitin-fold modifier conjugating enzyme 1	2	-1.32	11.8	1;1;-;1;1	transmembrane receptor protein tyrosine kinase, protein amino acid phosphorylation
25	Etfb	electron transferring flavoprotein, beta polypeptide	4	-1.32	23.9	-;3;1;2;2	hydroxylase
26	Acp1	acid phosphatase 1, soluble	3	-1.33	24.4	-;1;2;2;1	protein phosphatase, reducatase
27	Gstp1	glutathione S-transferase, pi 1	4	-1.63	28.6	3;4;1;5;5	transferase

1000 mGy - Cortex

#	Symbol	Entrez Gene Name	Unique Peptides	n-fold change from ICPL-6/ICPL-0	ICPL-6/ICPL-0 Variability [%]	ICPL_6 / ICPL_0 Count	PANTHER protein class
1	Cox6a1	cytochrome c oxidase, subunit VI a, polypeptide 1	2	2.34	27.6	-;2;1;1;1	oxidase
2	Hebp1	heme binding protein 1	3	1.99	28.3	2;2;1;-;2	heme metabolic process, heme binding
3	Uqcrc1	ubiquinol-cytochrome c reductase core protein 1	11	1.92	27.1	4;6;8;5;6	metalloprotease, reductase, esterase
4	Hnrnpl	heterogeneous nuclear ribonucleoprotein L	2	1.68	13.6	-;2;2;2;1	mRNA splicing factor, ribonucleoprotein
5	mt-Co2	mitochondrially encoded cytochrome c oxidase II	3	1.68	27.8	-;2;2;2;3	electron transport chain, hydrogen ion transmembrane transport
6	Ndufa10	NADH dehydrogenase (ubiquinone) 1 alpha subcomplex 10	7	1.47	24.5	5;1;4;3;6	nucleotide kinase, oxidoreductase
7	Necap1	NECAP endocytosis associated 1	3	1.43	7.1	-;1;2;1;1	endocytosis
8	Gnb2	guanine nucleotide binding protein (G protein), beta 2	6	1.42	27.6	3;7;7;8;4	hydrolyse, heterotrimeric G-protein
9	Anxa5	annexin A5	9	1.42	28.5	3;2;4;2;5	transfer / carrier protein, annexin
10	Atp6v1b2	ATPase, H+ transporting, lysosomal V1 subunit B2	15	1.37	16.1	13;8;16;17;16	ATP synthase, anion channel , hydrolase
11	Aldh5a1	aldhehyde dehydrogenase family 5, subfamily A1	9	1.36	28.3	5;2;4;9;3	dehydrogenase
12	Gdi1	guanosine diphosphate (GDP) dissociation inhibitor 1	7	1.36	26.1	7;13;5;4;8	acyltransferase, G-protein modulator
13	Acta1	actin, alpha 1, skeletal muscle	3	1.34	17.7	2;1;5;4;5	actin and actin related protein
14	Chmp5	charged multivesicular body protein 5	2	1.34	9.8	-;1;2;2;1	transfer / carrier protein
15	Gnb1	guanine nucleotide binding protein (G protein), beta 1	7	1.33	15.8	13;18;5;11;13	hydrolyse, heterotrimeric G-protein
16	Tuba4a	tubulin, alpha 4A	7	1.33	22.6	19;36;26;35;38	tubulin complex
17	Ppp1ca	protein phosphatase 1, catalytic subunit, alpha isoform	3	1.33	14.7	-;1;2;2;2	protein phosphatase, calcium-binding protein
18	Bphl	biphenyl hydrolase-like (serine hydrolase, breast epithelial mucin-associated antigen)	8	1.31	21.9	3;-;4;2;1	serine protease
19	-	predicted pseudogene 9762	2	-1.40	9.9	1;2;2;2;1	not known
20	Chchd3	coiled-coil-helix-coiled-coil-helix domain containing 3	6	-1.44	16.6	-;2;3;2;3	mitochondrial function and structure
21	Pcp4	Purkinje cell protein 4	2	-1.48	20.3	-;1;1;1;1	calmodulin binding
22	Prrt2	proline-rich transmembrane protein 2	3	-1.53	14.6	2;1;3;3;4	response to biotic stimulus, cell junction

Table 26: List of deregulated proteins 7 months post-irradiation from 20 mGy, 100 mGy, 500 mGy and 1000 mGy within the hippocampus (NMRI mouse study).

The table shows the up-regulated or down-regulated proteins with the fold-changes, their variability, their number of unique peptides used for protein identification and number of identifications in the biological replicates (ICPLx/ICPL0-Count). "PANTHER protein class" represents the protein class where the protein of interest can be annotated based on PANTHER software tool and UniProt database. Grey / brown highlighted "PANTHER protein classes" belong to the protein class of "small GTPase / associated G-protein" / "cytoskeleton / cytoskeleton-binding protein", respectively

20 mGy - Hippocampus

#	Symbol	Entrez Gene Name	Unique Peptides	n-fold change from ICPL-4/ICPL-0	ICPL-4/ICPL-0 Variability [%]	ICPL_4 / ICPL_0 Count	PANTHER protein class
1	Gad2	glutamic acid decarboxylase 2	3	1.46	20.7	5;5;4;5	decarboxylase
2	Cap1	CAP, adenylate cyclase-associated protein 1	3	1.44	9.5	7;2;1;-	actin family cytoskeletal protein
3	Hebp1	heme binding protein 1	3	1.43	10.1	1;2;1;1	heme metabolic process, heme binding
4	Cct6a	chaperonin containing Tcp1, subunit 6a (zeta)	4	1.37	19.9	2;1;1;-	chaperonin
5	Sfxn1	sideroflexin 1	6	1.31	10.6	1;2;1;1	cation transporter, transfer/carrier protein
6	Glod4	glyoxalase domain containing 4	3	-1.61	23.0	3;-;2;1	glyoxalase
7	Sirpa	signal-regulatory protein alpha	5	-1.73	28.7	5;3;-;3	chemokine

100 mGy - Hippocampus

#	Symbol	Entrez Gene Name	Unique Peptides	n-fold change from ICPL-4/ICPL-0	ICPL-4/ICPL-0 Variability [%]	ICPL_4 / ICPL_0 Count	PANTHER protein class
1	Vim	vimentin	7	1.45	25.2	2;1;4;2	structural protein, intermediate filament
2	Mbp	myelin basic protein	2	1.41	29.2	9;12;17;6	myelin
3	Trf	transferrin	5	1.37	12.2	2;-;2;3	iron binding transport protein
4	Uqcrc1	ubiquinol-cytochrome c reductase core protein 1	15	1.37	10.2	3;5;5;2	metalloprotease, reductase
5	Ndufa10	NADH dehydrogenase (ubiquinone) 1 alpha subcomplex 10	7	1.35	15.4	8;6;8;3	dehydrogenase
6	Sirt2	sirtuin 2 (silent mating type information regulation 2, homolog) 2 (S. cerevisiae)	7	1.34	12.2	2;5;8;2	chormatin/chromatin-binding protein, deacetylase
7	Ppp1ca	protein phosphatase 1, catalytic subunit, alpha isoform	2	1.31	25.1	1;2;2;-	protein phosphatase, calcium-binding protein
8	Gad2	glutamic acid decarboxylase 2	3	1.30	24.1	5;3;3;5	decarboxylase
9	Ndufa8	NADH dehydrogenase (ubiquinone) 1 alpha subcomplex, 8	2	-1.33	26.4	2;3;2;2	nucleotide kinase
10	Ak4	adenylate kinase 4	8	-1.35	18.5	2;5;3;2	nucleotide kinase
11	Hint1	histidine triad nucleotide binding protein 1	3	-1.38	4.9	2;2;2;2	nucleotide phsophatase
12	Pcca	propionyl-Coenzyme A carboxylase, alpha polypeptide	6	-1.99	21.3	1;1;2;1	ligase

500 mGy - Hippocampus

#	Symbol	Entrez Gene Name	Unique Peptides	n-fold change from ICPL-6/ICPL-0	ICPL-6/ICPL-0 Variability [%]	ICPL_6 / ICPL_0 Count	PANTHER protein class
1	Cap1	CAP, adenylate cyclase-associated protein 1 (yeast)	3	2.41	7.3	-;7;2;1	actin family cytoskeletal protein
2	Mog	myelin oligodendrocyte glycoprotein	7	1.92	24.1	1;2;3;1	myelin protein

3	Rtn3	reticulon 3	6	1.67	26.6	1;4;1;4	membrane traffic protein
4	Cdc42	cell division cycle 42 homolog (S. cerevisiae)	3	1.66	26.6	2;2;4;2	small GTPase, cytoskeletal protein
5	Ppp1ca	protein phosphatase 1, catalytic subunit, alpha isoform	3	1.63	11.6	2;1;1;1	protein phosphatase, calcium-binding protein
6	Rap1gds1	RAP1, GTP-GDP dissociation stimulator 1	5	1.61	18.0	4;8;2;6	GDP/GTP exchange of small GTPases
7	Pde2a	phosphodiesterase 2A, cGMP-stimulated	4	1.59	19.6	1;3;3;-	phosphodiesterase
8	Ndufv1	NADH dehydrogenase (ubiquinone) flavoprotein 1	9	1.59	28.4	4;7;8;4	dehydrogenase, reductase
9	Uqcrc1	ubiquinol-cytochrome c reductase core protein 1	12	1.58	24.8	1;3;1;3	metalloprotease, reductase
10	Slc25a3	solute carrier family 25 (mitochondrial carrier, phosphate carrier), member 3	5	1.55	25.2	-;6;3;2	amino acid transporter, mitochondrial carrier protein, calmodulin
11	Tomm34	translocase of outer mitochondrial membrane 34	3	1.53	9.7	-;1;1;1	chaperone
12	Mbp	myelin basic protein	2	1.51	27.9	21;6;7;8	myelin protein
13	Ank2	ankyrin 2, brain	2	1.49	21.8	1;7;7;3	cytoskeletal protein
14	Cnp	2',3'-cyclic nucleotide 3' phosphodiesterase	11	1.47	17.0	26;29;43;27	phosphodiesterase
15	Ywhah	tyrosine 3-monooxygenase/tryptophan 5-monooxygenase activation protein, eta polypeptide	4	1.43	11.8	1;2;2;2	chaperone
16	Gnb1	guanine nucleotide binding protein (G protein), beta 1	8	1.42	6.6	20;15;21;10	hydrolyse, heterotrimeric G-protein
17	Cnrip1	cannabinoid receptor interacting protein 1	4	1.42	13.7	4;4;4;5	cannabinoid receptor signalling
18	Gnb2	guanine nucleotide binding protein (G protein), beta 2	7	1.37	3.5	9;5;7;7	hydrolyse, heterotrimeric G-protein
19	Cntn1	contactin 1	13	1.36	29.7	25;27;26;20	immunoglobulin receptor superfamily (cell adhesion molecule), protein phosphatase, extracellular matrix linker protein
20	Acta1	actin, alpha 1, skeletal muscle	3	1.36	3.7	8;6;5;6	actin and actin related
21	Bin1	bridging integrator 1	5	1.35	16.2	2;2;1;-	membrane trafficking regulatory protein
22	Tubb3	tubulin, beta 3 class III	7	1.33	7.8	26;17;23;17	tubulin complex
23	Tuba4a	tubulin, alpha 4A	7	1.32	7.9	40;36;38;43	tubulin complex
24	Nptx1	neuronal pentraxin 1	6	1.31	13.9	3;5;1;2	immune / stress response
25	Rpl19	ribosomal protein L19	4	1.31	28.5	2;3;4;5	ribosomal protein
26	Pfn2	profilin 2	3	1.30	5.0	4;2;2;3	cytoskeletal regulation
27	Sgip1	SH3-domain GRB2-like (endophilin) interacting protein 1	7	-1.31	17.9	1;5;6;2	energy homeostasis, clathrin mediated endocyosis
28	Srgap3	SLIT-ROBO Rho GTPase activating protein 3	9	-1.32	10.4	1;5;4;1	G-protein modulator
29	Lonp1	lon peptidase 1, mitochondrial	8	-1.33	15.5	-;4;2;1	serine protease
30	Add3	adducin 3 (gamma)	4	-1.34	17.2	2;2;-;1	non-motor actin binding protein
31	Ogdhl	oxoglutarate dehydrogenase-like	12	-1.35	18.3	-;5;3;3	dehydrogenase
32	Trim28	tripartite motif-containing 28	2	-1.40	13.4	-;3;1;1	transcriptional repressor
33	Gstp1	glutathione S-transferase, pi 1	4	-1.47	17.7	5;3;2;4	transferase
34	Necab2	N-terminal EF-hand calcium binding protein 2	6	-1.51	25.5	1;1;1;2	calcium-binding protein

1000 mGy - Hippocampus

#	Symbol	Entrez Gene Name	Unique Peptides	n-fold change from ICPL-6/ICPL-0	ICPL-6/ICPL-0 Variability [%]	ICPL_6 / ICPL_0 Count	PANTHER protein class
1	Numbl	numb-like	5	2.79	11.8	-;2;2;1	signaling molecule
2	Uqcrc1	ubiquinol-cytochrome c reductase core protein 1	15	2.19	25.1	2;5;5;3	metalloprotease, reductase
3	Sept8	septin 8	6	1.89	29.0	5;1;1;6	small GTPase, cytoskeletal protein
4	Fscn1	fascin homolog 1, actin bundling protein	8	1.82	22.6	-;3;2;1	non-motor actin binding protein
5	Ank2	ankyrin 2, brain	4	1.79	24.0	2;5;2;3	cytoskeletal protein
6	Prdx5	peroxiredoxin 5	3	1.75	25.5	-;4;2;2	proxidase
7	Rap1gds1	RAP1, GTP-GDP dissociation stimulator 1	5	1.59	14.5	6;8;8;3	GDP/GTP exchange of small GTPases
8	Atp1b2	ATPase, Na+/K+ transporting, beta 2 polypeptide	6	1.57	27.1	3;8;9;5	cation transporter
9	Me3	malic enzyme 3, NADP(+)-dependent, mitochondrial	6	1.52	21.0	-;3;3;3	acyltransferase, dehydrogenase, decarboxylase
10	Mbp	myelin basic protein	2	1.52	26.7	6;12;17;9	myelin
11	Rab7	RAB7, member RAS oncogene family	2	1.51	22.4	-;1;2;1	endosomal traffic, lipid metabolism, small GTPase
12	Gdi1	guanosine diphosphate (GDP) dissociation inhibitor 1	7	1.46	21.5	3;11;8;5	acyltransferase, G-protein modulator
13	Dnaja1	DnaJ (Hsp40) homolog, subfamily A, member 1	4	1.45	25.9	-;2;2;1	chaperone
14	Ppp1ca	protein phosphatase 1, catalytic subunit, alpha isoform	2	1.43	23.5	1;2;2;-	protein phosphatase, calcium-binding protein
15	Tubb3	tubulin, beta 3 class III	8	1.41	7.0	15;19;17;21	tubulin complex
16	Tagln3	transgelin 3	5	1.41	19.7	1;3;1;-	non-motor actin binding protein
17	N28178	expressed sequence N28178	8	1.37	20.9	2;1;1;-	not known
18	Gnb1	guanine nucleotide binding protein (G protein), beta 1	5	1.37	4.6	5;14;18;15	hydrolyse, heterotrimeric G-protein
19	Gpc1	glypican 1	9	1.36	4.0	-;2;6;1	extracellular matrix glycoprotein, cell adhesion molecule
20	Tuba4a	tubulin, alpha 4A	7	1.36	9.3	35;29;38;38	tubulin complex
21	Gnb2	guanine nucleotide binding protein (G protein), beta 2	4	1.35	6.4	7;7;8;7	hydrolyse, heterotrimeric G-protein
22	Tpt1	tumor protein, translationally-controlled 1	2	1.34	9.4	1;2;1;1	non-motor microtubule binding protein
23	Cnrip1	cannabinoid receptor interacting protein 1	5	1.34	11.2	3;4;4;2	cannabinoid receptor signalling
24	Ckb	creatine kinase, brain	14	1.34	9.4	43;50;53;44	amino acid kinase
25	Lap3	leucine aminopeptidase 3	5	1.31	9.7	1;1;5;-	metalloprotease
26	Sgip1	SH3-domain GRB2-like (endophilin) interacting protein 1	7	-1.30	27.5	-;2;1;5	energy homeostasis, clathrin mediated endocyosis
27	Sez6l	seizure related 6 homolog like	5	-1.31	23.4	-;1;1;4	apolipoprotein, metalloprotease, serine protease, cell adhesion molecule
22	Tpt1	tumor protein, translationally-controlled 1	2	1.34	9.4	1;2;1;1	non-motor microtubule binding protein
23	Cnrip1	cannabinoid receptor interacting protein 1	5	1.34	11.2	3;4;4;2	cannabinoid receptor signalling
24	Ckb	creatine kinase, brain	14	1.34	9.4	43;50;53;44	amino acid kinase
25	Lap3	leucine aminopeptidase 3	5	1.31	9.7	1;1;5;-	metalloprotease

26	Sgip1	SH3-domain GRB2-like (endophilin) interacting protein 1	7	-1.30	27.5	-;2;1;5	energy homeostasis, clathrin-mediated endocyosis
27	Sez6l	seizure related 6 homolog like	5	-1.31	23.4	-;1;1;4	apolipoprotein, metalloprotease, serine protease, cell adhesion molecule
28	Hint1	histidine triad nucleotide binding protein 1	3	-1.31	7.0	2;2;2;2	nucleotide phosphatase
29	Ehd1	EH-domain containing 1	5	-1.31	17.3	-;1;1;1	membrane traffic protein, G-protein modulator, calcimu-binding protein
30	Ran	RAN, member RAS oncogene family	4	-1.32	18.6	5;9;5;6	small GTPase
31	Cnksr2	connector enhancer of kinase suppressor of Ras 2	6	-1.36	18.7	-;1;1;1	kinase modulator
32	Psat1	phosphoserine aminotransferase 1	3	-1.37	22.4	1;2;1;-	transaminase
33	Necab2	N-terminal EF-hand calcium binding protein 2	3	-1.52	28.3	-;1;3;1	calcium-binding protein
34	Ndufa8	NADH dehydrogenase (ubiquinone) 1 alpha subcomplex, 8	2	-1.53	17.4	2;3;2;2	dehydrogenase
35	Synpo	synaptopodin	11	-1.58	26.6	2;4;1;3	non-motor actin binding protein
36	Pcca	propionyl-Coenzyme A carboxylase, alpha polypeptide	6	-2.12	25.7	1;1;2;1	ligase

Table 27: List of deregulated proteins 4 weeks post-irradiation from 100 mGy, 500 mGy and 2000 mGy within the cortex (C57Bl6 study).

The table shows the up-regulated or down-regulated proteins with the fold-changes, their variability, their number of unique peptides used for protein identification and number of identifications in the biological replicates (ICPLx/ICPL0-Count). "PANTHER protein class" represents the protein class where the protein of interest can be annotated based on PANTHER software tool and UniProt database. Grey / brown highlighted "PANTHER protein classes" belong to the protein class of "small GTPase / associated G-protein" / "cytoskeleton / cytoskeleton-binding protein", respectively

100 mGy - Cortex - 4 weeks post irradiation

#	Symbol	Entrez Gene Name	Unique Peptides	n-fold change from ICPL-4/ICPL-0	ICPL-4/ICPL-0 Variability [%]	ICPL_4 / ICPL_0 Count	PANTHER protein class
1	Actb	actin, beta	7	1.580	24.6	1;12;3;1;2;4	actin and actin related protein
2	Ank2	ankyrin 2, brain	3	1.460	24.2	-;1;1;1;2;2	cytoskeletal protein
3	Phactr1	phosphatase and actin regulator 1	11	1.371	21.7	1;1;6;4;4;1	phosphatase modulator, cytoskeleton organisation protein
4	Uqcrc1	ubiquinol-cytochrome c reductase core protein 1	12	1.334	21.2	3;1;2;4;2;1	metalloprotease, reductase, esterase
5	Fam49b	family with sequence similarity 49, member B	4	1.304	9.1	1;1;2;2;1;1	-
6	Srsf7	serine/arginine-rich splicing factor 7	3	-1.319	26.9	-;3;2;2;1;2	mRNA splicing factor
7	Gnai1	guanine nucleotide binding protein (G protein), alpha inhibiting 1	4	-1.343	10.0	2;2;2;2;3;2	heterotrimeric G-protein
8	Rtn3	reticulon 3	7	-1.420	25.0	1;-;1;1;1;1	membrane traffic protein
9	Cbr1	carbonyl reductase 1	4	-1.740	14.7	1;1;1;1;1;1	dehydrogenase, reductase

500 mGy - Cortex - 4 weeks post irradiation

#	Symbol	Entrez Gene Name	Unique Peptides	n-fold change from ICPL-6/ICPL-0	ICPL-6/ICPL-0 Variability [%]	ICPL_6 / ICPL_0 Count	PANTHER protein class
1	Uqcrc1	ubiquinol-cytochrome c reductase core protein 1	12	2.644	12.8	-;1;1;2;2;1	metalloprotease, reductase, esterase
2	Ywhae	tyrosine 3-monooxygenase/tryptophan 5-monooxygenase activation protein, epsilon polypeptide	3	2.365	540.27	3;-;2;2;1;1	chaperone
3	Coro1b	coronin, actin binding protein 1B	6	1.967	26.8	-;1;3;1;1;2	non-motor actin binding protein

4	Ank2	ankyrin 2, brain	3	1.794	20.7	1;-;4;4;5;1	cytoskeletal protein
5	Rap1gds1	RAP1, GTP-GDP dissociation stimulator 1	7	1.650	28.8	3;6;7;4;4;5	GDP / GTP exchange*
6	Gnb1	guanine nucleotide binding protein (G protein), beta 1	8	1.608	26.2	3;7;5;3;6;5	hydrolase, heterotrimeric G-protein
7	Gnb2	guanine nucleotide binding protein (G protein), beta 2	5	1.599	29.5	2;4;3;3;3;1	hydrolase, heterotrimeric G-protein
8	Atp1b2	ATPase, Na+/K+ transporting, beta 2 polypeptide	5	1.581	29.2	4;4;4;4;3;1	ATP synthase
9	Sept11	septin 11	4	1.52	19.8	3;1;4;3;1;4	small GTPase, cytoskeletal protein
10	Sept8	septin 8	6	1.50	20.2	2;5;3;2;5;1	small GTPase, cytoskeletal protein
11	Lsamp	limbic system-associated membrane protein	5	1.49	14.6	2;3;1;2;1;1	immunoglobulin superfamily cell adhesion molecule
12	Rtn3	reticulon 3	7	1.44	23.4	3;5;3;4;3;3	membrane traffic protein
13	Eif2s1	eukaryotic translation initiation factor 2, subunit 1 alpha	5	1.43	28.9	1;1;2;1;2;-	translation initiation factor
14	Ckb	creatine kinase, brain	14	1.41	16.2	23;23;43;31;29;33	amino acid kinase
15	Sod1	superoxide dismutase 1, soluble	3	1.40	23.3	2;3;4;1;2;2	oxidoreductase
16	Sept7	septin 7	8	1.38	12.8	1;4;4;3;5;5	small GTPase, cytoskeletal protein
17	Tuba4a	tubulin, alpha 4A	7	1.36	9.0	13;15;20;21;20;21	tubulin
18	Tubb3	tubulin, beta 3 class III	8	1.34	8.0	13;18;27;20;12;22	tubulin
19	Sept5	septin 5	5	1.34	11.8	4;6;9;7;7;5	small GTPase, cytoskeletal protein
20	Slc17a7	solute carrier family 17 (sodium-dependent inorganic phosphate cotransporter), member 7	5	1.32	21.4	3;1;3;3;2;1	cation transporter
21	Pcx	pyruvate carboxylase	15	1.32	23.1	1;3;2;2;3;1	ligase
22	Bin1	bridging integrator 1	4	1.31	20.4	1;4;6;3;3;2	membrane trafficking regulatory protein
23	Lancl2	bacterial lantibiotic synthetase component C)-like 2	4	-1.30	7.2	1;1;1;3;1;2	phasphatidylinositol-3/4/5-phosphate binding*
24	Iqsec1	IQ motif and Sec7 domain 1	9	-1.30	8	-;1;2;2;3;1	guanyl-nucleotide exchange factor
25	Prrt2	proline-rich transmembrane protein 2	2	-1.31	9.2	2;2;3;2;2;3	AMPA receptor complex protein*
26	Prkcc	protein kinase C, gamma	13	-1.32	12.4	8;6;8;8;8;8	ATP binding, calcium-dependent protein kinase C activity*
27	Gm9762	predicted pseudogene 9762	2	-1.33	8.2	1;-;1;2;1;3	-
28	Pura	purine rich element binding protein A	7	-1.35	19.3	2;-;4;1;1;1	transcription factor, DNA binding protein
29	Rapgef2	Rap guanine nucleotide exchange factor (GEF) 2	11	-1.36	26.0	2;-;2;2;3;2	guanyl-nucleotide exchange factor
30	Fam49b	family with sequence similarity 49, member B	4	-1.37	8.1	2;2;2;2;3;2	-
31	Rac1	RAS-related C3 botulinum substrate 1	4	-1.47	16.1	5;4;6;7;5;9	small GTPase

2000 mGy - Cortex - 4 weeks post irradiation

#	Symbol	Entrez Gene Name	Unique Peptides	n-fold change from ICPL-10/ICPL-0	ICPL-10/ICPL-0 Variability [%]	ICPL_10 / ICPL_0 Count	PANTHER protein class
1	Ywhae	tyrosine 3-monooxygenase/tryptophan 5-monooxygenase activation protein, epsilon polypeptide	3	1.77	18.3	3;-;2;2;1;1	chaperone
2	Uqcrc1	ubiquinol-cytochrome c reductase core protein 1	12	1.55	20.8	1;1;2;2;1;1	metalloprotease, reductase, esterase
3	Sod1	superoxide dismutase 1, soluble	3	1.38	16.6	2;2;4;1;2;2	oxidoreductase
4	Sept8	septin 8	6	1.37	14.1	2;1;5;2;2;2	small GTPase, cytoskeletal protein
5	Atp5h	ATP synthase, H+ transporting, mitochondrial F0 complex, subunit d	2	1.30	27.4	1;1;3;1;3;5	hydrogen ion transmembrane transcription activity protein, mitochondrial respiration*
6	Prrt2	proline-rich transmembrane protein 2	2	-1.30	9.7	2;3;2;1;2;2	AMPA receptor complex protein*
7	Rac1	RAS-related C3 botulinum substrate 1	4	-1.30	9.9	5;6;5;1;4;4	small GTPase

8	Hspa2	heat shock protein 2	7	-1.30	14.1	1;2;2;2;2;3	Hsp70 family chaperone
9	Gm9762	predicted pseudogene 9762	2	-1.32	6.7	1;-;1;2;1;3	-
10	Ywhab	tyrosine 3-monooxygenase/tryptophan 5-monooxygenase activation protein, beta polypeptide	6	-1.33	23.3	2;-;3;3;4;5	chaperone
11	Ctbp1	C-terminal binding protein 1	5	-1.36	11.5	1;1;1;1;2;-	transcription cofactor, dehydrogenase
12	Srsf1	serine/arginine-rich splicing factor 1	8	-1.42	13.1	1;2;3;2;2;2	mRNA splicing factor
13	Fam49b	family with sequence similarity 49, member B	4	-1.43	17.6	2;2;2;2;3;2	-
14	Rapgef2	Rap guanine nucleotide exchange factor (GEF) 2	11	-1.46	23.2	2;-;2;2;3;2	guanyl-nucleotide exchange factor

Table 28: List of deregulated proteins 4 weeks post-irradiation from 100 mGy, 500 mGy and 2000 mGy within the hippocampus (C57Bl6 study).

The table shows the up-regulated or down-regulated proteins with the fold-changes, their variability, their number of unique peptides used for protein identification and number of identifications in the biological replicates (ICPLx/ICPL0-Count). "PANTHER protein class" represents the protein class where the protein of interest can be annotated based on PANTHER software tool and UniProt database. Grey / brown highlighted "PANTHER protein classes" belong to the protein class of "small GTPase / associated G-protein" / "cytoskeleton / cytoskeleton-binding protein", respectively

100 mGy - Hippocampus - 4 weeks post irradiation

#	Symbol	Entrez Gene Name	Unique Peptides	n-fold change from ICPL-4/ICPL-0	ICPL-4/ICPL-0 Variability [%]	ICPL_4 / ICPL_0 Count	PANTHER protein class
1	Stip1	stress-induced phosphoprotein 1	8	1.59	26.2	4;3;3;4;6;2	chaperone
2	Uqcrc1	ubiquinol-cytochrome c reductase core protein 1	8	1.36	9.4	1;1;1;1;1;1	metalloprotease, reductase, esterase
3	Prkar2b	protein kinase, cAMP dependent regulatory, type II beta	4	-1.55	20.2	-;1;1;1;1;1	kinase modulator
4	Gnai1	guanine nucleotide binding protein (G protein), alpha inhibiting 1	4	-1.92	23.2	1;1;1;1;1;2	heterotrimeric G-protein

500 mGy - Hippocampus - 4 weeks post irradiation

#	Symbol	Entrez Gene Name	Unique Peptides	n-fold change from ICPL-6/ICPL-0	ICPL-6/ICPL-0 Variability [%]	ICPL_6 / ICPL_0 Count	PANTHER protein class
1	Hbb-b1	hemoglobin, beta adult major chain	2	2.86	27.7	3;2;5;1;3;5	oxygen transport*
2	Uqcrc1	ubiquinol-cytochrome c reductase core protein 1	8	1.94	15.7	1;1;1;1;1;1	metalloprotease, reductase, esterase
3	Aldoa	aldolase A, fructose-bisphosphate	4	1.69	15.5	9;7;5;6;10;5	fructose-bisphosphate aldolase activity, protease binding*
4	Slc17a7	solute carrier family 17 (sodium-dependent inorganic phosphate cotransporter), member 7	3	1.57	13.9	1;1;-;1;1;1	cation transporter
5	Rap1gds1	RAP1, GTP-GDP dissociation stimulator 1	6	1.54	26.6	3;4;3;1;3;3	GDP / GTP exchange*
6	Hnrnpl	heterogeneous nuclear ribonucleoprotein L	3	1.50	28.2	3;3;3;3;3;1	mRNA splicing factor, ribonucleoprotein
7	Actb	actin, beta	5	1.48	16.1	2;-;16;5;2;1	actin and actin related protein

8	Nfasc	neurofascin	21	1.38	28.4	2;4;3;-;7;1	immunoglobulin receptor sumperfamily, protein phosphatase, immunoglobulin superfamily cell adhesion molecule
9	Spna2	spectrin alpha 2	2	1.36	28.7	5;7;6;4;4;6	actin capping*
10	Gnb2	guanine nucleotide binding protein (G protein), beta 2	4	1.33	11.6	1;1;2;1;1;2	hydrolase, heterotrimeric G-protein
11	Park7	Parkinson disease (autosomal recessive, early onset) 7	2	1.32	13.9	2;2;2;2;1;2	transcription factor, cysteine protease, RNA binding protein
12	Gnb1	guanine nucleotide binding protein (G protein), beta 1	5	1.31	4.4	2;5;3;5;4;3	hydrolase, heterotrimeric G-protein
13	Cct7	chaperonin containing Tcp1, subunit 7 (eta)	3	1.30	26.5	2;2;1;7;3;4	chaperonin
14	Gdi1	guanosine diphosphate (GDP) dissociation inhibitor 1	7	1.30	26.8	7;5;7;5;4;5	acyltransferase, G-protein modulator
15	Phgdh	3-phosphoglycerate dehydrogenase	6	1.30	23.5	2;2;3;1;1;1	dehydrogenase
16	Bin1	bridging integrator 1	4	1.30	15.6	4;2;4;2;2;3	membrane trafficking regulatory protein
17	Ndufs3	NADH dehydrogenase (ubiquinone) Fe-S protein 3	4	-1.31	14.6	1;2;2;1;2;2	oxidoreductase*
18	Phb2	prohibitin 2	9	-1.31	8.5	1;1;1;1;-;1	estrogen receptor-selective coregulator*
19	Ncam1	neural cell adhesion molecule 1	5	-1.32	17.5	12;10;11;12;	immunoglobulin receptor sumperfamily, protein phosphatase, immunoglobulin superfamily cell adhesion molecule
20	Rac1	RAS-related C3 botulinum substrate 1	4	-1.36	23.1	3;3;4;2;4;7	small GTPase
21	Tubb6	tubulin, beta 6 class V	2	-1.37	28.0	1;3;6;1;-;2	tubulin
22	Prrt2	proline-rich transmembrane protein 2	2	-1.39	10.5	3;2;1;3;1;2	AMPA receptor complex protein*
23	Gnai1	guanine nucleotide binding protein (G protein), alpha inhibiting 1	4	-1.53	14.1	1;1;1;1;1;2	heterotrimeric G-protein
24	Prkar2b	protein kinase, cAMP dependent regulatory, type II beta	4	-1.55	13.7	-;1;1;1;1;1	kinase modulator

2000 mGy - Hippocampus - 4 weeks post irradiation

#	Symbol	Entrez Gene Name	Unique Peptides	n-fold change from ICPL-10/ICPL-0	ICPL-10/ICPL-0 Variability [%]	ICPL_10 / ICPL_0 Count	PANTHER protein class
1	Uqcrc1	ubiquinol-cytochrome c reductase core protein 1	8	1.48	10.1	1;1;1;1;1;1	metalloprotease, reductase, esterase
2	Aldoa	aldolase A, fructose-bisphosphate	4	1.44	19.9	5;7;5;5;7;9	glycolysis and gluconeogenesis*
3	Nfasc	neurofascin	21	1.34	14.6	7;4;2;2;-;4	immunoglobulin receptor sumperfamily, protein phosphatase, immunoglobulin superfamily cell adhesion molecule
4	Ogdhl	oxoglutarate dehydrogenase-like	12	1.31	24.5	3;1;1;1;1;1	oxidoreductase*
5	Hist1h2bp	histone cluster 1, H2bp	3	-1.30	16.9	3;2;1;2;1;2	histone
6	Rac1	RAS-related C3 botulinum substrate 1	4	-1.31	19.8	3;4;2;4;7;3	small GTPase
7	Phb2	prohibitin 2	9	-1.32	4.2	1;1;1;1;-;1	estrogen receptor-selective coregulator*
8	Gnai1	guanine nucleotide binding protein (G protein), alpha inhibiting 1	4	-1.34	21.2	1;1;1;1;1;2	heterotrimeric G-protein
9	Hist1h4j	histone cluster 1, H4j	6	-1.46	19.2	1;7;10;8;10;1	histone*
10	Prrt2	proline-rich transmembrane protein 2	2	-1.51	23.1	3;2;1;3;1;2	AMPA receptor complex protein*

Table 29: List of deregulated proteins 24 weeks post-irradiation from 100 mGy, 500 mGy and 2000 mGy within the cortex (C57Bl6 study).

The table shows the up-regulated or down-regulated proteins with the fold-changes, their variability, their number of unique peptides used for protein identification and number of identifications in the biological replicates (ICPLx/ICPL0-Count). "PANTHER protein class" represents the protein class where the protein of interest can be annotated based on PANTHER software tool and UniProt database. Grey / brown highlighted "PANTHER protein classes" belong to the protein class of "small GTPase / associated G-protein" / "cytoskeleton / cytoskeleton-binding protein", respectively

100 mGy - Cortex - 24 weeks post irradiation

#	Symbol	Entrez Gene Name	Unique Peptides	n-fold change from ICPL-4/ICPL-0	ICPL-4/ICPL-0 Variability [%]	ICPL_4 / ICPL_0 Count	PANTHER protein class
1	H3f3b	H3 histone, family 3B	2	1.80	27.6	5;2;6;6;4;2	histone*
2	Vcl	vinculin	7	1.34	5.5	1;2;1;3;3;-	non-motor actin binding protein, cell adhesion molecule
3	Hnrnpa2b1	heterogeneous nuclear ribonucleoprotein A2/B1	9	1.32	12.8	1;3;3;2;9;6	mRNA polyadeylation factor, mRNA splicing factor, ribosomal protein, ribonucleoprotein
4	Add1	adducin 1 (alpha)	9	-1.31	24.0	9;7;5;3;5;6	non-motor actin binding protein
5	Rpl10	ribosomal protein 10	10	-1.32	20.1	-;3;4;2;3;3	ribosomal protein
6	Cnp	2',3'-cyclic nucleotide 3' phosphodiesterase	11	-1.33	9.2	7;11;16;16;15;17	phosphodiesterase

500 mGy - Cortex - 24 weeks post irradiation

#	Symbol	Entrez Gene Name	Unique Peptides	n-fold change from ICPL-6/ICPL-0	ICPL-6/ICPL-0 Variability [%]	ICPL_6 / ICPL_0 Count	PANTHER protein class
1	Uqcrc1	ubiquinol-cytochrome c reductase core protein 1	10	2.46	28.2	2;3;5;2;3;2	metalloprotease, reductase, esterase
2	Gripap1	GRIP1 associated protein 1	11	1.57	26.3	1;1;3;1;2;1	AMPA receptor interacting protein*
3	Slc3a2	solute carrier family 3 (activators of dibasic and neutral amino acid transport), member 2	4	1.51	18.3	2;3;2;2;1;1	amylase
4	Sept5	septin 5	5	1.47	22.2	3;3;10;5;8;4	small GTPase, cytoskeletal protei
5	Actg1	actin, gamma, cytoplasmic 1	6	1.46	18.6	25;7;19;4;4;5	actin and actin related protein
6	Nono	non-POU-domain-containing, octamer binding protein	9	1.46	26.2	-;1;1;2;2;2	mRNA splicing factor
7	Sept3	septin 3	2	1.40	4.2	3;3;5;1;2;-	small GTPase, cytoskeletal protei
8	Atp6v1d	ATPase, H+ transporting, lysosomal V1 subunit D	8	1.39	24.6	1;2;4;7;5;4	ATP synthase, hydrolase
9	Sept7	septin 7	6	1.39	15.2	3;-;2;3;3;2	small GTPase, cytoskeletal protei
10	Ogdhl	oxoglutarate dehydrogenase-like	9	1.37	29.7	3;4;4;1;1;-	oxidoreductase
11	Rdx	radixin	3	1.36	26.7	1;1;1;1;1;-	actin family cytoskeletal protein
12	Gnb2	guanine nucleotide binding protein (G protein), beta 2	7	1.36	25.3	3;5;8;8;8;3	hydrolase, heterotrimeric G-protein
13	Gnb1	guanine nucleotide binding protein (G protein), beta 1	8	1.35	27.9	9;15;15;18;17;9	hydrolase, heterotrimeric G-protein
14	Ppp2r2a	protein phosphatase 2 (formerly 2A), regulatory subunit B (PR 52), alpha isoform	7	1.35	27.9	-;1;1;3;3;3	protein phosphatase

15	Lrp1	low density lipoprotein receptor-related protein 1	19	1.34	18.3	2;1;1;-;1;2	receptor, extracellular matrix glycoprotein
16	Lsamp	limbic system-associated membrane protein	4	1.31	29.0	2;2;1;3;2;1	immunoglobulin superfamily cell adhesion molecule
17	Ctbp1	C-terminal binding protein 1	8	-1.31	10	1;2;1;2;2;2	transcription cofactor, dehydrogenase
18	Nptn	neuroplastin	7	-1.32	12.4	2;6;9;3;6;6	transmembrane receptor regulatory / adaptor protein
19	Rac1	RAS-related C3 botulinum substrate 1	4	-1.33	18.5	3;5;7;5;7;4	small GTPase
20	Cnp	2',3'-cyclic nucleotide 3' phosphodiesterase	11	-1.39	18.3	11;11;16;17;14;18	phosphodiesterase
21	Synj1	synaptojanin 1	7	-1.43	25.2	1;1;1;-;1;1	phosphatase
22	Prrt2	proline-rich transmembrane protein 2	2	-1.43	7.8	3;1;3;-;2;3	AMPA receptor complex component*

2000 mGy - Cortex - 24 weeks post irradiation

#	Symbol	Entrez Gene Name	Unique Peptides	n-fold change from ICPL-10/ICPL-0	ICPL-10/ICPL-0 Variability [%]	ICPL_10 / ICPL_0 Count	PANTHER protein class
1	Uqcrc1	ubiquinol-cytochrome c reductase core protein 1	10	1.97	22.3	3;5;2;3;3;2	metalloprotease, reductase, esterase
2	Ehd3	EH-domain containing 3	4	1.52	23.6	2;-;1;1;3;1	membrane traffic protein, G-protein modulator, calcium-binding protein
3	Gripap1	GRIP1 associated protein 1	11	1.51	22.7	1;1;3;1;2;1	AMPA receptor interacting protein*
4	Erc2	ELKS/RAB6-interacting/CAST family member 2	7	1.49	13.1	2;1;3;2;-;1	membrane traffic protein - G-protein modulator
5	Rpl35	ribosomal protein L35	2	1.45	24.6	1;1;2;-;1;1	glycosyltransferase, ribosomal protein
6	Snap91	synaptosomal-associated protein 91	5	1.45	29.6	3;3;4;5;2;3	vesicle coat protein
7	Anxa6	annexin A6	7	1.43	29.8	2;3;3;1;3;2	calcium ion binding, calcium-dependent phospholipid binding*
8	Cpne6	copine VI	8	1.42	12.8	4;4;2;2;1;2	membrane traffic protein
9	Ywhae	tyrosine 3-monooxygenase/tryptophan 5-monooxygenase activation protein, epsilon polypeptide	3	1.42	22.1	1;-;1;1;2;2	chaperone
10	Nono	non-POU-domain-containing, octamer binding protein	9	1.37	20.0	1;1;2;-;3;2	mRNA splicing factor
11	Hnrnpl	heterogeneous nuclear ribonucleoprotein L	5	1.36	12.4	2;1;2;2;-;3	mRNA splicing factor, ribonucleoprotein
12	Ap2b1	adaptor-related protein complex 2, beta 1 subunit	2	1.34	26.5	3;3;3;1;-;2	membrane traffic protein
13	L1cam	L1 cell adhesion molecule	13	1.33	18.7	9;5;5;4;4;4	immunoglobulin receptor superfamily, protein phosphatase, immunoglobulin superfamily cell adhesion molecule
14	Gpd2	glycerol phosphate dehydrogenase 2, mitochondrial	18	1.32	29.8	4;4;3;2;1;1	oxidoreductase
15	Sept9	septin 9	4	1.31	20.2	1;2;2;1;2;3	small GTPase, cytoskeletal protei

16	Nefh	neurofilament, heavy polypeptide	14	-1.30	16.5	2;11;3;4;3;5	structural protein, intermediate filament*
17	Nptn	neuroplastin	7	-1.31	15.8	2;6;8;3;5;5	transmembrane receptor regulatory / adaptor protein
18	Nefm	neurofilament, medium polypeptide	17	-1.31	20	19;28;33;26;29;21	structural protein, intermediate filament
19	Vapa	vesicle-associated membrane protein, associated protein A	3	-1.31	26.8	1;2;2;2;4;4	membrane trafficking regulatory protein
20	Hspa2	heat shock protein 2	7	-1.32	23.9	3;2;1;2;6;4	Hsp70 family chaperone
21	Ddt	D-dopachrome tautomerase	3	-1.32	28.9	1;1;2;1;-;1	cytokine, isomerase
22	Lingo1	leucine rich repeat and Ig domain containing 1	7	-1.33	27.3	1;1;1;1;1;-	receptor, extracellular matrix protein
23	Ctbp1	C-terminal binding protein 1	8	-1.33	21.7	2;2;2;-;2;3	transcription cofactor, dehydrogenase
24	Prrt2	proline-rich transmembrane protein 2	2	-1.34	24.1	1;3;-;3;2;3	AMPA receptor complex component*
25	Rac1	RAS-related C3 botulinum substrate 1	4	-1.35	25.3	4;5;7;5;7;2	small GTPase
26	Hint1	histidine triad nucleotide binding protein 1	2	-1.35	9.6	2;2;2;1;2;2	nucleotide phosphatase
27	Mbp	myelin basic protein	2	-1.39	13.7	9;4;14;7;8;5	myelin protein
28	Rps20	ribosomal protein S20	3	-1.41	10.7	1;-;3;2;3;2	ribosomal protein
29	Cnp	2',3'-cyclic nucleotide 3' phosphodiesterase	11	-1.48	25.2	11;16;17;8;14;18	phoshodiesterase

Table 30: List of deregulated proteins 24 weeks post-irradiation from 100 mGy, 500 mGy and 2000 mGy within the hippocampus (C57Bl6 study).

The table shows the up-regulated or down-regulated proteins with the fold-changes, their variability, their number of unique peptides used for protein identification and number of identifications in the biological replicates (ICPLx/ICPL0-Count). "PANTHER protein class" represents the protein class where the protein of interest can be annotated based on PANTHER software tool and UniProt database. Grey / brown highlighted "PANTHER protein classes" belong to the protein class of "small GTPase / associated G-protein" / "cytoskeleton / cytoskeleton-binding protein", respectively

100 mGy - Hippocampus - 24 weeks post irradiation

#	Symbol	Entrez Gene Name	Unique Peptides	n-fold change from ICPL-4/ICPL-	ICPL-4/ICPL-0 Variability [%]	ICPL_4 / ICPL_0 Count	PANTHER protein class
1	Prdx5	peroxiredoxin 5	2	1.649	24.7	2;2;4;4;3;3	radical scavenger*
2	Nfasc	neurofascin	2	1.376	14.4	1;3;2;2;2;2	immunoglobulin receptor superfamily, protein phosphatase, immunoglobulin superfamily cell adhesion molecule
3	Phb	prohibitin	9	1.340	20.9	3;1;6;2;3;4	estrogen receptor-selective coregulator*
4	Atp6v1f	ATPase, H+ transporting, lysosomal V1 subunit F	4	1.307	19.5	1;1;1;1;-;1	proton-transporting ATPase activity*
5	Vim	vimentin	18	-1.318	24.1	-;9;7;6;6;3	structural protein, intermediate filament
6	Idh3b	isocitrate dehydrogenase 3 (NAD+) beta	6	-1.323	28.8	-;4;4;2;5;3	dehydrogenase

500 mGy - Hippocampus - 24 weeks post irradiation

#	Symbol	Entrez Gene Name	Unique Peptides	n-fold change from ICPL-6/ICPL-0	ICPL-6/ICPL-0 Variability [%]	ICPL_6 / ICPL_0 Count	PANTHER protein class
1	Uqcrc1	ubiquinol-cytochrome c reductase core protein 1	12	1.86	18.5	1;2;3;1;2;2	metalloprotease, reductase, esterase
2	Prdx5	peroxiredoxin 5	2	1.83	24.4	2;4;3;4;3;3	radical scavenger*
3	Rap1gds1	RAP1, GTP-GDP dissociation stimulator 1	5	1.77	23.1	1;-;3;2;5;1	GDP / GTP exchange*
4	Nfasc	neurofascin	2	1.75	24.3	1;3;2;2;2;2	immunoglobulin receptor superfamily, protein phosphatase, immunoglobulin superfamily cell adhesion molecule
5	Bin1	bridging integrator 1	4	1.54	16.2	1;2;1;3;2;-	membrane trafficking regulatory protein

6	L1cam	L1 cell adhesion molecule	10	1.51	28.1	4;1;2;2;7;-	immunoglobulin receptor superfamily, protein phosphatase, immunoglobulin superfamily cell adhesion
7	Dnajc5	DnaJ (Hsp40) homolog, subfamily C, member 5	2	1.42	24.1	-;1;2;2;1;1	chaperone
8	Gnb1	guanine nucleotide binding protein (G protein), beta 1	8	1.41	16.3	10;20;8;8;9;8	hydrolase, heterotrimeric G-protein
9	Nptx1	neuronal pentraxin 1	7	1.38	13.3	1;1;3;2;3;3	uptake of synaptic material, synaptic clustering of AMPA receptors*
10	Csnk2a1	casein kinase 2, alpha 1 polypeptide	9	1.38	9.3	-;4;6;2;2;1	serine / theronine-protein kinase catalytic unit, ATP binding*
11	Atp1b2	ATPase, Na+/K+ transporting, beta 2 polypeptide	6	1.37	28.9	2;4;6;5;3;3	ATP synthase
12	Atp6v1f	ATPase, H+ transporting, lysosomal V1 subunit F	4	1.37	19.6	1;2;2;1;2;-	ATPase subunit*
13	Sfxn3	sideroflexin 3	9	1.36	20.9	1;1;4;3;3;2	cation transporter, transfer / carrier protein
14	Ppp1ca	protein phosphatase 1, catalytic subunit, alpha isoform	3	1.36	18.2	-;1;1;1;1;1	protein phosphatase, calcium-binding protein
15	Lsamp	limbic system-associated membrane protein	4	1.35	15.6	1;1;2;2;2;2	immunoglobulin superfamily cell adhesion molecule
16	Sirpa	signal-regulatory protein alpha	6	1.35	28.5	1;2;2;1;3;2	chemokine
17	Cnrip1	cannabinoid receptor interacting protein 1	4	1.35	15.7	3;3;2;4;1;1	voltage-gated calcium channel activity*
18	Ndufs8	NADH dehydrogenase (ubiquinone) Fe-S protein 8	4	1.33	21.7	1;1;2;2;2;2	mitochondrial respiration, NADH dehydrogenase*
19	Gnb2	guanine nucleotide binding protein (G protein), beta 2	7	1.33	13.4	4;4;10;2;2;2	hydrolase, heterotrimeric G-protein
20	Sptan1	spectrin alpha 2	2	1.33	11.7	6;6;6;7;7;8	non-motor actin binding protein
21	Atp6v1b2	ATPase, H+ transporting, lysosomal V1 subunit B2	12	1.32	11.2	3;9;9;6;7;5	ATP synthase, anion channel, ligand-gated ion channel, DNA binding protein, hydrolase
22	Erc2	ELKS/RAB6-interacting/CAST family member 2	7	1.31	22.9	3;2;3;2;2;2	membrane traffic protein, G-protein modulator
23	Ckb	creatine kinase, brain	12	1.31	17.0	33;41;24;28;37;24	amino acid kinase
24	Dclk1	doublecortin-like kinase 1	7	1.30	26.6	-;4;2;3;5;3	non-receptor serine / threonine protein
25	Rac1	RAS-related C3 botulinum substrate 1	5	-1.31	6.5	3;3;5;2;1;2	small GTPase
26	Gfap	glial fibrillary acidic protein	2	-1.31	23.3	1;2;4;1;1;2	structural protein, intermediate filament
27	Rph3a	rabphilin 3A	12	-1.31	9.1	-;3;1;2;3;3	membrane trafficking regulatory protein
28	Nptn	neuroplastin	6	-1.33	16.6	-;4;5;5;6;4	transmembrane receptor regulatory / adaptor protein
29	Cyc1	cytochrome c-1	5	-1.52	29.3	2;3;6;5;5;4	electron acceptor, mitochondrial respiration*

2000 mGy - Hippocampus - 24 weeks post irradiation

#	Symbol	Entrez Gene Name	Unique Peptides	n-fold change from ICPL-10/ICPL-0	ICPL-10/ICPL-0 Variability [%]	ICPL_10 / ICPL_0 Count	PANTHER protein class
1	Prdx5	peroxiredoxin 5	2	1.537	20.7	2;2;4;4;4;3	radical scavenger*

2	Erc2	ELKS/RAB6-interacting/CAST family member 2	7	1.449	18.2	1;3;2;-;2;2	membrane traffic protein, G-protein modulator
3	Pdia3	protein disulfide isomerase associated 3	8	1.355	19.4	6;2;4;3;6;3	isomerase
4	Nfasc	neurofascin	2	1.354	20.3	1;3;2;2;2;2	immunoglobulin receptor superfamily, protein phosphatase, immunoglobulin superfamily cell adhesion molecule
5	Nefh	neurofilament, heavy polypeptide	11	1.337	28.6	1;-;2;1;3;5	structural protein, intermediate filament*
6	Actb	actin, beta	2	1.334	12.9	1;3;6;4;1;-	actin and actin related protein
7	Atp6v1f	ATPase, H+ transporting, lysosomal V1 subunit F	4	1.321	15.4	1;1;2;1;-;1	ATPase activity*
8	Pdhx	pyruvate dehydrogenase complex, component X	3	1.302	15.3	1;3;2;1;3;3	acetyltransferase, acyltransferase
9	Ppp2r1a	protein phosphatase 2 (formerly 2A), regulatory subunit A (PR 65), alpha isoform	9	-1.301	23.2	11;18;4;11;11;4	protein phosphatase
10	Tkt	transketolase	10	-1.328	30	7;4;6;5;7;10	transketolase, dehydrogenase, lyase
11	Rac1	RAS-related C3 botulinum substrate 1	5	-1.385	25.8	4;2;5;2;2;5	small GTPase

Table 31: List of deregulated proteins 5 weeks post-irradiation from 100 mGy, 500 mGy and 2000 mGy within the isolated synaptosomes of cortex (C57Bl6 study).

The table shows the up-regulated or down-regulated proteins with the fold-changes, their variability, their number of unique peptides used for protein identification and number of identifications in the biological replicates (ICPLx/ICPL0-Count). "PANTHER protein class" represents the protein class where the protein of interest can be annotated based on PANTHER software tool and UniProt database. Grey / brown highlighted "PANTHER protein classes" belong to the protein class of "small GTPase / associated G-protein" / "cytoskeleton / cytoskeleton-binding protein", respectively

100 mGy - Synaptosomes of cortex - 5 weeks post irradiation

#	Symbol	Entrez Gene Name	Unique Peptides	n-fold change from ICPL-4/ICPL-0	ICPL-4/ICPL-0 Variability [%]	ICPL_4 / ICPL_0 Count	PANTHER protein class
1	Ctnnb1	catenin (cadherin associated protein), beta 1	6	2.06	25.0	1;-;2	storage protein, signaling molecule, cytoskeletal protein, cell adhesion molecule
2	Cask	calcium/calmodulin-dependent serine protein kinase (MAGUK family)	5	1.79	0.3	1;-;1	nucleotide kinase, protein kinase, cell junction protein
3	Rab3a	RAB3A, member RAS oncogene family	2	1.76	17.0	3;-;1	GTPase activity, GTP binding, ATPase activator activity*
4	Cotl1	coactosin-like 1 (Dictyostelium)	3	1.70	20.3	1;-;1	non-motor actin binding protein
5	Uqcrc1	ubiquinol-cytochrome c reductase core protein 1	13	1.65	30.0	1;3;3	metalloprotease, reductase, esterase
6	Lrp1	low density lipoprotein receptor-related protein 1	16	1.59	16.1	1;1;2	receptor, extracellular matrix glycoprotein
7	Rpn1	ribophorin I	3	1.47	2.2	1;-;1	glycosyltransferase
8	Otub1	OTU domain, ubiquitin aldehyde binding 1	4	1.44	5.1	2;-;2	hydrolase
9	Rasal1	RAS protein activator like 1 (GAP1 like)	9	1.42	13.4	1;-;1	signaling molecule, G-protein modulator
10	Cox4i1	cytochrome c oxidase subunit IV isoform 1	3	1.41	20.4	1;-;1	mitochondrial cytochrome-c oxidase activity*
11	Ap2b1	adaptor-related protein complex 2, beta 1 subunit	2	1.40	20.4	1;1;2	membrane traffic protein
12	Mbp	myelin basic protein	11	1.39	10.2	13;11;15	myelin protein

13	Cand1	cullin associated and neddylation disassociated 1	4	1.39	28.1	2;1;2	transcription factor
14	Prkce	protein kinase C, epsilon	2	1.37	25.9	2;-;2	non-receptor serine / threonine protein kinase, transfer / carrier protein, annexin, calmodulin
15	Prkcsh	protein kinase C substrate 80K-H	5	1.37	11.0	1;-;1	transferase, enzyme modulator
16	Rap1gds1	RAP1, GTP-GDP dissociation stimulator 1	4	1.36	27.5	1;2;2	GTPase activator activity*
17	Pdia3	protein disulfide isomerase associated 3	8	1.36	27.7	1;6;8	isomerase
18	C2cd2l	C2 calcium-dependent domain containing 2-like	4	1.35	19.7	1;1;1	membrane protein*
19	Mapt	microtubule-associated protein tau	2	1.34	28.3	2;2;2	microtubule binding*
20	Coro1a	coronin, actin binding protein 1A	11	1.34	23.1	10;7;10	non-motor actin binding protein
21	Vapa	vesicle-associated membrane protein, associated protein A	3	1.33	23.2	4;2;4	membrane trafficking regulatory protein
22	Cpne6	copine VI	5	1.32	8.3	3;1;3	membrane traffic protein
23	Dnajc5	DnaJ (Hsp40) homolog, subfamily C, member 5	2	1.31	12.6	2;1;3	chaperone
24	Lsamp	limbic system-associated membrane protein	6	1.31	20.2	4;-;2	immunoglobulin superfamily cell adhesion molecule
25	Cct4	chaperonin containing Tcp1, subunit 4 (delta)	4	-1.31	1.5	3;1;-	chaperonin
26	Uqcrb	ubiquinol-cytochrome c reductase binding protei	5	-1.31	16.1	2;6;2	reductase
27	Dctn2	dynactin 2	5	-1.32	26.1	1;1;1	microtubule binding motor protein
28	Cct2	chaperonin containing Tcp1, subunit 2 (beta)	9	-1.32	1.5	2;-;3	chaperonin
29	Plec	plectin	39	-1.32	24.2	2;3;5	non-motor actin binding protein
30	Epb4.1l3	erythrocyte protein band 4.1-like 3	8	-1.32	11.9	7;4;5	structural constituent of cytoskeleton*
31	Atp5o	ATP synthase, H+ transporting, mitochondrial F1 complex, O subunit	5	-1.33	17.8	10;7;6	ATP synthase, hydrolase
32	Napg	N-ethylmaleimide sensitive fusion protein attachment protein gamma	3	-1.33	12.6	-;1;2	membrane traffic protein
33	Hadhb	hydroxyacyl-Coenzyme A dehydrogenase/3-ketoacyl-Coenzyme A thiolase/enoyl-Coenzyme A hydratase (trifunctional protein), beta	6	-1.37	0.2	1;1;-	acetyltransferase
34	Ndufa9	NADH dehydrogenase (ubiquinone) 1 alpha subcomplex, 9	7	-1.38	18.4	3;2;5	dehydrogenase, reductase
35	Homer1	homer homolog 1 (Drosophila)	5	-1.38	14.0	3;3;3	signaling molecule
36	720456B07R	RIKEN cDNA 6720456B07 gene	2	-1.38	13.2	2;2;-	cyotskeletal protein*
37	Ube2d3	ubiquitin-conjugating enzyme E2D 3 (UBC4/5 homolog, yeast)	2	-1.39	12.9	1;-;2	ligase
38	Aldh6a1	aldehyde dehydrogenase family 6, subfamily A1	3	-1.40	20.7	3;1;1	dehydrogenase
39	Strn	striatin, calmodulin binding protein	5	-1.40	5.0	1;1;-	calmodulin binding, scaffolding protein*
40	Ndufa1	NADH dehydrogenase (ubiquinone) 1 alpha subcomplex, 1	2	-1.41	3.0	1;1;1	mitochondrial NADH dehydrogenase*
41	Shank3	SH3/ankyrin domain gene 3	22	-1.42	3	-;3;1	interconnector of receptors to cytoskeleton*
42	Mdh1	malate dehydrogenase 1, NAD (soluble)	2	-1.42	2.4	1;-;1	dehydrogenase
43	Cs	citrate synthase	5	-1.43	26.3	1;2;3	transferase, lyase
44	Prkar2a	protein kinase, cAMP dependent regulatory, type II alpha	5	-1.43	13.0	2;3;-	kinase modulator
45	Bsg	basigin	3	-1.44	26.8	1;-;1	transmembrane receptor regulatory adaptor protein

46	Atp6v1c1	ATPase, H+ transporting, lysosomal V1 subunit C1	5	-1.45	5.7	4;9;4	ATP synthase, hydrolase
47	Ywhab	tyrosine 3-monooxygenase/tryptophan 5-monooxygenase activation protein, beta polypeptide	4	-1.47	8.6	1;-;2	chaperone

500 mGy -Synaptosomes of cortex- 5 weeks post irradiation

#	Symbol	Entrez Gene Name	Unique Peptides	n-fold change from ICPL-6/ICPL-0	ICPL-6/ICPL-0 Variability [%]	ICPL_6 / ICPL_0 Count	PANTHER protein class
1	Cox4i1	cytochrome c oxidase subunit IV isoform 1	3	2.20	14.3	1;1;-	mitochondrial cytochrome c activity*
2	Prkar2a	protein kinase, cAMP dependent regulatory, type II alpha	5	1.81	3.2	2;3;-	kinase modulator
3	Cand1	cullin associated and neddylation disassociated 1	4	1.74	24.2	1;2;1	transcription factor
4	Tpm3	tropomyosin 3, gamma	6	1.73	20.7	2;1;-	actin binding motor protein
5	Wdr7	WD repeat domain 7	5	1.70	14.2	-;2;1	mRNA splicing factor, esterase, kinase inhibitor
6	Rap1gds1	RAP1, GTP-GDP dissociation stimulator 1	4	1.67	6.2	2;2;-	GTPase activator activity*
7	Pi4ka	phosphatidylinositol 4-kinase, catalytic, alpha polypeptide	5	1.63	0.9	1;1;-	kinase
8	Uqcrc1	ubiquinol-cytochrome c reductase core protein 1	13	1.62	16.6	3;1;3	metalloprotease, reductase, esterase
9	Otub1	OTU domain, ubiquitin aldehyde binding 1	4	1.55	9.4	2;2;-	hydrolase
10	Sept3	septin 3	2	1.48	24.7	2;5;3	small GTPase, cytoskeletal protein
11	Hsph1	heat shock 105kDa/110kDa protein 1	5	1.48	12.2	2;3;-	Hsp70 family chaperone
12	Ctnnb1	catenin (cadherin associated protein), beta 1	6	1.47	4.3	2;1;-	storage protein, signaling molecule, cytoskeletal protein, cell adhesion molecule
13	Opa1	optic atrophy 1 homolog (human)	9	1.46	18.5	2;2;2	hydrolase, small GTPase, microtubule family cytoskeletal protein
14	Atp5h	ATP synthase, H+ transporting, mitochondrial F0 complex, subunit d	2	1.39	27.0	5;3;4	mitochondrial ATP synthase*
15	Git1	G protein-coupled receptor kinase-interactor 1	13	1.39	6.2	4;3;-	nucleic acid binding, G-protein modulator
16	Pdhx	pyruvate dehydrogenase complex, component X	4	1.39	7.3	-;3;2	acetyltransferase, acyltransferase
17	Mtap4	microtubule-associated protein 4	5	1.38	22.5	4;6;5	microtuble assembly promotor*
18	Pdia4	protein disulfide isomerase associated 4	4	1.37	12.2	4;6;1	isomerase
19	Ndufs8	NADH dehydrogenase (ubiquinone) Fe-S protein	4	1.35	20.0	-;2;1	mitochondrial NADH dehydrogenase*
20	Mtdh	metadherin	4	1.34	24.2	1;2;-	NF-kappaB binding, RNA binding, transcription coactivator activity*
21	Pdia3	protein disulfide isomerase associated 3	8	1.33	21.7	6;9;2	isomerase
22	Dld	dihydrolipoamide dehydrogenase	7	1.33	24.3	6;6;4	deydrogenase, oxidase, reductase
23	Sept7	septin 7	6	1.33	15.5	7;7;4	small GTPase, cytoskeletal protein
24	Pfkp	phosphofructokinase, platelet	6	1.33	28.9	1;8;4	carbohydrate kinase
25	Tuba4a	tubulin, alpha 4A	8	1.32	28.1	12;15;12	tubulin
26	Ckb	creatine kinase, brain	13	1.32	5.1	31;32;22	amino acid kinase
27	Cask	calcium/calmodulin-dependent serine protein kinase (MAGUK family)	5	1.31	2.3	1;3;-	nucleotide kinase, protein kinase, cell junction protein
28	Tubb3	tubulin, beta 3 class III	8	1.31	23.6	13;16;10	tubulin
29	Rac1	RAS-related C3 botulinum substrate 1	4	-1.32	19.9	7;4;7	small GTPase
30	Rab11b	RAB11B, member RAS oncogene family	2	-1.33	22.5	3;1;1	GDP / GTP binding, GTPase activity*
31	Cct2	chaperonin containing Tcp1, subunit 2 (beta)	9	-1.34	14.3	3;2;-	chaperonin
32	Dlat	dihydrolipoamide S-acetyltransferase (E2 component of pyruvate dehydrogenase complex)	2	-1.35	19.2	2;4;2	acetyltransferase, acyltransferase
33	Ube2d3	ubiquitin-conjugating enzyme E2D 3 (UBC4/5 homolog, yeast)	2	-1.36	0.8	2;1;-	ligase
34	Gm20390	predicted gene 20390	6	-1.37	23.5	7;9;7	-
35	Atp6v1c1	ATPase, H+ transporting, lysosomal V1 subunit C1	5	-1.37	13	4;9;4	ATP synthase, hydrolase
36	Uqcrb	ubiquinol-cytochrome c reductase binding protein	5	-1.39	19.3	2;6;-	reductase

37	Slc25a11	solute carrier family 25 (mitochondrial carrier oxoglutarate carrier), member 11	2	-1.39	14.6	-;1;1	amino acid transporter, mitochondrial carrier protein, transfer / carrier protein, calmodulin
38	Ntrk2	neurotrophic tyrosine kinase, receptor, type 2	3	-1.42	3.7	1;2;-	ATP binding, brain-derived neurothrophic factor binding, protein homodimerization activity*
39	Cct4	chaperonin containing Tcp1, subunit 4 (delta)	4	-1.43	4.2	-;3;1	chaperonin
40	Pdia6	protein disulfide isomerase associated 6	5	-1.43	2.7	4;1;-	isomerase
41	Rab5c	RAB5C, member RAS oncogene family	2	-1.52	3.1	-;1;1	GDP / GTP binding, GTPase activity*
42	Ppp5c	protein phosphatase 5, catalytic subunit	2	-1.60	1.3	1;1;-	protein phosphatase, calcium-binding protein
43	Rasal1	RAS protein activator like 1 (GAP1 like)	9	-1.60	4.0	1;1;-	signaling molecule, G-protein modulator

2000 mGy - Synaptosomes of cortex - 5 weeks post irradiation

#	Symbol	Entrez Gene Name	Unique Peptides	n-fold change from ICPL-10/ICPL-0	ICPL-10/ICPL-0 Variability [%]	ICPL_10 / ICPL_0 Count	PANTHER protein class
1	Ppfia3	protein tyrosine phosphatase, receptor type, f polypeptide (PTPRF), interacting protein (liprin), alpha 3	15	2.83	26.8	3;2;3	focal adhesion regulation*
2	Prkar2a	protein kinase, cAMP dependent regulatory, type II alpha	5	2.08	1.6	2;3;-	kinase modulator
3	Plcb1	phospholipase C, beta 1	9	1.98	22.7	2;3;4	signaling molecule, guanyl-nucleotide exchange factor, calcium-binding protein, phospholipase
4	Prkcsh	protein kinase C substrate 80K-H	5	1.92	17.7	1;-;1	transferase, enzyme modulator
5	Cadm1	cell adhesion molecule 1	3	1.91	14.8	1;-;4	receptor, defense / immunity protein, cell adhesion molecule
6	Itsn1	intersectin 1 (SH3 domain protein 1A)	7	1.90	20.8	2;2;5	G-protein modulator, calcium-binding protein, membrane traffic protein
7	Strn	striatin, calmodulin binding protein	5	1.88	18.6	2;1;-	calmodulin binding, scaffolding protein*
8	Rasal1	RAS protein activator like 1 (GAP1 like)	9	1.86	15.2	1;-;1	signaling molecule, G-protein modulator
9	Kif2a	kinesin family member 2A	6	1.84	5.1	2;1;-	microtubule binding motor protein
10	Nsfl1c	NSFL1 (p97) cofactor (p47)	5	1.75	16.2	1;-;2	membrane trafficking regulatory protein
11	Ezr	ezrin	5	1.75	8.7	1;-;1	actin family cytoskeletal protein
12	Git1	G protein-coupled receptor kinase-interactor 1	13	1.72	4.2	3;-;4	nucleic acid binding, G-protein modulator
13	Prkar2b	protein kinase, cAMP dependent regulatory, type II beta	9	1.68	16.5	3;3;5	kinase modulator
14	Epb4.1l2	erythrocyte protein band 4.1-like 2	7	1.67	18.5	3;2;-	actin binding, structural molecule activity*
15	430548M08Ri	RIKEN cDNA 6430548M08 gene	4	1.67	29.4	3;2;-	-
16	Sh3glb2	SH3-domain GRB2-like endophilin B2	8	1.62	27.7	2;4;1	membrane trafficking regulatory protein, actin family cytoskeletal protein
17	Ppp1r7	protein phosphatase 1, regulatory (inhibitor) subunit 7	4	1.59	21.5	2;1;1	protein phosphatase*
18	C2cd2l	C2 calcium-dependent domain containing 2-like	4	1.58	8.7	1;1;1	membrane protein*
19	Mtap7d1	microtubule-associated protein 7 domain containing 1	4	1.57	16.2	1;1;-	microtuble protein*
20	Epn1	epsin 1	5	1.57	19.4	2;-;1	lipid binding, transcription factor binding*
21	Sept3	septin 3	2	1.57	19.9	2;5;3	small GTPase, cytoskeletal protein
22	Palm	paralemmin	5	1.56	29.6	3;1;4	axonal and dendritic filopodia induction protein*
23	Mtap6	microtubule-associated protein 6	19	1.55	24.5	15;12;25	microtubule protein*
24	Prkce	protein kinase C, epsilon	2	1.52	26.7	2;-;2	non-receptor serine / threonine protein kinase, transfer / carrier protein, annexin, calmodulin
25	Uqcrc1	ubiquinol-cytochrome c reductase core protein 1	13	1.52	27.5	1;3;3	metalloprotease, reductase, esterase
26	Dlg4	discs, large homolog 4 (Drosophila)	12	1.52	22.4	4;-;10	transmembrane receptor regulatory adaptor protein
27	Cacna2d1	calcium channel, voltage-dependent, alpha2/delta subunit 1	8	1.49	19.9	9;9;7	metal ion binding, voltage-gated calcium channel activity*

28	Usp5	ubiquitin specific peptidase 5 (isopeptidase T)	15	1.49	17.7	1;3;4	cysteine protease, mRNA splicing factor, ubiquitin
29	Icam5	intercellular adhesion molecule 5, telencephalin	11	1.48	29.9	1;2;2	signaling molecule, immunoglobulin superfamily cell adhesion molecule
30	Dnm1l	dynamin 1-like	8	1.47	17	1;-;6	hydrolase, small GTPase, microtubule family cytoskeletal protein
31	Sept7	septin 7	6	1.47	4.0	6;6;4	small GTPase, cytoskeletal protein
32	Gprin1	G protein-regulated inducer of neurite outgrowth 1	13	1.47	20.7	11;8;11	protein involved in neurite outgrowth, G-protein*
33	Dpysl3	dihydropyrimidinase-like 3	9	1.45	6.6	11;5;4	cytoskeletal remodelling*
34	Mtap4	microtubule-associated protein 4	5	1.45	21.0	6;5;4	microtubule protein*
35	Tmod2	tropomodulin 2	4	1.44	25.6	2;3;2	non-motor actin binding protein
36	Dlg1	discs, large homolog 1 (Drosophila)	10	1.44	28	1;4;1	transmembrane receptor regulatory / adaptor protein
37	Pdia4	protein disulfide isomerase associated 4	4	1.43	29.8	1;4;5	isomerase
38	Arfgap1	ADP-ribosylation factor GTPase activating protein 1	7	1.43	27.5	6;3;2	nucleic acid binding, G-protein modulator
39	Tom1l2	target of myb1-like 2 (chicken)	6	1.42	22.2	1;-;1	transporter, membrane traffic protein, kinase activator, cytoskeletal protein
40	Ppp2r2a	protein phosphatase 2 (formerly 2A), regulatory subunit B (PR 52), alpha isoform	6	1.42	6.4	4;2;-	protein phosphatase
41	Epb4.1l1	erythrocyte protein band 4.1-like 1	10	1.40	27.1	7;4;13	structural constituent of cytoskeleton*
42	Pdhx	pyruvate dehydrogenase complex, component X	4	1.39	2.2	3;2;-	acetyltransferase, acyltransferase
43	Mpp2	membrane protein, palmitoylated 2 (MAGUK p55 subfamily member 2)	10	1.39	23.3	2;-;1	nucleotide kinase, cell junction protein
44	Aak1	AP2 associated kinase 1	7	1.38	15.4	2;4;5	non-receptor serine / threonine protein kinase
45	Ogdhl	oxoglutarate dehydrogenase-like	6	1.38	25.8	1;-;2	dehydrogenase*
46	Fscn1	fascin homolog 1, actin bundling protein (Strongylocentrotus purpuratus)	11	1.38	26.7	5;4;4	non-motor actin binding protein
47	Mtap1b	microtubule-associated protein 1B	12	1.37	9.8	8;6;11	microtubule protein*
48	Pi4ka	phosphatidylinositol 4-kinase, catalytic, alpha polypeptide	5	1.37	22.8	1;1;-	kinase
49	Eif4b	eukaryotic translation initiation factor 4B	4	1.37	28.2	2;-;2	translation initiation factor
50	Hspa9	heat shock protein 9	9	1.36	20.9	14;-;14	heat shock protein*
51	Aldh5a1	aldhehyde dehydrogenase family 5, subfamily A1	7	1.36	28.9	1;4;2	dehydrogenase
52	Nrcam	neuron-glia-CAM-related cell adhesion molecule	5	1.35	23.8	5;4;5	immunoglobulin receptor superfamily, protein phosphatase, immunoglobulin superfamily cell adhesion molecule
53	Abi2	abl-interactor 2	7	1.35	27.1	1;1;2	G-protein modulator
54	Coro1a	coronin, actin binding protein 1A	11	1.34	16.6	10;7;10	non-motor actin binding protein
55	Sgip1	SH3-domain GRB2-like (endophilin) interacting protein 1	7	1.34	26.6	2;2;3	membrane trafficking regulatory protein, actin family cytoskeletal protein
56	Add1	adducin 1 (alpha)	9	1.34	11.9	7;5;1	non-motor actin binding protein
57	Gphn	gephyrin	3	1.33	21.6	1;-;2	microtuble-associated protein*
58	Immt	inner membrane protein, mitochondrial	10	1.32	18.3	7;-;3	mitochondrial membrane protein*
59	Dlg3	discs, large homolog 3 (Drosophila)	10	1.32	19.8	3;4;8	transmembrane receptor regulatory / adaptor protein
60	Cct3	chaperonin containing Tcp1, subunit 3 (gamma)	5	1.32	1.4	2;-;1	chaperonin
61	Myh10	myosin, heavy polypeptide 10, non-muscle	16	1.32	23.9	7;3;3	G-protein modulator, actin binding motor protein, cell junction protein
62	Uba1	ubiquitin-like modifier activating enzyme 1	9	1.32	29.3	2;1;1	transfer / carrier protein, ligase
63	Myo5a	myosin VA	13	1.32	20.0	6;7;8	G-protein modulator, actin binding motor protein, cell junction protein
64	Dld	dihydrolipoamide dehydrogenase	7	1.32	23.6	4;4;6	dehydrogenase, oxidase, reductase
65	Stxbp1	syntaxin binding protein 1	3	1.31	30	4;9;9	transporter, membrane trafficking regulatory protein
66	Fh1	fumarate hydratase 1	5	1.31	16.2	3;3;3	fumarate hydratase activity*
67	Pld3	phospholipase D family, member 3	4	-1.31	2.6	2;3;5	phospholipase

68	Eno1	enolase 1, alpha non-neuron	5	-1.31	8.3	22;14;20	lyase
69	Ywhab	tyrosine 3-monooxygenase/tryptophan 5-monooxygenase activation protein, beta polypeptide	4	-1.32	22.0	1;-;2	chaperone
70	Atp6v0d1	ATPase, H+ transporting, lysosomal V0 subunit D1	3	-1.32	6.6	5;4;2	ATP synthase, hydrolase
71	Eif4h	eukaryotic translation initiation factor 4H	3	-1.34	1.3	1;-;1	translation initiation factor
72	Rpl4	ribosomal protein L4	2	-1.35	11.3	4;3;-	ribosomal protein
73	720456B07R	RIKEN cDNA 6720456B07 gene	2	-1.35	2.8	2;2;-	-
74	Camkv	CaM kinase-like vesicle-associated	5	-1.36	7.7	2;5;1	non-receptor serine / threonine protein kinase
75	Arhgdia	Rho GDP dissociation inhibitor (GDI) alph	3	-1.37	9.6	2;2;-	signaling molecule, G-protein modulator
76	Ywhae	tyrosine 3-monooxygenase/tryptophan 5-monooxygenase activation protein, epsilon polypeptide	4	-1.37	21.6	4;3;7	chaperone
77	Gstp1	glutathione S-transferase, pi 1	3	-1.37	22.9	2;2;2	gluthatione transferase activity*
78	Syngap1	synaptic Ras GTPase activating protein 1 homolog (rat)	9	-1.37	18.0	3;1;-	signaling molecule, G-protein modulator
79	Gad2	glutamic acid decarboxylase 2	2	-1.37	11.5	5;4;5	decarboxylase
80	Cyc1	cytochrome c-1	5	-1.38	17.9	8;7;6	mitochondrial cytochrome c activity*
81	Ube2d3	ubiquitin-conjugating enzyme E2D 3 (UBC4/5 homolog, yeast)	2	-1.38	10.4	1;-;2	ligase
82	Slc25a5	solute carrier family 25 (mitochondrial carrier, adenine nucleotide translocator), member 5	6	-1.40	23.1	10;15;12	mitochondrial ADP exchange*
83	Phb2	prohibitin	10	-1.41	18.7	2;3;4	estrogen-receptor coregulator*
84	Rac1	RAS-related C3 botulinum substrate 1	4	-1.42	28.7	7;11;6	small GTPase
85	Calm3	calmodulin 3	4	-1.42	16.5	6;4;7	calcium ion binding, protein phosphatase activator activity*
86	Ndufa1	NADH dehydrogenase (ubiquinone) 1 alpha subcomplex, 1	2	-1.45	10.8	1;1;1	mitochondrial NADH dehydrogenase*
87	Abhd12	abhydrolase domain containing 12	3	-1.45	23.6	2;2;1	acylglycerol lipase activity*
88	Rab5c	RAB5C, member RAS oncogene family	2	-1.49	5.8	1;1;-	GTPase activity, GTP / GDP binding*
89	Gm20390	predicted gene 20390	6	-1.49	20.2	8;7;10	ATP binding, nucleoside diphosphate kinase activity*
90	Arhgap1	Rho GTPase activating protein 1	3	-1.50	6.2	1;1;3	G-protein modulator
91	Ndufa9	NADH dehydrogenase (ubiquinone) 1 alpha subcomplex, 9	7	-1.50	13.3	3;2;5	dehydrogenase, reductase
92	Cnp	2',3'-cyclic nucleotide 3' phosphodiesterase	7	-1.50	9.9	8;6;3	phosphodiesterase
93	Rpl8	ribosomal protein L8	3	-1.52	19.9	1;4;3	ribosomal protein*
94	Atp6v1c1	ATPase, H+ transporting, lysosomal V1 subunit C1	5	-1.52	6.7	10;4;5	ATP synthase, hydrolase
95	Hspa8	heat shock protein 8	11	-1.52	27.7	53;43;50	Hsp70 family chaperone
96	Rps14	ribosomal protein S14	2	-1.55	21.6	2;2;2	ribosomal protein
97	Dlat	dihydrolipoamide S-acetyltransferase (E2 component of pyruvate dehydrogenase complex)	2	-1.60	9.2	4;2;2	acetyltransferase, acyltransferase
98	Arpc4	actin related protein 2/3 complex, subunit 4	3	-1.61	5.5	4;2;-	actin family cytoskeletal protein
99	Rab35	RAB35, member RAS oncogene family	2	-1.64	15.5	2;-;1	small GTPase, GDP / GTP binding*
100	Atp1a3	ATPase, Na+/K+ transporting, alpha 3 polypeptide	9	-1.70	9.0	15;9;6	cation transporter, ion channel, hydrolase
101	Fkbp2	FK506 binding protein 2	2	-1.71	22.7	2;-;2	isomerase, chaperone, calcium-binding protein
102	Atp1a2	ATPase, Na+/K+ transporting, alpha 2 polypeptide	7	-1.73	14.8	3;1;2	cation transporter, ion channel, hydrolase
103	Cct4	chaperonin containing Tcp1, subunit 4 (delta)	4	-1.80	19.1	3;1;-	chaperonin
104	Slc25a11	solute carrier family 25 (mitochondrial carrier oxoglutarate carrier), member 11	2	-1.85	11.4	1;1;-	amino acid transporter, mitochondrial carrier protein, transfer / carrier protein, calmodulin
105	Ndufb10	NADH dehydrogenase (ubiquinone) 1 beta subcomplex, 1	3	-1.89	12.2	2;2;2	mitochondrial NADH dehydrogenase*
106	Slc12a5	solute carrier family 12, member 5	2	-2.09	10.6	2;-;1	cation transporter

Table 32: List of deregulated proteins 5 weeks post-irradiation from 100 mGy, 500 mGy and 2000 mGy within the isolated synaptosomes of hippocampus (C57Bl6 study).

The table shows the up-regulated or down-regulated proteins with the fold-changes, their variability, their number of unique peptides used for protein identification and number of identifications in the biological replicates (ICPLx/ICPL0-Count). "PANTHER protein class" represents the protein class where the protein of interest can be annotated based on PANTHER software tool and UniProt database. Grey / brown highlighted "PANTHER protein classes" belong to the protein class of "small GTPase / associated G-protein" / "cytoskeleton / cytoskeleton-binding protein", respectively

100 mGy - Synaptosomes of hippocampus - 5 weeks post irradiation

#	Symbol	Entrez Gene Name	Unique Peptides	n-fold change from ICPL-4/ICPL-	ICPL-4/ICPL-0 Variability [%]	ICPL_4 / ICPL_0 Count	PANTHER protein class
1	Lrp1	low density lipoprotein receptor-related protein 1	11	1.92	11.2	1;-;1	receptor, extracellular matrix glycoprotein
2	Ctnnb1	catenin (cadherin associated protein), beta 1	11	1.83	21.8	1;1;-	cell adhesion molecule, signaling molecule, storage protein, cytoskeletal protein
3	Lasp1	LIM and SH3 protein 1	2	1.80	18.0	2;1;2	actin-based cytoskeletal activity*
4	Clasp2	CLIP associating protein 2	6	1.76	4.0	1;1;-	structural protein
5	Fasn	fatty acid synthase	11	1.74	5.1	1;1;-	acyltransferase, methyltransferase,
6	Acot7	acyl-CoA thioesterase 7	4	1.74	21.3	5;1;4	esterase
7	Fscn1	fascin homolog 1, actin bundling protein (Strongylocentrotus purpuratus)	9	1.73	17.8	2;1;2	non-motor actin binding protein
8	Hsp90b1	heat shock protein 90, beta (Grp94), member 1	7	1.70	3.3	2;5;8	Hsp90 family chaperone
9	Rpl4	ribosomal protein L4	3	1.58	0.8	3;-;1	ribosomal protein
10	Ndufs5	NADH dehydrogenase (ubiquinone) Fe-S protein 5	3	1.57	10.6	2;-;1	mitochondrial NADH dehydrogenase*
11	Uqcrh	ubiquinol-cytochrome c reductase hinge protein	4	1.52	13.2	1;-;2	reductase
12	Cox6a1	cytochrome c oxidase, subunit VI a, polypeptide 1	2	1.52	9.4	1;-;1	oxidase
13	Ctnnd2	catenin (cadherin associated protein), delta 2	11	1.51	12.5	2;1;-	intermediate filament binding protein, cell junction protein, cell adhesion molecule
14	Arhgap1	Rho GTPase activating protein 1	2	1.47	7.2	2;-;5	G-protein modulator
15	Rasal1	RAS protein activator like 1 (GAP1 like)	7	1.46	24.4	1;1;1	signaling molecule, G-protein modulator
16	Eef2	eukaryotic translation elongation factor 2	8	1.46	28.9	3;1;4	translation elongation / inititation factor, G-protein, hydrolase
17	Hspa5	heat shock protein 5	10	1.44	2.0	7;11;7	Hsp70 family chaperone
18	Pdia4	protein disulfide isomerase associated 4	3	1.43	16.4	1;1;2	isomerase
19	Rap1gds1	RAP1, GTP-GDP dissociation stimulator 1	4	1.41	1.3	3;1;-	GTPase activator activity*
20	Rpl35	ribosomal protein L35	3	1.41	6.7	2;1;-	ribosomal protein, glycosyltransferase
21	Prkce	protein kinase C, epsilon	2	1.40	23.2	3;2;-	non-receptor serine / threonine protein kinase, transfer / carrier protein, annexin, calmodulin

22	Pdia3	protein disulfide isomerase associated 3	6	1.38	11.1	3;3;4	isomerase
23	Stmn1	stathmin 1	2	1.38	8.2	3;1;2	microtuble destabilizing protein*
24	Coro1a	coronin, actin binding protein 1A	8	1.37	27.8	10;6;9	non-motor actin binding protein
25	Sfxn1	sideroflexin 1	4	1.36	1.0	1;-;1	cation transporter, transfer / carrier protein
26	Psd3	pleckstrin and Sec7 domain containing 3	2	1.35	4.1	2;-;3	guanyl-nucleotide exchange factor
27	Tubb5	tubulin, beta 5 class I	3	1.34	13.3	7;7;6	tubulin
28	Atp1b2	ATPase, Na+/K+ transporting, beta 2 polypeptid	6	1.34	24.6	4;2;2	ATP synthase
29	Magi2	membrane associated guanylate kinase, WW and PDZ domain containing 2	2	1.33	19.5	1;1;-	nucletotide kinase, cell junction protein
30	Prkcb	protein kinase C, beta	6	1.32	2.4	3;-;4	non-receptor serine / threonine protein kinase, transfer / carrier protein, annexin, calmodulin
31	Ehd3	EH-domain containing 3	4	1.32	23.1	3;2;-	membrane traffic protein
32	Cadm1	cell adhesion molecule 1	4	1.32	18.5	2;2;1	receptor, defense, / immunity protein, cell adehsion molecule
33	L1cam	L1 cell adhesion molecule	10	1.31	20.2	4;3;4	immunoglobulin receptor superfamily, protein phosphatase, immunoglobulin superfamily cell adhesion molecule
34	Igsf8	immunoglobulin superfamily, member 8	9	1.31	23.2	1;1;3	membrane protein*
35	Gdi1	guanosine diphosphate (GDP) dissociation inhibitor 1	8	1.31	26.3	2;3;6	acyltransferase, G-protein modulator
36	Tubb3	tubulin, beta 3 class III	6	1.30	7.0	16;10;11	tubulin
37	Opcml	opioid binding protein/cell adhesion molecule-like	3	1.30	7.8	1;1;1	immunoglobulin superfamily cell adhesion molecule
38	Lsamp	limbic system-associated membrane protein	5	1.30	11.9	1;1;2	immunoglobulin superfamily cell adhesion molecule
39	Coro1c	coronin, actin binding protein 1C	5	-1.30	24.9	1;2;2	non-motor actin binding protein
40	Syngap1	synaptic Ras GTPase activating protein 1 homolog (rat)	16	-1.30	13.9	5;5;6	signalling molecule, G-protein modulator
41	Gstm1	glutathione S-transferase, mu 1	7	-1.31	8.4	1;3;9	glutathione binding, glutathione transferase activity*
42	Ap1b1	adaptor protein complex AP-1, beta 1 subunit	3	-1.33	20.6	3;3;4	membrane traffic protein
43	Hrsp12	heat-responsive protein 12	2	-1.33	12.3	1;1;1	endoribonuclease*
44	Rala	v-ral simian leukemia viral oncogene homolog A (ras related)	3	-1.33	8.6	2;-;4	small GTPase
45	Tmod2	tropomodulin 2	2	-1.33	0.9	1;-;2	non-motor actin binding protein
46	Ndufa1	NADH dehydrogenase (ubiquinone) 1 alpha subcomplex, 1	2	-1.35	11.1	1;2;1	mitochondrial NADH dehydrogenase*
47	Abi2	abl-interactor 2	7	-1.37	27.0	4;2;2	G-protein modulator
48	Kif21a	kinesin family member 21A	5	-1.38	10.7	1;2;2	microtubule binding motor protein
49	Phb	prohibitin	9	-1.39	4.2	5;4;6	estrogen-selective coregulator*

50	Arpc5l	actin related protein 2/3 complex, subunit 5-like	2	-1.45	7.8	1;-;2	actin family cytoskeletal protein
51	Slc25a3	solute carrier family 25 (mitochondrial carrier, phosphate carrier), member 3	3	-1.45	28.7	3;-;1	amino acid transporter, mitochondrial carrier protein, transfer / carrier protein, calmodulin
52	Ywhab	tyrosine 3-monooxygenase/tryptophan 5-monooxygenase activation protein	5	-1.48	12.1	1;3;3	chaperone
53	Dlg4	discs, large homolog 4 (Drosophila)	14	-1.51	17.9	9;7;11	transmembrane receptor regulatory / adaptor protein
54	Ndufa9	NADH dehydrogenase (ubiquinone) 1 alpha subcomplex, 9	11	-1.52	26	7;1;9	dehydrogenase, reductase
55	Csnk2a1	casein kinase 2, alpha 1 polypeptide	4	-1.54	23.3	2;1;1	ATP binding, kinase activity, protein serine / threonine kinase activity*
56	Atp6v1h	ATPase, H+ transporting, lysosomal V1 subunit H	5	-1.54	20.7	2;-;6	ATP synthase, hydrolase
57	Nipsnap1	4-nitrophenylphosphatase domain and non-neuronal SNAP25-like protein homolog 1 (C. elegans)	7	-1.97	15.0	3;1;1	neurotransmitter binding*
58	Coq9	coenzyme Q9 homolog (yeast)	3	-2.02	11.9	1;-;2	coenzyme Q biosynthesis*
59	Hist1h4j	histone cluster 1, H4j	3	-5.57	8.1	1;2;-	histone*

500 mGy - Synaptosomes of hippocampus - 5 weeks post irradiation

#	Symbol	Entrez Gene Name	Unique Peptides	n-fold change from ICPL-6/ICPL-	ICPL-6/ICPL-0 Variability [%]	ICPL_6 / ICPL_0 Count	PANTHER protein class
1	Cox6a1	cytochrome c oxidase, subunit VI a, polypeptide 1	2	2.35	11.9	-;1;1	mitochondrial oxidase
2	Uqcrc1	ubiquinol-cytochrome c reductase core protein 1	13	2.16	24.7	2;2;2	metalloprotease, reductase, esterase
3	Sfxn1	sideroflexin 1	4	2.07	20.0	-;1;1	cation transporter, transfer / carrier protein
4	Psd3	pleckstrin and Sec7 domain containing 3	2	2.06	24.0	-;3;2	guanyl-nucleotide exchange factor
5	Ctnnb1	catenin (cadherin associated protein), beta 1	11	1.84	15.2	1;1;1	storage protein, signaling molecule, cytoskeletal protein, cell adhesion molecule
6	mt-Co2	mitochondrially encoded cytochrome c oxidase II	3	1.83	2.7	2;1;2	mitochondrial cytochrome C*
7	Lsamp	limbic system-associated membrane protein	5	1.81	10.7	-;1;2	immunoglobulin superfamily cell adhesion molecule
8	Rap1gds1	RAP1, GTP-GDP dissociation stimulator 1	4	1.74	1.7	3;1;-	GTPase activator activity*
9	Atp1b2	ATPase, Na+/K+ transporting, beta 2 polypeptide	6	1.72	19.7	4;2;3	ATP synthase
10	Dlgap1	discs, large (Drosophila) homolog-associated protein 1	5	1.69	29.3	3;2;1	transmembrane receptor regulatory / adaptor protein
11	Ndufb10	NADH dehydrogenase (ubiquinone) 1 beta subcomplex, 10	4	1.66	18.7	-;4;5	mitochondrial NADH dehydrogenase*
12	Arpc3	actin related protein 2/3 complex, subunit 3	4	1.65	3.2	-;1;2	actin family cytoskeletal protein
13	Uqcrh	ubiquinol-cytochrome c reductase hinge protein	4	1.61	12.2	-;2;2	reductase
14	Aldh1b1	aldehyde dehydrogenase 1 family, member B1	3	1.57	16.0	3;1;-	dehydrogenase
15	Cand1	cullin associated and neddylation disassociated 1	4	1.56	14.5	1;1;-	transcription factor
16	Dmxl2	Dmx-like 2	20	1.55	12.5	-;3;3	scaffold protein on synaptic vesicles*
17	Nipsnap3b	nipsnap homolog 3B (C. elegans)	3	1.55	14.5	-;1;1	mitochondrial protein, vesicular structure protein*
18	Magi2	membrane associated guanylate kinase, WW and PDZ domain containing 2	2	1.54	26.4	1;1;-	nucleotide kinase, cell junction protein
19	Ttyh1	tweety homolog 1 (Drosophila)	3	1.52	16.3	1;1;-	anion channel
20	Sirpa	signal-regulatory protein alpha	4	1.51	4.8	3;3;2	chemokine
21	Igsf8	immunoglobulin superfamily, member	9	1.50	23.1	1;1;3	integrin-dependent morphology and motility function, neurite outgrowth and neural network
22	Dlg2	discs, large homolog 2 (Drosophila	7	1.48	22.5	2;1;2	transmembrane receptor regulatory / adaptor protein

23	Gnb1	guanine nucleotide binding protein (G protein), beta 1	8	1.46	13.8	10;10;10	hydrolase, heterotrimeric G-protein
24	Cyfip2	cytoplasmic FMR1 interacting protein 2	7	1.46	14.0	1;1;1	G-protein modulator
25	Prkcsh	protein kinase C substrate 80K-H	3	1.45	11.7	2;1;1	transferase, enzyme modulator
26	Sod1	superoxide dismutase 1, soluble	3	1.44	8.3	1;1;2	oxidoreductase
27	Tom1l2	target of myb1-like 2 (chicken)	6	1.42	2.6	1;1;-	transporter, membrane traffic protein, kinase activator, cytoskeletal protein
28	Synj1	synaptojanin 1	17	1.41	18.2	8;2;10	phosphatase
29	Dclk1	doublecortin-like kinase 1	6	1.39	27.6	-;2;1	non-receptor serine / threonine protein kinase
30	Pfkl	phosphofructokinase, liver, B-type	6	1.38	19.1	-;1;1	carbohydrate kinase
31	Coro1a	coronin, actin binding protein 1A	8	1.37	26.8	6;9;9	non-motor actin binding protein
32	Rasal1	RAS protein activator like 1 (GAP1 like)	7	1.36	28.5	1;1;1	signaling molecule, G-protein modulator
33	Ctbp1	C-terminal binding protein 1	6	1.36	12.0	-;1;2	transcription cofactor, dehydrogenase
34	Tubb3	tubulin, beta 3 class III	6	1.36	14.7	16;10;12	tubulin
35	Clasp2	CLIP associating protein 2	6	1.35	6.5	1;2;-	structural protein
36	Tubb5	tubulin, beta 5 class I	3	1.35	12.2	7;6;5	tubulin
37	Ncan	neurocan	11	1.35	27.8	3;1;3	extracellular matrix glycoprotein
38	Ndufs5	NADH dehydrogenase (ubiquinone) Fe-S protein	3	1.35	13.9	-;1;2	mitochondrial NADH dehydrogenase*
39	Aldh6a1	aldehyde dehydrogenase family 6, subfamily A1	5	1.34	10.0	-;1;1	dehydrogenase
40	Fscn1	fascin homolog 1, actin bundling protein (Strongylocentrotus	9	1.34	1.5	-;2;2	non-motor actin binding protein
41	Ap2b1	adaptor-related protein complex 2, beta 1 subunit	2	1.34	19.4	4;1;4	membrane traffic protein
42	Dbn1	drebrin 1	10	1.33	29.4	6;3;2	non-motor actin binding protein
43	Cadm3	cell adhesion molecule 3	5	1.33	20.5	7;3;6	receptor, defense / immunity protein, cell adehsion molecule
44	Tuba4a	tubulin, alpha 4A	8	1.32	10.5	13;11;10	tubulin
45	Plch2	phospholipase C, eta 2	6	1.32	3.7	1;1;-	signaling molecule, phosphatase, guanyl-nucleotide exchange factor, calcium-binding protein
46	Negr1	neuronal growth regulator	7	1.31	7.6	2;3;2	immunoglobulin superfamily cell adhesion molecule
47	Cnksr2	connector enhancer of kinase suppressor of Ras 2	5	1.31	27.8	1;-;1	kinase modulator
48	Gnb2	guanine nucleotide binding protein (G protein), beta 2	7	1.31	6.1	6;6;4	hydrolase, heterotrimeric G-protein
49	Gpc1	glypican 1	5	1.30	8.1	1;1;-	extracellular matrix glycoprotein, cell adhesion molecule
50	Prdx1	peroxiredoxin 1	2	-1.30	16.2	1;3;3	peroxidase
51	Carkd	carbohydrate kinase domain containing	2	-1.31	9.4	-;1;1	ATP binding, ATP-dependent NAD(P)H-hydrate dehydratase activity*
52	Kif21a	kinesin family member 21A	5	-1.31	23.0	3;2;1	microtubule binding motor protein
53	Snap91	synaptosomal-associated protein 91	4	-1.32	18.8	7;5;6	vesicle coat protein
54	Ptprd	protein tyrosine phosphatase, receptor type, D	8	-1.34	4.6	-;1;2	receptor, protein phosphatase
55	Ap2m1	adaptor protein complex AP-2, mu1	6	-1.36	17.3	19;6;16	membrane traffic protein
56	Pdxp	pyridoxal (pyridoxine, vitamin B6)	10	-1.38	28.8	2;1;3	phosphatase
57	Shank3	SH3/ankyrin domain gene 3	19	-1.41	11.4	3;1;-	scaffold protein for interconnecting NMDA receptors and metabotropic glutamate receptors to actin-based cytoskeleton*
58	Immt	inner membrane protein, mitochondrial	10	-1.42	18.9	6;9;11	mitochondrial inner membrane protein*
59	Abi2	abl-interactor 2	7	-1.42	2.5	4;2;2	G-protein modulator
60	Kras	v-Ki-ras2 Kirsten rat sarcoma viral oncogene homolog	3	-1.48	30	-;1;5	small GTPase

61	Nipsnap1	4-nitrophenylphosphatase domain and non-neuronal SNAP25-like protein homolog 1 (C. elegans)	7	-1.48	19.1	1;1;2	neurotransmitter binding*
62	Epb4.1l2	erythrocyte protein band 4.1-like 2	6	-1.50	26.8	1;2;5	actin binding, structural molecule activity*
63	Ywhab	tyrosine 3-monooxygenase/tryptophan 5-monooxygenase activation protein,	5	-1.60	12.2	1;3;3	chaperone
64	Arhgap1	Rho GTPase activating protein 1	2	-1.92	1.5	-;4;2	G-protein modulator

2000 mGy - Synaptosomes of hippocampus - 5 weeks post irradiation

#	Symbol	Entrez Gene Name	Unique Peptides	n-fold change from ICPL-10/ICPL-	ICPL-10/ICPL-0 Variability [%]	ICPL_10 / ICPL_0 Count	PANTHER protein class
1	Ppp1r9b	protein phosphatase 1, regulatory subunit 9B	5	2.164	9.5	3;2;-	actin binding, cross-linking activity at synaptic junction, protein phosphatase*
2	330407J23F	RIKEN cDNA 6330407J23 gene	8	2.102	15.0	2;1;-	membrane protein*
3	Cox6a1	cytochrome c oxidase, subunit VI a, polypeptide 1	2	1.993	4.1	1;-;1	mitochondrial oxidase
4	Nsfl1c	NSFL1 (p97) cofactor (p47)	3	1.973	28.0	2;-;1	membrane trafficking regulatory protein
5	Nefl	neurofilament, light polypeptide	10	1.929	12.6	4;-;3	structural protein, intermediate filament
6	Hyou1	hypoxia up-regulated 1	8	1.857	5.7	3;3;2	Hsp70 family chaperone
7	Oxr1	oxidation resistance 1	12	1.797	29.2	9;8;6	mitochondrial oxidative damage protection protein*
8	Plch2	phospholipase C, eta 2	6	1.780	25.4	1;1;-	signaling molecule, guanyl-nucleotide exchange factor, phospholipase, calcium-binding protein
9	Prkcsh	protein kinase C substrate 80K-H	3	1.760	6.5	1;2;1	transferase, intermediate modulator
10	Mtap6	microtubule-associated protein 6	19	1.756	25.2	15;25;18	microtuble stabilization protein, microtuble binding protein*
11	Eif4b	eukaryotic translation initiation factor 4B	5	1.752	29.2	3;2;3	translation initiation factor
12	Gdi1	guanosine diphosphate (GDP) dissociation inhibitor 1	8	1.723	17.1	2;3;6	acyltransferase, G-protein modulator
13	Cttn	cortactin	6	1.704	22.1	4;7;6	basic helix-loop-helix transcription factor, actin family cytoskeletal protein
14	Cadm1	cell adhesion molecule 1	4	1.681	20.4	2;-;2	receptor, defense / immunity protein, cell adehsion molecule
15	Uqcrh	ubiquinol-cytochrome c reductase hinge protein	4	1.674	0.5	2;-;2	reductase
16	Dlg3	discs, large homolog 3 (Drosophila	12	1.655	23.9	8;8;8	transmembrane receptor regulatory / adaptor protein
17	Plec	plectin	42	1.636	25.4	3;2;9	non-motor actin binding protein
18	Numbl	numb-like	6	1.612	27.9	2;1;1	signaling molecule
19	Begain	brain-enriched guanylate kinase-associated	9	1.601	23.9	2;1;-	structural protein of postsynaptic density*
20	Lasp1	LIM and SH3 protein 1	2	1.593	21.9	2;1;2	actin-based cytoskeletal activity, actin binding, guanylate kinase*
21	Synpo	synaptopodin	8	1.585	20.2	4;2;2	non-motor actin binding protein
22	Strn	striatin, calmodulin binding protein	7	1.584	27.5	2;1;3	calmodulin binding, protein phosphatase 2A binding, protein complex binding*
23	Lsamp	limbic system-associated membrane protein	5	1.583	19.7	3;1;1	immunoglobulin superfamily cell adhesion molecule
24	Sorbs1	sorbin and SH3 domain containing	5	1.580	24.3	2;1;-	membrane trafficking regulatory protein, actin family cytoskeletal protein
25	Ctnnb1	catenin (cadherin associated protein), beta 1	11	1.569	22.5	1;1;-	storage protein, signaling molecule, cytoskeletal protein, cell adhesion
26	Ppfia3	protein tyrosine phosphatase, receptor type, f polypeptide (PTPRF), interacting protein (liprin), alpha 3	14	1.564	27.9	3;1;4	focal adhesion disassembly, localization of receptor-like tyrosine phosphatases type 2a on plasma membrane*

27	Hspa5	heat shock protein 5	10	1.562	14.2	7;11;7	Hsp70 family chaperone
28	Sh3glb2	SH3-domain GRB2-like endophilin B2	10	1.561	16.7	1;1;4	membrane trafficking regulatory protein, actin family cytoskeletal protein
29	Arpc3	actin related protein 2/3 complex, subunit 3	4	1.557	17.3	2;-;1	actin family cytoskeletal protein
30	Magi2	membrane associated guanylate kinase, WW and PDZ domain containing 2	2	1.552	23.5	1;1;-	nucleotide kinase, cell junction protein
31	Ncan	neurocan	11	1.538	25.7	2;1;3	extracellular matrix glycoprotein
32	Tom1l2	target of myb1-like 2 (chicken)	6	1.524	11.2	1;-;1	transporter, membrane traffic protein, kinase activator, cytoskeletal protein
33	Srcin1	SRC kinase signaling inhibitor 1	31	1.513	8.4	20;20;23	protein kinase binding, dendrite spine morphology regulation via lamellopodia, cortical actin and actin stress fibers*
34	Gprin1	G protein-regulated inducer of neurite outgrowth 1	15	1.470	15.9	14;13;14	neurite outgrowth protein*
35	Pclo	piccolo (presynaptic cytomatrix protein)	25	1.465	27.2	11;4;12	scaffolding protein*
36	Stmn1	stathmin 1	2	1.458	22.1	3;1;2	microtubule filament regulatory protein by destabilzing microtubule*
37	L1cam	L1 cell adhesion molecule	10	1.454	10.2	4;3;4	immunoglobulin receptor superfamily, protein phosphatase, immunoglobulin superfamily cell adhesion molecule
38	Pdia4	protein disulfide isomerase associated 4	3	1.438	12.2	1;2;2	isomerase
39	Sgip1	SH3-domain GRB2-like (endophilin) interacting protein 1	7	1.424	23.9	2;2;3	membrane trafficking regulatory protein, actin family cytoskeletal protein
40	Uqcrc1	ubiquinol-cytochrome c reductase core protein 1	13	1.420	17.6	2;3;2	metalloprotease, reductase, esterase
41	Mtap1a	microtubule-associated protein 1 A	26	1.420	24.9	12;16;7	structural protein involved in the cross-bridging between micortubules and other skeletal elements, microtubule binding*
42	Vcp	valosin containing protein	20	1.417	15.9	17;16;15	ATP binding, ATPase
43	Arfgap1	ADP-ribosylation factor GTPase activating protein 1	4	1.413	14.7	4;-;6	nucleic acid binding, G-protein modulator
44	Epb4.1l3	erythrocyte protein band 4.1-like 3	7	1.413	27.5	5;10;8	structural constituent of cytoskeleton*
45	Dlg2	discs, large homolog 2 (Drosophila)	7	1.395	9.2	1;2;1	transmembrane receptor regulatory / adaptor protein
46	Hspa9	heat shock protein 9	10	1.381	14.3	21;16;18	heast shock protein*
47	Mapt	microtubule-associated protein tau	8	1.378	19.4	9;10;8	microtubule binding protein*
48	Dnajc6	DnaJ (Hsp40) homolog, subfamily C, member 6	5	1.368	7.4	3;2;2	non-receptor serine / threonine protein kinase, chaperone
49	Ndufv2	NADH dehydrogenase (ubiquinone) flavoprotein 2	3	1.367	25.5	2;-;1	dehydrogenase, reductase
50	Epb4.1l1	erythrocyte protein band 4.1-like 1	12	1.366	3.2	10;14;16	structural constituent of cytoskeleton*
51	Mbp	myelin basic protein	10	1.347	27.3	9;16;9	myelin protein
52	Atp5d	ATP synthase, H+ transporting, mitochondrial F1 complex, delta subunit	3	1.341	21.0	5;3;3	proton-transporting ATP synhtase, activity*
53	Pdhx	pyruvate dehydrogenase complex, component X	2	1.334	27.8	2;2;3	acetyltransferase, acyltransferase
54	Bsn	bassoon	66	1.332	21.7	40;46;31	neurotransmitter release organisation*
55	Hsp90b1	heat shock protein 90, beta (Grp94), member 1	7	1.327	24.2	2;5;8	Hsp90 family chaperone
56	Cdh13	cadherin 13	3	1.326	25.8	2;1;1	cell junction protein,
57	Shank2	SH3/ankyrin domain gene 2	8	1.322	16.9	1;2;-	adapter protein connecting NMDA and metabortropic glutamate receptors to actin-based cytoskeleton*

58	Dpysl3	dihydropyrimidinase-like 3	8	1.321	16.3	11;9;9	hydrolase
59	Pacsin1	protein kinase C and casein kinase substrate in neurons 1	11	1.318	27.4	13;9;12	membrane trafficking regulatory protein
60	Caskin1	CASK interacting protein 1	14	1.318	23.9	7;11;6	transmembrane receptor regulatory / adaptor protein
61	Dld	dihydrolipoamide dehydrogenase	6	1.317	21.9	7;7;8	dehydrogenase, oxidase, reductase
62	Epn1	epsin 1	4	1.316	19.7	1;3;3	lipid binding*
63	Mpp6	membrane protein, palmitoylated 6 (MAGUK p55 subfamily member 6)	4	1.316	24.0	1;1;-	nucleotide kinase, cell junction protein
64	Uchl1	ubiquitin carboxy-terminal hydrolase	3	1.314	13.1	2;3;5	cysteine protease
65	Picalm	phosphatidylinositol binding clathrin assembly protein	4	-1.301	13.1	1;3;2	vesicle coat protein
66	Ywhaz	tyrosine 3-monooxygenase/tryptophan 5-monooxygenase activation protein,	7	-1.305	6.3	5;3;6	chaperone
67	Coq9	coenzyme Q9 homolog (yeast)	3	-1.306	19.0	1;-;2	coenzyme Q biosynthesis'
68	Atp6v1a	ATPase, H+ transporting, lysosomal V1 subunit A	18	-1.306	22.5	17;11;9	ATP synthase, anion channel, ligand-gated ion channel, DNA binding protein, hydrolase
69	Coro1c	coronin, actin binding protein 1C	5	-1.308	19.6	1;2;2	non-motor actin binding protein
70	Slc25a5	solute carrier family 25 (mitochondrial carrier, adenine nucleotide translocator), member 5	6	-1.308	27.2	29;21;24	amino acid transporter, mitochondrial carrier protei transfer / carrier protein, calmodulin
71	Slc3a2	solute carrier family 3 (activators of dibasic and neutral amino acid transport), member 2	5	-1.309	18.9	2;1;3	amylase
72	Gda	guanine deaminase	4	-1.311	21	1;1;3	hydrolase
73	Abat	4-aminobutyrate aminotransferase	9	-1.311	28.9	10;9;14	transaminase
74	Atp6v1d	ATPase, H+ transporting, lysosomal V1 subunit D	8	-1.333	17	4;4;8	ATP synthase, hydrolase
75	Tomm20	translocase of outer mitochondrial membrane 20 homolog (yeast)	3	-1.345	3.1	1;-;2	mitochondrial transporter
76	Acat2	acetyl-Coenzyme A acetyltransferase 2	2	-1.355	29.1	1;-;1	acetyltransferase
77	Cntnap1	contactin associated protein-like 1	22	-1.378	17.9	3;1;1	transporter, cell adhesion molecule, oxidase, recepto
78	Rala	v-ral simian leukemia viral oncogene homolog A (ras related)	3	-1.389	13.8	5;-;2	small GTPase
79	Nptn	neuroplastin	7	-1.391	24.6	4;9;10	transmembrane receptor regulatory / adaptor protei
80	Brp44l	brain protein 44-like	2	-1.400	29.2	1;3;2	pyruvate uptake into mitochondria regulatory protein*
81	Phb2	prohibitin 2	12	-1.400	9.3	8;-;2	estrogen-selective coregulator*
82	Nipsnap1	4-nitrophenylphosphatase domain and non-neuronal SNAP25-like protein homolog 1 (C. elegans)	7	-1.415	16.5	3;1;1	neurotransmitter binding*
83	Mapk1	mitogen-activated protein kinase 1	5	-1.437	23.7	4;1;3	non-receptor serine / threonine protein kinase
84	Ap1b1	adaptor protein complex AP-1, beta 1 subunit	3	-1.445	25.2	3;3;3	membrane traffic protein
85	Atp6v0a1	ATPase, H+ transporting, lysosomal V0 subunit A1	14	-1.459	15.4	8;4;6	ATP synthase, hydrolase
86	Atp6v1c1	ATPase, H+ transporting, lysosomal V1 subunit C1	6	-1.460	9	10;2;9	ATP synthase, hydrolase
87	Hspa4	heat shock protein 4	8	-1.468	29.8	1;3;2	Hsp70 family chaperone
88	Rac1	RAS-related C3 botulinum substrate 1	3	-1.488	15.2	8;11;13	small GTPase
89	Atp6v1h	ATPase, H+ transporting, lysosomal V1 subunit H	5	-1.490	2.7	6;-;2	ATP synthase, hydrolase
90	Ldhb	lactate dehydrogenase B	2	-1.512	17.9	8;5;6	dehydrogenase
91	Camk2a	calcium/calmodulin-dependent protein kinase II alpha	15	-1.528	29.6	46;37;33	non-receptor serine / threonine protein kinase
92	Ppp2r1a	protein phosphatase 2 (formerly 2A), regulatory subunit A (PR 65), alpha isoform	10	-1.536	24.1	10;8;7	protein phosphatase
93	Ganab	alpha glucosidase 2 alpha neutral subunit	7	-1.546	12.6	1;-;1	glucosidase
94	Atp1a3	ATPase, Na+/K+ transporting, alpha 3 polypeptide	12	-1.565	22.4	13;16;20	cation transporter, ion channel, hydrolase

95	Arpc2	actin related protein 2/3 complex, subunit 2	6	-1.570	26.3	9;2;1	actin-binding protein for actin polymerization, structural constituent of cytoskeleton*
96	Cacng8	calcium channel, voltage-dependent, gamma subunit 8	2	-1.614	16.1	3;-;2	voltage-gated ion / calcium channel
97	Wdr7	WD repeat domain 7	7	-1.639	17.0	2;3;5	mRNA splicing factor, esterase, kinase inhibitor
98	Ywhab	tyrosine 3-monooxygenase/tryptophan 5-monooxygenase activation protein,	5	-1.646	5.9	1;3;3	chaperone
99	Psmb2	proteasome (prosome, macropain) subunit, beta type 2	4	-1.655	14.0	1;1;1	protease
100	Pld3	phospholipase D family, member 3	4	-1.664	12.6	3;-;1	phospholipase
101	Atp1a1	ATPase, Na+/K+ transporting, alpha 1 polypeptide	6	-1.802	28.5	2;1;4	cation transporter, ion channel, hydrolase
102	Ndufa9	NADH dehydrogenase (ubiquinone) 1 alpha subcomplex, 9	11	-1.917	27.5	10;1;7	dehydrogenase, reductase
103	Mapk3	mitogen-activated protein kinase 3	3	-1.920	0.5	1;-;1	non-receptor serine / threonine protein kinase
104	Rab11b	RAB11B, member RAS oncogene family	5	-2.079	10.5	2;-;3	GDP / GTP binding, GTPase activity*
105	Grin1	glutamate receptor, ionotropic, NMDA1 (zeta 1)	6	-2.502	24.9	1;-;1	ionotropic glutamate receptor
106	Slc1a2	solute carrier family 1 (glial high affinity glutamate transporter),	2	-2.545	16.6	2;-;2	cation transporter

Table 33: List of deregulated proteins 24 weeks post-irradiation from 100 mGy, 500 mGy and 2000 mGy within the isolated synaptosomes of cortex (C57Bl6 study).

The table shows the up-regulated or down-regulated proteins with the fold-changes, their variability, their number of unique peptides used for protein identification and number of identifications in the biological replicates (ICPLx/ICPL0-Count). "PANTHER protein class" represents the protein class where the protein of interest can be annotated based on PANTHER software tool and UniProt database. Grey / brown highlighted "PANTHER protein classes" belong to the protein class of "small GTPase / associated G-protein" / "cytoskeleton / cytoskeleton-binding protein", respectively

100 mGy - Synaptosomes of cortex - 24 weeks post irradiation

#	Symbol	Entrez Gene Name	Unique Peptides	n-fold change from ICPL-4/ICPL-0	ICPL-4/ICPL-0 Variability [%]	ICPL_4 / ICPL_0 Count	PANTHER protein class
1	Grm2	glutamate receptor, metabotropic 2	5	2.79	20.0	1;-;1	G-protein coupled receptor
2	Arfgap1	ADP-ribosylation factor GTPase activating protein 1	4	2.20	11.6	2;5;-	nucleic acid binding, G-protein modulator
3	Gja1	gap junction protein, alpha 1	2	2.18	17.7	1;-;1	gap junction
4	Slc4a4	solute carrier family 4 (anion exchanger), member 4	5	2.06	8.6	3;-;2	cation transporter
5	Glud1	glutamate dehydrogenase 1	10	2.04	20.3	8;9;6	dehydrogenase
6	Ak4	adenylate kinase 4	5	1.93	25.8	1;1;-	nucleotide kinase
7	Car2	carbonic anhydrase 2	3	1.87	3.6	1;-;1	carbonate dehydratase activity*
8	Dlg2	discs, large homolog 2 (Drosophila)	6	1.76	10.9	1;-;1	transmembrane receptor regulatory adaptor protein
9	Acot7	acyl-CoA thioesterase 7	3	1.74	1.8	2;-;4	esterase
10	Slc9a3r1	solute carrier family 9 (sodium/hydrogen exchanger), member 3 regulator 1	7	1.59	27.8	1;2;1	-

11	Atp2b3	ATPase, Ca++ transporting, plasma membrane 3	5	1.57	19.1	2;-;5	cation transporter, ion channel, hydrolase
12	Glul	glutamate-ammonia ligase (glutamine synthetase)	11	1.55	5.0	11;11;11	ligase
13	Mif	macrophage migration inhibitory factor	2	1.54	23.1	1;1;-	chemoattractant activity, cytokine activity*
14	Kcnq2	potassium voltage-gated channel, subfamily Q, member 2	4	1.54	9.7	1;-;1	voltage-gated potassium channel, voltage-gated ion channel
15	Aldoc	aldolase C, fructose-bisphosphate	13	1.50	14.5	8;7;6	fructose-bisphosphate aldolase activity*
16	Sdhb	succinate dehydrogenase complex, subunit B, iron sulfur (Ip)	4	1.49	17.4	6;2;-	succinate dehydrogenase activity*
17	Add2	adducin 2 (beta)	6	1.48	29.3	2;2;3	non-motor actin binding protein
18	Tmod2	tropomodulin 2	5	1.48	26.1	2;1;2	non-motor actin binding protein
19	Aldh5a1	aldhehyde dehydrogenase family 5, subfamily A1	7	1.46	29.3	8;4;5	dehydrogenase
20	Prdx6	peroxiredoxin 6	5	1.44	1.8	1;1;-	peroxidase activity*
21	Sept4	septin 4	4	1.42	10.8	1;-;2	small GTPase, cytoskeletal protein
22	Mog	myelin oligodendrocyte glycoprotein	8	1.41	25.9	1;-;3	ubiquitin-protein ligase
23	Ogdhl	oxoglutarate dehydrogenase-like	7	1.41	23.3	1;-;1	mitochondrial oxoglutarate dehydrogenase (succinyl-transferring) activity*
24	Cox6b1	cytochrome c oxidase, subunit VIb polypeptide 1	4	1.40	18.3	2;3;1	oxidase
25	Pdxp	pyridoxal (pyridoxine, vitamin B6) phosphatase	9	1.40	22.7	2;1;-	phosphatase
26	Scn2a1	sodium channel, voltage-gated, type II, alpha 1	8	1.40	5.1	3;-;2	voltage-gated calcium / sodium / ion channel
27	Gabbr1	gamma-aminobutyric acid (GABA) B receptor, 1	3	1.38	15.9	1;-;2	G-protein coupled receptor
28	Grin1	glutamate receptor, ionotropic, NMDA1 (zeta 1)	10	1.38	19.7	1;-;1	involved in neurite outgrowth, phosphoprotein binding*
29	Nap1l1	nucleosome assembly protein 1-like 1	2	1.36	23.4	2;-;2	phosphatase inhibitor
30	Pip5k1c	phosphatidylinositol-4-phosphate 5-kinase, type 1 gamma	3	1.33	2.9	1;1;-	kinase
31	Cacng8	calcium channel, voltage-dependent, gamma subunit 8	2	1.33	5.1	1;-;1	voltage-gated calcium / ion channel
32	Fam49b	family with sequence similarity 49, member B	3	1.33	1.2	1;-;1	-
33	Prkar2b	protein kinase, cAMP dependent regulatory, type II beta	6	1.33	20.9	3;1;-	kinase modulator
34	Map2k1	mitogen-activated protein kinase kinase 1	3	1.33	6.0	3;3;3	MAP kinase kinase activity, ATP binding, protein serine / threonine / tyrosine kinase activity*
35	L1cam	L1 cell adhesion molecule	11	1.33	16.7	5;7;5	immunoglobulin receptor superfamily, protein phosphatase, immunoglobulin superfamily cell adhesion molecule
36	Pi4ka	phosphatidylinositol 4-kinase, catalytic, alpha polypeptide	9	1.32	26.3	2;-;1	kinase
37	Tuba4a	phosphatidylinositol 4-kinase, catalytic, alpha polypeptide	6	1.31	18.9	6;10;7	tubulin

38	Pfn2	profilin 2	3	1.31	15.1	3;-;2	actin binding protein for cytoskeleton structure*
39	Epb4.1l2	erythrocyte protein band 4.1-like 2	8	1.31	14.2	5;3;4	structural molecule activity, cytoskeletal organisation+
40	Usp5	ubiquitin specific peptidase 5 (isopeptidase T)	9	1.30	12.5	3;1;2	cysteine-type peptidase activity*
41	Tpm1	tropomyosin 1, alpha	3	1.30	29.5	1;1;1	actin binding motor protein
42	Fkbp2	FK506 binding protein 2	2	-1.31	12.2	2;3;3	isomerase, chaperone, calcium-binding protein
43	Gprin1	G protein-regulated inducer of neurite outgrowth 1	11	-1.33	28.0	5;5;8	neurite outgrowth, phosphoprotein binding+
44	Snap91	synaptosomal-associated protein 91	5	-1.33	0.5	8;8;10	vesicel coat protein
45	Anxa7	annexin A7	4	-1.35	1.4	1;2;-	calcium ion binding, calcium-dependent protein / phospholipid binding*
46	Epb4.1l3	erythrocyte protein band 4.1-like 3	9	-1.35	16.8	9;5;5	structural molecule activity, cytoskeletal organisation+
47	Cotl1	coactosin-like 1 (Dictyostelium)	4	-1.39	10.1	3;4;2	non-motor actin binding protein
48	Purb	purine rich element binding protein B	5	-1.39	2.2	1;-;2	transcription factor, DNA binding protein
49	Auh	AU RNA binding protein/enoyl-coenzyme A hydratase	5	-1.40	8.4	2;-;1	acetyltransferase, acyltransferase, dehydrogenase, hydratase, ligase, epimerase / racemase
50	Tmx2	thioredoxin-related transmembrane protein 2	5	-1.41	11.8	2;-;3	membrane protein*
51	Pabpc1	poly(A) binding protein, cytoplasmic 1	3	-1.47	8.1	2;-;2	transcription factor, DNA binding protein, mRNA polyadenylation factor / splicing factor, ribonucleoprotein
52	Rpl13	ribosomal protein L13	9	-1.52	10.8	4;2;2	ribosomal protein
53	Pdia3	protein disulfide isomerase associated 3	10	-1.54	17.3	8;9;8	isomerase
54	Rpl7	ribosomal protein L7	4	-1.60	22.6	2;1;-	ribosomal protein
55	Rpl3	ribosomal protein L3	3	-1.63	23.7	1;2;1	ribosomal protein
56	Rpl19	ribosomal protein L19	3	-1.63	14.1	3;2;3	ribosomal protein
57	Hexb	hexosaminidase B	5	-1.68	23.0	1;2;2	glyosidase
58	Rpl11	ribosomal protein L11	4	-1.68	17.8	4;4;4	ribosomal protein
59	Cct7	chaperonin containing Tcp1, subunit 7 (eta)	4	-1.73	22.2	1;1;3	chaperonin
60	Rpl4	ribosomal protein L4	3	-1.78	27	2;2;2	ribosomal protein
61	Snd1	staphylococcal nuclease and tudor domain containing 1	9	-1.79	23.3	2;3;2	nuclease activity, transcription cofactor activity*
62	Hsp90b1	heat shock protein 90, beta (Grp94), member 1	11	-1.80	21.9	12;11;10	Hsp90 family chaperone
63	Plec	plectin	74	-1.80	24.0	12;5;23	non-motor actin binding protein
64	Rpl35a	ribosomal protein L35A	4	-1.81	19.1	3;3;4	ribosomal protein
65	Hspa5	heat shock protein 5	12	-1.81	18.9	18;19;23	Hsp70 family chaperone
66	Rplp0	ribosomal protein, large, P0	2	-1.85	1.2	2;1;1	ribosomal protein
67	Mlec	malectin	2	-1.94	21.8	1;-;1	carbohydrate binding*
68	Ganab	alpha glucosidase 2 alpha neutral subunit	14	-1.97	17.0	2;3;3	glucosidase
69	Rpl13a	ribosomal protein L13A	3	-2.11	4.3	3;3;-	ribosomal protein

70	Rpn1	ribophorin I	3	-2.15	12.0	2;-;2	glycosyltransferase
71	Rps11	ribosomal protein S11	3	-2.19	4.6	2;2;-	ribosomal protein
72	Hyou1	hypoxia up-regulated 1	14	-2.27	29.8	3;9;12	Hsp70 family chaperone
73	Rpl10	ribosomal protein 10	8	-2.49	16.9	4;3;1	ribosomal protein

500 mGy -Synaptosomes of cortex- 24 weeks post irradiation

#	Symbol	Entrez Gene Name	Unique Peptides	n-fold change from ICPL-6/ICPL-0	ICPL-6/ICPL-0 Variability [%]	ICPL_6 / ICPL_0 Count	PANTHER protein class
1	Hadha	hydroxyacyl-Coenzyme A dehydrogenase/3-ketoacyl-Coenzyme A thiolase/enoyl-Coenzyme A hydratase (trifunctional protein), alpha	2	3.24	0.5	3;2;-	dehydrogenase, hydratase, epimerase / racemase
2	Cryz	crystallin, zeta	2	2.50	7.1	2;1;-	dehydrogenase, reductase
3	Grm2	glutamate receptor, metabotropic 2	5	2.02	2.8	-;1;1	G-protein coupled receptor
4	Acot7	acyl-CoA thioesterase 7	3	1.75	1	2;-;4	esterase
5	Psd3	pleckstrin and Sec7 domain containing 3	3	1.73	16.2	2;6;3	guanyl-nucleotide exchange factor
6	N28178	expressed sequence N28178	5	1.70	26.9	1;1;3	-
7	Mdh2	malate dehydrogenase 2, NAD (mitochondrial)	5	1.69	29.5	15;8;13	dehydrogenase
8	Gnb1	guanine nucleotide binding protein (G protein), beta 1	8	1.68	19.3	14;15;7	hydrolase, heterotrimeric G-protein
9	Dld	dihydrolipoamide dehydrogenase	6	1.68	22.0	5;9;4	dehydrogenase, oxidase, reductase
10	Immt	inner membrane protein, mitochondrial	10	1.68	18.5	-;2;5	mitochondrial membrane protein*
11	Abat	4-aminobutyrate aminotransferase	9	1.67	28.0	6;7;1	transaminase
12	Atp5a1	ATP synthase, H+ transporting, mitochondrial F1 complex, alpha subunit 1	18	1.65	28.6	49;39;65	ATP synthase, anion channel, ligand gated ion channel, DNA binding protein, hydrolase
13	Slc1a3	solute carrier family 1 (glial high affinity glutamate transporter), member 3	2	1.58	0.9	1;2;-	cation transporter
14	Atp5b	ATP synthase, H+ transporting mitochondrial F1 complex, beta subunit	11	1.58	25.8	10;7;9	ATP synthase, anion channel, ligand gated ion channel, DNA binding protein, hydrolase
15	Uqcrq	ubiquinol-cytochrome c reductase, complex III subunit VII	5	1.56	20.8	3;2;3	mitochondrial ubiquinol-cytochrome-c reductase activity*
16	Aldh6a1	aldehyde dehydrogenase family 6, subfamily A1	3	1.56	16.9	3;2;-	dehydrogenase
17	Slc25a3	solute carrier family 25 (mitochondrial carrier, phosphate carrier), member 3	3	1.55	17.4	1;1;-	amino acid transporter, mitochondria carrier protein, transfer / carrier protein, calmodulin
18	Atp5d	ATP synthase, H+ transporting, mitochondrial F1 complex, delta subunit S	2	1.52	14.4	3;1;3	mitochondrial proton-transporting ATP synthase activity*
19	Ndufs7	NADH dehydrogenase (ubiquinone) Fe-S protein 7	3	1.52	20.4	3;1;3	dehydrogenase, reductase
20	Ntm	neurotrimin	3	1.50	4.6	1;1;-	immunoglobulin superfamily cell adhesion molecule
21	Glud1	glutamate dehydrogenase 1	10	1.50	29.5	10;4;8	dehydrogenase
22	Bdh1	3-hydroxybutyrate dehydrogenase, type 1	4	1.49	3.6	1;3;-	dehydrogenase, reductase
23	Dlgap1	discs, large (Drosophila) homolog-associated protein 1	2	1.48	27.1	-;1;1	transmembrane receptor regulatory / adaptor protein
24	Sept3	septin 3	3	1.48	8.1	1;2;-	small GTPase, cytoskeletal protein
25	Gnb2	guanine nucleotide binding protein (G protein), beta 2	6	1.47	2.3	5;7;-	hydrolase, heterotrimeric G-protein
26	Dlgap3	discs, large (Drosophila) homolog-associated protein 3	5	1.46	7.8	-;1;2	transmembrane receptor regulatory / adaptor protein
27	Slc8a1	solute carrier family 8 (sodium/calcium exchanger), member 1	3	1.46	14.6	-;1;1	cation transporter
28	Cox6c	cytochrome c oxidase, subunit VIc	4	1.46	27.6	6;6;9	mitochondrial cytochrome c oxidase*

29	Tubb5	tubulin, beta 5 class I	3	1.45	16	8;4;6	tubulin
30	Ndufa2	NADH dehydrogenase (ubiquinone) 1 alpha subcomplex, 2	5	1.44	17.2	8;6;4	oxidoreductase
31	Slc1a2	solute carrier family 1 (glial high affinity glutamate transporter), member 2	3	1.44	14.3	5;3;4	cation transporter
32	Uqcrc2	ubiquinol cytochrome c reductase core protein 2	11	1.44	13.9	14;10;14	metalloprotease, reductase, esterase
33	Slc25a12	solute carrier family 25 (mitochondrial carrier, Aralar), member 12	18	1.43	13.1	7;7;3	amino acid transporter, mitochondrial carrier protein, transfer / carrier protein, calmodulin
34	Tubb3	tubulin, beta 3 class III	4	1.41	24.3	12;13;13	tubulin
35	Mif	macrophage migration inhibitory factor	2	1.41	2.4	1;-;1	cytokine activity, chemoattractant activity*
36	Pygb	brain glycogen phosphorylase	5	1.41	29.3	3;1;1	phosphorylase
37	Plcb1	phospholipase C, beta 1	7	1.40	29.6	2;3;3	signaling molecule, phospholipase, guanyl-nucleotide exchange factor, calcium-binding protein
38	Snd1	staphylococcal nuclease and tudor domain containing 1	9	1.38	21.5	5;4;2	transcription cofactor, nucleic acid binding
39	Atp5e	ATP synthase, H+ transporting, mitochondrial F1 complex, epsilon subunit	2	1.38	14.0	2;2;2	ATP synthase, hydrolase
40	Ndufs3	NADH dehydrogenase (ubiquinone) Fe-S protein 3	7	1.36	23.1	4;5;4	mitochondrial NADH dehydrogenase*
41	Atp5h	ATP synthase, H+ transporting, mitochondrial F0 complex, subunit d	2	1.36	8.8	1;2;-	mitochondrial hydrogen iontransmembrane transproter activity*
42	Uqcrfs1	ubiquinol-cytochrome c reductase, Rieske iron-sulfur polypeptide 1	8	1.35	10.2	10;12;7	reductase
43	Dclk1	doublecortin-like kinase 1	6	1.35	18.8	-;1;1	non-receptor serine / threonine protein kinase
44	Nipsnap1	4-nitrophenylphosphatase domain and non-neuronal SNAP25-like protein homolog 1 (C. elegans)	4	1.34	22.2	2;1;2	neurotransmitter binding*
45	Pclo	piccolo (presynaptic cytomatrix protein)	20	1.33	7.7	-;1;5	calcium ion binding, calcium-dependent protein / phospholipid binding*
46	Atp5k	ATP synthase, H+ transporting, mitochondrial F1F0 complex, subunit e	5	1.33	24.1	5;2;4	mitochondrial ATPase activity, hydrogen ion transmembrane transproter activity*
47	Sdha	succinate dehydrogenase complex, subunit A, flavoprotein (Fp)	11	1.33	19.0	5;7;5	dehydrogenase, oxidase
48	Cpne6	copine VI	6	1.32	5.7	-;1;4	membrane traffic protein
49	Tuba1a	tubulin, alpha 1A	5	1.31	14.0	12;9;16	tubulin
50	Ckb	creatine kinase, brain	11	1.30	8.3	23;18;11	amino acid kinase
51	Pdcd6ip	programmed cell death 6 interacting protein	4	1.30	16.2	-;1;1	transmembrane receptor regulatory / adaptor protein
52	Uqcrb	ubiquinol-cytochrome c reductase binding protein	6	1.30	13.6	4;5;4	reductase
53	Got1	glutamate oxaloacetate transaminase 1, soluble	12	-1.30	29.3	12;11;13	transaminase
54	Ablim2	actin-binding LIM protein 2	3	-1.30	29.7	-;1;1	structural protein, actin family cytoskeleton protein
55	St13	suppression of tumorigenicity 13	2	-1.31	20.5	-;1;1	chaperone
56	Rac1	RAS-related C3 botulinum substrate 1	3	-1.31	9.2	1;6;5	small GTPase
57	Rpl4	ribosomal protein L4	3	-1.32	22.2	2;2;2	ribosomal protein*
58	Synj1	synaptojanin 1	14	-1.33	20.9	4;6;3	phosphatase
59	Mapt	microtubule-associated protein tau	11	-1.33	26.4	12;10;12	promoting microtubule assembly and stability, microtubule binding*
60	Ywhab	tyrosine 3-monooxygenase/tryptophan 5-monooxygenase activation protein, beta polypeptide	6	-1.33	6.0	4;3;3	chaperone
61	Pacsin1	protein kinase C and casein kinase substrate in neurons 1	8	-1.33	27.3	11;9;6	membrane trafficking regulatory protein
62	Ufc1	ubiquitin-fold modifier conjugating enzyme 1	3	-1.33	0.6	-;2;1	UFM1 conjugating enyme activity*
63	Gstp1	glutathione S-transferase, pi 1	3	-1.34	15.4	1;2;2	glutathione transferase activity, kinase regulator activity*
64	Mapre2	microtubule-associated protein, RP/EB family, member 2	3	-1.34	6.5	-;1;1	non-motor microtubule binding protein
65	Rap1b	RAS related protein 1b	2	-1.34	28.4	1;2;2	small GTPase

66	Ezr	ezrin	6	-1.35	0.6	-;1;2	actin family cytoskeletal protein
67	Nefm	neurofilament, medium polypeptide	10	-1.35	27.5	3;8;7	structural protein, intermediate filament
68	Igsf8	immunoglobulin superfamily, member 8	11	-1.35	23.4	1;3;6	membrane protein*
69	Nptn	neuroplastin	6	-1.35	17.6	8;9;10	transmembrane receptor regulatory / adaptor protein
70	Ctnna2	catenin (cadherin associated protein), alpha 2	13	-1.37	28.4	1;2;1	non-motor actin binding protein, cell adhesion molecule
71	Kcnab2	potassium voltage-gated channel, shaker-related subfamily, beta member 2	7	-1.38	1.8	2;1;-	voltage-gated potassium channel, voltage-gated ion channel, reductase
72	Tmod2	tropomodulin 2	5	-1.38	28.7	2;2;2	non-motor actin binding protein
73	Cap2	CAP, adenylate cyclase-associated protein, 2 (yeast	5	-1.38	4.1	1;2;2	actin family cytoskeletal protein
74	Prkacb	protein kinase, cAMP dependent, catalytic, beta	4	-1.38	25.7	1;2;2	non-receptor serine / threonine protein kinase
75	Tpm1	tropomyosin 1, alpha	3	-1.39	25	1;1;1	actin family cytoskeletal protein
76	Dlgap2	discs, large (Drosophila) homolog-associated protein 2	4	-1.40	29.6	1;1;1	transmembrane receptor regulatory / adaptor protein
77	Nefl	neurofilament, light polypeptide	13	-1.41	19.1	8;7;8	structural protein, intermediate filament
78	Anks1b	ankyrin repeat and sterile alpha motif domain containing 1B	6	-1.41	15.4	3;3;-	transmembrane receptor regulatory / adaptor protein
79	Snap91	synaptosomal-associated protein 91	5	-1.42	15.2	9;9;9	vesicle coat protein
80	Gda	guanine deaminase	7	-1.43	14.6	3;2;4	hydrolase
81	Nrxn3	neurexin III	5	-1.44	20.4	1;1;2	transporter, apolipoprotein, cell adhesion molecule, serien protease, membrane-bound signaling molecule
82	Mdh1	malate dehydrogenase 1, NAD (soluble)	2	-1.44	20.3	2;3;2	dehydrogenase
83	Homer1	homer homolog 1 (Drosophila)	4	-1.45	8.8	2;3;3	signaling molecule
84	Sh3gl2	SH3-domain GRB2-like 2	7	-1.47	21.6	12;8;9	membrane trafficking regulatory protein, actin family cytoskeletal protein
85	Olfm1	olfactomedin 1	3	-1.48	24.0	1;1;-	structural protein, receptor
86	Slc12a5	solute carrier family 12, member 5	10	-1.49	22.6	2;6;6	cation transporter
87	Prrt2	proline-rich transmembrane protein 2	2	-1.57	13.1	3;5;4	component of the outer core of AMPA receptor complex*
88	Ncam2	neural cell adhesion molecule 2	6	-1.69	19.6	1;2;-	immunoglobulin receptor superfamily, protein phosphatase, immunoglobulin superfamily cell adhesion molecule
89	Cct2	chaperonin containing Tcp1, subunit 2 (beta)	9	-1.87	6.1	4;1;-	chaperonin
90	Sh3gl1	SH3-domain GRB2-like 1	2	-1.89	20.9	1;1;-	membrane trafficking regulatory protein, actin family cytoskeletal protein
91	Nucb1	nucleobindin 1	10	-1.92	28.9	4;3;-	nucleic acid binding, annexin, calmodulin

2000 mGy - Synaptosomes of cortex - 24 weeks post irradiation

#	Symbol	Entrez Gene Name	Unique Peptides	n-fold change from ICPL-10/ICPL-0	ICPL-10/ICPL-0 Variability [%]	ICPL_10 / ICPL_0 Count	PANTHER protein class
1	Aars	alanyl-tRNA synthetase	4	**3.09**	19.2	**1;1;-**	RNA binding protein
2	Ap2b1	adaptor-related protein complex 2, beta 1 subunit	2	**3.05**	8.4	**2;1;-**	membrane traffic protein
3	Ndufb6	NADH dehydrogenase (ubiquinone) 1 beta subcomplex, 6	3	**2.65**	19.5	**1;1;2**	mitochondrial NADH dehydrogenase*
4	Myh10	myosin, heavy polypeptide 10, non-muscle	19	**2.63**	14.2	**3;7;7**	G-protein modulator, actin binding motor protein, cell junction protein
5	Cct4	chaperonin containing Tcp1, subunit 4 (delta)	3	**2.35**	27.6	**1;3;-**	chaperonin
6	Opcml	opioid binding protein/cell adhesion molecule-like	3	**2.27**	6.5	**1;1;-**	immunoglobulin superfamily cell adhesion molecule
7	Atp1b2	ATPase, Na+/K+ transporting, beta 2 polypeptide	6	**2.25**	15.5	**3;2;1**	ATP synthase
8	Ap2a2	adaptor protein complex AP-2, alpha 2 subunit	9	**2.12**	18	**3;3;1**	transmembrane receptor regulatory adaptor protein

9	Cask	calcium/calmodulin-dependent serine protein kinase (MAGUK family)	5	2.09	17.9	1;1;-	nucleotide kinase, protein kinase, cell junction protein
10	Plec	plectin	74	2.09	28.4	6;22;12	non-motor actin binding protein
11	Ezr	ezrin	6	2.08	9.3	1;1;1	actin family cytoskeletal protein
12	Uqcrc1	ubiquinol-cytochrome c reductase core protein 1	10	2.07	23.3	3;1;1	metalloprotease, reductase, esterase
13	Pip5k1c	phosphatidylinositol-4-phosphate 5-kinase, type 1 gamma	3	2.07	16.5	1;1;-	kinase
14	Prkar2b	protein kinase, cAMP dependent regulatory, type II beta	6	2.06	9.1	3;1;-	kinase modulator
15	Kif5c	kinesin family member 5C	4	2.05	21.3	2;1;-	microtubule binding motor protein
16	Ncan	neurocan	11	2.01	23.9	2;1;1	extracellular matrix glycoprotein
17	Coro1a	coronin, actin binding protein 1A	6	1.97	28.7	12;9;9	non-motor acting binding protein
18	Ntm	neurotrimin	3	1.94	24.3	1;-;1	protein methyltransferase activity*
19	Gphn	gephyrin	5	1.91	14.6	1;1;-	cytoskeletal protein binding, ATP binding, microtubule-associated protein*
20	Ckap4	cytoskeleton-associated protein 4	8	1.88	25.2	3;4;3	chromatin / chromatin-binding protein, hydrolase
21	Nap1l1	nucleosome assembly protein 1-like 1	2	1.86	27.7	2;-;2	phosphatase inhibitor
22	Usp5	ubiquitin specific peptidase 5 (isopeptidase T)	9	1.85	28.7	3;1;3	cysteine protease, mRNA splicing factor ubiquitn-protein ligase
23	Dpysl3	dihydropyrimidinase-like 3	5	1.84	14.9	2;-;2	hydrolase
24	Hsph1	heat shock 105kDa/110kDa protein 1	5	1.79	25.9	2;2;2	alpha-tubulin binding, ATP binding*
25	Ywhah	tyrosine 3-monooxygenase/tryptophan 5-monooxygenase activation protein, eta polypeptide	2	1.79	15.2	1;1;-	chaperone
26	Rgs7	regulator of G protein signaling 7	7	1.74	13.8	3;3;1	G-protein modulator
27	Cct3	chaperonin containing Tcp1, subunit 3 (gamma)	5	1.72	22.6	2;3;3	chaperonin
28	Gnb5	guanine nucleotide binding protein (G protein), beta 5	5	1.69	14.4	3;2;1	hydrolase, heterotrimeric G-protein
29	Caskin1	CASK interacting protein 1	12	1.68	11.9	3;2;3	transmembrane receptor regulatory adaptor protein
30	Camk2b	calcium/calmodulin-dependent protein kinase II, beta	6	1.66	26	8;6;4	non-receptor serine / threonine protein kinase
31	Ctnna2	catenin (cadherin associated protein), alpha 2	13	1.66	12.9	2;1;2	non-motor actin binding protein, cell adhesion molecule
32	Wdr1	WD repeat domain 1	4	1.66	5.6	1;1;-	non-motor actin binding protein
33	Mpp3	membrane protein, palmitoylated 3 (MAGUK p55 subfamily member 3)	4	1.66	16.9	1;-;1	nucleotide kinase, cell junction protein
34	Epb4.1l2	erythrocyte protein band 4.1-like 2	8	1.65	6.3	5;3;4	actin binding, spectrin binding, structural molecule activity*
35	Hsp90ab1	heat shock protein 90 alpha (cytosolic), class B member 1	6	1.64	15.1	1;1;-	Hsp90 family chaperone
36	Pin1	protein (peptidyl-prolyl cis/trans isomerase) NIMA-interacting 1	3	1.64	27.2	1;-;1	isomerase
37	Gnb1	guanine nucleotide binding protein (G protein), beta 1	8	1.63	23.0	14;7;13	hydrolase, heterotrimeric G-protein
38	Cntn1	contactin 1	10	1.63	6.6	11;8;2	immunoglobulin receptor superfamily, protein phosphatase, immunoglobulin superfamily cell adhesion molecule
39	Tubb5	tubulin, beta 5 class I	3	1.62	27.8	7;4;6	tubulin
40	Dpysl4	dihydropyrimidinase-like 4	10	1.60	28.4	3;2;3	hydrolase
41	Cadm1	cell adhesion molecule 1	3	1.59	16.9	1;1;-	receptor, defense / immunity protein, cell adhesion
42	Nefl	neurofilament, light polypeptide	13	1.58	23.6	8;8;7	structural protein, intermediate filament
43	Ap2a1	adaptor protein complex AP-2, alpha 1 subunit	14	1.58	15.2	9;9;10	transmembrane receptor regulatory / adaptor protein
44	Shank3	SH3/ankyrin domain gene 3	21	1.55	29	2;1;2	scaffold protein interconnectin NMDA and metabotropic glutamate receptors with actin-based cytoskeleton*
45	Ppfia3	protein tyrosine phosphatase, receptor type, f polypeptide (PTPRF), interacting protein (liprin), alpha 3	7	1.55	18.4	1;-;1	Regulating disassembly of focal adhesions*

46	Mtap6	microtubule-associated protein 6	17	1.54	8.3	17;15;20	microtubule stabilization protein*
47	Gpd2	glycerol phosphate dehydrogenase 2, mitochondrial	13	1.54	25.5	11;8;9	calcium ion binding, sn-glycerol-3-phosphate:ubiquinone-8 oxidoreductase activity*
48	Ehd3	EH-domain containing 3	2	1.54	11.2	1;1;-	membrane traffic protein, G-protein modulator, calcium-binding protein
49	Gnaz	guanine nucleotide binding protein, alpha z subunit	3	1.53	17.5	2;-;1	heterotrimeric G-protein
50	Cacna2d1	calcium channel, voltage-dependent, alpha2/delta subunit 1	9	1.51	11.6	8;5;6	voltage-gated calcium channel activity*
51	Ncam1	neural cell adhesion molecule 1	7	1.51	19.9	18;12;15	immunoglobulin receptor superfamily, protein phosphatase, immunoglobulin superfamily cell adhesion molecule
52	Aak1	AP2 associated kinase	8	1.50	28.9	3;1;-	non-receptor serine / threonine protein kinase
53	Plcb1	phospholipase C, beta 1	7	1.50	22.9	3;2;3	signaling molecule, phospholipase, guanyl-nucleotide exchange factor, calcium-binding protein
54	Sept7	septin 7	9	1.47	12.2	4;-;2	small GTPase, cytoskeletal protein
55	Gnb2	guanine nucleotide binding protein (G protein), beta 2	6	1.47	18.7	7;-;5	hydrolase, heterotrimeric G-protein
56	Ncam2	neural cell adhesion molecule 2	6	1.45	26.8	2;2;-	immunoglobulin receptor superfamily, protein phosphatase, immunoglobulin superfamily cell adhesion molecule
57	N28178	expressed sequence N28178	5	1.44	3.9	1;-;2	-
58	Pabpc1	poly(A) binding protein, cytoplasmic 1	3	1.44	8.6	2;-;2	transcription factor, DNA binding protein, mRNA splicing / polyadenylation factor, ribonucleoprotein
59	Negr1	neuronal growth regulator 1	6	1.43	24.5	4;4;2	immunoglobulin superfamily cell adhesion molecule
60	Agap2	ArfGAP with GTPase domain, ankyrin repeat and PH domain 2	12	1.43	24.1	1;4;2	nucleic acid binding, G-protein modulator
61	Bsn	bassoon	62	1.42	9.3	19;10;20	neurotransmitter release organisation*
62	L1cam	L1 cell adhesion molecule	11	1.40	24.1	4;5;5	immunoglobulin receptor superfamily, protein phosphatase, immunoglobulin superfamily cell adhesion molecule
63	Sgip1	SH3-domain GRB2-like (endophilin) interacting protein 1	5	1.40	22.3	1;2;2	membrane trafficking regulatory protein, actin family cytoskeletal protein
64	Ap1b1	adaptor protein complex AP-1, beta 1 subunit	3	1.37	20.6	1;1;4	membrane traffic protein
65	Pacs1	phosphofurin acidic cluster sorting protein 1	5	1.37	11.3	1;-;1	coat protein for localization of trans-Golgi network membrane proteins*
66	Pcdh1	protocadherin 1	5	1.37	19.9	1;2;2	cadherin
67	Ckb	creatine kinase, brain	11	1.37	13.0	17;11;22	amino acid kinase
68	Cbr1	carbonyl reductase 1	3	1.37	11.9	1;1;1	dehydrogenase, reductase
69	Gda	guanine deaminase	7	1.36	17.6	1;4;3	hydrolase
70	Slc8a1	solute carrier family 8 (sodium/calcium exchanger), member 1	3	1.35	1.5	1;-;1	cation transporter
71	Dclk1	doublecortin-like kinase 1	6	1.35	17.2	1;-;1	non-receptor serine / threonine protein kinase
72	Mtap2	microtubule-associated protein 2	20	1.34	27.0	6;16;19	stabilizing microtubules agains depolymerization*
73	Acot7	acyl-CoA thioesterase 7	3	1.34	19.6	2;-;4	esterase
74	Kcnq2	potassium voltage-gated channel, subfamily Q, member 2	4	1.34	7.5	1;-;1	voltage-gated potassium / ion channel
75	Idh3g	isocitrate dehydrogenase 3 (NAD+), gamma	9	1.34	27.7	5;3;4	dehydrogenase
76	Dlg2	discs, large homolog 2 (Drosophila)	6	1.32	1.8	1;-;1	transmembrane receptor regulatory adaptor protein
77	Add2	adducin 2 (beta)	6	1.32	6.9	3;1;1	non-motor acting binding protein
78	Epb4.1l1	erythrocyte protein band 4.1-like 1	9	1.31	6.4	6;6;8	structural molecule activity, cytoskeletal organisation*
79	Ganab	alpha glucosidase 2 alpha neutral subunit	14	1.31	15.9	2;3;3	glucosidase
80	Mtx3	metaxin 3	2	-1.30	7.6	1;-;1	mitochondrial protein for protein transport*
81	Baiap2	brain-specific angiogenesis inhibitor 1-associated protein 2	5	-1.30	14.2	5;4;2	cytoskeletal adaptor activity linking small G-proteins to effector proteins*
82	Arpc4	actin related protein 2/3 complex, subunit 4	6	-1.30	15.7	5;5;7	actin-binding component regulating actin polymerization*
83	Rac1	RAS-related C3 botulinum substrate 1	3	-1.31	16.8	2;4;6	small GTPase

84	Syn2	synapsin II	7	-1.31	10.7	14;10;9	membrane trafficking regulatory protein, non-motor actin binding protein
85	Ppp2r2a	protein phosphatase 2 (formerly 2A), regulatory subunit B (PR 52), alpha isoform	5	-1.32	25.7	2;1;2	protein phosphatase
86	Atp5d	ATP synthase, H+ transporting, mitochondrial F1 complex, delta subunit	2	-1.33	23.7	3;-;3	mitochondrial proton-transporting ATP synthase activity*
87	Rph3a	rabphilin 3A	12	-1.33	27.3	6;4;3	membrane trafficking regulatory protein
88	Cox6c	cytochrome c oxidase, subunit VIc	4	-1.34	29.8	6;6;6	mitochondrial cytochrome c oxidase*
89	Prkcb	protein kinase C, beta	5	-1.34	13.6	2;1;2	non-receptor serine / threonine protein kinase, transfer / carrier protein, annexin, calmodulin
90	Acat2	acetyl-Coenzyme A acetyltransferase 2	3	-1.34	8.6	1;1;1	acetyltransferase
91	Arpc4	actin related protein 2/3 complex, subunit 4	6	-1.35	13.9	5;6;5	actin family cytoskeletal protein
92	Glul	glutamate-ammonia ligase (glutamine synthetase)	11	-1.35	23.5	11;10;11	ligase
93	Dbn1	drebrin 1	10	-1.35	27.6	3;2;2	non-motor actin binding protein
94	Ckmt1	creatine kinase, mitochondrial 1, ubiquitou	17	-1.36	15.0	23;21;21	amino acid kinase
95	Uqcrc2	ubiquinol cytochrome c reductase core protein 2	11	-1.37	18.3	13;11;10	metalloprotease, reductase, esterase
96	Dld	dihydrolipoamide dehydrogenase	6	-1.37	3.3	5;9;2	dehydrogenase, oxidase, reductase
97	Pgam1	phosphoglycerate mutase 1	8	-1.37	5.7	8;6;5	bisphosphoglycerate 2-phosphatase activity*
98	Atp5a1	ATP synthase, H+ transporting, mitochondrial F1 complex, alpha subunit	18	-1.38	29.9	47;38;60	ATP synthase, anion channel, ligand gated ion channel, DNA binding protein, hydrolase
99	Gstm1	glutathione S-transferase, mu 1	7	-1.38	10.0	4;3;2	glutathione transferase activity*
100	Baiap2	brain-specific angiogenesis inhibitor 1-associated protein 2	5	-1.39	18.4	3;2;5	receptor
101	Cyc1	cytochrome c-1	5	-1.39	28.7	3;1;4	mitchondrial cytochrome c activity*
102	Epb4.1l3	erythrocyte protein band 4.1-like 3	9	-1.39	27.3	5;3;7	structural molecule activity, cytoskeletal organisation*
103	Cap2	CAP, adenylate cyclase-associated protein, 2 (yeast)	5	-1.41	5.2	3;1;1	actin family cytoskeletal protein
104	Nceh1	arylacetamide deacetylase-like 1	3	-1.41	14.3	1;-;1	ligase
105	Sh3gl2	SH3-domain GRB2-like 2	7	-1.43	27.3	10;8;9	membrane trafficking regulatory protein, actin family cytoskeletal protein
106	Kcnab2	potassium voltage-gated channel, shaker-related subfamily, beta member 2	7	-1.44	4.1	2;2;-	voltage-gated potassium / ion channel, reductase
107	Ndufa1	NADH dehydrogenase (ubiquinone) 1 alpha subcomplex, 1	2	-1.45	17.3	1;1;1	mitochondrial NADH dehydrogenase*
108	Actb	actin, beta	5	-1.45	11.8	14;20;6	actin and actin related protein
109	Olfm1	olfactomedin 1	3	-1.45	6.8	1;1;-	structural protein, receptor
110	Nucb1	nucleobindin 1	10	-1.46	4.0	3;1;-	nucleic acid binding, annexin, calmodulin
111	Atp2b3	ATPase, Ca++ transporting, plasma membrane 3	5	-1.47	17.2	1;1;4	cation transporter, ion channel, hydrolase
112	Atp6v1e1	ATPase, H+ transporting, lysosomal V1 subunit E1	6	-1.49	29.1	9;8;9	mitochondrial ATPase activity, hydrogen ion transmembrane transporter activity*
113	Rtn4	reticulon 4	2	-1.50	21.0	1;1;1	membrane traffic protein
114	Arhgdia	Rho GDP dissociation inhibitor (GDI) alpha	4	-1.50	25.4	5;6;5	signaling molecule, G-protein modulator
115	Anxa7	annexin A7	4	-1.51	11.5	1;2;-	calcium ion binding protein*
116	Pygb	brain glycogen phosphorylase	5	-1.51	24.1	1;2;1	phosphorylase
117	Hspd1	heat shock protein 1 (chaperonin)	8	-1.51	22.3	9;7;10	chaperonin
118	Ywhab	tyrosine 3-monooxygenase/tryptophan 5-monooxygenase activation protein, beta polypeptide	6	-1.53	24.7	3;3;4	chaperone
119	Anks1b	ankyrin repeat and sterile alpha motif domain containing 1B	6	-1.57	12.4	3;4;-	transmembrane receptor regulatory adaptor protein
120	Hexb	hexosaminidase B	5	-1.58	12.1	1;2;2	glycosidase
121	Pebp1	phosphatidylethanolamine binding protein 1	2	-1.59	28.5	1;2;2	ATP binding, protein kinase binding*
122	Arpc2	actin related protein 2/3 complex, subunit 2	5	-1.59	16.5	2;2;-	structural constituent of cytoskeleton, actin-binding component*
123	Prkacb	protein kinase, cAMP dependent, catalytic, beta	4	-1.61	16.2	2;-;2	non-receptor serine / threonine protein kinase
124	Dlst	dihydrolipoamide S-succinyltransferase (E2 component of 2-oxo-glutarate complex)	4	-1.61	13.4	7;5;5	acetyltransferase, acyltransferase
125	Rab35	RAB35, member RAS oncogene family	2	-1.64	1.7	1;-;2	GDP / GTP binding, small GTPase*
126	Gbas	glioblastoma amplified sequence	2	-1.65	2.6	1;1;-	ATP biosynthetic processing protein*

127	Sept6	septin 6	3	-1.66	22.7	4;3;5	small GTPase, cytoskeletal protein
128	Got2	glutamate oxaloacetate transaminase 2, mitochondrial	14	-1.77	6.4	20;12;19	transaminase
129	Mapre2	microtubule-associated protein, RP/EB family, member 2	3	-1.78	27.8	1;1;-	non-motor microtubule binding protein
130	Phb2	prohibitin 2	13	-1.81	18.0	3;4;5	transketolase, dehydrogenase, lyase
131	Grin1	glutamate receptor, ionotropic, NMDA1 (zeta 1)	10	-1.81	22.0	1;-;1	ionotropic glutamate receptor
132	Fkbp1a	FK506 binding protein 1a	5	-1.81	25.5	4;3;2	isomerase, chaperone, calcium-binding protein
133	Ppp1r7	protein phosphatase 1, regulatory (inhibitor) subunit 7	4	-1.83	24.6	2;-;2	regulatory subuni of protein phosphatase 1*
134	Ldhb	lactate dehydrogenase B	2	-1.87	17.9	5;4;5	dehydrogenase
135	Stmn1	stathmin 1	4	-1.87	27	3;5;3	regulation of microtubule filament system by destabilizing microtubules*
136	Ndufs5	NADH dehydrogenase (ubiquinone) Fe-S protein 5	3	-1.89	14.6	1;2;2	mitochondrial NADH dehydrogenase*
137	Cnp	2',3'-cyclic nucleotide 3' phosphodiesterase	10	-2.00	14.5	12;7;15	phosphodiesterase
138	Pdhb	pyruvate dehydrogenase (lipoamide) beta	4	-2.02	19.2	1;-;1	transferase activity, transferring acyl groups*
139	Dlat	dihydrolipoamide S-acetyltransferase (E2 component of pyruvate dehydrogenase complex)	3	-2.04	15.0	1;4;2	acetyltransferase, acyltransferase
140	Cops8	COP9 (constitutive photomorphogenic) homolog, subunit 8 (Arabidopsis thaliana)	3	-2.04	24.4	1;1;1	signaling molecule
141	Sod1	superoxide dismutase 1, soluble	3	-2.08	25.8	4;3;1	oxidoreductase
142	Mbp	myelin basic protein	10	-2.12	19.5	6;25;16	myelin protein
143	Gad2	glutamic acid decarboxylase 2	2	-2.13	17.0	2;-;2	decarboxylase
144	Ywhaz	tyrosine 3-monooxygenase/tryptophan 5-monooxygenase activation protein, zeta polypeptid	7	-2.21	20.4	9;7;9	chaperone
145	Fam49b	family with sequence similarity 49, member B	3	-2.27	4.9	1;-;1	-
146	Dlgap2	discs, large (Drosophila) homolog-associated protein 2	4	-2.35	15.5	1;1;1	transmembrane receptor regulatory adaptor protein
147	Rab2a	RAB2A, member RAS oncogene family	5	-2.36	21.6	3;-;2	GDP / GTP binding, GTPase activity*
148	Asah1	N-acylsphingosine amidohydrolase 1	3	-2.57	20.2	1;1;1	ceramidase activity*
149	Atp5o	ATP synthase, H+ transporting, mitochondrial F1 complex, O subunit	6	-2.64	15.8	10;9;9	ATP synthase, hydrolase
150	Ppt1	palmitoyl-protein thioesterase 1	4	-2.70	28.6	2;1;1	esterase
151	Tomm20	translocase of outer mitochondrial membrane 20 homolog (yeast)	2	-4.51	12.5	2;1;-	mitochondrial transporter
152	H3f3a	H3 histone, family 3A	3	-6.57	10.1	1;-;2	histone

Table 34: List of deregulated proteins 24 weeks post-irradiation from 100 mGy, 500 mGy and 2000 mGy within the isolated synaptosomes of hippocampus (C57Bl6 study).

The table shows the up-regulated or down-regulated proteins with the fold-changes, their variability, their number of unique peptides used for protein identification and number of identifications in the biological replicates (ICPLx/ICPL0-Count). "PANTHER protein class" represents the protein class where the protein of interest can be annotated based on PANTHER software tool and UniProt database. Grey / brown highlighted "PANTHER protein classes" belong to the protein class of "small GTPase / associated G-protein" / "cytoskeleton / cytoskeleton-binding protein", respectively

100 mGy - Synaptosomes of hippocampus - 24 weeks post irradiation

#	Symbol	Entrez Gene Name	Unique Peptides	n-fold change from ICPL-4/ICPL-0	ICPL-4/ICPL-0 Variability [%]	ICPL_4 / ICPL_0 Count	PANTHER protein class
1	Tcp1	t-complex protein 1	5	1.63	25.8	1;3;-	chaperonin
2	Lgi1	leucine-rich repeat LGI family, member 1	2	1.62	5.9	1;1;-	receptor, extracellular matrix protein
3	Sfxn1	sideroflexin 1	4	1.58	29.4	1;1;-	cation transporter, transfer / carrier protein
4	Sept3	septin 3	3	1.46	29.3	1;1;-	small GTPase, cytoskeletal protein

5	Ehd3	EH-domain containing 3	3	1.43	1.8	1;-;1	membrane traffic protein, G-protein modulator, calcium-
6	Dmxl2	Dmx-like 2	17	1.40	19.5	4;4;-	scaffold protein on synaptic vesicles*
7	Hrsp12	heat-responsive protein 12	3	1.38	24.2	2;2;2	deaminase activity, endonuclease activity*
8	Ppfia3	protein tyrosine phosphatase, receptor type, f polypeptide (PTPRF), interacting protein (liprin), alpha 3	13	1.34	11.6	4;4;-	protein regulating disassembly of focal adhesions*
9	Dlgap2	discs, large (Drosophila) homolog-associated protein 2	4	1.34	17.2	2;2;-	transmembrane receptor regulatory / adaptor protein
10	Uqcrc1	ubiquinol-cytochrome c reductase core protein 1	10	1.34	7.5	1;1;1	metalloprotease, reductase, esterase
11	Dlgap1	discs, large (Drosophila) homolog-associated protein 1	5	1.33	6.5	3;2;1	transmembrane receptor regulatory / adaptor protein
12	Coro1c	coronin, actin binding protein 1C	5	1.32	11.7	2;4;-	non-motor actin binding protein
13	Arfgap1	ADP-ribosylation factor GTPase activating protein 1	3	1.30	6.2	3;4;3	nucleic acid binding, G-protein modulator
14	Arhgef2	rho/rac guanine nucleotide exchange factor (GEF) 2	9	1.30	6.3	1;1;-	guanyl-nucleotide exchange factor
15	Rpl11	ribosomal protein L11	2	-1.30	6.0	2;2;2	ribosomal protein
16	Phgdh	3-phosphoglycerate dehydrogenase	4	-1.30	7.3	1;1;-	dehydrogenase
17	Slc25a4	solute carrier family 25 (mitochondrial carrier, adenine nucleotide translocator), member 4	4	-1.33	19.5	7;6;1	amino acid transporter, mitochondrial carrier protein, transfer / carrier protein, calmodulin
18	Fbxo41	F-box protein 41	6	-1.35	23.4	1;1;-	component of E3 ubiquitin ligase complex*
19	Snd1	staphylococcal nuclease and tudor domain containing 1	7	-1.35	11.9	1;2;-	transcription cofactor, nucleic acid binding
20	Mink1	misshapen-like kinase 1 (zebrafish)	10	-1.36	25.2	1;3;-	ATP binding, small GTPase regulator activity*
21	Nefl	neurofilament, light polypeptide	12	-1.36	17.0	7;10;10	structural protein, intermediate filament
22	Chchd3	coiled-coil-helix-coiled-coil-helix domain containing 3	4	-1.37	13.1	3;1;2	protein for mitochondrial crista integrity and function*
23	Rps19	ribosomal protein S19	3	-1.38	15.5	1;3;2	ribosomal protein
24	Hsp90b1	heat shock protein 90, beta (Grp94), member 1	10	-1.39	18.1	5;6;2	Hsp90 family chaperone
25	Slc25a11	solute carrier family 25 (mitochondrial carrier oxoglutarate carrier), member 11	5	-1.41	3.5	3;1;-	amino acid transporter, mitochondrial carrier protein, transfer / carrier protein, calmodulin
26	Fam49b	family with sequence similarity 49, member B	3	-1.42	9.0	1;2;-	-
27	Pld3	phospholipase D family, member 3	4	-1.43	4.4	2;5;2	phospholipase
28	Tom1l2	target of myb1-like 2 (chicken)	7	-1.46	21.9	1;-;1	transporter, membrane traffic protein, kinase activator, cytoskeletal protein
29	Hyou1	hypoxia up-regulated 1	12	-1.53	22.6	4;7;2	Hsp70 family chaperone

30	Cct7	chaperonin containing Tcp1, subunit 7 (eta)	3	-1.53	24.3	2;2;-	chaperonin
31	Gna11	guanine nucleotide binding protein, alpha 11	2	-1.55	28.9	1;1;-	heterotrimeric G-protein
32	Srgap3	SLIT-ROBO Rho GTPase activating protein 3	10	-1.56	12.8	1;1;-	G-protein modulator
33	Ckap4	cytoskeleton-associated protein 4	2	-1.56	8.0	1;1;1	chromatin / chromatin-binding protein, hydrolase
34	Hsd17b10	hydroxysteroid (17-beta) dehydrogenase 10	4	-1.57	12.5	1;2;-	dehydrogenase, reductase
35	Ivd	isovaleryl coenzyme A dehydrogenase	2	-1.63	23.9	1;1;-	transferase, dehydrogenase, oxidase
36	Nt5dc3	5'-nucleotidase domain containing 3	4	-1.84	4.3	2;2;-	nucleotide phosphatase
37	Ndufa9	NADH dehydrogenase (ubiquinone) 1 alpha subcomplex, 9	11	-1.92	5.9	3;5;1	dehydrogenase, reductase
38	Prkacb	protein kinase, cAMP dependent, catalytic, beta	5	-1.96	18.8	3;3;-	non-receptor serine / threonine protein kinase
39	Rab39b	RAB39B, member RAS oncogene family	2	-2.16	22.6	1;-;1	GTP binding, small GTPase mediated signal transduction*
40	Coq9	coenzyme Q9 homolog (yeast)	3	-2.21	27.8	1;-;1	coenzyme Q9 biosynthesis*

500 mGy - Synaptosomes of hippocampus - 24 weeks post irradiation

#	Symbol	Entrez Gene Name	Unique Peptides	n-fold change from ICPL-6/ICPL-0	ICPL-6/ICPL-0 Variability [%]	ICPL_6 / ICPL_0 Count	PANTHER protein class
1	Uqcrc1	ubiquinol-cytochrome c reductase core protein 1	10	2.40	24.0	1;1;1	metalloprotease, reductase, esterase
2	Tagln3	transgelin 3	3	2.08	14.0	1;1;1	non-motor actin binding protein
3	Sfxn1	sideroflexin 1	4	1.97	24.0	-;1;1	cation transporter, transfer / carrier protein
4	Sept3	septin 3	3	1.83	23.6	-;1;1	small GTPase, cytoskeletal protein
5	mt-Co2	mitochondrially encoded cytochrome c oxidase II	2	1.71	23.9	2;1;1	mitochondrial cytochrome c activity*
6	Sucla2	succinate-Coenzyme A ligase, ADP-forming, beta subunit	3	1.67	26.2	-;1;1	ligase
7	Ndufb10	NADH dehydrogenase (ubiquinone) 1 beta subcomplex, 10	6	1.65	28.4	2;7;4	mitochondrial NADH dehydrogenase activity*
8	Nefm	neurofilament, medium polypeptide	10	1.59	18.8	8;9;6	structural protein, intermediate filament
9	Ndufs8	NADH dehydrogenase (ubiquinone) Fe-S protein 8	4	1.56	28.5	-;1;3	mitochondrial NADH dehydrogenase activity*
10	Bin1	bridging integrator 1	2	1.56	12.8	1;1;-	membrane trafficking regulatory protein
11	Tcp1	t-complex protein 1	5	1.56	9.6	-;1;3	chaperonin
12	Sars	seryl-aminoacyl-tRNA synthetase	5	1.53	26.2	-;1;1	RNA binding protein, aminoacyl-tRNA synthetase
13	Gnb1	guanine nucleotide binding protein (G protein), beta 1	9	1.52	17.6	5;8;15	hydrolase, heterotrimeric G-protein
14	Ppt1	palmitoyl-protein thioesterase 1	3	1.52	24.5	-;2;1	esterase
15	Gnb2	guanine nucleotide binding protein (G protein), beta 2	6	1.49	28.8	1;3;6	hydrolase, heterotrimeric G-protein
16	Gm8226	predicted gene 8226	4	1.46	16.0	2;1;-	-
17	Atp5d	ATP synthase, H+ transporting, mitochondrial F1 complex, delta subunit	2	1.46	17.8	4;2;4	mitochondrial membrane ATP synthase*
18	Tsfm	Ts translation elongation factor, mitochondrial	2	1.45	12.7	1;1;-	translation elongation factor, guanyl-nucleotide exchange factor
19	Cox6b1	cytochrome c oxidase, subunit Vlb polypeptide 1	4	1.42	25.2	4;5;3	oxidase
20	Tom1l2	target of myb1-like 2 (chicken)	7	1.41	29.3	1;1;-	transporter, membrane traffic protein, kinase activator, cytoskeletal protein
21	Uqcrb	ubiquinol-cytochrome c reductase binding protein	5	1.41	21.1	4;6;6	reductase
22	Slc44a2	solute carrier family 44, member 2	2	1.41	10.2	1;1;-	transporter
23	Ndufa7	NADH dehydrogenase (ubiquinone) 1 alpha subcomplex, 7 (B14.5a)	2	1.41	18.9	2;3;-	mitochondrial NADH dehydrogenase activity*
24	Trap1	TNF receptor-associated protein 1	5	1.40	26.9	1;1;-	Hsp90 family chaperone
25	Sept7	septin 7	7	1.40	20.4	1;2;5	filament-forming cytoskeletal GTPase*
26	Mdh2	malate dehydrogenase 2, NAD (mitochondrial	5	1.39	1.7	6;12;14	dehydrogenase

27	Pdhx	pyruvate dehydrogenase complex, component X	3	1.39	6.0	3;3;-	acetyltransferase, acyltransferase
28	Ogdhl	oxoglutarate dehydrogenase-like	8	1.39	16.1	2;3;-	oxoglutarate dehydrogenase activity*
29	Fech	ferrochelatase	3	1.38	22.8	1;1;-	ferrochelatase activity, ferrous iron binding, iron-responsive element binding*
30	Rimbp2	RIMS binding protein 2	7	1.38	9.9	2;1;-	synaptic transmission*
31	Ivd	isovaleryl coenzyme A dehydrogenase	2	1.37	3.1	-;1;1	transferase, dehydrogenase, oxidase
32	Snd1	staphylococcal nuclease and tudor domain containing 1	7	1.37	0.1	1;3;-	transcription cofactor, nucleic acid binding
33	Arhgef2	rho/rac guanine nucleotide exchange factor (GEF) 2	9	1.36	0.9	1;1;-	guanyl-nucleotide exchange factor
34	Psd3	pleckstrin and Sec7 domain containing 3	4	1.36	12.4	-;4;4	guanyl-nucleotide exchange factor
35	Arhgef2	rho/rac guanine nucleotide exchange factor (GEF) 2	9	1.36	1	1;1;-	guanyl-nucleotide exchange factor
36	Dpysl5	dihydropyrimidinase-like 5	4	1.36	15.4	-;1;1	hydrolase
37	Aldh6a1	aldehyde dehydrogenase family 6, subfamily A1	6	1.35	7.8	3;5;-	ATP synthase, hydrolase
38	Hspa5	heat shock protein 5	10	1.35	1.8	-;7;12	Hsp70 family chaperone
39	Atp5e	ATP synthase, H+ transporting, mitochondrial F1 complex, epsilon subunit	2	1.35	17.3	2;2;2	ATP synthase, hydrolase
40	Etfa	electron transferring flavoprotein, alpha polypeptide	2	1.34	13.8	2;3;2	transferase, dehydrogenase, oxidase
41	Nefl	neurofilament, light polypeptide	12	1.33	5.5	10;7;10	structural protein, intermediate filament
42	Atp5c1	ATP synthase, H+ transporting, mitochondrial F1 complex, gamma polypeptide 1	7	1.33	19.1	7;7;3	mitochondrial ATP synthase*
43	Sdhb	succinate dehydrogenase complex, subunit B, iron sulfur (Ip)	4	1.32	15.2	7;5;8	dehydrogenase
44	Ndufa2	NADH dehydrogenase (ubiquinone) 1 alpha subcomplex, 2	5	1.31	25.9	6;6;3	oxidoreductase
45	Pdia3	protein disulfide isomerase associated 3	7	1.31	5.8	5;6;-	isomerase
46	Tubb5	tubulin, beta 5 class I	3	1.30	15.4	3;9;2	tubulin
47	Ap2m1	adaptor protein complex AP-2, mu1	5	-1.30	12.8	9;12;5	membrane traffic protein
48	Pdxp	pyridoxal (pyridoxine, vitamin B6) phosphatase	11	-1.31	29.2	2;2;1	phosphatase
49	Prkacb	protein kinase, cAMP dependent, catalytic, beta	5	-1.31	15.1	-;3;3	non-receptor serine / threonine protein kinase
50	Agap2	ArfGAP with GTPase domain, ankyrin repeat and PH domain 2	13	-1.31	14.7	5;4;-	nucleic acid binding, G-protein modulator
51	Srgap3	SLIT-ROBO Rho GTPase activating protein 3	10	-1.31	10.5	1;1;-	G-protein modulator
52	Ufc1	ubiquitin-fold modifier conjugating enzyme 1	2	-1.32	18.9	-;1;1	UFM1 conjugating enzyme activity*
53	Gnaq	guanine nucleotide binding protein, alpha q polypeptide	4	-1.32	19.4	-;1;1	heterotrimeric G-protein
54	Fbxo41	F-box protein 41	6	-1.32	11.0	-;1;1	E3 ubiquitin ligase complex*
55	Rab11b	RAB11B, member RAS oncogene family	5	-1.32	22.4	3;3;2	GDP / GTP binding, GTPase activity*
56	Phyhip	phytanoyl-CoA hydroxylase interacting	4	-1.33	21.6	2;2;1	hydroxylase*
57	Arpc4	actin related protein 2/3 complex, subunit 4	6	-1.34	3.6	6;7;3	actin family cytoskeletal protein
58	Gria1	glutamate receptor, ionotropic, AMPA1 (alpha 1)	5	-1.34	8.7	1;2;-	ionotropic glutamate receptor
59	Madd	MAP-kinase activating death domain	10	-1.35	7.7	-;3;2	guanyl-nucleotide exchange factor
60	Pcdh1	protocadherin 1	8	-1.35	20.2	4;6;5	cadherin
61	Rufy3	RUN and FYVE domain containing 3	3	-1.36	0.5	-;1;1	zinc finger transcription factor, membrane traffic protein, G-protein modulator, kinase activator
62	Cadm1	cell adhesion molecule 1	2	-1.36	14.0	1;1;-	receptor, defense / immunity response, cell adhesion protein
63	Slc25a5	solute carrier family 25 (mitochondrial carrier, adenine nucleotide translocator), member 5	4	-1.36	16.5	13;16;4	amino acid transporter, mitochondrial carrier protein, transfer / carrier protein, calmodulin
64	Acly	ATP citrate lyase	7	-1.38	16.5	1;2;-	transferase, lyase, ligase
65	Cand1	cullin associated and neddylation disassociated 1	8	-1.39	1.0	4;4;-	transcription factor
66	Ezr	ezrin	8	-1.39	26.4	4;3;-	actin family cytoskeletal protein
67	Rab35	RAB35, member RAS oncogene family	2	-1.42	29.4	2;3;-	GDP / GTP binding, GTPase activity*

68	Slc25a4	solute carrier family 25 (mitochondrial carrier, adenine nucleotide translocator), member 4	4	-1.42	27.4	7;8;1	amino acid transporter, mitochondrial carrier protein, transfer / carrier protein, calmodulin
69	Mink1	misshapen-like kinase 1 (zebrafish)	10	-1.44	7.2	-;1;3	ATP binding, small GTPase regulator activity*
70	Gstm5	glutathione S-transferase, mu 5	2	-1.47	9.7	-;1;1	glutathione transferase activity*
71	Slc4a4	solute carrier family 4 (anion exchanger), member 4	4	-1.48	0.5	1;3;-	cation transporter
72	Diras2	DIRAS family, GTP-binding RAS-like 2	2	-1.49	6.0	1;1;-	small GTPase
73	Psmb2	proteasome (prosome, macropain) subunit, beta type 2	5	-1.50	23.4	2;2;-	protease
74	Brp44l	brain protein 44-like	2	-1.50	29.99	1;2;-	mediates uptake of pyruvate into mitochondria*
75	Atp5v0d1	ATPase, H+ transporting, lysosomal V0 subunit D1	4	-1.52	22.0	4;4;6	mitochondrial ATP synthase*
76	Gnas	GNAS (guanine nucleotide binding protein, alpha stimulating) complex locus	5	-1.54	17.4	-;1;1	heterotrimeric G-protein
77	Gpd1	glycerol-3-phosphate dehydrogenase 1 (soluble)	2	-1.54	5.3	-;1;1	dehydrogenase
78	Rac1	RAS-related C3 botulinum substrate 1	3	-1.57	25.4	7;5;7	small GTPase
79	Ndufa9	NADH dehydrogenase (ubiquinone) 1 alpha subcomplex, 9	11	-1.62	13.2	3;5;-	dehydrogenase, reductase
80	Fam49b	family with sequence similarity 49, member B	3	-1.75	15.7	-;1;2	-
81	Nudt3	nudix (nucleotide diphosphate linked moiety X)-type motif 3	3	-1.76	25.6	-;1;1	phosphatase
82	Alcam	activated leukocyte cell adhesion molecule	3	-1.98	12.0	1;1;-	receptor, immunoglobulin superfamily cell adhesion molecule
83	Wdr7	WD repeat domain 7	9	-2.07	24.2	2;3;-	mRNA splicing factor, esterase, kinase inhibitor
84	Nptx1	neuronal pentraxin 1	5	-5.64	8.0	3;1;-	mediating uptake of synaptic metrial during synapse remodeling*

2000 mGy - Synaptosomes of hippocampus - 24 weeks post irradiation

#	Symbol	Entrez Gene Name	Unique Peptides	n-fold change from ICPL-10/ICPL-	ICPL-10/ICPL-0 Variability [%]	ICPL_10 / ICPL_0 Count	PANTHER protein class
1	Gad1	glutamic acid decarboxylase 1	3	3.41	3.9	2;2;-	decarboxylase
2	Nefm	neurofilament, medium polypeptide	10	2.63	26.1	4;4;5	structural protein, intermediate filament
3	Ina	internexin neuronal intermediate filament protein, alpha	12	2.34	29.5	5;3;7	intermediate filament binding protein, structural molecule activity*
4	Vcp	valosin containing protein	12	2.30	6.4	4;7;3	ADP / ATP binding, ATPase activity*
5	Dctn1	dynactin 1	8	2.13	2.5	3;5;-	non-motor actin binding protein, chaperone
6	Hyou1	hypoxia up-regulated 1	12	2.11	10.2	4;7;2	Hsp70 family chaperone
7	Ckap4	cytoskeleton-associated protein 4	2	2.05	16.1	1;1;1	chromatin / chromatin-binding protein, hydrolase
8	Ina	internexin neuronal intermediate filament protein, alpha	12	1.99	6	5;3;4	structural protein, intermediate filament
9	Efhd2	EF hand domain containing 2	5	1.94	9.5	1;-;1	calcium-binding protein
10	Csnk2a1	casein kinase 2, alpha 1 polypeptide	6	1.88	26.9	2;2;2	ATP binding, kinase activity, protein phosphatase regulator activity, protein serine / threonine kinase activity*
11	Tcp1	t-complex protein 1	5	1.88	20.0	1;3;-	chaperonin
12	Tagln3	transgelin 3	3	1.82	9.8	1;1;2	non-motor actin binding protein
13	Numbl	numb-like	6	1.82	0.9	2;2;-	signaling molecule
14	Add3	adducin 3 (gamma)	4	1.79	23.8	2;2;-	non-motor actin binding protein
15	Hsp90b1	heat shock protein 90, beta (Grp94), member 1	10	1.77	11.1	5;6;2	Hsp90 family chaperone
16	Mtap6	microtubule-associated protein 6	11	1.77	5.3	7;5;6	microtubuli stabilization protein*
17	Sept3	septin 3	3	1.76	6.0	1;1;-	small GTPase, cytoskeletal protein
18	Git1	G protein-coupled receptor kinase-interactor 1	12	1.73	10.7	1;3;-	nucleic acid binding, G-protein modulator
19	Sgip1	SH3-domain GRB2-like (endophilin) interacting protein 1	7	1.70	25.5	2;3;1	membrane trafficking regulatory protein, actin family cytoskeletal protein
20	Tpm3	tropomyosin 3, gamma	7	1.67	12.1	4;2;4	actin binding motor protein
21	Dbnl	drebrin-like	6	1.65	15.1	1;2;2	non-motor actin binding protein
22	Tpm1	tropomyosin 1, alpha	3	1.64	23.5	2;1;2	actin binding motor protein
23	Pdia3	protein disulfide isomerase associated 3	7	1.61	6.8	5;5;-	isomerase

24	Shank3	SH3/ankyrin domain gene 3	19	1.60	4.1	1;2;-	scaffold protein, interconnecting NMDA and metabotropic glutamate receptors with actin-based cytoskeleton*
25	Pip5k1c	phosphatidylinositol-4-phosphate 5-kinase, type 1 gamma	4	1.60	13.7	2;1;-	kinase
26	Snd1	staphylococcal nuclease and tudor domain containing 1	7	1.58	19.1	1;2;-	transcription cofactor, nucleic acid binding
27	Sars	seryl-aminoacyl-tRNA synthetase	5	1.58	23.8	1;1;-	RNA binding protein, aminoacyl-tRNA synthetase
28	Cltb	clathrin, light polypeptide (Lcb)	3	1.58	21.2	3;1;-	vesicle coat protein
29	Pabpc1	poly(A) binding protein, cytoplasmic 1	3	1.57	6.0	1;1;-	transcription factor, DNA binding protein, mRNA splicing / polyadenylation factor, ribonucleoprotein
30	Itsn1	intersectin 1 (SH3 domain protein 1A)	5	1.56	1.9	2;3;-	membrane traffic protein, G-protein modulator, calcium-binding protein
31	Gm10237	predicted gene 10237	2	1.56	20.5	2;2;3	-
32	Uqcrc1	ubiquinol-cytochrome c reductase core protein 1	10	1.55	16.8	1;1;1	metalloprotease, reductase, esterase
33	Me1	malic enzyme 1, NADP(+)-dependent, cytosolic	4	1.53	4.4	1;2;-	acyltransferase, dehydrogenase, decarboxylase
34	Dlgap1	discs, large (Drosophila) homolog-associated protein 1	5	1.52	29.8	1;2;1	transmembrane receptor regulatory / adaptor protein
35	Tpi1	triosephosphate isomerase 1	3	1.52	28.2	5;4;4	isomerase
36	L1cam	L1 cell adhesion molecule	8	1.51	13.1	5;5;3	immunoglobulin receptor superfamily, protein phosphatase, immunoglobulin superfamily cell adhesion molecule
37	Arhgef2	rho/rac guanine nucleotide exchange factor (GEF) 2	9	1.49	7.2	1;1;-	guanyl-nucleotide exchange factor
38	Gdi1	guanosine diphosphate (GDP) dissociation inhibitor 1	8	1.49	11.8	9;7;2	acyltransferase, G-protein modulator
39	010300C02R	RIKEN cDNA 2010300C02 gene	7	1.47	12.3	1;1;-	-
40	Hspa12a	heat shock protein 12A	9	1.46	17.7	3;6;1	non-receptor serine / threonine protein kinase, Hsp70 family chaperone
41	Ppp1r9b	protein phosphatase 1, regulatory subunit 9B	5	1.46	27.9	1;2;-	protein phosphatase 1 binding, binds to actin filaments and cross-linking activity*
42	Mtap1b	microtubule-associated protein 1B	11	1.46	11.0	7;11;4	cytoskeletal regulatory protein binding, microtubuli binding*
43	Gmfb	glia maturation factor, beta	3	1.45	6.2	1;1;-	signaling molecule, kinase modulator
44	Tmod2	tropomodulin 2	5	1.45	23.4	3;2;5	non-motor actin binding protein
45	Gprin1	G protein-regulated inducer of neurite outgrowth 1	7	1.44	29.2	1;1;3	phosphoprotein binding, involved in neurite outgrowth*
46	Pfkp	phosphofructokinase, platelet	9	1.44	13.1	6;7;-	carbohydrate kinase
47	Pdxk	pyridoxal (pyridoxine, vitamin B6) kinase	4	1.41	9.0	2;3;2	kinase
48	Ndufb6	NADH dehydrogenase (ubiquinone) 1 beta subcomplex, 6	3	1.41	27.3	1;2;2	ATP binding, pyridoxal kinase activity*
49	Dnm3	dynamin 3	2	1.40	22.8	2;2;-	hydrolase, small GTPase, microtubule family cytoskeletal protein
50	Pld3	phospholipase D family, member 3	4	1.40	16.4	2;2;5	phospholipase
51	Cnrip1	cannabinoid receptor interacting protein 1	4	1.38	12.4	3;4;1	voltage-gated calcium channels regulation*
52	Mtap1a	microtubule-associated protein 1 A	28	1.38	19.9	7;11;7	structural protein involved in cross-bridging between microtubules and skeletal elements*
53	Ganab	alpha glucosidase 2 alpha neutral subunit	10	1.38	6.5	2;3;-	glucosidase
54	Hspa4l	heat shock protein 4 like	10	1.37	2.4	1;3;-	Hsp70 family chaperone
55	Cox6b1	cytochrome c oxidase, subunit VIb polypeptide 1	4	1.37	15.5	4;5;3	oxidase
56	Oxr1	oxidation resistance 1	11	1.37	18.7	6;5;2	protection from oxidative damage*
57	Tom1l2	target of myb1-like 2 (chicken)	7	1.37	13.0	1;-;1	transporter, membrane traffic protein, kinase activator, cytoskeletal protein
58	Camkv	CaM kinase-like vesicle-associated	6	1.36	21.5	4;3;1	non-receptor serine / threonine kinases
59	Mif	macrophage migration inhibitory factor	2	1.36	5.9	1;-;1	chemoattractant activity, cytokine activity*
60	Sept5	septin 5	5	1.36	27.1	5;7;3	small GTPase, cytoskeletal protein

61	Spnb3	spectrin beta 3	60	1.36	27.1	5;16;24	structural constitutent of cytoskeleton*
62	Purb	purine rich element binding protein B	4	1.35	26.5	2;1;1	transcription factor, DNA binding protein
63	Actn4	actinin alpha 4	3	1.35	0.4	1;4;-	non-motor actin binding protein
64	Arpc3	actin related protein 2/3 complex, subunit 3	2	1.34	10	1;1;-	actin family cytoskeletal protein
65	Atp6v1b2	ATPase, H+ transporting, lysosomal V1 subunit B2	14	1.34	11.1	11;13;17	ATP synthase, anion channel, ligand-gated ion channel. DNA binding protein, hydrolase
66	Gnb5	guanine nucleotide binding protein (G protein), beta 5	4	1.34	12.5	2;1;-	hydrolase, heterotrimeric G-protein
67	Dnajc6	DnaJ (Hsp40) homolog, subfamily C, member 6	5	1.34	15.7	1;2;-	non-receptor serine / threonine kinases, chaperone
68	Fscn1	fascin homolog 1, actin bundling protein (Strongylocentrotus purpuratus)	5	1.34	23.1	2;3;-	non-motor actin binding protein
69	Rgs7	regulator of G protein signaling 7	7	1.34	13.7	3;4;-	G-protein modulator
70	Nudt3	nudix (nucleotide diphosphate linked moiety X)-type motif 3	3	1.33	15.5	1;-;1	phosphatase
71	Epb4.1l3	erythrocyte protein band 4.1-like 3	7	1.33	4.8	5;8;5	structural molecule activity, cytoskeletal organisation+
72	Ank3	ankyrin 3, epithelial	13	1.33	2.2	10;7;-	cytoskeletal protein
73	Ppp2r2a	protein phosphatase 2 (formerly 2A), regulatory subunit B (PR 52), alpha isoform	6	1.33	13.6	2;2;-	protein phosphatase
74	Epb4.1l1	erythrocyte protein band 4.1-like 1	9	1.32	3.8	12;9;3	structural molecule activity, cytoskeletal organisation+
75	720456B07R	RIKEN cDNA 6720456B07 gene	2	1.32	18.9	2;1;2	-
76	Hspa4	heat shock protein 4	7	1.32	25.6	3;5;1	Hsp70 family chaperone
77	Cntn1	contactin 1	11	1.32	12.9	8;9;-	immunoglobulin receptor superfamily, protein phosphatase, immunoglobulin superfamily cell adhesion molecule
78	Uqcrb	ubiquinol-cytochrome c reductase binding protein	5	1.31	15.1	6;6;4	reductase
79	Vcp	valosin containing protein	21	1.31	8.6	15;17;6	ADP / ATP binding, ATPase activity*
80	Lsamp	limbic system-associated membrane protein	5	1.31	14.7	2;1;1	immunoglobulin superfamily cell adhesion molecule
81	Anxa6	annexin A6	5	1.31	7.8	2;4;-	calcium ion binding, calcium-dependent phospholipid binding*
82	Pdha1	pyruvate dehydrogenase E1 alpha 1	15	-1.30	22	10;11;9	dehydrogenase
83	Atp2b2	ATPase, Ca++ transporting, plasma membrane 2	9	-1.31	5.8	5;8;2	cation transporter, ion channel, hydrolase
84	Atp2a2	ATPase, Ca++ transporting, cardiac muscle, slow twitch 2	9	-1.31	11	6;5;2	cation transporter, ion channel, hydrolase
85	Atp2b3	ATPase, Ca++ transporting, plasma membrane 3	8	-1.31	14.4	1;7;-	cation transporter, ion channel, hydrolase
86	Gpi1	glucose phosphate isomerase 1	8	-1.31	16.5	15;16;7	phosphatidylinositol N-acetylglucosaminyltransferase activity*
87	Sv2a	synaptic vesicle glycoprotein 2 a	6	-1.31	28.0	3;3;2	transfer / carrier protein
88	Uqcrfs1	ubiquinol-cytochrome c reductase, Rieske iron-sulfur polypeptide 1	8	-1.31	15.2	6;11;8	reductase
89	Pfkm	phosphofructokinase, muscle	10	-1.31	0.7	1;5;-	carbohydrate kinase
90	Aldh5a1	aldhehyde dehydrogenase family 5, subfamily A1	8	-1.32	19.6	6;8;3	dehydrogenase
91	Slc25a22	solute carrier family 25 (mitochondrial carrier, glutamate), member 22	7	-1.32	15.7	5;2;1	amino acid transporter, mitochondrial carrier protein, transfer / carrier protein, calmodulin
92	Gpd1	glycerol-3-phosphate dehydrogenase 1 (soluble)	2	-1.32	13.4	1;1;-	dehydrogenase
93	Fkbp1a	FK506 binding protein 1a	5	-1.32	8.4	3;4;2	isomerase, chaperone, calcium-binding protein
94	Cadps	Ca2+-dependent secretion activator	15	-1.32	23.2	16;16;5	calcium-binding protein
95	Slc25a12	solute carrier family 25 (mitochondrial carrier, Aralar), member 12	20	-1.32	24.8	7;14;4	amino acid transporter, mitochondrial carrier protein, transfer / carrier protein, calmodulin
96	Gpm6a	glycoprotein m6a	3	-1.33	25.9	3;4;2	myelin protein
97	Hspd1	heat shock protein 1 (chaperonin)	10	-1.34	16.0	11;14;6	chaperonin
98	Arpc4	actin related protein 2/3 complex, subunit 4	6	-1.34	20	6;7;3	actin family cytoskeletal protein
99	Tspan7	tetraspanin 7	2	-1.36	2.9	1;1;-	membrane-bound signaling molecule, receptor, cell adhesion molecule
100	Atp5k	ATP synthase, H+ transporting, mitochondrial F1F0 complex, subunit e	5	-1.36	21.1	2;6;5	ATPase activity, hydrogen ion transmembrane transporter activity*

101	Cct7	chaperonin containing Tcp1, subunit 7 (eta)	3	-1.36	22.4	2;2;-	chaperonin
102	Uqcrc2	ubiquinol cytochrome c reductase core protein 2	12	-1.37	7.1	16;11;10	metalloprotease, reductase, esterase
103	Ran	RAN, member RAS oncogene family	3	-1.37	16.8	2;1;3	small GTPase
104	Dlst	dihydrolipoamide S-succinyltransferase (E2 component of 2-oxo-glutarate complex)	5	-1.37	11.6	7;8;5	acetyltransferase, acyltransferase
105	Ndufs7	NADH dehydrogenase (ubiquinone) Fe-S protein 7	4	-1.38	15.4	4;2;2	dehydrogenase, reductase
106	Atp6v0d1	ATPase, H+ transporting, lysosomal V0 subunit D1	4	-1.38	11.6	4;4;6	ATP synthase, hydrolase
107	Ldhb	lactate dehydrogenase B	2	-1.38	8.0	4;4;4	dehydrogenase
108	Pgam1	phosphoglycerate mutase 1	6	-1.39	20.0	5;9;4	phosphoglycerate mutase activity, bisphosphoglycerate mutase activity*
109	Ctnnd2	catenin (cadherin associated protein), delta 2	9	-1.39	10.8	1;2;-	intermediate filament binding protein, cell junction protein, cell adhesion molecule
110	Grin1	glutamate receptor, ionotropic, NMDA1 (zeta 1)	11	-1.41	29.2	2;4;1	ionotropic glutamate receptor
111	Syt1	synaptotagmin I	2	-1.41	20.7	4;2;2	membrane trafficking regulatory protein
112	Ndufa1	NADH dehydrogenase (ubiquinone) 1 alpha subcomplex,	2	-1.41	19.2	1;1;1	mitochondrial NADH dehydrogenase activity*
113	Aldh6a1	aldehyde dehydrogenase family 6, subfamily A1	6	-1.41	21.7	4;5;-	dehydrogenase
114	Tubb4a	tubulin, beta 4A class IVA	2	-1.42	28.9	2;5;1	tubulin
115	Cacng8	calcium channel, voltage-dependent, gamma subunit 8	2	-1.42	4.5	3;3;-	voltage-gated calcium / ion channel
116	Baiap2	brain-specific angiogenesis inhibitor 1-associated protein 2	4	-1.43	7	2;2;-	receptor
117	Arl6ip5	ADP-ribosylation factor-like 6 interacting protein 5	3	-1.45	6.7	1;1;-	amino acid transporter
118	Slc4a4	solute carrier family 4 (anion exchanger), member 4	4	-1.46	25.2	1;3;-	cation transporter
119	Tmx2	thioredoxin-related transmembrane protein 2	4	-1.49	14.3	2;2;-	membrane protein*
120	Gnao1	guanine nucleotide binding protein, alpha O	9	-1.49	8.1	11;15;6	heterotrimeric G-protein
121	Rab6a	RAB6A, member RAS oncogene family	2	-1.49	14.2	1;1;-	ATPase activity, GTP binding, GTPase activity*
122	Fam126b	family with sequence similarity 126, member B	4	-1.49	28.1	1;1;-	-
123	Atp5a1	ATP synthase, H+ transporting, mitochondrial F1 complex, alpha subunit 1	19	-1.50	15.2	33;56;63	ATP synthase, anion channel, ligand-gated ion channel. DNA binding protein, hydrolase
124	Coq9	coenzyme Q9 homolog (yeast)	3	-1.50	14.7	1;-;1	coenzyme Q9 biosynthesis*
125	Ndufb10	NADH dehydrogenase (ubiquinone) 1 beta subcomplex, 10	6	-1.53	28.8	1;1;7	mitochondrial NADH dehydrogenase activity*
126	Gnai1	guanine nucleotide binding protein (G protein), alpha inhibiting 1	5	-1.55	10.4	2;4;-	heterotrimeric G-protein
127	Srgap3	SLIT-ROBO Rho GTPase activating protein 3	10	-1.56	8.0	1;1;-	G-protein modulator
128	Ap2s1	adaptor-related protein complex 2, sigma 1 subunit	2	-1.57	9.0	1;1;1	vesicle coat protein
129	Atp6v0a1	ATPase, H+ transporting, lysosomal V0 subunit A1	12	-1.58	18.7	7;8;6	ATP synthase, hydrolase
130	Psmb2	proteasome (prosome, macropain) subunit, beta type 2	5	-1.58	2.8	1;2;-	protease
131	Atp5h	ATP synthase, H+ transporting, mitochondrial F0 complex, subunit d	2	-1.59	0.0	3;-;3	mitochondrial ATP synthase*
132	Sfxn3	sideroflexin 3	8	-1.61	25.3	1;3;-	cation transporter, transfer / carrier protein
133	Oxct1	3-oxoacid CoA transferase 1	6	-1.61	21.1	6;7;3	transferse
134	Atp6v1h	ATPase, H+ transporting, lysosomal V1 subunit H	6	-1.61	25.4	2;2;-	ATP synthase, hydrolase
135	Idh3b	isocitrate dehydrogenase 3 (NAD+) beta	6	-1.62	24.0	5;6;2	dehydrogenase
136	Cand1	cullin associated and neddylation disassociated 1	8	-1.62	29.0	4;4;-	transcription factor
137	Dnajc5	DnaJ (Hsp40) homolog, subfamily C, member 5	2	-1.63	4.7	1;1;-	chaperone
138	Atp1a2	ATPase, Na+/K+ transporting, alpha 2 polypeptide	13	-1.64	22.4	6;7;10	cation transporter, ion channel, hydrolase
139	Sept2	septin 2	3	-1.64	3.9	1;1;-	small GTPase, cytoskeletal protein
140	Chchd3	coiled-coil-helix-coiled-coil-helix domain containing 3	4	-1.64	10.6	3;1;2	protein complex scaffold, mitochondrial crista integrity and function*
141	Gna11	guanine nucleotide binding protein, alpha 11	2	-1.65	12.0	1;1;-	heterotrimeric G-protein

142	Ndufa10	NADH dehydrogenase (ubiquinone) 1 alpha subcomplex 10	6	-1.65	25.1	2;3;3	nucleotide kinase
143	Vps35	vacuolar protein sorting 35	7	-1.65	1.2	1;2;-	membrane traffic protein
144	Glud1	glutamate dehydrogenase 1	11	-1.66	22.2	11;18;8	dehydrogenase
145	Nt5dc3	5'-nucleotidase domain containing 3	4	-1.66	23.6	2;2;-	nucleotide phosphatase
146	Glul	glutamate-ammonia ligase (glutamine synthetase)	10	-1.69	23.9	11;14;10	ligase
147	Dlgap2	discs, large (Drosophila) homolog-associated protein 2	4	-1.72	17.0	2;2;-	transmembrene receptor regulatory / adaptor protein
148	Tuba1a	tubulin, alpha 1A	5	-1.72	26.8	17;15;6	tubulin
149	Slc1a2	solute carrier family 1 (glial high affinity glutamate transporter), member 2	3	-1.73	14.8	6;4;2	cation transporter
150	Rab2a	RAB2A, member RAS oncogene family	4	-1.73	4.3	2;2;-	GDP binding, GTP binding, GTPase activity*
151	Nnt	nicotinamide nucleotide transhydrogenase	2	-1.74	7.7	1;1;-	dehydrogenase
152	Pdhb	pyruvate dehydrogenase (lipoamide) beta	4	-1.76	5.7	3;4;1	transketolase, dehydrogenase, lyase
153	Vamp2	vesicle-associated membrane protein 2	4	-1.78	21.5	4;4;5	SNARE protein
154	Atp5o	ATP synthase, H+ transporting, mitochondrial F1 complex, O subunit	6	-1.79	25.8	11;11;10	ATP synthase, hydrolase
155	Rab35	RAB35, member RAS oncogene family	2	-1.86	4.7	2;3;-	GDP binding, GTP binding, GTPase activity*
156	Rab11b	RAB11B, member RAS oncogene family	5	-1.87	4.1	3;3;2	GDP binding, GTP binding, GTPase activity*
156	Rab11b	RAB11B, member RAS oncogene family	5	-1.87	4.1	3;3;2	GDP binding, GTP binding, GTPase activity*
157	Gdi2	guanosine diphosphate (GDP) dissociation inhibitor 2	4	-1.88	4.9	2;2;-	acyltransferase, G-protein modulator
158	Mosc2	MOCO sulphurase C-terminal domain containing 2	4	-1.90	19.7	3;1;-	mitochondrial nitrate reductase activity*
159	Rac1	RAS-related C3 botulinum substrate 1	3	-1.94	25.3	7;5;7	small GTPase
160	Atp5b	ATP synthase, H+ transporting mitochondrial F1 complex, beta subunit	12	-1.94	23.1	7;10;3	ATP synthase, anion channel, ligand-gated ion channel. DNA binding protein, hydrolase
161	Mog	myelin oligodendrocyte glycoprotein	7	-1.98	27.0	1;3;2	ubiquitin-protein ligase
162	Nckap1	NCK-associated protein 1	6	-2.03	2.2	3;4;-	lamellipodium, lamellipodium membrane, actin filament reorganization*
163	Dlat	dihydrolipoamide S-acetyltransferase (E2 component of pyruvate dehydrogenase complex)	3	-2.10	14.2	2;5;-	acetyltransferase, acyltransferase
164	Cnp	2',3'-cyclic nucleotide 3' phosphodiesterase	9	-2.15	23.8	14;13;11	phosphodiesterase
165	Ndufa9	NADH dehydrogenase (ubiquinone) 1 alpha subcomplex, 9	11	-2.18	21.0	3;5;-	dehydrogenase, reductase
166	Fam49b	family with sequence similarity 49, member B	3	-2.21	28.8	1;2;-	-
167	Prkacb	protein kinase, cAMP dependent, catalytic, beta	5	-2.28	2.2	3;3;-	non-receptor serine / threonine protein kinase
168	Cyfip2	cytoplasmic FMR1 interacting protein 2	6	-2.95	1.0	2;4;-	G-protein modulator

Table 35: List of mRNAs quantified via the RT^2 Profiler arrays "PI3k/Akt signalling pathway", "synaptic plasticity" and "circadian rhythm".

Highlighted mRNAs: turquoise – membrane receptors; red: circadian clock; green: Circadian regulated transcription factors and circadian regulated genes. They are grouped according to manufacturer´s information and uniprot-database.

UniGene	RefSeq	Symbol	Description	Gene Name
Mm.42233	NM_009591	Aanat	Arylalkylamine N-acetyltransferase	AA-NAT, MGC151344, Nat-2, Nat4, Snat
Mm.328431	NM_007393	Actb	Actin, beta	Actx, E430023M04Rik, beta-actin
Mm.3037	NM_007399	Adam10	A disintegrin and metallopeptidase domain 10	1700031C13Rik, MADM, kuz, kuzbanian
Mm.316628	NM_019655	Adar	Adenosine deaminase, RNA-specific	AV242451, Adar1, mZaADAR
Mm.259733	NM_009622	Adcy1	Adenylate cyclase 1	AC1, D11Bwg1392e, I-AC, KIAA4070, brl, mKIAA4070
Mm.1425	NM_009623	Adcy8	Adenylate cyclase 8	AC8, AW060868
Mm.6645	NM_009652	Akt1	Rac-alpha serine / threonine protein kinase	Akt, PKB, PKB, Akt, PKBalpha, Rac
Mm.177194	NM_007434	Akt2	Rac-beta serine / threonine protein kinase	2410016A19Rik, AW554154, MGC14031, PKB, PKBbeta
Mm.235194	NM_011785	Akt3	Rac-gamma serine / threonine protein kinase	AI851531, D930002M15Rik, Nmf350
Mm.290578	NM_020559	Alas1	Aminolevulinic acid synthase 1	ALAS, ALAS-N, Alas-1, Alas-h
Mm.384171	NM_007462	Apc	Adenomatosis polyposis coli	AI047805, AU020952, AW124434, CC1, Min, mAPC
Mm.25405	NM_018790	Arc	Activity regulated cytoskeletal-associated protein	Arc3.1, C86064, arg3.1
Mm.440371	NM_007489	Arntl	Aryl hydrocarbon receptor nuclear translocator-like	Arnt3, BMAL1b, Bmal1, MOP3, bHLHe5, bmal1b'
Mm.333500	NM_172309	Arntl2	Aryl hydrocarbon receptor nuclear translocator-like 2	4632430A05Rik, BMAL2, CLIF, MGC124257, MOP9, bHLHe6
Mm.163	NM_009735	B2m	Beta-2 microglobulin	Ly-m11, beta2-m, beta2m
Mm.4387	NM_007522	Bad	BCL2-associated agonist of cell death	AI325008, Bbc2

Mm.1442	NM_007540	Bdnf	Brain derived neurotrophic factor	-
Mm.2436	NM_011498	Bhlhe40	Basic helix-loop-helix family, member e40	Bhlhb2, C130042M06Rik, CR8, Clast5, Dec1, Sharp2, Stra13, Stra14
Mm.154529	NM_024469	Bhlhe41	Basic helix-loop-helix family, member e41	Bhlhb2l, Bhlhb3, DEC2, Sharp1
Mm.4475	NM_013482	Btk	Bruton agammaglobulinemia tyrosine kinase	AI528679, xid
Mm.131530	NM_177407	Camk2a	Calcium/calmodulin-dependent protein kinase II alpha	CaMKII, R74975, mKIAA0968
Mm.439733	NM_007595	Camk2b	Calcium/calmodulin-dependent protein kinase II, beta	Camk2d, MGC90738
Mm.255822	NM_023813	Camk2d	Calcium/calmodulin-dependent protein kinase II, delta	2810011D23Rik, 8030469K03Rik, KIAA4163, MGC60852, [d]-CaMKII, mKIAA4163
Mm.235182	NM_178597	Camk2g	Calcium/calmodulin-dependent protein kinase II gamma	5930429P18Rik, Camkg
Mm.75498	NM_013732	Cartpt	CART prepropeptide	Cart
Mm.88829	NM_015733	Casp9	Caspase 9	AI115399, AW493809, Caspase-9, ICE-LAP6, Mch6
Mm.273049	NM_007631	Ccnd1	Cyclin D1	AI327039, Cyl-1, PRAD1, bcl-1, cD1
Mm.86541	NM_009834	Ccrn4l	CCR4 carbon catabolite repression 4-like (S. cerevisiae)	AU043840, Ccr4, nocturnin
Mm.3460	NM_009841	Cd14	CD14 antigen	-
Mm.1022	NM_009861	Cdc42	Cell division cycle 42 homolog (S. cerevisiae)	AI747189, AU018915
Mm.257437	NM_007664	Cdh2	Cadherin 2	CDHN, N-cadherin, Ncad
Mm.2958	NM_009875	Cdkn1b	Cyclin-dependent kinase inhibitor 1B	AA408329, AI843786, Kip1, p27, p27Kip1
Mm.439656	NM_009883	Cebpb	CCAAT/enhancer binding protein (C/EBP), beta	C, EBPbeta, CRP2, IL-6DBP, LAP, LIP, NF-IL6, NF-M, Nfil6
Mm.347407	NM_007679	Cebpd	CCAAT/enhancer binding protein (C/EBP), delta	-

Mm.35088	NM_009602	Chrnb2	Cholinergic receptor, nicotinic, beta polypeptide 2 (neuronal)	Acrb-2, Acrb2, C030030P04Rik, [b]2-nAchR
Mm.3996	NM_007700	Chuk	Conserved helix-loop-helix ubiquitous kinase	AI256658, Chuk1, Fbx24, Fbxo24, IKBKA, IKK1, Ikka, MGC25325, NFKBIKA
Mm.3552	NM_007715	Clock	Circadian locomotor output cycles kaput	5330400M04Rik, KAT13D, bHLHe8, mKIAA0334
Mm.7992	NM_007726	Cnr1	Cannabinoid receptor 1 (brain)	CB-R, CB1, CB1R
Mm.453295	NM_133828	Creb1	CAMP responsive element binding protein 1	2310001E10Rik, 3526402H21Rik, AV083133, Creb, Creb-1
Mm.12407	NM_013497	Creb3	CAMP responsive element binding protein 3	AU044960, AW538053, C80076, LZIP, LZIP-1, LZIP-2, Luman
Mm.5244	NM_013498	Crem	CAMP responsive element modulator	ICER
Mm.441911	NM_007770	Crx	Cone-rod homeobox containing gene	Crx1
Mm.26237	NM_007771	Cry1	Cryptochrome 1 (photolyase-like)	AU020726, AU021000, Phll1
Mm.254181	NM_009963	Cry2	Cryptochrome 2 (photolyase-like)	AV006279, D130054K12Rik
Mm.26908	NM_146087	Csnk1a1	Casein kinase 1, alpha 1	2610208K14Rik, 4632404G05Rik, 5430427P18Rik, CK1a, Csnk1a, MGC29354, MGC30571
Mm.216227	NM_139059	Csnk1d	Casein kinase 1, delta	1200006A05Rik, AA409348, D930010H05Rik
Mm.30199	NM_013767	Csnk1e	Casein kinase 1, epsilon	AI426939, AI551861, AW457082, CK1epsilon, CKIe, KC1epsilon, tau
Mm.23692	NM_007788	Csnk2a1	Casein kinase 2, alpha 1 polypeptide	Csnk2a1-rs4, MGC102141
Mm.440348	NM_009974	Csnk2a2	Casein kinase 2, alpha prime polypeptide	1110035J23Rik, C77789, CK2
Mm.291928	NM_007614	Ctnnb1	Catenin (cadherin associated protein), beta 1	Bfc, Catnb, Mesc
Mm.378235	NM_016974	Dbp	D site albumin promoter binding protein	-
Mm.27256	NM_007864	Dlg4	Discs, large homolog 4 (Drosophila)	Dlgh4, PSD-95, PSD95, SAP90, SAP90A

Mm.181959	NM_007913	Egr1	Early growth response 1	A530045N19Rik, ETR103, Egr-1, Krox-1, Krox-24, Krox24, NGF1-A, NGFI-A, NGFIA, TIS8, Zenk, Zfp-6, Zif268, egr
Mm.290421	NM_010118	Egr2	Early growth response 2	Egr-2, Krox-20, Krox20, NGF1-B, Zfp-25, Zfp-6
Mm.103737	NM_018781	Egr3	Early growth response 3	MGC124006, MGC124009, Pilot
Mm.44137	NM_020596	Egr4	Early growth response 4	NGF1-C, NGFI-C, NGFIC, pAT133
Mm.378990	NM_011163	Eif2ak2	Eukaryotic translation initiation factor 2-alpha kinase 2	2310047A08Rik, 4732414G15Rik, AI467567, AI747578, Pkr, Prkr, Tik
Mm.290022	NM_145625	Eif4b	Eukaryotic translation initiation factor 4B	2310046H11Rik, AL024095, C85189, Eif4a2
Mm.3941	NM_007917	Eif4e	Eukaryotic translation initiation factor 4E	EG668879, Eif4e-ps, If4e, MGC103177, eIF-4E
Mm.6700	NM_007918	Eif4ebp 1	Eukaryotic translation initiation factor 4E binding protein 1	4e-bp1, AA959816, PHAS-I
Mm.260256	NM_001005 331	Eif4g1	Eukaryotic translation initiation factor 4, gamma 1	E030015G23Rik, MGC37551, MGC90776, eIF4GI
Mm.405823	NM_007922	Elk1	ELK1, member of ETS oncogene family	Elk-1
Mm.250981	NM_010142	Ephb2	Eph receptor B2	Cek5, Drt, ETECK, Erk, Hek5, Nuk, Prkm5, Qek5, Sek3, Tyro5
Mm.349116	NM_007942	Epo	Erythropoietin	-
Mm.386776	NM_007953	Esrra	Estrogen related receptor, alpha	ERRalpha, Err1, Estrra, Nr3b1
Mm.3355	NM_010177	Fasl	Fas ligand (TNF superfamily, member 6)	APT1LG1, CD178, CD95-L, CD95L, Fas-L, Faslg, Tnfsf6, gld
Mm.233904	NM_178674	Fbxl21	F-box and leucine-rich repeat protein 21	D630045D17Rik, FBL3B, FBXL3B
Mm.214746	NM_015822	Fbxl3	F-box and leucine-rich repeat protein 3	AU041772, AW212966, FBK, Fbl3a, Fbxl3a, Ovtm
Mm.278458	NM_008019	Fkbp1a	FK506 binding protein 1a	12kDa, FKBP12, FKBP12-T1, FKBP12-T2, Fkbp, Fkbp1, mFKBP1, mFKBP12
Mm.246513	NM_010234	Fos	c-Fos transcription factor	D12Rfj1, c-fos, cFos
Mm.29891	NM_019739	Foxo1	Forkhead box O1	AI876417, Afxh, FKHR, Fkhr1, Foxo1a

Mm.338613	NM_019740	Foxo3	Forkhead box O3	1110048B16Rik, 2010203A17Rik, C76856, FKHRL1, Fkhr2, Foxo3a
Mm.273114	NM_176942	Gabra5	Gamma-aminobutyric acid (GABA) A receptor, subunit alpha 5	A230018I05Rik
Mm.343110	NM_008084	Gapdh	Glyceraldehyde-3-phosphate dehydrogenase	Gapd, MGC102544, MGC102546, MGC103190, MGC103191, MGC105239
Mm.378921	NM_010288	Gja1	Gap junction protein, alpha 1	AU042049, AW546267, Cnx43, Cx43, Cx43alpha1, Gja-1, Npm1, connexin43
Mm.254629	NM_010305	Gnai1	Guanine nucleotide binding protein (G protein), alpha inhibiting 1	AU046200, Gialpha1, Gnai-1
Mm.273117	NM_010345	Grb10	Growth factor receptor bound protein 10	5730571D09Rik, AI325020, Meg1, mKIAA0207
Mm.439649	NM_008163	Grb2	Growth factor receptor bound protein 2	AA408164, Ash
Mm.4920	NM_008165	Gria1	Glutamate receptor, ionotropic, AMPA1 (alpha 1)	2900051M01Rik, AI853806, Glr-1, Glr1, GluA1, GluR-A, GluRA, Glur-1, Glur1, HIPA1
Mm.220224	NM_013540	Gria2	Glutamate receptor, ionotropic, AMPA2 (alpha 2)	GluA2, GluR-B, Glur-2, Glur2
Mm.327681	NM_016886	Gria3	Glutamate receptor, ionotropic, AMPA3 (alpha 3)	2900064I19Rik, GluA3, GluR-C, GluR-K3, Glur-3, Glur3, Gluralpha3, KIAA4184, mKIAA4184
Mm.209263	NM_019691	Gria4	Glutamate receptor, ionotropic, AMPA4 (alpha 4)	GluA4, GluR-D, Glur-4, Glur4, Gluralpha4, spkw1
Mm.278672	NM_008169	Grin1	Glutamate receptor, ionotropic, NMDA1 (zeta 1)	GluRdelta1, GluRzeta1, M100174, NMDAR1, NR1, Nmdar, Rgsc174
Mm.2953	NM_008170	Grin2a	Glutamate receptor, ionotropic, NMDA2A (epsilon 1)	GluN2A, NMDAR2A, NR2A
Mm.436649	NM_008171	Grin2b	Glutamate receptor, ionotropic, NMDA2B (epsilon 2)	AW490526, NR2B, Nmdar2b
Mm.39090	NM_010350	Grin2c	Glutamate receptor, ionotropic, NMDA2C (epsilon 3)	NMDAR2C, NR2C

Mm.322594	NM_008172	Grin2d	Glutamate receptor, ionotropic, NMDA2D (epsilon 4)	GluN2D, NMDAR2D, NR2D
Mm.196692	NM_133442	Grip1	Glutamate receptor interacting protein 1	4931400F03Rik, KIAA4223, eb, mKIAA4223
Mm.391904	NM_016976	Grm1	Glutamate receptor, metabotropic 1	4930455H15Rik, ENSMUSG00000075319, Gm10828, Gprc1a, MGC90744, mGluR1, nmf373, rcw, wobl
Mm.410822	NM_001160353	Grm2	Glutamate receptor, metabotropic 2	4930441L02Rik, Gprc1b, mGluR2, mGluR7
Mm.318966	NM_181850	Grm3	Glutamate receptor, metabotropic 3	0710001G23Rik, Gprc1c, mGlu3, mGluR3
Mm.358940	NM_001013385	Grm4	Glutamate receptor, metabotropic 4	Gprc1d, mGluR4
Mm.235018	NM_001081414	Grm5	Glutamate receptor, metabotropic 5	6430542K11Rik, AI850523, Gprc1e, mGluR5, mGluR5b
Mm.240881	NM_177328	Grm7	Glutamate receptor, metabotropic 7	6330570A01Rik, BB176677, C030018L03, E130018M02Rik, Gpr1g, Gprc1g, MGC90857, mGluR7
Mm.320732	NM_008174	Grm8	Glutamate receptor, metabotropic 8	A230002O04, Gprc1h, mGluR8
Mm.394930	NM_019827	Gsk3b	Glycogen synthase kinase 3 beta	7330414F15Rik, 8430431H08Rik, C86142, GSK-3, GSK-3beta, GSK3
Mm.3317	NM_010368	Gusb	Glucuronidase, beta	AI747421, Gur, Gus, Gus-r, Gus-s, Gus-t, Gus-u, Gut, asd, g
Mm.378937	NM_013546	Hebp1	Heme binding protein 1	Hebp
Mm.158903	NM_172563	Hlf	Hepatic leukemia factor	E230015K02Rik
Mm.37533	NM_152134	Homer1	Homer homolog 1 (Drosophila)	PSD-Zip45, SYN47, Ves-1
Mm.299381	NM_013556	Hprt	Hypoxanthine guanine phosphoribosyl transferase	C81579, HPGRT, Hprt1, MGC103149
Mm.334313	NM_008284	Hras1	GTPase Hras	H-ras, Ha-ras, Harvey-ras, Hras-1, Kras2, c-H-ras, c-Ha-ras, c-rasHa, ras
Mm.2180	NM_008302	Hsp90ab1	Heat shock protein 90 alpha (cytosolic), class B member 1	90kDa, AL022974, C81438, Hsp84, Hsp84-1, Hsp90, Hspcb, MGC115780
Mm.13849	NM_013560	Hspb1	Heat shock protein 1	27kDa, Hsp25

Mm.254266	NM_008315	Htr7	5-hydroxytryptamine (serotonin) receptor 7	5-HT7, MGC151363
Mm.268521	NM_010512	Igf1	Insulin-like growth factor 1	C730016P09Rik, Igf-1, Igf-I
Mm.275742	NM_010513	Igf1r	Insulin-like growth factor I receptor	A330103N21Rik, CD221, D930020L01, IGF-1R, hyft
Mm.274846	NM_010562	Ilk	Integrin linked kinase	AA511515, ESTM24
Mm.8042	NM_008380	Inhba	Inhibin beta-A	-
Mm.38241	NM_008363	Irak1	Interleukin-1 receptor-associated kinase 1	AA408924, IRAK, IRAK-1, IRAK1-S, Il1rak, Plpk, mPLK
Mm.105218	NM_008390	Irf1	Interferon regulatory factor 1	AU020929, Irf-1
Mm.4952	NM_010570	Irs1	Insulin receptor substrate 1	G972R, IRS-1
Mm.263396	NM_010578	Itgb1	Integrin beta 1 (fibronectin receptor beta)	4633401G24Rik, AA409975, AA960159, CD29, ENSMUSG00000051907, Fnrb, Gm9863, gpIIa
Mm.275071	NM_010591	Jun	Jun transcription factor	AP-1, Junc, c-jun
Mm.1167	NM_008416	Junb	Jun-B transcription factor	-
Mm.343607	NM_010610	Kcnma1	Potassium large conductance calcium-activated channel, subfamily M, alpha member 1	5730414M22Rik, BKCa, MaxiK, Slo, Slo1, mSlo, mSlo1
Mm.347452	NM_010623	Kif17	Kinesin family member 17	5930435E01Rik, AW492270, Kif17b, mKIAA1405
Mm.4292	NM_013692	Klf10	Kruppel-like factor 10	AI115143, EGR[a], Egral, Gdnfif, Tieg, Tieg1, mGIF
Mm.248907	NM_008927	Map2k1	Mitogen-activated protein kinase kinase 1	MAPKK1, MEKK1, Mek1, Prkmk1
Mm.196581	NM_011949	Mapk1	Mitogen-activated protein kinase 1	9030612K14Rik, AA407128, AU018647, C78273, ERK, Erk2, MAPK2, PRKM2, Prkm1, p41mapk, p42mapk
Mm.311337	NM_011951	Mapk14	Mitogen-activated protein kinase 14	CSBP2, Crk1, Csbp1, MGC102436, Mxi2, PRKM14, PRKM15, p38, p38-alpha, p38MAPK, p38a, p38alpha
Mm.8385	NM_011952	Mapk3	Mitogen-activated protein kinase 3	Erk-1, Erk1, Ert2, Esrk1, Mnk1, Mtap2k, Prkm3, p44, p44erk1, p44mapk
Mm.21495	NM_016700	Mapk8	Mitogen-activated protein kinase 8	AI849689, JNK, JNK1, Prkm8, SAPK1

Mm.29815	NM_145569	Mat2a	Methionine adenosyltransferase II, alpha	D630045P18Rik, MGC6545
Mm.4406	NM_013599	Mmp9	Matrix metallopeptidase 9	AW743869, B, MMP9, Clg4b, MMP-9, pro-MMP-9
Mm.16366	NM_010839	Mtcp1	Mature T-cell proliferation 1	-
Mm.5133	NM_008639	Mtnr1a	Melatonin receptor 1A	MGC151277, MR, MelR
Mm.222631	NM_145712	Mtnr1b	Melatonin receptor 1B	MGC129286, MGC129287, Mel-1B-R, Mel1b, Mt2
Mm.21158	NM_020009	Mtor	Mechanistic target of rapamycin (serine/threonine kinase)	2610315D21Rik, AI327068, FRAP, FRAP2, Frap1, MGC118056, RAFT1, RAPT1, flat
Mm.213003	NM_010851	Myd88	Myeloid differentiation primary response gene 88	-
Mm.1526	NM_010866	Myod1	Myogenic differentiation 1	AI503393, MYF3, MyoD, Myod-1, bHLHc1
Mm.4974	NM_010875	Ncam1	Neural cell adhesion molecule 1	CD56, E-NCAM, NCAM-1, Ncam
Mm.476883	NM_008679	Ncoa3	Nuclear receptor coactivator 3	2010305B15Rik, AW321064, Actr, Aib1, KAT13B, Rac3, Src3, Tram-1, Tram1, bHLHe42, p, Cip, pCip
Mm.136604	NM_017373	Nfil3	Nuclear factor, interleukin 3, regulated	AV225605, E4BP4
Mm.256765	NM_008689	Nfkb1	Nuclear factor of kappa light polypeptide gene enhancer in B-cells 1, p105	NF-KB1, NF-kappaB, NF-kappaB1, p105, p50, p50, p105
Mm.170515	NM_010907	Nfkbia	Nuclear factor of kappa light polypeptide gene enhancer in B-cells inhibitor, alpha	AI462015, Nfkbi
Mm.220333	NM_010908	Nfkbib	Nuclear factor of kappa light polypeptide gene enhancer in B-cells inhibitor, beta	IKB-beta, IKappaBbeta, IkB, IkBb, MGC36057
Mm.1259	NM_013609	Ngf	Nerve growth factor	Ngfb
Mm.283893	NM_033217	Ngfr	Nerve growth factor receptor (TNFR superfamily, member 16)	LNGFR, Tnfrsf16, p75, p75NGFR, p75NTR

Mm.41974	NM_008700	Nkx2-5	NK2 transcription factor related, locus 5 (Drosophila)	Csx, Nkx-2.5, Nkx2.5, tinman
Mm.333709	NM_001011684	Nms	Neuromedin S	AB164466
Mm.44249	NM_008712	Nos1	Nitric oxide synthase 1, neuronal	2310005C01Rik, NO, NOS-I, Nos-1, bNOS, nNOS
Mm.2380	NM_008719	Npas2	Neuronal PAS domain protein 2	MGC129355, MOP4, bHLHe9
Mm.10099	NM_016789	Nptx2	Neuronal pentraxin 2	Narp, np2
Mm.390397	NM_145434	Nr1d1	Nuclear receptor subfamily 1, group D, member 1	A530070C09Rik, R75201
Mm.26587	NM_011584	Nr1d2	Nuclear receptor subfamily 1, group D, member 2	RVR, Rev-erb
Mm.28989	NM_010150	Nr2f6	Nuclear receptor subfamily 2, group F, member 6	AV090102, COUP-TF3, EAR2, Erbal2
Mm.119	NM_010444	Nr4a1	Nuclear receptor subfamily 4, group A, member 1	GFRP1, Gfrp, Hbr-1, Hbr1, Hmr, N10, NGFI-B, NGFIB, NP10, TIS1, TR3, nur77
Mm.267570	NM_008742	Ntf3	Neurotrophin 3	AI316846, AI835689, Nt3, Ntf-3
Mm.20344	NM_198190	Ntf5	Neurotrophin 5	2900040K06Rik, AI462899, NT-4, NT4, NT4, 5, Ntf-5, Ntf4
Mm.130054	NM_008745	Ntrk2	Neurotrophic tyrosine kinase, receptor, type 2	AI848316, C030027L06Rik, Tkrb, trkB
Mm.32744	NM_010098	Opn3	Opsin 3	ERO, Ecpn, MGC124138, panopsin
Mm.103670	NM_013887	Opn4	Opsin 4 (melanopsin)	1110007J02Rik, Gm533
Mm.371570	NM_008774	Pabpc1	Poly(A) binding protein, cytoplasmic 1	PABP, Pabp1, PabpI, Pabpl1, ePAB
Mm.260227	NM_011035	Pak1	P21 protein (Cdc42/Rac)-activated kinase 1	AW045634, PAK-1, Paka
Mm.8026	NM_011038	Pax4	Paired box gene 4	Pax-4
Mm.390715	NM_021543	Pcdh8	Protocadherin 8	1700080P15Rik, Papc
Mm.221403	NM_011058	Pdgfra	Platelet derived growth factor receptor, alpha polypeptide	AI115593, CD140a, Pdgfr-2
Mm.34411	NM_172665	Pdk1	Pyruvate dehydrogenase kinase, isoenzyme 1	B830012B01, D530020C15Rik

Mm.29768	NM_133667	Pdk2	Pyruvate dehydrogenase kinase, isoenzyme 2	-
Mm.10504	NM_011062	Pdpk1	3-phosphoinositide dependent protein kinase 1	Pdk1
Mm.7373	NM_011065	Per1	Period homolog 1 (Drosophila)	MGC102121, Per, m-rigui, mPer1
Mm.482463	NM_011066	Per2	Period homolog 2 (Drosophila)	mKIAA0347, mPer2
Mm.121361	NM_011067	Per3	Period homolog 3 (Drosophila)	2810049O06Rik, mPer3
Mm.259464	NM_008837	Pick1	Protein interacting with C kinase 1	Prkcabp
Mm.260521	NM_008839	Pik3ca	Phosphatidylinositol 3-kinase, catalytic, alpha polypeptide	6330412C24Rik, MGC161268, caPI3K, p110, p110alpha
Mm.101369	NM_020272	Pik3cg	Phosphoinositide-3-kinase, catalytic, gamma polypeptide	5830428L06Rik, PI3Kgamma, p110gamma
Mm.259333	NM_001024955	Pik3r1	Phosphatidylinositol 3-kinase, regulatory subunit, polypeptide 1 (p85 alpha)	AA414921, C530050K14, PI3K, p50alpha, p55alpha, p85alpha
Mm.12945	NM_008841	Pik3r2	Phosphatidylinositol 3-kinase, regulatory subunit, polypeptide 2 (p85 beta)	p85beta
Mm.405293	NM_008842	Pim1	Serine/threonine-protein kinase pim-1	Pim-1
Mm.154660	NM_008872	Plat	Plasminogen activator, tissue	AU020998, AW212668, D8Ertd2e, MGC18508, tPA
Mm.44463	NM_021280	Plcg1	Phospholipase C, gamma 1	AI894140, Cded, Plc-1, Plc-gamma1, Plcg-1
Mm.245261	NM_198934	Pou2f1	POU domain, class 2, transcription factor 1	2810482H01Rik, Oct-1, Oct1, Otf-1, Otf1
Mm.212789	NM_011144	Ppara	Peroxisome proliferator activated receptor alpha	4933429D07Rik, AW742785, Nr1c1, PPAR-alpha, PPARalpha, Ppar
Mm.259072	NM_008904	Ppargc1a	Peroxisome proliferative activated receptor, gamma, coactivator 1 alpha	A830037N07Rik, ENSMUSG00000079510, Gm11133, PGC-1, PGC-1v, Pgc-1alpha, Pgc1, Pgco1, Ppargc1
Mm.1970	NM_031868	Ppp1ca	Protein phosphatase 1, catalytic subunit, alpha isoform	Ppp1c, dism2

Mm.280784	NM_013636	Ppp1cc	Protein phosphatase 1, catalytic subunit, gamma isoform	PP1, dis2m1
Mm.2343	NM_026731	Ppp1r14a	Protein phosphatase 1, regulatory (inhibitor) subunit 14A	1110001M11Rik, Cpi17
Mm.260288	NM_019411	Ppp2ca	Protein phosphatase 2 (formerly 2A), catalytic subunit, alpha isoform	PP2A, R75353
Mm.331389	NM_008913	Ppp3ca	Protein phosphatase 3, catalytic subunit, alpha isoform	2900074D19Rik, AI841391, AW413465, CN, Caln, Calna, CnA, MGC106804
Mm.240313	NM_011073	Prf1	Perforin 1 (pore forming protein)	Pfn, Pfp, Prf-1
Mm.19111	NM_008854	Prkaca	Protein kinase, cAMP dependent, catalytic, alpha	Cs, PKA, PKCD, Pkaca
Mm.16766	NM_011100	Prkacb	Protein kinase, cAMP dependent, catalytic, beta	Pkacb
Mm.30039	NM_021880	Prkar1a	Protein kinase, cAMP dependent regulatory, type I, alpha	1300018C22Rik, RIalpha, Tse-1, Tse1
Mm.306163	NM_008923	Prkar1b	Protein kinase, cAMP dependent regulatory, type I beta	AI385716, RIbeta
Mm.253102	NM_008924	Prkar2a	Protein kinase, cAMP dependent regulatory, type II alpha	1110061A24Rik, AI317181, AI836829, RII(alpha)
Mm.25594	NM_011158	Prkar2b	Protein kinase, cAMP dependent regulatory, type II beta	AI451071, AW061005, Pkarb2, RII(beta)
Mm.222178	NM_011101	Prkca	Protein kinase C, alpha	AI875142, Pkca
Mm.207496	NM_008855	Prkcb	Protein kinase C, beta	A130082F03Rik, PKC-Beta, Pkcb, Prkcb1, Prkcb2
Mm.7980	NM_011102	Prkcc	Protein kinase C, gamma	MGC130440, PKCgamma, Pkcc, Prkcg
Mm.28561	NM_008860	Prkcz	Protein kinase C, zeta	AI098070, C80388, Pkcz, R74924, aPKCzeta, zetaPKC
Mm.381172	NM_011160	Prkg1	Protein kinase, cGMP-dependent, type I	AW125416, CGKI, MGC132849, Prkg1b, Prkgr1b
Mm.283777	NM_144944	Prokr2	Prokineticin receptor 2	B830005M06Rik, EG-VEGRF2, Gpcr73l1, Gpr73l1, PKR2
Mm.245395	NM_008960	Pten	Phosphatase and tensin homolog	2310035O07Rik, A130070J02Rik, AI463227, B430203M17Rik, MGC183880, MMAC1, TEP1

Mm.1008	NM_008963	Ptgds	Prostaglandin D2 synthase (brain)	21kDa, L-PGDS, PGD2, PGDS, PGDS2, Ptgs3
Mm.254494	NM_007982	Ptk2	PTK2 protein tyrosine kinase 2	FAK, FRNK, Fadk, KIAA4203, mKIAA4203
Mm.8681	NM_011202	Ptpn11	Protein tyrosine phosphatase, non-receptor type 11	2700084A17Rik, AW536184, PTP1D, PTP2C, SAP-2, SH-PTP2, SH-PTP3, SHP-2, Shp2, Syp
Mm.5083	NM_009001	Rab3a	Ras-related protein Rab-3A	-
Mm.292510	NM_009007	Rac1	RAS-related C3 botulinum substrate 1	AL023026, D5Ertd559e
Mm.184163	NM_029780	Raf1	RAF serine/threonine-protein kinase	6430402F14Rik, AA990557, BB129353, Craf1, D830050J10Rik, MGC102375, Raf-1, c-Raf, v-Raf
Mm.259653	NM_145452	Rasa1	RAS p21 protein activator 1	Gap, MGC7759, RasGAP, Rasa
Mm.235580	NM_011250	Rbl2	Retinoblastoma-like 2	Rb2, p130
Mm.249966	NM_009045	Rela	V-rel reticuloendotheliosis viral oncogene homolog A (avian)	p65
Mm.425236	NM_011261	Reln	Reelin	reeler, rl
Mm.28262	NM_009061	Rgs2	Regulator of G-protein signalling 2	GOS8
Mm.319175	NM_053075	Rheb	Ras homolog enriched in brain	-
Mm.757	NM_016802	Rhoa	Ras homolog gene family, member A	Arha, Arha1, Arha2
Mm.378450	NM_013646	Rora	RAR-related orphan receptor alpha	9530021D13Rik, Nr1f1, ROR1, ROR2, ROR3, nmf267, sg, staggerer, tmgc26
Mm.485649	NM_146095	Rorb	RAR-related orphan receptor beta	MGC38728, Nr1f2, RZR-beta, RZRB, Rorbeta
Mm.4372	NM_011281	Rorc	RAR-related orphan receptor gamma	Nr1f3, RORgamma, TOR, Thor
Mm.301827	NM_009097	Rps6ka1	Ribosomal protein S6 kinase polypeptide 1	Rsk1, p90rsk, rsk
Mm.394280	NM_028259	Rps6kb1	Ribosomal protein S6 kinase, polypeptide 1	2610318I15Rik, 4732464A07Rik, 70kDa, AA959758, AI256796, AI314060, S6K1, p70, 85s6k, p70s6k

Mm.86595	NM_011368	Shc1	Src homology 2 domain-containing transforming protein C1	Shc, ShcA, p66, p66shc
Mm.351459	NM_019812	Sirt1	Sirtuin 1 (silent mating type information regulation 2, homolog) 1 (S. cerevisiae)	AA673258, MGC150273, SIR2L1, Sir2, Sir2a, Sir2alpha
Mm.261564	NM_001081060	Slc9a3	Solute carrier family 9 (sodium/hydrogen exchanger), member 3	9030624O13Rik, AI930210, NHE-3, NHE3
Mm.100399	NM_008540	Smad4	MAD homolog 4 (Drosophila)	AW743858, D18Wsu70e, DPC4, Madh4
Mm.434583	NM_009231	Sos1	Son of sevenless homolog 1 (Drosophila)	4430401P03Rik, 9630010N06, AI449023
Mm.4618	NM_013672	Sp1	Trans-acting transcription factor 1	1110003E12Rik, AA450830, AI845540, Sp1-1
Mm.278701	NM_011480	Srebf1	Sterol regulatory element binding transcription factor 1	ADD-1, ADD1, D630008H06, SREBP-1, SREBP-1a, SREBP-1c, SREBP1, SREBP1c, bHLHd1
Mm.45044	NM_020493	Srf	Serum response factor	AW049942, AW240594
Mm.277403	NM_011488	Stat5a	Signal transducer and activator of transcription 5A	AA959963, STAT5
Mm.252321	NM_177340	Synpo	Synaptopodin	9030217H17Rik, 9130229N11, 9330140I15Rik, AW046661
Mm.85544	NM_011547	Tcfap2a	Transcription factor AP-2, alpha	AP-2, AP2alpha, Ap2, Ap2tf, Tfap2a
Mm.18154	NM_009337	Tcl1	T-cell lymphoma breakpoint 1	Tcl1a
Mm.270278	NM_017376	Tef	Thyrotroph embryonic factor	2310028D20Rik
Mm.248380	NM_011577	Tgfb1	Transforming growth factor, beta 1	TGF-beta1, TGFbeta1, Tgfb, Tgfb-1
Mm.6458	NM_011589	Timeless	Timeless homolog (Drosophila)	C77407, Debt69, tim
Mm.8245	NM_011593	Timp1	Tissue inhibitor of metalloproteinase 1	Clgi, MGC7143, TIMP-1, Timp
Mm.23987	NM_054096	Tirap	Toll-interleukin 1 receptor (TIR) domain-containing adaptor protein	AA407980, C130027E04Rik, Mal, Tlr4ap, Wyatt
Mm.38049	NM_021297	Tlr4	Toll-like receptor 4	Lps, Ly87, Ran, M1, Rasl2-8
Mm.1293	NM_013693	Tnf	Tumor necrosis factor	DIF, MGC151434, TNF-alpha, TNFSF2, TNFalpha, Tnfa, Tnfsf1a

Mm.103551	NM_023764	Tollip	Toll interacting protein	4930403G24Rik, 4931428G15Rik
Mm.224354	NM_022887	Tsc1	Tuberous sclerosis 1	hamartin, mKIAA0243
Mm.30435	NM_011647	Tsc2	Tuberous sclerosis 2	Tcs2
Mm.1574	NM_028459	Wasl	Wiskott-Aldrich syndrome-like (human)	2900021I12Rik, 3110031I02Rik, N-WASP
Mm.287173	NM_009516	Wee1	WEE 1 homolog 1 (S. pombe)	Wee1A
Mm.332314	NM_011738	Ywhah	Tyrosine 3-monooxygenase/tryptophan 5-monooxygenase activation protein, eta polypeptide	-
Mm.289630	NM_011739	Ywhaq	Tyrosine 3-monooxygenase/tryptophan 5-monooxygenase activation protein, theta polypeptide	2700028P07Rik, AA409740, AU021156, MGC118161, R74690

Signaling by Rho Family GTPases

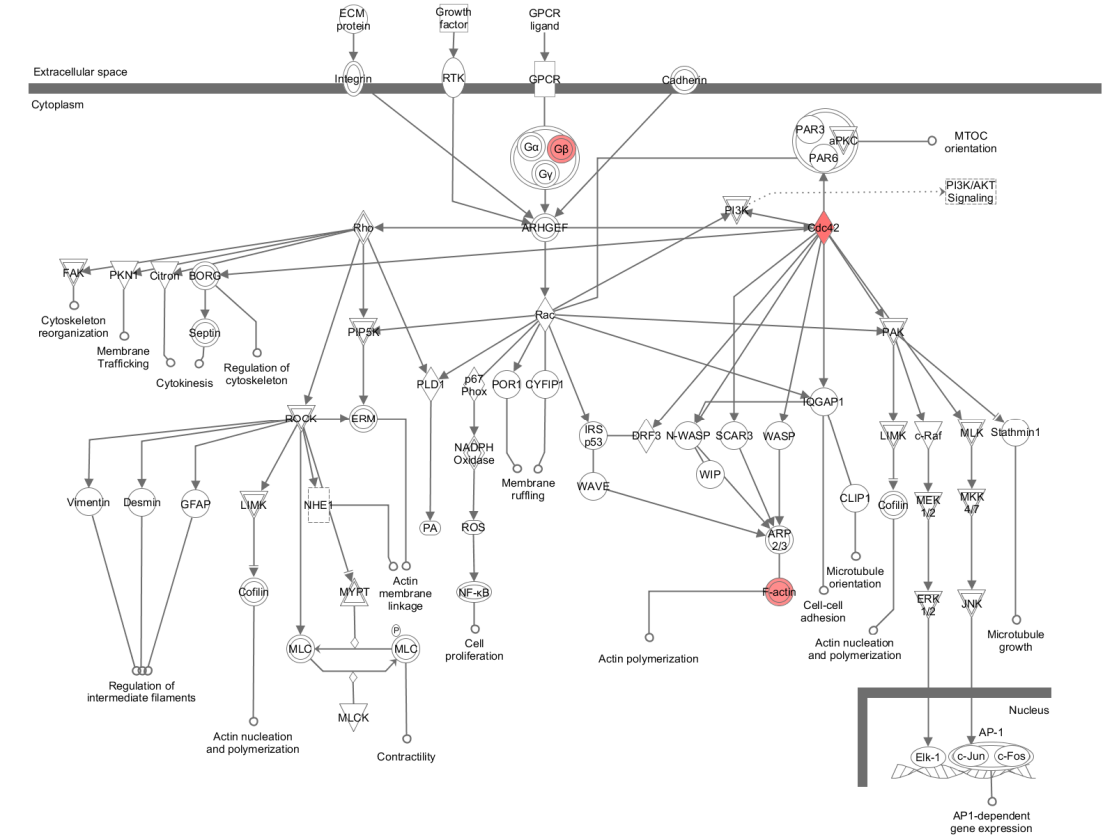

Ephrin B Signaling

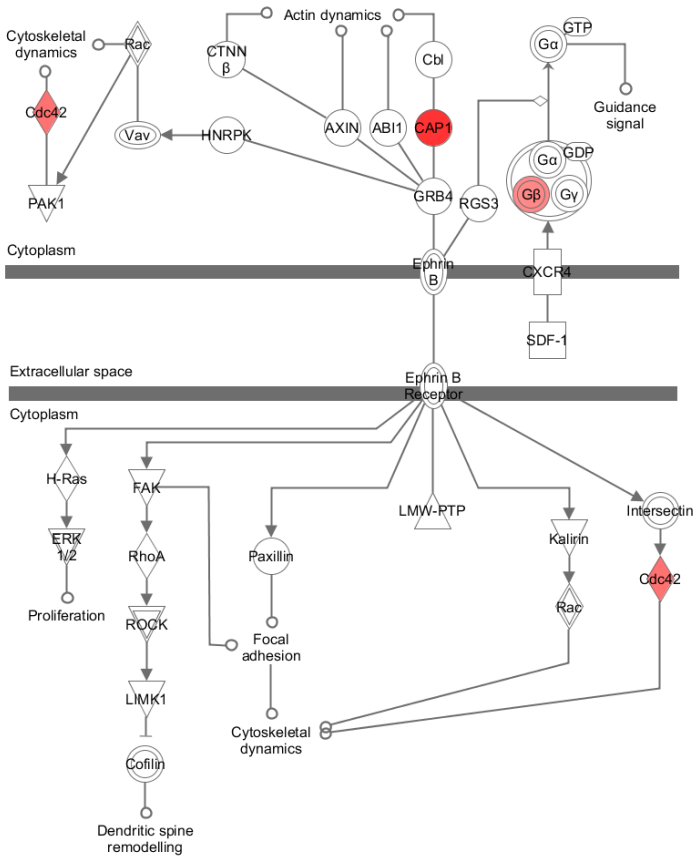

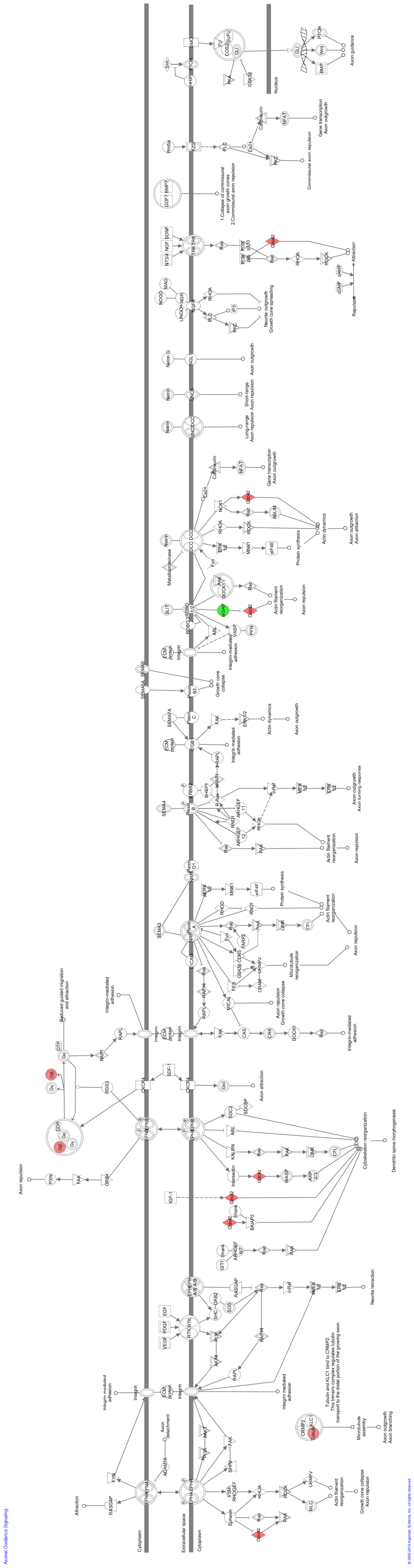

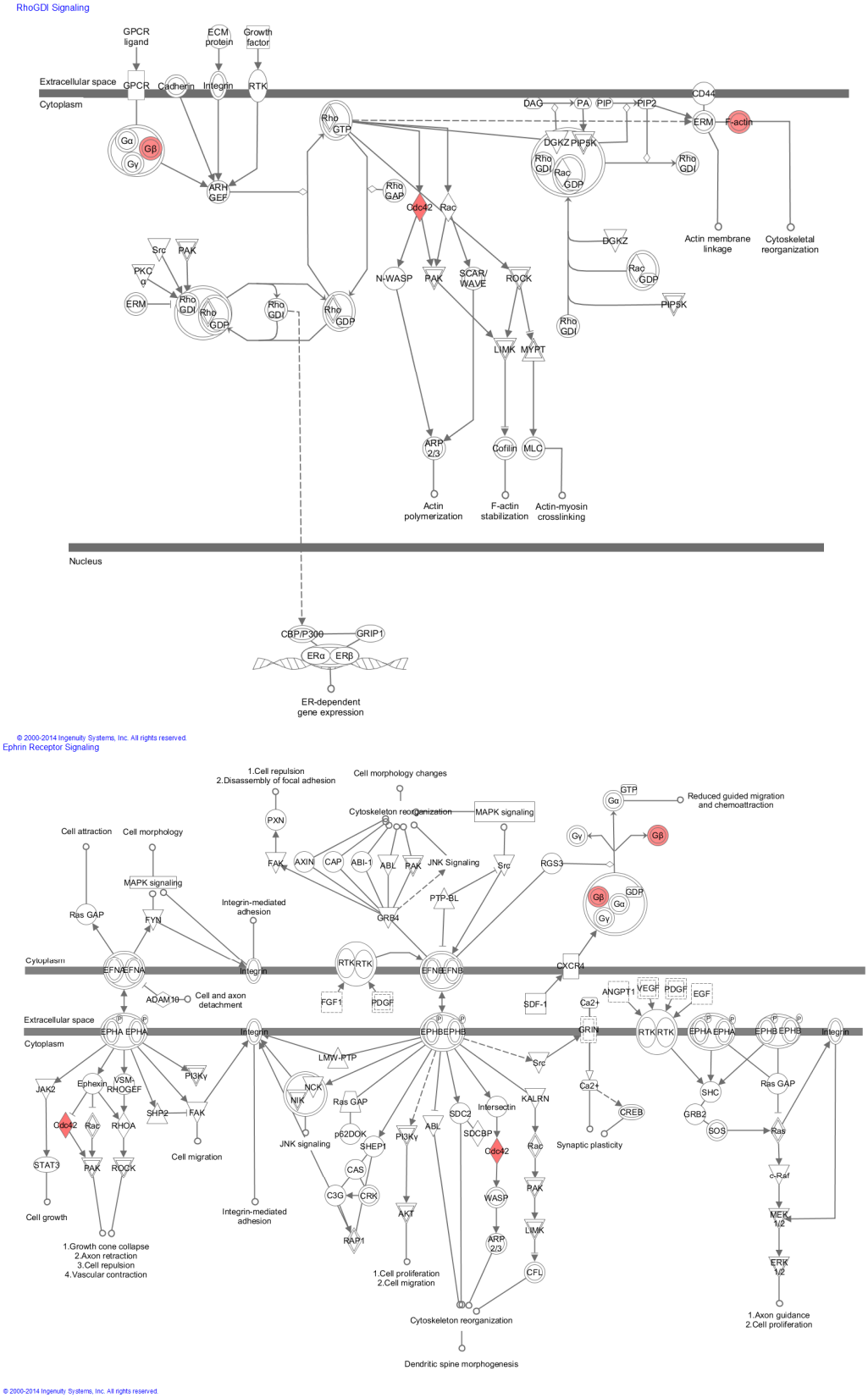

Figure 40: Visualisation of persistently affected pathways after irradiation adapted from the Ingenuity Pathway analysis software tool (Qiagen)

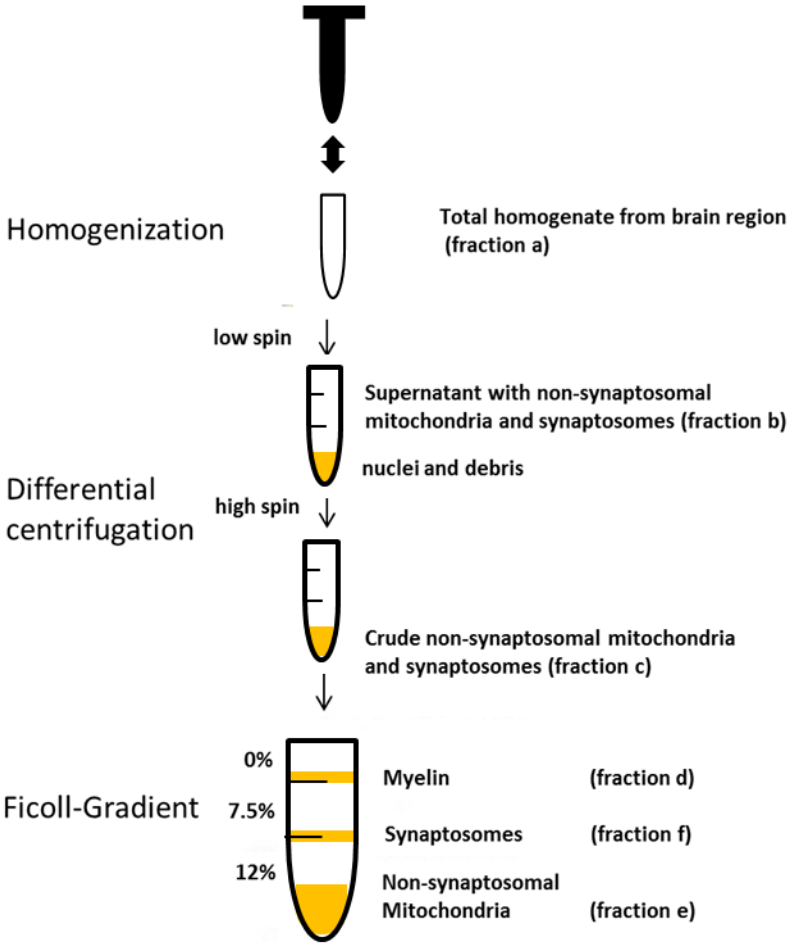

Figure 41: Workflow for isolation of non-synaptosomal mitochondria and synaptosomes from brain tissue

12 Figure and table index

13 Abbreviations

ADP	adenosine diphosphate
APS	ammonium persulfate
BSA	bovine serum albumin
CA1/3	Cornu ammonis area 1/3
CR	crest area (of hippocampus)
CNS	central nervous system
CT	computed tomography
C	cortex
CVD	cerebrovascular disease
DAB	diaminobenzidine
DG	dentate gyrus
ECL	enhanced chemiluminescence
EDTA	ethylenediaminetetraacetic acid
ESI	electrospray ionisation
DNA	deoxyribonucleic acid
DMSO	dimethyl sulfoxide
FA	formic acid
FCCP	carbonyl cyanide-4-(trifluoromethoxy)phenylhydrazone
FDR	false discovery rate
Gy	Gray
g	gravity acceleration
GnHCl	guanidine hydrochloride
H	hippocampus
HPLC	high-performance liquid chromatography
IB	infrapyramidal blade (of hippocampus)
IBS	isolation buffer for synaptosomes and mitochondria
IPA	Ingenuity Pathway Analysis
ICPL	isotope-coded protein label
(k)DA	(kilo) Dalton
LTP	long-term potentiation
LTD	long-term depression
LC-MS/MS	liquid chromatography-mass spectrometry / mass spectrometry
LNT	linear no-threshold
LTQ-MS/MS	linear trap quadrupole-mass spectrometry / mass-spectrometry
(m)RNA	(messenger) ribonucleic acid
MS	mass spectrometry
M	molar
miRNA	microRNA
n	number of biological replicates

OD	optical density
ppm	parts per million
PEI	polyethyleinamine
PBS	phosphate buffered saline
PND10	postnatal day 10
qPCR	quantitative polymerase chain reaction
RIN	RNA integrity number
RT	room temperature
SAS	Assay puffer for XF96 Seahorse
SB	suprapyramidal blade
snoRNA	small nucleolar ribonucleic acid
TFA	trifluoroacetic acid
(SDS-)PAGE	(sodium dodecyl sulphate-)polyacrylamide gel electrophoresis
SCN	suprachiasmatic nucleus
SDS	sodium dodecyl sulfate
SGZ	subgranular zone
TEMED	tetramethylethylenediamine
Tris	Tris(hydroxmethyl)aminomethane
TBST	Tris-buffered Saline Tween 20
TES	N-[tris(hydroxymethyl)methyl]-2-aminoethanesulfonic acid
UCP	uncoupling protein
vol	volume
v / v	volume per volume
w / v	weight per volume

14 Acknowledgements

I wish to express sincere gratitude to my supervisor Dr. **Soile Tapio** for her supervision, scientific discussion, valuable suggestions and inspiration towards my work. It has been a great pleasure to work with you.

I am profoundly grateful to Prof. Dr. **Mike Atkinson,** Prof. Dr. **Jerzy Adamski** and Prof. Dr. **Michael W. Pfaffl** for valuable suggestions, support and discussions.

My special thanks to **Sonja Buratovic,** Prof. Dr. **Bo Stenerlöw** and Prof Dr. **Per Eriksson** for animal irradiation (NMRI mouse study) and their personal communications regarding their behavioural design and analysis. I am also very grateful for **Jacqueline Mueller**, Dr. **Dirk Janik**, Dr**. Frauke Neff, Sandra Helm,** Dr. **Christine von Toerne,** Dr. **Stefanie Hauck,** Prof. Dr. **Marius Ueffing,** Dr. **Simonetta Pazzaglia,** Dr. **Arianna Casciati,** Prof. Dr. **Anna Saran,** Dr. **Simone Moertl** and **Klaudia Winkler** for their support and collaboration.

I am thankful to Dr. **Omid Azimzadeh**, Dr. **Zarko Barjaktarovic**, Dr. **Ramesh Yentrapalli**, Dr. **Arundhathi Sriharshan**, Dr. **Melanie Maier**, **Mayur Bakshi and Stefanie Winkler** for their knowledge, support and fruitful group discussions. It was a pleasure to work with you. A special thanks to all my colleagues at the Institute of Radiation Biology, Helmholtz Zentrum Munich, Germany.

I am highly grateful for Dr. **Pier Giorgio Mastroberardino** and Dr. **Sara Sepe** for their support, animal irradiation (C57BL/6 mouse study) and warm welcome during my stay at their institute. Further, thanks to Dr. **Martin Jastroch** and **Maria Kutschke** to run mitochondrial respiration experiments at their institute.

My gratitude to kind administrative persons **Solvejg Schroeder** and **Silvia Koehn**.

I am also thankful for the support of a grant from the **European Community´s Seventh Framework Programme (EURATOM) contract no. 29552 (CEREBRAD).**

To my beloved family – **Hannelore, Alois** and **Michael Kempf** and **friends**: Thank you all for your kind support during that intense time.

15 Publication list

Long-term effects of ionising radiation on the brain: cause for concern?
Kempf SJ, Azimzadeh O, Atkinson MJ, Tapio S.
Radiat Environ Biophys 2013 – accepted

Ionising radiation immediately impairs synaptic plasticity-associated cytoskeletal signalling pathways in HT22 cells and in mouse brain: An in vitro / in vivo comparison study
Kempf SJ, Buratovic S, von Toerne C, Moertl S, Stenerloew B, Hauck SM, Atkinson MJ, Eriksson P, Tapio S
PloS One 2014 - accepted

Long-term effects of acute low-dose ionizing radiation on the neonatal mouse heart: a proteomic study.
Bakshi MV, Barjaktarovic Z, Azimzadeh O, **Kempf SJ**, Merl J, Hauck SM, Eriksson P, Buratovic S, Atkinson MJ, Tapio S.
Radiat Environ Biophys 2013 – accepted

Total body exposure to low-dose ionizing radiation induces long-term alterations to the liver proteome of neonatally exposed mice
Bakshi MV, Azimzadeh O, Barjaktarovic Z, **Kempf SJ**, Merl J, Hauck SM, Buratovic S, Eriksson P, Atkinson MJ, Tapio S
J Proteome Research 2014 - accepted

The cognitive defects of neonatally irradiated mice are accompanied by changed synaptic plasticity, adult neurogenesis and neuroinflammation
Kempf SJ, Casciati A, Buratovic S, Janik D, von Toerne C, Ueffing M, Neff F, Moertl S, Stenerloew B, Atkinson MJ, Eriksson P, Pazzaglia S, Tapio S - submitted

Low-dose ionising radiation rapidly affects mitochondrial and synaptic signalling pathways in hippocampus and cortex
Kempf SJ, Moertl S, Sepe S, von Toerne C, Hauck SM, Atkinson MJ, Mastroberardino PG, Tapio S - submitted

Long-term effects of ionising radiation include defects in synaptic plasticity-related signalling pathways and mitochondrial dysfunction
Kempf SJ, Sepe S, von Toerne C, Moertl S, Hauck SM, Atkinson MJ, Mastroberardino PG, Tapio S - in preparation

Chronic low-dose ionising radiation induce alterations in synaptic plasticity-related signalling pathways in Apoe$^{-/-}$ mice
Kempf SJ, Janik D, von Toerne C, Hauck SM, Neff F, Braga-Tanaka I, Atkinson MJ, Tapio S - in preparation

Ionizing radiation induces immediate protein deacetylation in the human cardiac microvascular endothelial cells
Barjaktarovic Z, **Kempf SJ**, Sriharshan A, Merl J, Atkinson MJ, Tapio S – in preparation

16 References

ABDUL, H. M. & BUTTERFIELD, D. A. 2007. Involvement of PI3K/PKG/ERK1/2 signalling pathways in cortical neurons to trigger protection by cotreatment of acetyl-L-carnitine and alpha-lipoic acid against HNE-mediated oxidative stress and neurotoxicity: implications for Alzheimer's disease. *Free Radic Biol Med,* 42, 371-84.

ALLEN, A. R., EILERTSON, K., SHARMA, S., SCHNEIDER, D., BAURE, J., ALLEN, B., ROSI, S., RABER, J. & FIKE, J. R. 2013. Effects of radiation combined injury on hippocampal function are modulated in mice deficient in chemokine receptor 2 (CCR2). *Radiat Res,* 180, 78-88.

ALVAREZ-SAAVEDRA, M., ANTOUN, G., YANAGIYA, A., OLIVA-HERNANDEZ, R., CORNEJO-PALMA, D., PEREZ-IRATXETA, C., SONENBERG, N. & CHENG, H. Y. 2011. miRNA-132 orchestrates chromatin remodeling and translational control of the circadian clock. *Hum Mol Genet,* 20, 731-51.

AMARAL, D. G. & WITTER, M. P. 1989. The three-dimensional organization of the hippocampal formation: a review of anatomical data. *Neuroscience,* 31, 571-91.

ANWYL, R. 1999. Metabotropic glutamate receptors: electrophysiological properties and role in plasticity. *Brain Res Brain Res Rev,* 29, 83-120.

ARMSTRONG, D. D., DUNN, K. & ANTALFFY, B. 1998. Decreased dendritic branching in frontal, motor and limbic cortex in Rett syndrome compared with trisomy 21. *J Neuropathol Exp Neurol,* 57, 1013-7.

ASRAR, S. & JIA, Z. 2013. Molecular mechanisms coordinating functional and morphological plasticity at the synapse: role of GluA2/N-cadherin interaction-mediated actin signalling in mGluR-dependent LTD. *Cell Signal,* 25, 397-402.

AZIMZADEH, O., SIEVERT, W., SARIOGLU, H., YENTRAPALLI, R., BARJAKTAROVIC, Z., SRIHARSHAN, A., UEFFING, M., JANIK, D., AICHLER, M., ATKINSON, M. J., MULTHOFF, G. & TAPIO, S. 2013. PPAR alpha: a novel radiation target in locally exposed Mus musculus heart revealed by quantitative proteomics. *J Proteome Res,* 12, 2700-14.

AZIZOVA, T. V., MUIRHEAD, C. R., DRUZHININA, M. B., GRIGORYEVA, E. S., VLASENKO, E. V., SUMINA, M. V., O'HAGAN, J. A., ZHANG, W., HAYLOCK, R. G. & HUNTER, N. 2010. Cerebrovascular diseases in the cohort of workers first employed at Mayak PA in 1948-1958. *Radiat Res,* 174, 851-64.

AZIZOVA, T. V., MUIRHEAD, C. R., MOSEEVA, M. B., GRIGORYEVA, E. S., SUMINA, M. V., O'HAGAN, J., ZHANG, W., HAYLOCK, R. J. & HUNTER, N. 2011. Cerebrovascular diseases in nuclear workers first employed at the Mayak PA in 1948-1972. *Radiat Environ Biophys,* 50, 539-52.

BARJAKTAROVIC, Z., SCHMALTZ, D., SHYLA, A., AZIMZADEH, O., SCHULZ, S., HAAGEN, J., DORR, W., SARIOGLU, H., SCHAFER, A., ATKINSON, M. J., ZISCHKA, H. & TAPIO, S. 2011. Radiation-induced signalling results in mitochondrial impairment in mouse heart at 4 weeks after exposure to X-rays. *PLoS One,* 6, e27811.

BARJAKTAROVIC, Z., SHYLA, A., AZIMZADEH, O., SCHULZ, S., HAAGEN, J., DORR, W., SARIOGLU, H., ATKINSON, M. J., ZISCHKA, H. & TAPIO, S. 2013. Ionising radiation induces persistent alterations in the cardiac mitochondrial function of C57BL/6 mice 40 weeks after local heart exposure. *Radiother Oncol,* 106, 404-10.

BASAK, O. & TAYLOR, V. 2009. Stem cells of the adult mammalian brain and their niche. *Cell Mol Life Sci,* 66, 1057-72.

BAUMANS, V., HAVENAAR, R. & VAN HERCK, H. 1988. The use of repeated treatment with Ivomec and Neguvon spray in the control of murine fur mites and oxyurid worms. *Lab Anim,* 22, 246-9.

BECKER, L. E., ARMSTRONG, D. L. & CHAN, F. 1986. Dendritic atrophy in children with Down's syndrome. ***Ann Neurol,*** **20, 520-6.**

BELLOT, A., GUIVERNAU, B., TAJES, M., BOSCH-MORATO, M., VALLS-COMAMALA, V. & MUNOZ, F. J. 2014a. The structure and function of actin cytoskeleton in mature glutamatergic dendritic spines. ***Brain Res*****.**

BELLOT, A., GUIVERNAU, B., TAJES, M., BOSCH-MORATO, M., VALLS-COMAMALA, V. & MUNOZ, F. J. 2014b. The structure and function of actin cytoskeleton in mature glutamatergic dendritic spines. ***Brain Res,*** **1573, 1-16.**

BENARROCH, E. E. 2012. Insulin-like growth factors in the brain and their potential clinical implications. ***Neurology,*** **79, 2148-53.**

BERNIER, M. O., REHEL, J. L., BRISSE, H. J., WU-ZHOU, X., CAER-LORHO, S., JACOB, S., CHATEIL, J. F., AUBERT, B. & LAURIER, D. 2012. Radiation exposure from CT in early childhood: a French large-scale multicentre study. ***Br J Radiol,*** **85, 53-60.**

BERO, A. W., MENG, J., CHO, S., SHEN, A. H., CANTER, R. G., ERICSSON, M. & TSAI, L. H. 2014. Early remodeling of the neocortex upon episodic memory encoding. ***Proc Natl Acad Sci U S A,*** **111, 11852-7.**

BIFFI, A., SABUNCU, M. R., DESIKAN, R. S., SCHMANSKY, N., SALAT, D. H., ROSAND, J. & ANDERSON, C. D. 2014. Genetic variation of oxidative phosphorylation genes in stroke and Alzheimer's disease. ***Neurobiol Aging,*** **35, 1956 e1-8.**

BLISS, T. V. & GARDNER-MEDWIN, A. R. 1973. Long-lasting potentiation of synaptic transmission in the dentate area of the unanaestetized rabbit following stimulation of the perforant path. ***J Physiol,*** **232, 357-74.**

BOURNE, J. N. & HARRIS, K. M. 2008. Balancing structure and function at hippocampal dendritic spines. ***Annu Rev Neurosci,*** **31, 47-67.**

BRADFORD, M. M. 1976. A rapid and sensitive method for the quantitation of microgram quantities of protein utilizing the principle of protein-dye binding. ***Anal Biochem,*** **72, 248-54.**

BREITSPRECHER, D., KOESTLER, S. A., CHIZHOV, I., NEMETHOVA, M., MUELLER, J., GOODE, B. L., SMALL, J. V., ROTTNER, K. & FAIX, J. 2011. Cofilin cooperates with fascin to disassemble filopodial actin filaments. ***J Cell Sci,*** **124, 3305-18.**

BROSCH, M., YU, L., HUBBARD, T. & CHOUDHARY, J. 2009. Accurate and sensitive peptide identification with Mascot Percolator. ***J Proteome Res,*** **8, 3176-81.**

CACERES, L. G., URAN, S. L., ZORRILLA ZUBILETE, M. A., ROMERO, J. I., CAPANI, F. & GUELMAN, L. R. 2011. An early treatment with 17-beta-estradiol is neuroprotective against the long-term effects of neonatal ionizing radiation exposure. ***J Neurochem,*** **118, 626-35.**

CALKINS, M. J., MANCZAK, M., MAO, P., SHIRENDEB, U. & REDDY, P. H. 2011. Impaired mitochondrial biogenesis, defective axonal transport of mitochondria, abnormal mitochondrial dynamics and synaptic degeneration in a mouse model of Alzheimer's disease. ***Hum Mol Genet,*** **20, 4515-29.**

CAMERON, H. A. & MCKAY, R. D. 2001. Adult neurogenesis produces a large pool of new granule cells in the dentate gyrus. ***J Comp Neurol,*** **435, 406-17.**

CAO, H., CUI, Y. H., ZHAO, Z. Q., CAO, X. H. & ZHANG, Y. Q. 2009. Activation of extracellular signal-regulated kinase in the anterior cingulate cortex contributes to the induction of long-term potentiation in rats. ***Neurosci Bull,*** **25, 301-8.**

CAVALLUCCI, V., NOBILI, A. & D'AMELIO, M. 2013. Emerging role of mitochondria dysfunction in the onset of neurodegenerative diseases. ***J Biol Regul Homeost Agents,*** **27, 1-9.**

CHAUDHURY, D., WANG, L. M. & COLWELL, C. S. 2005. Circadian regulation of hippocampal long-term potentiation. ***J Biol Rhythms,*** **20, 225-36.**

CHIU, S. L., CHEN, C. M. & CLINE, H. T. 2008. Insulin receptor signalling regulates synapse number, dendritic plasticity, and circuit function in vivo. ***Neuron,*** **58, 708-19.**

CHOI, S. W., GERENCSER, A. A., LEE, D. W., RAJAGOPALAN, S., NICHOLLS, D. G., ANDERSEN, J. K. & BRAND, M. D. 2011. Intrinsic bioenergetic properties and stress sensitivity of dopaminergic synaptosomes. ***J Neurosci,*** **31, 4524-34.**

CLOPATH, C. 2012. Synaptic consolidation: an approach to long-term learning. ***Cogn Neurodyn,*** **6, 251-7.**

COHEN, P. T. 1997. Novel protein serine/threonine phosphatases: variety is the spice of life. ***Trends Biochem Sci,*** **22, 245-51.**

COHEN, R. S., CHUNG, S. K. & PFAFF, D. W. 1985. Immunocytochemical localization of actin in dendritic spines of the cerebral cortex using colloidal gold as a probe. ***Cell Mol Neurobiol,*** **5, 271-84.**

COLBRAN, R. J. 2004. Protein phosphatases and calcium/calmodulin-dependent protein kinase II-dependent synaptic plasticity. ***J Neurosci,*** **24, 8404-9.**

CORTES-MENDOZA, J., DIAZ DE LEON-GUERRERO, S., PEDRAZA-ALVA, G. & PEREZ-MARTINEZ, L. 2013. Shaping synaptic plasticity: the role of activity-mediated epigenetic regulation on gene transcription. ***Int J Dev Neurosci,*** **31, 359-69.**

DAENEN, E. W., VAN DER HEYDEN, J. A., KRUSE, C. G., WOLTERINK, G. & VAN REE, J. M. 2001. Adaptation and habituation to an open field and responses to various stressful events in animals with neonatal lesions in the amygdala or ventral hippocampus. ***Brain Res,*** **918, 153-65.**

DAULATZAI, M. A. 2014. Role of Stress, Depression, and Aging in Cognitive Decline and Alzheimer's Disease. ***Curr Top Behav Neurosci*****.**

DAVIS, R. C., MARSDEN, I. T., MALONEY, M. T., MINAMIDE, L. S., PODLISNY, M., SELKOE, D. J. & BAMBURG, J. R. 2011. Amyloid beta dimers/trimers potently induce cofilin-actin rods that are inhibited by maintaining cofilin-phosphorylation. ***Mol Neurodegener,*** **6, 10.**

DE JAEGER, X., COURTEY, J., BRUS, M., ARTINIAN, J., VILLAIN, H., BACQUIE, E. & ROULLET, P. 2014. Characterization of spatial memory reconsolidation. ***Learn Mem,*** **21, 316-24.**

DEKABAN, A. S. 1978. Changes in brain weights during the span of human life: relation of brain weights to body heights and body weights. ***Ann Neurol,*** **4, 345-56.**

DEKOSKY, S. T. & SCHEFF, S. W. 1990. Synapse loss in frontal cortex biopsies in Alzheimer's disease: correlation with cognitive severity. ***Ann Neurol,*** **27, 457-64.**

DEKOSKY, S. T., SCHEFF, S. W. & STYREN, S. D. 1996. Structural correlates of cognition in dementia: quantification and assessment of synapse change. ***Neurodegeneration,*** **5, 417-21.**

DERMARDIROSSIAN, C., SCHNELZER, A. & BOKOCH, G. M. 2004. Phosphorylation of RhoGDI by Pak1 mediates dissociation of Rac GTPase. ***Mol Cell,*** **15, 117-27.**

DHAR, M., ZHU, M., IMPEY, S., LAMBERT, T. J., BLAND, T., KARATSOREOS, I. N., NAKAZAWA, T., APPLEYARD, S. M. & WAYMAN, G. A. 2014. Leptin induces hippocampal synaptogenesis via CREB-regulated microRNA-132 suppression of p250GAP. ***Mol Endocrinol,*** **28, 1073-87.**

DI FILIPPO, M., CHIASSERINI, D., GARDONI, F., VIVIANI, B., TOZZI, A., GIAMPA, C., COSTA, C., TANTUCCI, M., ZIANNI, E., BORASO, M., SILIQUINI, S., DE IURE, A., GHIGLIERI, V., COLCELLI, E., BAKER, D., SARCHIELLI, P., FUSCO, F. R., DI LUCA, M. & CALABRESI, P. 2013. Effects of central and peripheral inflammation on hippocampal synaptic plasticity. ***Neurobiol Dis,*** **52, 229-36.**

DI PENTA, A., MORENO, B., REIX, S., FERNANDEZ-DIEZ, B., VILLANUEVA, M., ERREA, O., ESCALA, N., VANDENBROECK, K., COMELLA, J. X. & VILLOSLADA, P. 2013. Oxidative stress and proinflammatory cytokines contribute to demyelination and axonal damage in a cerebellar culture model of neuroinflammation. ***PLoS One,*** **8, e54722.**

DIANA, G., VALENTINI, G., TRAVAGLIONE, S., FALZANO, L., PIERI, M., ZONA, C., MESCHINI, S., FABBRI, A. & FIORENTINI, C. 2007. Enhancement of learning and memory after activation of cerebral Rho GTPases. ***Proc Natl Acad Sci U S A,*** **104, 636-41.**

DOBBING, J. & SANDS, J. 1973. Quantitative growth and development of human brain. *Arch Dis Child,* 48, 757-67.

DOBBING, J. & SANDS, J. 1979. Comparative aspects of the brain growth spurt. *Early Hum Dev,* 3, 79-83.

DUBOFF, B., FEANY, M. & GOTZ, J. 2013. Why size matters - balancing mitochondrial dynamics in Alzheimer's disease. *Trends Neurosci,* 36, 325-35.

ECKEL-MAHAN, K. L., PATEL, V. R., DE MATEO, S., OROZCO-SOLIS, R., CEGLIA, N. J., SAHAR, S., DILAG-PENILLA, S. A., DYAR, K. A., BALDI, P. & SASSONE-CORSI, P. 2013. Reprogramming of the circadian clock by nutritional challenge. *Cell,* 155, 1464-78.

ECKERT, A., NISBET, R., GRIMM, A. & GOTZ, J. 2013. March separate, strike together - Role of phosphorylated TAU in mitochondrial dysfunction in Alzheimer's disease. *Biochim Biophys Acta*.

ERIKSSON, P., ANKARBERG, E. & FREDRIKSSON, A. 2000. Exposure to nicotine during a defined period in neonatal life induces permanent changes in brain nicotinic receptors and in behaviour of adult mice. *Brain Res,* 853, 41-8.

ERIKSSON, P., FISCHER, C., STENERLOW, B., FREDRIKSSON, A. & SUNDELL-BERGMAN, S. 2010. Interaction of gamma-radiation and methyl mercury during a critical phase of neonatal brain development in mice exacerbates developmental neurobehavioural effects. *NeuroToxicology,* 31, 223-9.

FERREIRA, S. T., CLARKE, J. R., BOMFIM, T. R. & DE FELICE, F. G. 2014. Inflammation, defective insulin signalling, and neuronal dysfunction in Alzheimer's disease. *Alzheimers Dement,* 10, S76-S83.

FIFKOVA, E. & DELAY, R. J. 1982. Cytoplasmic actin in neuronal processes as a possible mediator of synaptic plasticity. *J Cell Biol,* 95, 345-50.

FISCHER, M., KAECH, S., WAGNER, U., BRINKHAUS, H. & MATUS, A. 2000. Glutamate receptors regulate actin-based plasticity in dendritic spines. *Nat Neurosci,* 3, 887-94.

FLEISCHMANN, A., HVALBY, O., JENSEN, V., STREKALOVA, T., ZACHER, C., LAYER, L. E., KVELLO, A., RESCHKE, M., SPANAGEL, R., SPRENGEL, R., WAGNER, E. F. & GASS, P. 2003. Impaired long-term memory and NR2A-type NMDA receptor-dependent synaptic plasticity in mice lacking c-Fos in the CNS. *J Neurosci,* 23, 9116-22.

FULGA, T. A., ELSON-SCHWAB, I., KHURANA, V., STEINHILB, M. L., SPIRES, T. L., HYMAN, B. T. & FEANY, M. B. 2007. Abnormal bundling and accumulation of F-actin mediates tau-induced neuronal degeneration in vivo. *Nat Cell Biol,* 9, 139-48.

GEMMA, C. & BACHSTETTER, A. D. 2013. The role of microglia in adult hippocampal neurogenesis. *Front Cell Neurosci,* 7, 229.

GERBER, T. C., KANTOR, B. & MCCOLLOUGH, C. H. 2009. Radiation dose and safety in cardiac computed tomography. *Cardiol Clin,* 27, 665-77.

GERSTNER, J. R., LYONS, L. C., WRIGHT, K. P., JR., LOH, D. H., RAWASHDEH, O., ECKEL-MAHAN, K. L. & ROMAN, G. W. 2009. Cycling behavior and memory formation. *J Neurosci,* 29, 12824-30.

GLAZE, D. G. 2004. Rett syndrome: of girls and mice--lessons for regression in autism. *Ment Retard Dev Disabil Res Rev,* 10, 154-8.

GOLD, A. E. & KESNER, R. P. 2005. The role of the CA3 subregion of the dorsal hippocampus in spatial pattern completion in the rat. *Hippocampus,* 15, 808-14.

GREER, P. L. & GREENBERG, M. E. 2008. From synapse to nucleus: calcium-dependent gene transcription in the control of synapse development and function. *Neuron,* 59, 846-60.

GRINBERG, Y. Y., VAN DRONGELEN, W. & KRAIG, R. P. 2012. Insulin-like growth factor-1 lowers spreading depression susceptibility and reduces oxidative stress. *J Neurochem,* 122, 221-9.

GROVES, P. M. & THOMPSON, R. F. 1970. Habituation: a dual-process theory. *Psychol Rev,* 77, 419-50.

GUZOWSKI, J. F. 2002. Insights into immediate-early gene function in hippocampal memory consolidation using antisense oligonucleotide and fluorescent imaging approaches. *Hippocampus,* 12, 86-104.

GUZOWSKI, J. F., LYFORD, G. L., STEVENSON, G. D., HOUSTON, F. P., MCGAUGH, J. L., WORLEY, P. F. & BARNES, C. A. 2000. Inhibition of activity-dependent arc protein expression in the rat hippocampus impairs the maintenance of long-term potentiation and the consolidation of long-term memory. *J Neurosci,* 20, 3993-4001.

GUZOWSKI, J. F., MCNAUGHTON, B. L., BARNES, C. A. & WORLEY, P. F. 1999. Environment-specific expression of the immediate-early gene Arc in hippocampal neuronal ensembles. *Nat Neurosci,* 2, 1120-4.

HADDY, N., MOUSANNIF, A., TUKENOVA, M., GUIBOUT, C., GRILL, J., DHERMAIN, F., PACQUEMENT, H., OBERLIN, O., EL-FAYECH, C., RUBINO, C., THOMAS-TEINTURIER, C., LE-DELEY, M. C., HAWKINS, M., WINTER, D., CHAVAUDRA, J., DIALLO, I. & DE VATHAIRE, F. 2011. Relationship between the brain radiation dose for the treatment of childhood cancer and the risk of long-term cerebrovascular mortality. *Brain,* 134, 1362-72.

HADITSCH, U., LEONE, D. P., FARINELLI, M., CHROSTEK-GRASHOFF, A., BRAKEBUSCH, C., MANSUY, I. M., MCCONNELL, S. K. & PALMER, T. D. 2009. A central role for the small GTPase Rac1 in hippocampal plasticity and spatial learning and memory. *Mol Cell Neurosci,* 41, 409-19.

HALL, P., ADAMI, H. O., TRICHOPOULOS, D., PEDERSEN, N. L., LAGIOU, P., EKBOM, A., INGVAR, M., LUNDELL, M. & GRANATH, F. 2004. Effect of low doses of ionising radiation in infancy on cognitive function in adulthood: Swedish population based cohort study. *BMJ,* 328, 19.

HARADA, A., TENG, J., TAKEI, Y., OGUCHI, K. & HIROKAWA, N. 2002. MAP2 is required for dendrite elongation, PKA anchoring in dendrites, and proper PKA signal transduction. *J Cell Biol,* 158, 541-9.

HECKMAN, L. D., CHAHROUR, M. H. & ZOGHBI, H. Y. 2014. Rett-causing mutations reveal two domains critical for MeCP2 function and for toxicity in MECP2 duplication syndrome mice. *Elife*, e02676.

HOFFMAN, K. E. & YOCK, T. I. 2009. Radiation therapy for pediatric central nervous system tumors. *J Child Neurol,* 24, 1387-96.

HOLLAND, B. A., HAAS, D. K., NORMAN, D., BRANT-ZAWADZKI, M. & NEWTON, T. H. 1986. MRI of normal brain maturation. *AJNR Am J Neuroradiol,* 7, 201-8.

HOLSCHER, C., GIGG, J. & O'MARA, S. M. 1999. Metabotropic glutamate receptor activation and blockade: their role in long-term potentiation, learning and neurotoxicity. *Neurosci Biobehav Rev,* 23, 399-410.

HOTULAINEN, P. & HOOGENRAAD, C. C. 2010. Actin in dendritic spines: connecting dynamics to function. *J Cell Biol,* 189, 619-29.

HSIEH, H., BOEHM, J., SATO, C., IWATSUBO, T., TOMITA, T., SISODIA, S. & MALINOW, R. 2006. AMPAR removal underlies Abeta-induced synaptic depression and dendritic spine loss. *Neuron,* 52, 831-43.

HUGHES, J. R. 1958. Post-tetanic potentiation. *Physiol Rev,* 38, 91-113.

HUTTENLOCHER, P. R. & DABHOLKAR, A. S. 1997. Regional differences in synaptogenesis in human cerebral cortex. *J Comp Neurol,* 387, 167-78.

IMPEY, S., DAVARE, M., LESIAK, A., FORTIN, D., ANDO, H., VARLAMOVA, O., OBRIETAN, K., SODERLING, T. R., GOODMAN, R. H. & WAYMAN, G. A. 2010. An activity-induced microRNA controls dendritic spine formation by regulating Rac1-PAK signalling. *Mol Cell Neurosci,* 43, 146-56.

JOHANNESSEN, M., DELGHANDI, M. P. & MOENS, U. 2004. What turns CREB on? *Cell Signal,* 16, 1211-27.

JOHANNESSEN, M. & MOENS, U. 2007. Multisite phosphorylation of the cAMP response element-binding protein (CREB) by a diversity of protein kinases. *Front Biosci,* 12, 1814-32.

KADAR, E., HUGUET, G., ALDAVERT-VERA, L., MORGADO-BERNAL, I. & SEGURA-TORRES, P. 2013. Intracranial self stimulation upregulates the expression of synaptic plasticity related genes and Arc protein expression in rat hippocampus. ***Genes Brain Behav,*** **12, 771-9.**

KAIBARA, T. & LEUNG, L. S. 1993. Basal versus apical dendritic long-term potentiation of commissural afferents to hippocampal CA1: a current-source density study. ***J Neurosci,*** **13, 2391-404.**

KASAI, H., MATSUZAKI, M., NOGUCHI, J., YASUMATSU, N. & NAKAHARA, H. 2003. Structure-stability-function relationships of dendritic spines. ***Trends Neurosci,*** **26, 360-8.**

KELLY, S. J., GOODLETT, C. R., HULSETHER, S. A. & WEST, J. R. 1988. Impaired spatial navigation in adult female but not adult male rats exposed to alcohol during the brain growth spurt. ***Behav Brain Res,*** **27, 247-57.**

KEMPF, S. J., AZIMZADEH, O., ATKINSON, M. J. & TAPIO, S. 2013. Long-term effects of ionising radiation on the brain: cause for concern? ***Radiat Environ Biophys,*** **52, 5-16.**

KESNER, R. P. 2007. Behavioral functions of the CA3 subregion of the hippocampus. ***Learn Mem,*** **14, 771-81.**

KIEBISH, M. A., HAN, X., CHENG, H., LUNCEFORD, A., CLARKE, C. F., MOON, H., CHUANG, J. H. & SEYFRIED, T. N. 2008. Lipidomic analysis and electron transport chain activities in C57BL/6J mouse brain mitochondria. ***J Neurochem,*** **106, 299-312.**

KIRWAN, C. B., WIXTED, J. T. & SQUIRE, L. R. 2008. Activity in the medial temporal lobe predicts memory strength, whereas activity in the prefrontal cortex predicts recollection. ***J Neurosci,*** **28, 10541-8.**

KITAMURA, T., SAITOH, Y., TAKASHIMA, N., MURAYAMA, A., NIIBORI, Y., AGETA, H., SEKIGUCHI, M., SUGIYAMA, H. & INOKUCHI, K. 2009. Adult neurogenesis modulates the hippocampus-dependent period of associative fear memory. ***Cell,*** **139, 814-27.**

KLEIN, M. E., LIOY, D. T., MA, L., IMPEY, S., MANDEL, G. & GOODMAN, R. H. 2007. Homeostatic regulation of MeCP2 expression by a CREB-induced microRNA. ***Nat Neurosci,*** **10, 1513-4.**

KOVACS, K. J. 2008. Measurement of immediate-early gene activation- c-fos and beyond. ***J Neuroendocrinol,*** **20, 665-72.**

KULLANDER, K. & KLEIN, R. 2002. Mechanisms and functions of Eph and ephrin signalling. ***Nat Rev Mol Cell Biol,*** **3, 475-86.**

KURATA, T., MIYAZAKI, K., KOZUKI, M., MORIMOTO, N., OHTA, Y., IKEDA, Y. & ABE, K. 2011. Progressive neurovascular disturbances in the cerebral cortex of Alzheimer's disease-model mice: protection by atorvastatin and pitavastatin. ***Neuroscience,*** **197, 358-68.**

LAEMMLI, U. K. 1970. Cleavage of structural proteins during the assembly of the head of bacteriophage T4. ***Nature,*** **227, 680-5.**

LAN, Y. L., ZHAO, J. & LI, S. 2014. Update on the Neuroprotective Effect of Estrogen Receptor Alpha Against Alzheimer's Disease. ***J Alzheimers Dis*****.**

LANAHAN, A. & WORLEY, P. 1998. Immediate-early genes and synaptic function. ***Neurobiol Learn Mem,*** **70, 37-43.**

LAU, P., BOSSERS, K., JANKY, R., SALTA, E., FRIGERIO, C. S., BARBASH, S., ROTHMAN, R., SIERKSMA, A. S., THATHIAH, A., GREENBERG, D., PAPADOPOULOU, A. S., ACHSEL, T., AYOUBI, T., SOREQ, H., VERHAAGEN, J., SWAAB, D. F., AERTS, S. & DE STROOPER, B. 2013. Alteration of the microRNA network during the progression of Alzheimer's disease. ***EMBO Mol Med,*** **5, 1613-34.**

LEE, C. C., HUANG, C. C. & HSU, K. S. 2011. Insulin promotes dendritic spine and synapse formation by the PI3K/Akt/mTOR and Rac1 signalling pathways. ***Neuropharmacology,*** **61, 867-79.**

LEE, H. K., KAMEYAMA, K., HUGANIR, R. L. & BEAR, M. F. 1998. NMDA induces long-term synaptic depression and dephosphorylation of the GluR1 subunit of AMPA receptors in hippocampus. ***Neuron,*** **21, 1151-62.**

LI, Y. Q., AUBERT, I. & WONG, C. S. 2010. Abrogation of early apoptosis does not alter late inhibition of hippocampal neurogenesis after irradiation. ***Int J Radiat Oncol Biol Phys,*** **77, 1213-22.**

LIMOLI, C. L., GIEDZINSKI, E., ROLA, R., OTSUKA, S., PALMER, T. D. & FIKE, J. R. 2004. Radiation response of neural precursor cells: linking cellular sensitivity to cell cycle checkpoints, apoptosis and oxidative stress. ***Radiat Res,*** **161, 17-27.**

LISMAN, J. 2003. Actin's actions in LTP-induced synapse growth. ***Neuron,*** **38, 361-2.**

LITTLE, M. P. 2010. Do non-targeted effects increase or decrease low dose risk in relation to the linear-non-threshold (LNT) model? ***Mutat Res,*** **687, 17-27.**

LLORENS-MARTIN, M., TORRES-ALEMAN, I. & TREJO, J. L. 2010. Exercise modulates insulin-like growth factor 1-dependent and -independent effects on adult hippocampal neurogenesis and behaviour. ***Mol Cell Neurosci,*** **44, 109-17.**

LOGANOVSKY, K. 2009. Do Low Doses of Ionizing Radiation Affect the Human Brain? ***Data Science Journal,*** **advpub, 0906210142-0906210142.**

LOSONCZY, A., SOMOGYI, P. & NUSSER, Z. 2003. Reduction of excitatory postsynaptic responses by persistently active metabotropic glutamate receptors in the hippocampus. ***J Neurophysiol,*** **89, 1910-9.**

LUO, L. 2002. Actin cytoskeleton regulation in neuronal morphogenesis and structural plasticity. ***Annu Rev Cell Dev Biol,*** **18, 601-35.**

LUPIEN, S. J., MCEWEN, B. S., GUNNAR, M. R. & HEIM, C. 2009. Effects of stress throughout the lifespan on the brain, behaviour and cognition. ***Nat Rev Neurosci,*** **10, 434-45.**

LUSARDI, T. A., FARR, C. D., FAULKNER, C. L., PIGNATARO, G., YANG, T., LAN, J., SIMON, R. P. & SAUGSTAD, J. A. 2010. Ischemic preconditioning regulates expression of microRNAs and a predicted target, MeCP2, in mouse cortex. ***J Cereb Blood Flow Metab,*** **30, 744-56.**

LYFORD, G. L., YAMAGATA, K., KAUFMANN, W. E., BARNES, C. A., SANDERS, L. K., COPELAND, N. G., GILBERT, D. J., JENKINS, N. A., LANAHAN, A. A. & WORLEY, P. F. 1995. Arc, a growth factor and activity-regulated gene, encodes a novel cytoskeleton-associated protein that is enriched in neuronal dendrites. ***Neuron,*** **14, 433-45.**

MA, D. K., MARCHETTO, M. C., GUO, J. U., MING, G. L., GAGE, F. H. & SONG, H. 2010. Epigenetic choreographers of neurogenesis in the adult mammalian brain. ***Nat Neurosci,*** **13, 1338-44.**

MALAKHOVA, L., BEZLEPKIN, V. G., ANTIPOVA, V., USHAKOVA, T., FOMENKO, L., SIROTA, N. & GAZIEV, A. I. 2005. The increase in mitochondrial DNA copy number in the tissues of gamma-irradiated mice. ***Cell Mol Biol Lett,*** **10, 721-32.**

MANAHAN-VAUGHAN, D. 1997. Group 1 and 2 metabotropic glutamate receptors play differential roles in hippocampal long-term depression and long-term potentiation in freely moving rats. ***J Neurosci,*** **17, 3303-11.**

MARINISSEN, M. J. & GUTKIND, J. S. 2001. G-protein-coupled receptors and signalling networks: emerging paradigms. ***Trends Pharmacol Sci,*** **22, 368-76.**

MARTINEZ, L. A. & TEJADA-SIMON, M. V. 2011. Pharmacological inactivation of the small GTPase Rac1 impairs long-term plasticity in the mouse hippocampus. ***Neuropharmacology,*** **61, 305-12.**

MARZA, E., LONG, T., SAIARDI, A., SUMAKOVIC, M., EIMER, S., HALL, D. H. & LESA, G. M. 2008. Polyunsaturated fatty acids influence synaptojanin localization to regulate synaptic vesicle recycling. ***Mol Biol Cell,*** **19, 833-42.**

MASLIAH, E. 1995. Mechanisms of synaptic dysfunction in Alzheimer's disease. ***Histol Histopathol,*** **10, 509-19.**

MCGAUGH, J. L. 2000. Memory--a century of consolidation. ***Science,*** **287, 248-51.**

MENET, J. S. & ROSBASH, M. 2011. When brain clocks lose track of time: cause or consequence of neuropsychiatric disorders. ***Curr Opin Neurobiol,*** **21, 849-57.**

MENG, Y., ZHANG, Y., TREGOUBOV, V., JANUS, C., CRUZ, L., JACKSON, M., LU, W. Y., MACDONALD, J. F., WANG, J. Y., FALLS, D. L. & JIA, Z. 2002. Abnormal spine morphology and enhanced LTP in LIMK-1 knockout mice. ***Neuron,*** **35, 121-33.**

MERL, J., UEFFING, M., HAUCK, S. M. & VON TOERNE, C. 2012. Direct comparison of MS-based label-free and SILAC quantitative proteome profiling strategies in primary retinal Muller cells. ***Proteomics,*** **12, 1902-11.**

MESSAOUDI, E., KANHEMA, T., SOULE, J., TIRON, A., DAGYTE, G., DA SILVA, B. & BRAMHAM, C. R. 2007. Sustained Arc/Arg3.1 synthesis controls long-term potentiation consolidation through regulation of local actin polymerization in the dentate gyrus in vivo. ***J Neurosci,*** **27, 10445-55.**

METTLER, F. A., JR., WIEST, P. W., LOCKEN, J. A. & KELSEY, C. A. 2000. CT scanning: patterns of use and dose. ***J Radiol Prot,*** **20, 353-9.**

MILNER, B. 2005. The medial temporal-lobe amnesic syndrome. ***Psychiatr Clin North Am,*** **28, 599-611, 609.**

MING, G. L. & SONG, H. 2011. Adult neurogenesis in the mammalian brain: significant answers and significant questions. ***Neuron,*** **70, 687-702.**

MIZUMATSU, S., MONJE, M. L., MORHARDT, D. R., ROLA, R., PALMER, T. D. & FIKE, J. R. 2003. Extreme sensitivity of adult neurogenesis to low doses of X-irradiation. ***Cancer Res,*** **63, 4021-7.**

MONJE, M. L., TODA, H. & PALMER, T. D. 2003. Inflammatory blockade restores adult hippocampal neurogenesis. ***Science,*** **302, 1760-5.**

MONTEIRO-CARDOSO, V. F., OLIVEIRA, M. M., MELO, T., DOMINGUES, M. R., MOREIRA, P. I., FERREIRO, E., PEIXOTO, F. & VIDEIRA, R. A. 2014. Cardiolipin Profile Changes are Associated to the Early Synaptic Mitochondrial Dysfunction in Alzheimer's Disease. ***J Alzheimers Dis*****.**

MORRIS, K. A. & GOLD, P. E. 2012. Age-related impairments in memory and in CREB and pCREB expression in hippocampus and amygdala following inhibitory avoidance training. ***Mech Ageing Dev,*** **133, 291-9.**

MOSCOVITCH, M., NADEL, L., WINOCUR, G., GILBOA, A. & ROSENBAUM, R. S. 2006. The cognitive neuroscience of remote episodic, semantic and spatial memory. ***Curr Opin Neurobiol,*** **16, 179-90.**

MOSHER, K. I. & WYSS-CORAY, T. 2014. Microglial dysfunction in brain aging and Alzheimer's disease. ***Biochem Pharmacol,*** **88, 594-604.**

MOTA, S. I., FERREIRA, I. L. & REGO, A. C. 2014. Dysfunctional synapse in Alzheimer's disease - A focus on NMDA receptors. ***Neuropharmacology,*** **76 Pt A, 16-26.**

NAKATSUKA, H. & NATSUME, K. 2014. Circadian rhythm modulates long-term potentiation induced at CA1 in rat hippocampal slices. ***Neurosci Res,*** **6, 00289-7.**

NAKAZAWA, K., MCHUGH, T. J., WILSON, M. A. & TONEGAWA, S. 2004. NMDA receptors, place cells and hippocampal spatial memory. ***Nat Rev Neurosci,*** **5, 361-72.**

NAKAZAWA, K., QUIRK, M. C., CHITWOOD, R. A., WATANABE, M., YECKEL, M. F., SUN, L. D., KATO, A., CARR, C. A., JOHNSTON, D., WILSON, M. A. & TONEGAWA, S. 2002. Requirement for hippocampal CA3 NMDA receptors in associative memory recall. ***Science,*** **297, 211-8.**

NAMBA, T., MOCHIZUKI, H., ONODERA, M., MIZUNO, Y., NAMIKI, H. & SEKI, T. 2005. The fate of neural progenitor cells expressing astrocytic and radial glial markers in the postnatal rat dentate gyrus. ***Eur J Neurosci,*** **22, 1928-41.**

NISHIDA, H. & OKABE, S. 2007. Direct astrocytic contacts regulate local maturation of dendritic spines. ***J Neurosci,*** **27, 331-40.**

OLMOS, G. & LLADO, J. 2014. Tumor necrosis factor alpha: a link between neuroinflammation and excitotoxicity. ***Mediators Inflamm,*** **2014, 861231.**

OMRAN, A. R., SHORE, R. E., MARKOFF, R. A., FRIEDHOFF, A., ALBERT, R. E., BARR, H., DAHLSTROM, W. G. & PASTERNACK, B. S. 1978. Follow-up study of patients treated by X-ray epilation for tinea capitis: psychiatric and psychometric evaluation. ***Am J Public Health,*** **68, 561-7.**

OSTER, I., SHAMDEEN, G. M., ZIEGLER, K., EYMANN, R., GORTNER, L. & MEYER, S. 2012. Diagnostic approach to children with minor traumatic brain injury. ***Wien Med Wochenschr,*** **162, 394-9.**

OVERK, C. R. & MASLIAH, E. 2014. Pathogenesis of synaptic degeneration in Alzheimer's disease and Lewy body disease. ***Biochem Pharmacol,*** **88, 508-16.**

PARIHAR, V. K. & LIMOLI, C. L. 2013. Cranial irradiation compromises neuronal architecture in the hippocampus. ***Proc Natl Acad Sci U S A,*** **110, 12822-7.**

PARIHAR, V. K., PASHA, J., TRAN, K. K., CRAVER, B. M., ACHARYA, M. M. & LIMOLI, C. L. 2014. Persistent changes in neuronal structure and synaptic plasticity caused by proton irradiation. ***Brain Struct Funct*****.**

PAUL, C., STRATIL, C., HOFMANN, F. & KLEPPISCH, T. 2010. cGMP-dependent protein kinase type I promotes CREB/CRE-mediated gene expression in neurons of the lateral amygdala. ***Neurosci Lett,*** **473, 82-6.**

PEDROS, I., PETROV, D., ALLGAIER, M., SUREDA, F., BARROSO, E., BEAS-ZARATE, C., AULADELL, C., PALLAS, M., VAZQUEZ-CARRERA, M., CASADESUS, G., FOLCH, J. & CAMINS, A. 2014. Early alterations in energy metabolism in the hippocampus of APPSwe/PS1dE9 mouse model of Alzheimer's disease. ***Biochim Biophys Acta*****.**

PIZZIMENTI, S., CIAMPORCERO, E., DAGA, M., PETTAZZONI, P., ARCARO, A., CETRANGOLO, G., MINELLI, R., DIANZANI, C., LEPORE, A., GENTILE, F. & BARRERA, G. 2013. Interaction of aldehydes derived from lipid peroxidation and membrane proteins. ***Front Physiol,*** **4, 242.**

PRITHIVIRAJSINGH, S., STORY, M. D., BERGH, S. A., GEARA, F. B., ANG, K. K., ISMAIL, S. M., STEVENS, C. W., BUCHHOLZ, T. A. & BROCK, W. A. 2004. Accumulation of the common mitochondrial DNA deletion induced by ionizing radiation. ***FEBS Lett,*** **571, 227-32.**

RABER, J., ROLA, R., LEFEVOUR, A., MORHARDT, D., CURLEY, J., MIZUMATSU, S., VANDENBERG, S. R. & FIKE, J. R. 2004. Radiation-induced cognitive impairments are associated with changes in indicators of hippocampal neurogenesis. ***Radiat Res,*** **162, 39-47.**

REDMOND, L., KASHANI, A. H. & GHOSH, A. 2002. Calcium regulation of dendritic growth via CaM kinase IV and CREB-mediated transcription. ***Neuron,*** **34, 999-1010.**

REMENYI, J., HUNTER, C. J., COLE, C., ANDO, H., IMPEY, S., MONK, C. E., MARTIN, K. J., BARTON, G. J., HUTVAGNER, G. & ARTHUR, J. S. 2010. Regulation of the miR-212/132 locus by MSK1 and CREB in response to neurotrophins. ***Biochem J,*** **428, 281-91.**

RENNER, M., LACOR, P. N., VELASCO, P. T., XU, J., CONTRACTOR, A., KLEIN, W. L. & TRILLER, A. 2010. Deleterious Effects of Amyloid ? Oligomers Acting as an Extracellular Scaffold for mGluR5. ***Neuron,*** **66, 739-54.**

ROLA, R., RABER, J., RIZK, A., OTSUKA, S., VANDENBERG, S. R., MORHARDT, D. R. & FIKE, J. R. 2004a. Radiation-induced impairment of hippocampal neurogenesis is associated with cognitive deficits in young mice. ***Experimental Neurology,*** **188, 316-330.**

ROLA, R., RABER, J., RIZK, A., OTSUKA, S., VANDENBERG, S. R., MORHARDT, D. R. & FIKE, J. R. 2004b. Radiation-induced impairment of hippocampal neurogenesis is associated with cognitive deficits in young mice. ***Exp Neurol,*** **188, 316-30.**

RON, E., MODAN, B., FLORO, S., HARKEDAR, I. & GUREWITZ, R. 1982. Mental function following scalp irradiation during childhood. ***Am J Epidemiol,*** **116, 149-60.**

ROSI, S., ANDRES-MACH, M., FISHMAN, K. M., LEVY, W., FERGUSON, R. A. & FIKE, J. R. 2008. Cranial irradiation alters the behaviorally induced immediate-early gene arc (activity-regulated cytoskeleton-associated protein). ***Cancer Res,*** **68, 9763-70.**

SANEYOSHI, T., FORTIN, D. A. & SODERLING, T. R. 2010. Regulation of spine and synapse formation by activity-dependent intracellular signalling pathways. *Curr Opin Neurobiol,* 20, 108-15.

SANEYOSHI, T. & HAYASHI, Y. 2012. The Ca2+ and Rho GTPase signalling pathways underlying activity-dependent actin remodeling at dendritic spines. *Cytoskeleton (Hoboken),* 69, 545-54.

SAXTON, W. M. & HOLLENBECK, P. J. 2012. The axonal transport of mitochondria. *J Cell Sci,* 125, 2095-104.

SCHONFELD, S. J., LEE, C. & BERRINGTON DE GONZALEZ, A. 2011. Medical exposure to radiation and thyroid cancer. *Clin Oncol (R Coll Radiol),* 23, 244-50.

SCHRATT, G. M., TUEBING, F., NIGH, E. A., KANE, C. G., SABATINI, M. E., KIEBLER, M. & GREENBERG, M. E. 2006. A brain-specific microRNA regulates dendritic spine development. *Nature,* 439, 283-9.

SCHULZ, R. J. & ALBERT, R. E. 1968. Follow-up study of patients treated by x-ray epilation for tinea capitis. 3. Dose to organs of the head from the x-ray treatment of tinea capitis. *Arch Environ Health,* 17, 935-50.

SCOTT, H. L., TAMAGNINI, F., NARDUZZO, K. E., HOWARTH, J. L., LEE, Y. B., WONG, L. F., BROWN, M. W., WARBURTON, E. C., BASHIR, Z. I. & UNEY, J. B. 2012. MicroRNA-132 regulates recognition memory and synaptic plasticity in the perirhinal cortex. *Eur J Neurosci,* 36, 2941-8.

SHALTIEL, G., HANAN, M., WOLF, Y., BARBASH, S., KOVALEV, E., SHOHAM, S. & SOREQ, H. 2013. Hippocampal microRNA-132 mediates stress-inducible cognitive deficits through its acetylcholinesterase target. *Brain Struct Funct,* 218, 59-72.

SHENG, M. & HOOGENRAAD, C. C. 2007. The postsynaptic architecture of excitatory synapses: a more quantitative view. *Annu Rev Biochem,* 76, 823-47.

SHENG, Z. H. 2014. Mitochondrial trafficking and anchoring in neurons: New insight and implications. *J Cell Biol,* 204, 1087-98.

SHIMIZU, Y., KODAMA, K., NISHI, N., KASAGI, F., SUYAMA, A., SODA, M., GRANT, E. J., SUGIYAMA, H., SAKATA, R., MORIWAKI, H., HAYASHI, M., KONDA, M. & SHORE, R. E. 2010. Radiation exposure and circulatory disease risk: Hiroshima and Nagasaki atomic bomb survivor data, 1950-2003. *BMJ,* 340, b5349.

SHRUSTER, A. & OFFEN, D. 2014. Targeting neurogenesis ameliorates danger assessment in a mouse model of Alzheimer's disease. *Behav Brain Res,* 261, 193-201.

SLONIOWSKI, S. & ETHELL, I. M. 2012. Looking forward to EphB signalling in synapses. *Semin Cell Dev Biol,* 23, 75-82.

SMITH-BINDMAN, R., MIGLIORETTI, D. L. & LARSON, E. B. 2008. Rising use of diagnostic medical imaging in a large integrated health system. *Health Aff (Millwood),* 27, 1491-502.

SOKOLOW, S., HENKINS, K. M., WILLIAMS, I. A., VINTERS, H. V., SCHMID, I., COLE, G. M. & GYLYS, K. H. 2012. Isolation of synaptic terminals from Alzheimer's disease cortex. *Cytometry A,* 81, 248-54.

SONG, J., CHRISTIAN, K. M., MING, G. L. & SONG, H. 2012. Modification of hippocampal circuitry by adult neurogenesis. *Dev Neurobiol,* 72, 1032-43.

SPIEGLER, B. J., BOUFFET, E., GREENBERG, M. L., RUTKA, J. T. & MABBOTT, D. J. 2004. Change in neurocognitive functioning after treatment with cranial radiation in childhood. *J Clin Oncol,* 22, 706-13.

SQUIRE, L. R., STARK, C. E. & CLARK, R. E. 2004. The medial temporal lobe. *Annu Rev Neurosci,* 27, 279-306.

STAR, E. N., KWIATKOWSKI, D. J. & MURTHY, V. N. 2002. Rapid turnover of actin in dendritic spines and its regulation by activity. *Nat Neurosci,* 5, 239-46.

TAKEUCHI, T., DUSZKIEWICZ, A. J. & MORRIS, R. G. 2014. The synaptic plasticity and memory hypothesis: encoding, storage and persistence. *Philos Trans R Soc Lond B Biol Sci,* 369, 20130288.

TATAVARTY, V., DAS, S. & YU, J. 2012. Polarization of actin cytoskeleton is reduced in dendritic protrusions during early spine development in hippocampal neuron. *Mol Biol Cell,* 23, 3167-77.

TERRY, R. D., MASLIAH, E., SALMON, D. P., BUTTERS, N., DETERESA, R., HILL, R., HANSEN, L. A. & KATZMAN, R. 1991. Physical basis of cognitive alterations in Alzheimer's disease: synapse loss is the major correlate of cognitive impairment. *Ann Neurol,* 30, 572-80.

TONG, X. K., LECRUX, C. & HAMEL, E. 2012. Age-dependent rescue by simvastatin of Alzheimer's disease cerebrovascular and memory deficits. *J Neurosci,* 32, 4705-15.

TSAMIS, I. K., MYTILINAIOS, G. D., NJAU, N. S., FOTIOU, F. D., GLAFTSI, S., COSTA, V. & BALOYANNIS, J. S. 2010. Properties of CA3 dendritic excrescences in Alzheimer's disease. *Curr Alzheimer Res,* 7, 84-90.

UNSCEAR 2000. UNSCEAR 2000. The United Nations Scientific Committee on the Effects of Atomic Radiation. *Health Phys,* 79, 314.

URANGA, R. M., KATZ, S. & SALVADOR, G. A. 2013. Enhanced phosphatidylinositol 3-kinase (PI3K)/Akt signalling has pleiotropic targets in hippocampal neurons exposed to iron-induced oxidative stress. *J Biol Chem,* 288, 19773-84.

URBANSKA, M., SWIECH, L. & JAWORSKI, J. 2012. Developmental plasticity of the dendritic compartment: focus on the cytoskeleton. *Adv Exp Med Biol,* 970, 265-84.

VADODARIA, K. C. & JESSBERGER, S. 2013. Maturation and integration of adult born hippocampal neurons: signal convergence onto small Rho GTPases. *Front Synaptic Neurosci,* 5, 4.

VAN PRAAG, H., SCHINDER, A. F., CHRISTIE, B. R., TONI, N., PALMER, T. D. & GAGE, F. H. 2002. Functional neurogenesis in the adult hippocampus. *Nature,* 415, 1030-4.

VILLASANA, L. E., ROSENTHAL, R. A., DOCTROW, S. R., PFANKUCH, T., ZULOAGA, D. G., GARFINKEL, A. M. & RABER, J. 2013. Effects of alpha-lipoic acid on associative and spatial memory of sham-irradiated and 56Fe-irradiated C57BL/6J male mice. *Pharmacol Biochem Behav,* 103, 487-93.

VITICCHI, G., FALSETTI, L., VERNIERI, F., ALTAMURA, C., BARTOLINI, M., LUZZI, S., PROVINCIALI, L. & SILVESTRINI, M. 2012. Vascular predictors of cognitive decline in patients with mild cognitive impairment. *Neurobiol Aging,* 33, 1127 e1-9.

VO, N., KLEIN, M. E., VARLAMOVA, O., KELLER, D. M., YAMAMOTO, T., GOODMAN, R. H. & IMPEY, S. 2005. A cAMP-response element binding protein-induced microRNA regulates neuronal morphogenesis. *Proc Natl Acad Sci U S A,* 102, 16426-31.

VON TOERNE, C., KAHLE, M., SCHAFER, A., ISPIRYAN, R., BLINDERT, M., HRABE DE ANGELIS, M., NESCHEN, S., UEFFING, M. & HAUCK, S. M. 2013. Apoe, Mbl2, and Psp plasma protein levels correlate with diabetic phenotype in NZO mice--an optimized rapid workflow for SRM-based quantification. *J Proteome Res,* 12, 1331-43.

VOS, M., LAUWERS, E. & VERSTREKEN, P. 2010. Synaptic Mitochondria in Synaptic Transmission and Organization of Vesicle Pools in Health and Disease. *Front Synaptic Neurosci,* 2.

WANET, A., TACHENY, A., ARNOULD, T. & RENARD, P. 2012. miR-212/132 expression and functions: within and beyond the neuronal compartment. *Nucleic Acids Res,* 40, 4742-53.

WATT, A. J., VAN ROSSUM, M. C., MACLEOD, K. M., NELSON, S. B. & TURRIGIANO, G. G. 2000. Activity coregulates quantal AMPA and NMDA currents at neocortical synapses. *Neuron,* 26, 659-70.

WAYMAN, G. A., DAVARE, M., ANDO, H., FORTIN, D., VARLAMOVA, O., CHENG, H. Y., MARKS, D., OBRIETAN, K., SODERLING, T. R., GOODMAN, R. H. & IMPEY, S. 2008. An activity-regulated microRNA controls dendritic plasticity by down-regulating p250GAP. *Proc Natl Acad Sci U S A,* 105, 9093-8.

WAYMAN, G. A., IMPEY, S., MARKS, D., SANEYOSHI, T., GRANT, W. F., DERKACH, V. & SODERLING, T. R. 2006. Activity-dependent dendritic arborization mediated by CaM-kinase I activation and enhanced CREB-dependent transcription of Wnt-2. ***Neuron,*** **50, 897-909.**

WIEST, P. W., LOCKEN, J. A., HEINTZ, P. H. & METTLER JR, F. A. 2002. CT scanning: A major source of radiation exposure. ***Seminars in Ultrasound, CT, and MRI,*** **23, 402-410.**

WOODS, G. F., OH, W. C., BOUDEWYN, L. C., MIKULA, S. K. & ZITO, K. 2011. Loss of PSD-95 enrichment is not a prerequisite for spine retraction. ***J Neurosci,*** **31, 12129-38.**

XU, W., SCHLUTER, O. M., STEINER, P., CZERVIONKE, B. L., SABATINI, B. & MALENKA, R. C. 2008. Molecular dissociation of the role of PSD-95 in regulating synaptic strength and LTD. ***Neuron,*** **57, 248-62.**

YORK, J. M., BLEVINS, N. A., MELING, D. D., PETERLIN, M. B., GRIDLEY, D. S., CENGEL, K. A. & FREUND, G. G. 2012. The biobehavioral and neuroimmune impact of low-dose ionizing radiation. ***Brain Behav Immun,*** **26, 218-27.**

YOSHIDA, T., GOTO, S., KAWAKATSU, M., URATA, Y. & LI, T. S. 2012. Mitochondrial dysfunction, a probable cause of persistent oxidative stress after exposure to ionizing radiation. ***Free Radic Res,*** **46, 147-53.**

ZELINSKI, E. L., DEIBEL, S. H. & MCDONALD, R. J. 2014. The trouble with circadian clock dysfunction: Multiple deleterious effects on the brain and body. ***Neurosci Biobehav Rev,*** **40C, 80-101.**

ZHAO, C., DENG, W. & GAGE, F. H. 2008. Mechanisms and functional implications of adult neurogenesis. ***Cell,*** **132, 645-60.**

ZHENG, M., LIU, J., RUAN, Z., TIAN, S., MA, Y., ZHU, J. & LI, G. 2013. Intrahippocampal injection of Abeta1-42 inhibits neurogenesis and down-regulates IFN-gamma and NF-kappaB expression in hippocampus of adult mouse brain. ***Amyloid,*** **20, 13-20.**

ZHU, C., HUANG, Z., GAO, J., ZHANG, Y., WANG, X., KARLSSON, N., LI, Q., LANNERING, B., BJORK-ERIKSSON, T., GEORG KUHN, H. & BLOMGREN, K. 2009. Irradiation to the immature brain attenuates neurogenesis and exacerbates subsequent hypoxic-ischemic brain injury in the adult. ***J Neurochem,*** **111, 1447-56.**